

TECTONO-METAMORPHIC EVOLUTION OF THE NORTHERN MENDERES
MASSIF: EVIDENCE FROM THE HORST BETWEEN GÖRDES AND DEMİRCİ
BASINS (WEST ANATOLIA, TURKEY)

A THESIS SUBMITTED TO
THE GRADUATE SCHOOL OF NATURAL AND APPLIED SCIENCES
OF
MIDDLE EAST TECHNICAL UNIVERSITY


BY

ÇAĞRI BUĞDAYCIOĞLU


IN PARTIAL FULFILLMENT OF THE REQUIREMENTS
FOR
THE DEGREE OF MASTER OF SCIENCE
IN
GEOLOGICAL ENGINEERING

SEPTEMBER 2004

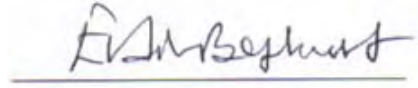
Approval of the Graduate School of Natural and Applied Sciences.


Prof. Dr. Canan Özgen
Director

I certify that this thesis satisfies all the requirements as a thesis for the degree of Master of Science.


Prof. Dr. Asuman Türkmenoğlu
Head of Department

This is to certify that we have read this thesis and that in our opinion it is fully adequate, in scope and quality, as a thesis for the degree of Master of Science.

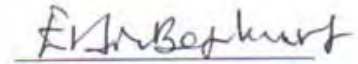

Prof. Dr. Erdin Bozkurt
Supervisor

Examining Committee Members

Prof. Dr. Vedat Toprak (METU, GEOE)



Prof. Dr. Erdin Bozkurt (METU, GEOE)



Assoc. Prof. Dr. Bora Rojay (METU, GEOE)



Assoc. Prof. Dr. Kadir Dirik (HU, GEOE)




Assist. Prof. Dr. İsmail Ömer Yılmaz (METU, GEOE)



I hereby declare that all information in this document has been obtained and presented in accordance with academic rules and ethical conduct. I also declare that, as required by these rules and conduct, I have fully cited and referenced all material and results that are not original to this work.

Name, Last name : Çaęrı Buędaycioęlu

Signature : 

ABSTRACT

TECTONO-METAMORPHIC EVOLUTION OF THE NORTHERN MENDERES MASSIF: EVIDENCE FROM THE HORST BETWEEN GÖRDES AND DEMİRCİ BASINS (WEST ANATOLIA, TURKEY)

Buğdaycıoğlu, Çağrı

M.Sc., Department of Geological Engineering

Supervisor : Prof.Dr. Erdin Bozkurt

September 2004, 163 pages

The Menderes Massif forms a large metamorphic culmination in western Turkey – an extensional province where continental lithosphere has been stretching following Palaeogene crustal thickening. Northern sector of the Massif on the horst between Gördes and Demirci Basins was chosen for structural analysis aimed to study the tectono-metamorphic evolution of the northern Menderes Massif.

Within the study area, four groups of rocks are recognized: (1) the metamorphic rocks – orthogneisses and metasediments; (2) pegmatoids; (3) Neogene sedimentary rocks; and (4) Quaternary alluvial sediments.

The tectono-metamorphic history of the region involves a regional metamorphism (M_1) at upper-amphibolite-facies conditions, coeval with a top-to-the-NNE contractional D_1 deformation during the northward backthrusting of Lycian Nappes (Eocene main Menderes metamorphism). Partial anatexis during the latest stages of the M_1 was speculated to be the main mechanism for the formation of the migmatites and the granitic magma. Pegmatoid domes and dikes/sills formed during late increments of this phase.

A second metamorphism (M_2) and coeval top-to-the-NNE deformation (D_2) took place during the Early Miocene exhumation of the metamorphic rocks along a presently low-angle normal fault in an extensional shear zone at presumably greenschist facies conditions during declining P-T conditions.

The latest deformation phase (D_3) is high-angle normal faulting due to N-S extension affecting western Anatolia. The E-W grabens dissecting the Massif into northern, central and southern submassifs are the result of this phase, commenced during Pliocene-Pleistocene and gave the western Anatolia much of its present-day shape. The evidence presented supports the idea of episodic two-stage extension in western Turkey.

Keywords: Menderes Massif, polydeformation, gneissic dome, episodic two-phase extension, northwestern Turkey.

ÖZ

KUZEY MENDERES MASIFI'NİN TEKTONO-METAMORFİK EVRİMİ: GÖRDES VE DEMİRCİ HAVZALARI ARASINDA KALAN HORSTTAN YENİ BULGULAR (BATI ANADOLU, TÜRKİYE)

Buğdaycıoğlu, Çağrı

Yüksek Lisans, Jeoloji Mühendisliği Bölümü

Tez Yöneticisi : Prof.Dr. Erdin Bozkurt

Eylül 2004, 163 sayfa

Menderes Masifi, kuzeybatı Türkiye'de Paleojen kıtasal kalınlaşmasını takip eden dönemde gerilme ile yüzeyleyen bölgesel ölçekli en önemli metamorfik parçalardan birini oluşturmaktadır. Kuzey Menderes Masifi'nin tektono-metamorfik evriminin çalışılması amacıyla yönelik olarak, masifin kuzey kısmının bir parçası olan ve Gördes (Manisa) kasabasının güneybatısında yer alan ve Gördes ve Demirci havzaları arasında kalan horst çalışma alanı olarak seçilmiştir.

Çalışma alanında dört kaya grubu yüzeylemektedir: (1) metamorfik kayalar – ortognayslar ve metasedimenterler; (2) pegmatoidler; (3) Neojen sedimenter kayalar; ve (4) Kuvaterner alüvyon sedimanları.

Kuzey Menderes Masifi'nin tektono-metamorfik evrimi, üst-ampfibolit fasiyesinde oluşmuş ve Likya Napları'nın kuzeye geri-bindirmesi sırasında oluşan ve kuzeye hareket veren D_1 deformasyonu ile eş zamanlı olarak gelişen bölgesel bir metamorfizmaya (M_1) sahiptir (Eosen ana Menderes metamorfizması). Çalışma alanındaki migmatitlerin ve granitik magmanın oluşumundaki ana mekanizmanın, M_1 'in son safhalarında oluşan kısmi ergime olduğu düşünülmektedir. Pegmatoid domları ve daykları/silleri bu fazın en son safhasında oluşmuşlardır.

Masif, Erken Eosen'de, yeşilşist fasiyesinde ve azalan P-T koşullarında gerçekleşen, ikinci bir metamorfizma (M_2) ve eş zamanlı olarak, metamorfik kayaların günümüzde düşük açılı olarak görülen normal fay boyunca yükseldiği, kuzeye hareket veren bir deformasyon (D_2) geçirmiştir.

Menderes Masifi'ni etkileyen en son deformasyon fazı (D_3), batı Anadolu'nun K-G yönlü gerilmesi sırasında oluşan yüksek açılı normal faylanmadır. Masifi kuzey, orta ve güney ara-masiflere ayıran bütün D-B yönlü grabenler, Pliyosen-Pleyistosen'de başlayan ve batı Türkiye'ye bugünkü yapısını kazandıran bu deformasyon sonucu oluşmuştur. Sunulan bulgular batı Türkiye'deki iki aşamalı gerilme hipotezini desteklemektedir.

Anahtar Kelimeler: Menderes Masifi, polideformasyon, gnays domu, iki aşamalı gerilme, kuzeybatı Türkiye.

ACKNOWLEDGMENTS

I am greatly indebted to Prof.Dr. Erdin Bozkurt for his guidance, continuous encouragement and interest, constructive discussions, critically reviewing and editing of the manuscript, and supervision throughout every stage of this study. Without him, this thesis could have never been completed.

I am grateful to Assist.Prof.Dr. Hasan Sözbilir for his help during the field studies and Ökmen Sümer for his guidance during İzmir journey.

Many thanks to Prof.Dr. Vedat Toprak, Assoc.Prof.Dr. Bora Rojay, Assist.Prof.Dr. Nuretdin Kaymakçı, and Assist.Prof.Dr. Mehmet Lütfi Süzen for their interest on the progress of the thesis and their endless offers for help during the preparation of this thesis and my M.Sc. education.

I ought to thank all examining committee members whose comments, critics and advice improved the text a lot.

I am also grateful to my friend Serhat Demirel for his valuable help, productive and provocative discussions and suggestions during the petrographic studies in the laboratory and his friendship and encouragement during the preparation of this thesis.

The technical assistance of Orhan Karaman during the preparation of thin sections from oriented samples for petrographic and microstructural analyses is gratefully acknowledged.

I would like to thank to all my friends, especially Gence Genç, Başak Şener, Alper Fulat, and Çağıl Kolat, who were with me during the stressful final preparation stages of the thesis, for their invaluable encouragement.

Last, but not the least, I offer my grateful thanks to my family, my mom, dad and brother, for their unlimited patience, unwavering support and encouragement in this study and all through my life.

This research was funded by METU Research Foundation grant BAP-2002-03-09-02.

TABLE OF CONTENTS

	PAGE
PLAGIARISM	iii
ABSTRACT	iv
ÖZ	vi
ACKNOWLEDGMENTS	viii
TABLE OF CONTENTS	ix
LIST OF TABLES	xii
LIST OF FIGURES	xiii

CHAPTERS

1. INTRODUCTION	1
1.1. Definition of the Problem	1
1.2. Purpose and Scope	7
1.3. Location of the Study Area	9
1.4. Methods of Study	11
1.5. Established Background Geology of Western Turkey	12
1.5.1. The Menderes Massif	14
1.5.1.1. Metamorphism.	16
1.5.1.2. Magmatism	20
1.5.1.3. Deformation	22
1.5.2. Current Problems	26
1.6. Previous Studies: the Gördes Region	30
2. STRATIGRAPHY.	38
2.1. Introduction	38
2.2. The Metamorphic Rocks.	41
2.2.1. Orthogneisses	41
2.2.2. Metasediments	51

2.2.2.1. Migmatites	51
2.2.2.2. Kyanite-Garnet-Biotite-Muscovite-Albite-Quartz Schists .	59
2.2.2.3. Quartz-Muscovite-Garnet Schists	63
2.3. Pegmatites	65
2.4. Neogene Sedimentary Rocks	71
2.5. Quaternary Alluvial Sediments	76
3. STRUCTURAL GEOLOGY	77
3.1. Introduction	77
3.2. Deformational Phases	77
3.3. D ₁ Deformation	78
3.3.1. F ₁ Folding	85
3.3.2. Microstructural Features of Deformed Grains in Orthogneisses	85
3.3.3. Shear-sense Indicators	94
3.4. D ₂ Deformation	94
3.4.1. Detachment Faulting	101
3.4.2. F ₂ Folding	101
3.5. D ₃ Deformation	104
3.5.1. Kınık-Mestanlı Area	104
3.5.2. Yardere Area	110
3.5.3. Dikilitaş Area	112
4. DISCUSSION AND CONCLUSION	115
4.1. Introduction	115
4.2. Metamorphism	115
4.2.1. M ₁ Metamorphism	115
4.2.2. M ₂ Metamorphism	120
4.3. Deformation	121
4.3.1. D ₁ Deformation	121
4.3.2. F ₁ Folding	123
4.3.3. D ₂ Deformation	124
4.3.4. F ₂ Folding	127
4.3.5. D ₃ Deformation	129

4.4. Significance of D ₂ and D ₃ Deformations130
4.5. Migmatization, Partial Anatexis and Intrusion of Pegmatoids132
4.6. Relationships among Migmatization, Crustal Melting, Extension and Intrusion.134
4.7. Is the Horst Between Gördes and Demirci Basins A Gneissic Dome?137
4.8. Geologic History139
4.9. Conclusions140

REFERENCES143
-----------------------------	-------------

LIST OF TABLES

TABLE	PAGE
1.1. Metamorphism in the Menderes Massif	16
1.2. Data concerning the age of main Menderes metamorphism	18
1.3. Magmatism in the Menderes Massif	21
1.4. Deformation in the Menderes Massif.	22
3.1. Selected fault plane measurements from Kınık – Mestanlı area.106
3.2. Fault plane measurements from Dikilitaş area.114

LIST OF FIGURES

FIGURE	PAGE
1.1. Back-arc extension models and its mechanisms	3
1.2. Location map of the study area	10
1.3. Simplified tectonic map of western Turkey	13
1.4. Simplified geological map of the Menderes Massif	15
1.5. Simplified map showing major structural elements of western Anatolia and the subdivision of the Menderes Massif after neotectonic (D ₄) deformation	25
1.6. General location map of the NNE-trending basins (Gördes, Demirci, Selendi, and Uşak-Güre basins) of western Anatolia	30
1.7. (a) Simplified geological map and (b) cross-section of the horst between Gördes and Demirci Basins	33
2.1. Geological map of the study area	39
2.2. Generalized columnar section of the study area	40
2.3. A porphyroclastic texture defined by a large feldspar augen with a more ductile fine grained matrix deflected around it	43
2.4. A field view from the orthogneisses displaying two distinct foliation with S ₂ shear band foliation overprinting the early S ₁ foliation	44
2.5. A view from the contact between the contact between kyanite-garnet- biotite-muscovite-albite-quartz schists and orthogneisses	44
2.6. Photomicrographs of orthogneisses	46
2.7. Field view showing the direct contact of migmatites with the pegmatoid dome	52
2.8. Different field views from pegmatites intruding into the migmatites discordantly or concordantly as dikes or both as dikes and sills.	53
2.9. A handspecimen of migmatite showing nomenclature used by Mehnert 1968 and Johannes 1983	54
2.10. Typical field view of migmatites with alternating dark (palaeosome) and light (neosome) layers	56
2.11. Phototomicrographs from migmatites	57

2.12. Photomicrographs from migmatites	58
2.13. A pegmatite dike intruded into kyanite-garnet-biotite-muscovite- albite-quartz schists near Mestanlı	60
2.14. Photomicrographs from kyanite-garnet-biotite-muscovite-albite- quartz schists	61
2.15. Photomicrographs from kyanite-garnet-biotite-muscovite-albite- quartz schists showing sporadically occurring garnet porphyroclasts.	62
2.16. Photomicrographs showing well developed S_1 foliation defined by parallel alignment of muscovite micas and quartz on quartz-muscovite- garnet schists	64
2.17. Typical dome shaped isolated pegmatite body known as ‘inselberg’ on the study area.	66
2.18. Photomicrographs showing different appearances of tourmaline crystals in pegmatites under plane polarized light	68
2.19. Photomicrographs illustrating different appearances of deformation twins in feldspar plagioclases in pegmatites	69
2.20. Photomicrographs showing different appearances of quartz crystals in pegmatites	70
2.21. General appearance of the Neogene sedimentary rocks exposed at Çavullar	72
2.22. Measured columnar section of the sedimentary sequence exposed near Çavullar village	73
2.23. Stratigraphical summary column of southern areas of Demirci basin	75
2.24. Quaternary alluvial sediments in the study area made up of loose sand-size material and fragments of various metamorphic rocks	76
3.1. Typical field views and the main regional foliation (S_1) developed on orthogneisses, kyanite-garnet-biotite-muscovite-albite-quartz schists and migmatites	79
3.2. Photomicrographs showing the main foliation defined by parallel alignment of biotites, muscovites and quartzes	80
3.3. Lower hemisphere stereonet (Schmidth net) projections and contour plots of poles to regional S_1 foliation on schists and migmatites; and L_1 lineations from metasediments	82
3.4. Lower hemisphere stereonet (Schmidth net) projections and contour plots of poles to regional S_1 foliation and L_1 lineations in the orthogneisses	84
3.5. Different field views from F_1 folding in migmatites	86
3.6. Photomicrographs from orthogneisses	88

3.7. Photomicrographs from orthogneisses showing different appearances of deformation twins in feldspars and myrmekitic intergrowth of vermicular quartz and plagioclase	90
3.8. Photomicrographs from orthogneisses showing different appearances of deformation twins in feldspars	91
3.9. Photomicrographs from orthogneisses	93
3.10. The main regional foliation (S_1) on the orthogneisses near Döğüşören and Çavullar villages	95
3.11. Photomicrographs from orthogneisses showing various shear sense indicators	96
3.12. Photomicrographs from orthogneisses showing muscovite minerals, defining well-developed mica-fish structures indicating a top-to-the-NNE deformation, in a matrix composed mainly of quartz	97
3.13. The S_2 foliation overprinting the main regional foliation (S_1) on the orthogneisses near Döğüşören village	98
3.14. Photomicrographs from orthogneisses showing the primary main regional foliation (S_1) defined by parallel alignment of quartzes, micas and elongated feldspar, and the secondary foliation (S_2) overprinting the first one.	99
3.15. Lower hemisphere stereonet (Schmidh net) projections and contour plot of poles to S_2 foliation on orthogneisses.	100
3.16. The presently low-angle fault comprising the boundary between orthogneisses and Neogene sedimentary rocks near Çavullar.	102
3.17. Close-up view of the metamorphic-sedimentary rock contact where the footwall rocks show evidence for brittle deformation with brecciation and iron-oxide development	102
3.18. Lower hemisphere stereonet (Schmidh net) projections of poles to foliations on migmatites and schists	103
3.19. General views of the faulted contact between orthogneisses and Neogene sedimentary rocks from the area between Kınık and Mestanlı and east of Kınık.	105
3.20. Close-up view of the fault plane and slip lineations on the same fault plane.	106
3.21. Schmidh lower hemisphere equal-area projections of fault slip data with higher rake angles from Kınık–Mestanlı area.	108
3.22. Schmidh lower hemisphere equal-area projections of fault slip data with lower rake angles from Kınık–Mestanlı area.	108
3.23. (a) Geological map of Kınık and surroundings; (b) cross-section along line A-B.	109

3.24. (a) Detailed geological map of Yardere region and surroundings;	
(b) cross-section along line A-B; (c) photograph along line A-B111
3.25. A close-up view an exposed small fault plane near Dikilitaş113
3.26. Schmidth lower hemisphere equal-area projections of fault slip data from the southern Dikilitaş Fault.114

CHAPTER 1

INTRODUCTION

1.1. Definition of the Problem

Crustal thickening is an important phenomenon during mountain formation at convergent continental margins and it reflects how collision is effective in changing the Earth's crust and topography. As the crust is too buoyant to be subducted, it thickens to accommodate the room problem during orogenesis. The thickened crust, over time, widens laterally, thus allowing the formation of continental plateaux (e.g., present-day Tibet and the Altiplano/Puna). Over the last three decades, the detailed structural analysis of orogens documents evidence for rapid extension of the upper crust and exhumation of the lower crust in metamorphic core complexes, i.e. orogenic collapse following crustal thickening (e.g., Dewey 1988; Ménard and Molnar 1988).

Although it is now commonly accepted that the extensional collapse of previously over-thickened crust is an important phenomenon in the evolution of orogens, the driving mechanism(s) of orogenic collapse forms the focus of a long-lasting debate and the proposed models fall into two distinct hypothesis: (1) *Thickened crust becomes too weak to support its own weight and flows under the action of gravity*: the occurrence of migmatites in the core of orogens form the main support of this hypothesis. Migmatization/partial melting suggests that the crust changes from a dominantly solid to a dominantly liquid state and that the strength of the crust decreases dramatically. The generation of partially molten rock during migmatization forms a weak layer, which then may decouple the upper part of the crust from the underlying lithospheric mantle. (2) *Change in the forces to the boundaries of the orogenic system*. The changes in the boundary conditions of the orogenic systems may cause the collapse of orogens. There are three possible mechanisms potentially leading to a change

in the boundary conditions of orogens: (i) *a change in the angle of subduction of the mantle lithosphere*: It is now commonly accepted that the angle of subduction may change from shallow to steep; this would affect the force budget that holds the orogen in contraction and results in extension. Similarly, a rollback of the subducted slab can induce extension in the orogen (Figure 1.1); (ii) *a decrease in convergence rate*: If global plate reorganization leads to a decrease in convergence rate at the boundary of an orogen, extension may also develop. The thick crust is maintained by continued contraction, and collapse occurs when this contraction decreases or vanishes because of gravitational potential energy stored in the elevated mountain belt and the thick crust drives orogenic collapse; or even (iii) *a change from plate convergence to plate divergence*: If the change in lateral boundary conditions is rapid, the response of the thickened crust can be swift, leading to rapid crustal extension and exhumation of deep rocks.

The continental extension following the crustal thickening at convergent plate margins is expressed, based on the structure of the extending terranes, by three modes (e.g., England 1983; Buck 1991): (1) *Narrow Rifting* – concentrated crustal and mantle lithospheric extension that give rise to narrow (up to 100–150 km wide) depressions bordered by high-angle normal faults. The thinning along rifts is accompanied by relative crustal thickening on the rift shoulders that give rise to local uplifts. Worldwide examples include East African Rift System, the Rio Grande Rift, the Baikal Rift, the northern Red Sea, the West Antarctic rift (Artemjev and Arthyushkov 1971; Illies and Greiner 1978; Bonatti 1985; Morgan *et al.* 1986; Rosendhal 1987; Steckler *et al.* 1988; Behrendt *et al.* 1991; Ziegler 1995; Prodehl *et al.* 1997; Corti *et al.* 2003; Ziegler and Cloetingh 2004 and references therein). (2) *Wide Rifting* – highly extended terranes or diffuse rifts with typical surface expression characterized by a large number of alternating grabens and intervening horsts over a region of up to 1000 km wide. Examples include Basin and Range Province of western North America, the Aegean (including western Anatolia) and the Tibet region (e.g., Armijo *et al.* 1986; Hamilton 1987; Jackson 1994; Şengör *et al.* 1985; Şengör 1987; Bozkurt 2000, 2001b). (3) *Core Complex* – high-grade metamorphic rocks originating in the

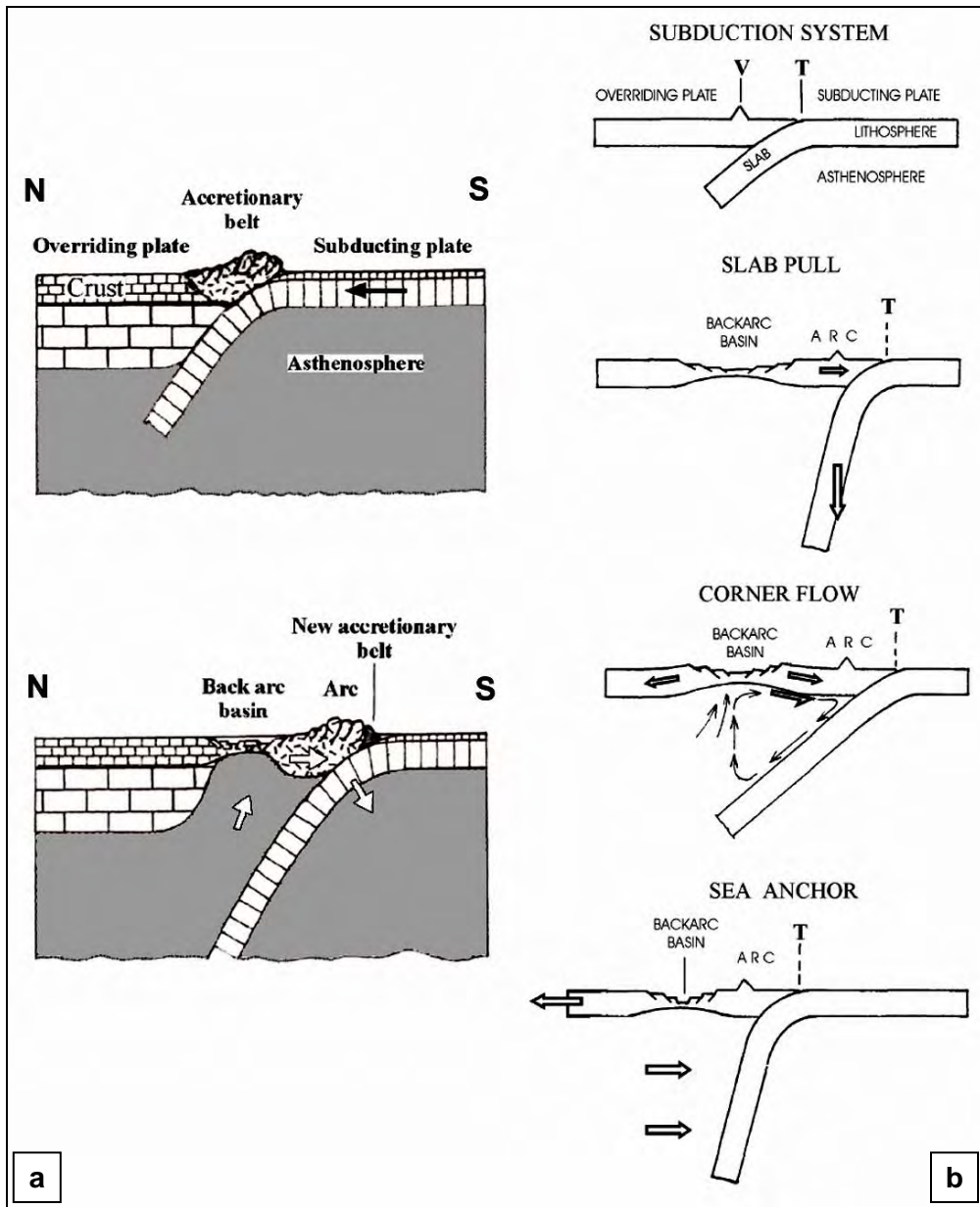


Figure 1.1. Back-arc extension models and its mechanisms (from Mantovani *et al.* 2001). **(a)** Model for the Aegean extensional province. Roll back of subducting slab is accompanied by southward migration of arc and N–S oriented extension in the region. **(b)** Proposed causes of back arc extension (T: position of the trench, V: volcanic arc). See Mantovani *et al.* (2001) for detailed discussion.

middle-lower crust are exposed at the surface, exhumed in the footwall of presently low-angle normal faults (detachments) (e.g., Coney 1980; Crittenden *et al.* 1980; Lister and Davis 1989; Gautier *et al.* 1990, 1993, 1999; King and Ellis 1990; Hill *et al.* 1992, 1995; Lister and Baldwin 1993; Sokoutis *et al.* 1993; Bozkurt and Park 1994, 1997a, 1997b, 1999, 2001; Brun and Van Den Driessche 1994; Brun *et al.* 1994; Gautier and Brunn 1994; Hetzel *et al.* 1995a, 1995b, 1998; Koçyiğit *et al.* 1999a; Bozkurt 2000, 2001a, 2001b, 2003, 2004; Bozkurt and Satır 2000; Okay and Satır 2000; Chéry 2001; Gessner *et al.* 2001a, 2001b, 2001c; Gökten *et al.* 2001; Işık and Tekeli 2001; Işık *et al.* 2003, 2004; Rimmelé *et al.* 2003a, 2003b; Ring *et al.* 2003; Bozkurt and Sözbilir 2004). Some of the core complexes worldwide are described from Basin and Range, Papua New Guinea and Aegean including western Anatolia. In these regions it is unequivocally demonstrated that the core complexes are usually associated with wide rifts. This, in turn, suggests successive rifting phases characterized by different styles of extension during core complex formation. Western Turkey, a region characterized by the widespread exposures of metamorphic rocks (known as the Menderes Massif – one of the largest metamorphic core complexes in the world) dissected by approximately E–W-trending grabens, forms a very good example for three modes of extension in the world (Figure 1.1). The northern parts of the Menderes Massif form the main subject of this thesis. In a very similar way, the origin, age and evolution of N–S continental extension in western Turkey is problematic and there are different models proposed to shed light on the existing controversies. This topic is summarized in the section 1.4.2, ‘*Current Problems*’.

The evolution of metamorphic core complexes represents dramatic, large-scale mass and heat transfer during continental deformation. Core complexes are exposures of high-grade metamorphic rocks unroofed during extension that typically follows crustal thickening (Dewey 1988), and are defined by the juxtaposition of high-grade and low-grade rocks across low-angle normal faults (detachments). They are comprised of several characteristic structural elements: (i) mid-crustal or deeper rocks exposed in the lower plate (high-grade metamorphic rocks and associated granitic intrusions); (ii) major ductile shear zones, typically dipping at a low angle ($< \sim 30^\circ$); and (iii) an upper plate

consisting of low-angle to unmetamorphosed, brittely deformed rocks. High-grade rocks of the lower plate, exposed below the detachment zones, cool rapidly, and rapid exhumation is typically inferred from the cooling history. The relation between cooling mechanisms and exhumation is, however, not well known.

It is now commonly agreed that extensional deformation and magma emplacement in the continental crust are closely related, and their interactions constitute a key factor in interpreting the structural evolution of the continental extensional terranes and metamorphic core complex formation. The emplacement of magmatic bodies within the continental crust modifies the initial thermal and mechanical properties of the continental lithosphere where the thermal weakening due to magmatic intrusions results in strain localization and enhancement particularly in the footwall of major low-angle normal faults (e.g., Lynch and Morgan 1987; Chèry *et al.* 1989; Tommasi *et al.* 1994; Hill *et al.* 1995; Brown and Solar 1998; Geoffroy 1989, 2001; Morley 1999a, 1999b; Simpson 1999; Callot *et al.* 2001, 2002; Ebinger and Casey 2001; Corti *et al.* 2003; Ziegler and Cloetingh 2004 and references therein).

In a similar fashion, the core complexes described worldwide are associated unequivocally with magmatism, thus suggesting an intimate relationship, both in space and time, between the magmatism and metamorphic core complex formation (e.g., Coney 1980; Crittenden *et al.* 1980; Lister *et al.* 1984, 1986; Gans 1987, 1997; Glazner and Bartley 1984; Gans *et al.* 1989; Lister and Davis 1989; Hutton *et al.* 1990; Ward 1991; Burchfiel *et al.* 1992; Axen *et al.* 1993; Lister and Baldwin 1993; Gautier *et al.* 1993; Parsons and Thompson 1993; Bozkurt 1994; Bozkurt and Park 1994, 1997b, 2001; Gautier and Brun 1994; Hetzel *et al.* 1995a, 1995b; Hill *et al.* 1995; Parsons 1995; Gans and Bohrsen 1998; Okay and Satir 2000; Bozkurt 2003, 2004). In such studies it is shown that the igneous rocks mainly intrudes the footwall of the major presently low-angle normal faults, thus suggesting a genetic/mechanic link between normal faulting and magmatism. However, the timing of magmatism with respect to extension is problematic and there are two possible hypothesis: (1) *Active Rifting* – Magmatism may predate extension where intrusion of magmatic bodies causes the generation of low-angle normal faults along which

the deeply seated high-grade metamorphic rocks in the footwall is progressively exhumed (e.g., Parsons and Thompson 1993). In this model, core complex formation is triggered by the plutonic activity (Lister and Baldwin 1993; Hill *et al.* 1995). (2) *Passive Rifting* – continental extension develops in response to regional tensional stresses due to plate boundary forces; i.e. lithosphere is thinned due to extension that enhances the passive upwelling of the asthenosphere and that, in turn, results in decompressional crustal melting, segregation and transport of melt, and final intrusion and emplacement of a pluton in an extending crust. On the other hand, many examples of continental extension worldwide is characterized by an early phase of passive rifting followed by an active phase (Wilson 1993; Merle and Michon 2001; Corti *et al.* 2003; Ziegler and Cloetingh 2004 and references therein).

The different models of continental extension highlight the intimate dynamic and temporal relationships between magmatism and crustal extension. However, the determination of the fundamental driving force of extension (passive vs active rifting) is hindered by lack of information about the timing and chemical/physical relationships among regional metamorphism, partial melting, pluton emplacement and deformation. The key question is to determine (1) whether crustal melting preceded extension and was therefore a contributing force for collapse/extension or (2) whether melting was a response of extension.

To distinguish between these competing hypotheses, detailed knowledge of the timing of orogenic collapse and plate-scale movements is necessary. The present research involves the study of the northern Menderes Massif (western Anatolia), where major extension occurred following crustal thickening. Previous work (see sections [1.4 and 1.5] on '*Established Background Geology of Western Turkey*' and '*Previous Studies: the Gördes Region*') has shown that extension has expressed itself in two distinct structural styles in the Menderes Massif area: rapid exhumation of metamorphic core complex under presently low-angle detachments, and late stretching of crust by high-angle normal faults (e.g., Koçyiğit *et al.* 1999a, 1999b; Bozkurt 2000, 2001a, 2001b, 2002, 2003, 2004; Bozkurt and Satır 2000; Sözbilir 2001, 2002; Koçyiğit and Özacar 2003; Bozkurt and Sözbilir 2004).

1.2. Purpose and Scope

The present work aims to study the tectono-metamorphic evolution of the northern Menderes Massif to discuss the relative timing of metamorphism/migmatization and partial melting/magmatism and, thus continental extension prevailed in the region. The Menderes Massif forms a large metamorphic culmination in western Anatolia – a major extensional province where continental lithosphere has been stretched following crustal thickening. The relative importance of likely driving forces for extension are debated, and a focus of discussion has been the origin and evolution of metamorphic core complexes, which represent mid-crust unroofed during extension (see section 1.4.2 on '*Current Problems*').

The Menderes Massif in western Anatolia forms an important metamorphic culmination where evidence for relationships among crustal melting, extension, and intrusion is preserved. Although there is an established background about the structure and metamorphism of the massif, the role of magmatism in the massifs is still unresolved because of lack of information about the timing of migmatization, magmatism and metamorphism. It is, therefore, essential to determine the timing and mutual relationships among these processes in the massif. Establishing the number and timing of phases of metamorphism and deformation, and coeval magmatism (if present), provides insights concerning the tectonic evolution of orogens and is a subject of major controversies and long-standing discussions of the study of metamorphic culminations. This relies on *field constraints* – age of the youngest metamorphosed lithology and the oldest unconformable unmetamorphosed sediments on top of the metamorphic rocks, and the application of the basic principles of relative dating (e.g., cross-cutting and overprinting relationships).

This research involves two-years study (field geological mapping and structural analysis) of the rocks of the least studied northern Menderes Massif (the metamorphic rocks exposed on the horst between Gördes and Demirci basins) in Gördes area to examine and understand the thermal and structural history of the submassif. This allows us (1) to assess the major factors that drive extension and influence the style, magnitude and the timing of exhumation of

mid-crustal terrains during large-scale extension; (2) to consider the constructional history of thickening/heating, metamorphism and magmatism; and (3) to evaluate unroofing mechanisms. The research combines the results of field-based structural geology and microstructural analysis with the available literature to better understand the evolution of Menderes core complex from the mid-lower crust to the Earth's surface.

More specifically, the main objectives of this research can be summarized as follows:

- (1) To examine the type and distribution of the metamorphic rocks of the northern Menderes Massif exposed in the horst between Gördes and Demirci basins;
- (2) To determine the nature and origin of boundary relationships among different lithologies and then discuss the geological significance of these relationships;
- (3) To study the petrology of metamorphic rocks in order to understand the number and nature of deformational and metamorphic phases that affected the northern Menderes Massif, and the metamorphic conditions prevailed during each phase;
- (4) To determine the kinematics (movement directions) and tectonic setting (where possible) of each deformational phase;
- (5) To discuss the mechanism of exhumation of the deep-seated metamorphic rocks of the Menderes Massif, i.e. to study the effects of extensional tectonics;
- (6) To discuss the relative timing of migmatization and magmatism with respect to each phase of deformational/metamorphism and then to discuss the role of migmatization and magmatism in exhuming the submassif;
- (7) To establish the chronology of the metamorphic, magmatic and deformational events that this part of the massif has experienced
- (8) Finally, to speculate/discuss and summarize the tectono-metamorphic evolution of the northern submassif.

The outline of this thesis is as follows: (1) firstly, Chapter 1 summarizes the state of art in western Turkey, particularly the established background on the

tectono-metamorphic evolution of the Menderes Massif as well as the origin and age of continental extension in western Turkey. A special emphasis will be given to the previous studies on the metamorphic rocks of the horst between Gördes and Demirci basins; (2) Chapter 2 focuses on the brief stratigraphy of the study area. General characteristics and structural/boundary relationships of various rock types exposed at the study area are given. A brief account of petrography of the metamorphic rocks exposed in the study area is described here; (3) the detailed description of main structural elements is given in Chapter 3. This chapter is also dedicated to the detailed classification, description and analysis of different deformational phases identified after both field and laboratory studies. The brief description of the shear sense indicators and kinematic analysis of each deformational phase, their importance and characteristics are all discussed here; (4) The discussion of tectonic significance of data present in the preceding chapters form the main subject of Chapter 4 together with a summary of main conclusions reached in this study. The relationship between migmatization/magmatism (plutonism), exhumation of the metamorphic rocks and metamorphic conditions of each deformational phase are also discussed here. Another section is devoted to the discussion of the relationship between metamorphic rocks and the Neogene basin-fill sediments of the Demirci Basin and their tectonic significance. The discussion of the tectono-metamorphic evolution of the northern Menderes Massif with special reference to the geotectonic evolution of western Turkey is also given in this chapter.

1.3. Location of the Study Area

The study area is located within the northern Menderes Massif in western Turkey, between southeast of Gördes and north of Köprübaşı (Manisa; Figure 1.2). The area lies in the horst bounded by Gördes Basin on the west and Demirci Basin on the east. The nearest main settlement to the study area is Köprübaşı. Total amount of area covered by the study area is approximately 100 km²; it is included on 1/25,000 scale Turkish topographic map sheets of İzmir K20-b1, K20-b2, K20-b3 and K20-b4 (Figure 1.2). The study area is about 8-km wide in E–W direction and 12-km long in N–S direction.

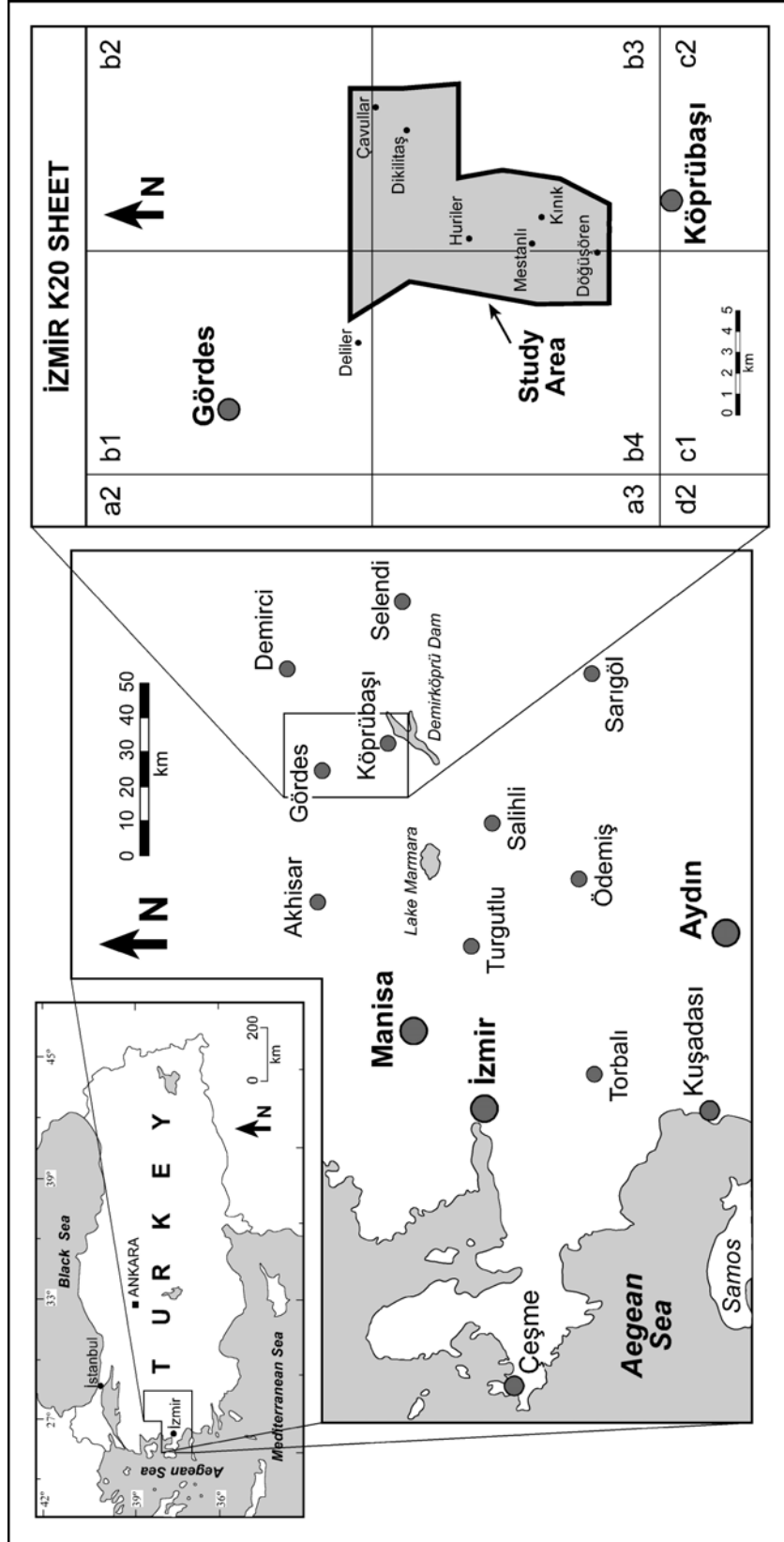


Figure 1.2. Location map of the study area.

1.4. Methods of Study

The results of this research are based on two years of (i) field studies carried out during the summer periods of the years 2002 and 2003 on a selected area near Gördes, and (ii) laboratory studies at the Tectonic Research Laboratory in the Geological Engineering Department of the Middle East Technical University.

The field studies include: (1) mapping of the various rock units and geological structures such as, faults, folds, foliation, lineation, shear zones, dikes and veins at a scale of 1/25,000; (2) preparation of detailed sketch maps, cross-sections and vertical stratigraphic sections in order to describe the meso-structures, boundary relationships, and lithological variations in defined rock units; (3) detailed structural/kinematic analysis of suitable outcrops to determine the number of deformational phases (where possible) and shear sense during each phase; (4) measurement of fault-slip data – attitude of fault plane and invariably associated slip-lines; (5) measurement of attitude for foliation and associated mineral lineation; and (6) collection of 105 oriented rock samples for petrographic and microstructural analysis. The structural analysis of deformed rocks requires oriented rock samples; therefore the oriented sample collection formed one of the most important part of the field studies. Following steps were followed during sampling: (i) the attitude of main foliation (strike, the direction and amount of dip) are measured and recorded in the field notebook; (ii) the measured strike is marked on a suitable surface by a long line with a half arrow above to indicate the strike direction whereas the dip is marked as thick line; (iii) the movement sense, if possible, is also marked and recorded; (iv) the detailed description and measured orientations of mesoscopic structures are also recorded in the notebook.

Laboratory studies include: (1) the detailed petrographic and fabric/microstructural examination of 105 oriented thin sections of metamorphic rocks under polarizer microscope in order to understand the metamorphic conditions of each deformation, and to support and/or control the results of kinematic analysis carried out during field studies. The thin sections prepared from the oriented rock samples are used for petrographic and structural

analysis. The sections are all cut parallel to the mineral stretching lineation and perpendicular to the main foliation in the rock sample; a direction parallel to the shear direction, and perpendicular to the flattening/finite shortening plane. All necessary marks from the oriented samples are transferred to the thin-section glass during preparation; (2) structural analysis of main foliation and mineral stretching lineation of metamorphic rocks by using stereographic projection techniques – preparation of stereograms using Schmidt net lower hemisphere projection; the data is computed using the stereonet utility of Rockworks 2002 software developed by Rockware Inc. in order to determine the dominant orientations for these structural elements (3) the fault kinematic analysis of fault slip data using the stress inversion method of Angelier (1984, 1991). The data is computed, using the software developed by Hardcastle and Hills (1991) in order to determine the kinematic framework of faulting during each phase.

1.5. Established Background Geology of Western Turkey

As mentioned earlier, western Anatolia forms one of the most seismically active and rapidly deforming regions in the world and currently experiences an approximately N–S continental extension. It is a part of the Aegean Extensional Province, which is a broad zone dominated by a distributed extension that extends from Bulgaria in the north to the Aegean Arc in the south (e.g., Bozkurt 2003 and references therein).

Western Anatolia comprises several continental fragments with distinctive stratigraphy, structural and metamorphic features. The boundaries of these continental fragments are defined by major suture zones, namely the Intra-Pontite Suture, the İzmir-Ankara Suture and the Inner-Tauride Suture, the amalgamation of which occurred during the Early Tertiary continent-continent collision across the Neotethys (Okay and Tüysüz 1999; Figure 1.3).

The Anatolide-Tauride platform, which is composed of several tectonic units bounded by major faults, lies at the south of the İzmir-Ankara Suture. These units include: (1) a blueschist belt (Tavşanlı Zone; Okay 1980a, 1980b, 1984a, 1984b, 1986; Okay *et al.* 1998; Sherlock *et al.* 1999), (2) the Bornova Flysch Zone, consisting of large Mesozoic limestone blocks within a matrix of

Maastrichtian–Palaeocene greywacke-shale (Erdoğan 1990; Okay and Siyako 1993), (3) the Afyon zone – a Palaeozoic–Mesozoic sedimentary sequence metamorphosed into the greenschist facies - (Akdeniz and Konak 1979; Okay 1984a, 1984b; Şengör *et al.* 1984; Göncüoğlu *et al.* 1996-1997; Özcan *et al.* 1988), (4) the Lycian Nappes, composed of Mesozoic sedimentary sequences and a peridotite thrust sheet (e.g., Brunn *et al.* 1970; de Graciansky 1972; Poisson 1977; Gutnic *et al.* 1979; Özkaya 1982, 1990, 1991; Okay 1989; Collins and Robertson 1997, 1998, 1999, 2003; Çelik and Delaloye 2003; Rimmelé *et al.* 2003a, 2003b), and (5) the Menderes Massif. The detailed information about the Menderes Massif will be given in the following section.



Figure 1.3. Simplified tectonic map of western Turkey (Okay and Tüysüz 1999).

1.5.1. The Menderes Massif

The Menderes Massif is a regional, large-scale, elongated metamorphic core complex with its long axis trending NE–SW, covering an area of more than 40,000 km² of western Turkey. It is made up of a Precambrian gneissic basement and the structurally overlying Palaeozoic–Palaeocene metasediments metamorphosed at greenschist- to amphibolite-facies conditions. The massif is conventionally subdivided into northern, central and southern submassifs, where the seismically active E–W-trending Gediz Graben in the north and Büyük Menderes Graben in the south are taken as dividing lines between the submassifs, respectively (Figure 1.4; e.g., Bozkurt 2001a; Bozkurt and Oberhänsli 2001 and references therein). The southern, central and northern submassifs are also known as Çine, Ödemiş-Kiraz and Gördes submassifs, respectively (e.g., Gessner *et al.* 2001a, 2001b, 2001c, 2004; Candan *et al.* 2001; Dora *et al.* 2001; Ring *et al.* 2003; Koralay *et al.* 2001, 2004).

The Menderes Massif is composed of an ‘augen gneiss core’ and an overlying ‘Palaeozoic–Cenozoic cover series’ with the intensity of metamorphism increasing towards the core. This relationship is well-exposed in the northern Menderes Massif.

Augen gneisses are the most dominant and widespread lithology of the so-called ‘core’ rocks. They are typical blastomylonites characterized by a well-developed mylonitic foliation and approximately N–S-trending mineral stretching lineation. The rocks are made up of asymmetric large feldspar porphyroclasts (reaching up to 8-cm along their long axes) within a more ductile matrix of primarily quartz, mica (both biotite and muscovite) and feldspars. Locally garnet porphyroclasts are also present. The matrix foliation wraps around the porphyroclasts (Bozkurt and Oberhänsli 2001; Bozkurt 2004 and references therein).

The origin of the augen gneisses has been subject of controversy for years. Before the geochemical studies of Bozkurt *et al.* (1992, 1993, 1995), it was largely believed that the protolith of augen gneisses was a sedimentary rock. However, these studies showed out that the protoliths are granitoid rocks

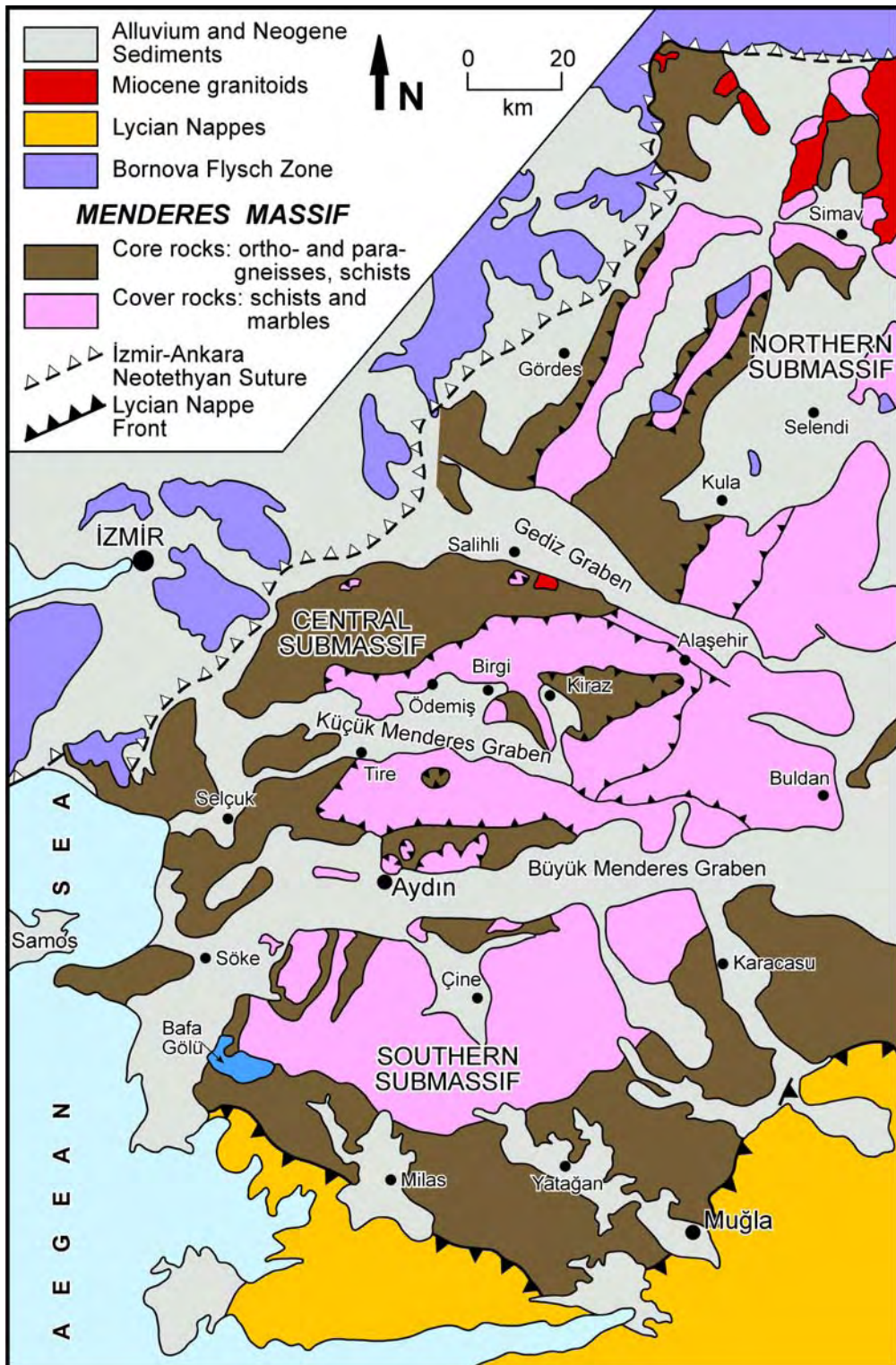


Figure 1.4. Simplified geological map of the Menderes Massif (Candan *et al.* 2001).

and the augen gneisses display young intrusive relationships with the structurally overlying metasediments rather than an unconformity as previously believed.

The 'cover' rocks consist of a pre-Upper Devonian to Lower Eocene metasedimentary sequence that comprises a variety of metamorphic rocks ranging from upper amphibolite to greenschist facies ('schist envelope', composed of garnet-, staurolite-, kyanite- and sillimanite-mica schists, garnet amphibolites, metapsammities, 'augen' schists and phyllites with limestone intercalations) and marble-dominated low-grade metasediments ('marble envelope') (e.g., Bozkurt and Oberhänsli 2001; Bozkurt 2001b; Özer *et al.* 2001; Güngör and Erdoğan 2002; Okay 2001, 2002; Özer and Sözbilir 2003; Bozkurt 2004; Erdoğan and Güngör 2004 and references therein).

1.5.1.1. Metamorphism

The Menderes Massif has undergone a complex metamorphism with six distinguished phases (Table 1.1; Bozkurt and Oberhänsli, 2001 and references therein; Whitney and Bozkurt 2002; Régnier *et al.* 2003; Rimmelé *et al.* 2003a, 2003b; Ring *et al.* 2003). Only the 'core' rocks were affected by the first two pre-Alpine phases (M₁ and M₂). Since the traces of these phases have been erased by subsequent Alpine events, evidence for pre-Alpine metamorphism is very rare.

Table 1.1. Metamorphism in the Menderes Massif (Bozkurt and Oberhänsli 2001).

Metamorphic phase	Grade	Age
M ₁₋₂	Granulite, eclogite, amphibolite	pre-550 Ma
M ₃	Greenschist	pre-230 Ma
M ₄	Blueschist	40 Ma
M ₅ (MMM)	Amphibolite-greenschist	35±5 – 36±2 Ma
M ₆	Greenschist	12.2±0.4 – 19.5±1.4 Ma

The first event (M_1) is evidenced by the occurrence of metagabbros with eclogite relics which suggest a HP/LT metamorphism at a pressure of ~15 kbar (Candan *et al.* 2001). Orthopyroxene relics in the gneisses and charnockites indicate a possible granulite-facies metamorphism prior to eclogite formation (Candan *et al.* 2001). The eclogites were later retrograded to garnet amphibolite during a Barrovian-type metamorphism. The absence of similar relics in augen gneisses and the presence of metagabbros as xenoliths in them suggest that the eclogite-facies metamorphism must have occurred prior to the emplacement of the precursors of the augen gneisses (pre-550 Ma: Candan *et al.* 2001). Candan *et al.* (2001) relates this phase to over-thrusting and consequent crustal thickening during Pan-African orogeny.

The second event (M_2) occurred at 502 ± 10 Ma with intense deformation at amphibolite-facies conditions associated with widespread migmatization and local anatexis. Deformed tonalitic-granitic intrusions dated at 470 ± 9 Ma mark the end of this episode (Satır and Friedrichsen 1986; Bozkurt and Oberhänsli 2001 and references therein). Şengör *et al.* (1984) related this event to the last Pan-African collision and associated post-collisional convergence.

Evidence for the third phase (M_3) is scarce and is from Derbent area of the central submassif (Akkök 1983). According to Akkök, this phase occurred at greenschist-facies conditions and was related to the closure of the Karakaya marginal basin of the Palaeotethyan ocean during the Late Triassic.

Blueschists and eclogites with strong greenschist-facies overprints, which suggest a HP metamorphism (M_4), have been documented from the central submassif, Dilek Peninsula. According to some scientists, these metamorphic units are similar to those on Samos Island in the Aegean Sea, so the high-pressure unit of the Dilek Peninsula is interpreted as the eastward lateral continuation of the HP unit of Samos Island (Okrusch *et al.* 1985; Candan *et al.* 1997; Oberhänsli *et al.* 1998). Oberhänsli *et al.* (1998) attributed this phase to a subduction-related HP metamorphism during the closure of Neotethys. However, Oberhänsli *et al.* (1998) and Okay (2001) suggested that this unit has no relation to the Menderes Massif but belongs to the Cycladic Massif and should be omitted in the definition of the Menderes Massif. According to this view, the HP unit of the Dilek Peninsula was thrust onto the

Menderes Massif during the Alpine orogeny. This view suggests that the Menderes and Cycladic massifs cannot be correlated (Bozkurt and Oberhänsli 2001 and references therein).

A major event affecting the whole massif is Alpine regional HT/MP Barrovian-type metamorphism termed the '*main Menderes metamorphism (MMM)*' (M_5), which was associated with intense top-to-the-N-NNE deformation (Bozkurt 1994, 1995, 1996, 2004; Hetzel *et al.* 1998; Bozkurt and Park 1999; Bozkurt and Satır 2000; Bozkurt 2001a; Arslan *et al.* 2002; Rimmelé *et al.* 2003a, 2003b) during Eocene times (Table 1.2). It reached upper-amphibolite-facies conditions in the central and northern submassifs, almandine-amphibolite grade associated with local anatectic melting in the structurally lower parts of the southern submassif, but only greenschist grade in the structurally upper parts of the 'cover' rocks. This metamorphism has long been considered to be the product of latest Palaeogene collision across the Neotethys and the consequent internal imbrication of the Menderes-Tauride block that resulted in the burial and intense shearing of the massif area within a broad zone along the base of the southward advancing Lycian Nappes, and must have been generated during and after their emplacement onto the Massif (Şengör and Yılmaz 1981; Şengör *et al.* 1984).

Table 1.2. Data concerning the age of main Menderes metamorphism.

Lithology	Location	Age (Ma)	Method	Reference
Schists	Southern Menderes Massif	35±5 (63–48 muscovite and 50–27 biotite)	Rb-Sr mica	Satır and Friedrichsen (1986)
Augen gneisses	Southern Menderes Massif	62–43	Rb-Sr mica	Bozkurt and Satır (2000)
Augen gneisses and schists	Southern Menderes Massif	43–37	⁴⁰ Ar- ³⁹ Ar muscovite	Hetzel and Reischmann (1996)
Augen gneisses	Northern margin of Büyük Menderes Graben	36±2	⁴⁰ Ar- ³⁹ Ar laser probe mica	Lips <i>et al.</i> (2001)

On the other hand, documentation of unambiguous top-to-the-N–NNE deformation associated with main foliation in the metasediments (Bozkurt 1994, 1995, 2001a, 2004; Hetzel *et al.* 1998; Bozkurt and Park 1999; Bozkurt and Satir 2000; Arslan *et al.* 2002; Rimmelé *et al.* 2003a, 2003b) suggest that the southward transport of Lycian Nappes has nothing to do with the main Menderes metamorphism but it is the northward back-thrusting of the Lycian nappes over the massif area (Bozkurt and Park 1999; Rimmelé *et al.* 2003b). The subsequent cooling occurred in the Early Tertiary, and it is commonly believed that the MMM affected the whole Massif and indeed gave it its '*massif*' character. The recent P–T work in the southern Menderes Massif showed that temperatures during the MMM reached conditions of 600–650°C in the metasediments within the orthogneisses (augen gneisses), >550°C in the structurally lowest cover rocks and ~450°C in the structurally highest, garnet-bearing schists to the south. Pressure estimated from the mineral paragenesis are 8–11 kbar in the core metasediments (Régnier *et al.* 2003) while it is \leq 5 kbar (Whitney and Bozkurt 2002) or 7 kbar (Régnier *et al.* 2003) in the cover schists. The estimated conditions in the central submassif are 450–660 °C and 5–8 kbar (Bozkurt and Oberhänsli 2001 and references therein).

In addition to all, it has been recently demonstrated that the schists of the southern Menderes Massif has experienced an Alpine HP metamorphism prior to the main Menderes metamorphism. The discovery of relict Fe-Mg-carpholite-chloritoid assemblages suggests P–T conditions of about 10–12 kbar and 440 °C (Rimmelé *et al.* 2003b). This is compatible with a burial depth of minimum 30 km and is contemporaneous with fast burial beneath the southward moving Lycian Nappes over the Menderes Massif area (Rimmelé *et al.* 2003b). The distribution of carpholites is not confined to the Menderes Massif only but magnesiocarpholites also occur in the Lycian nappes, suggesting the importance of HP event in western Turkey (Oberhänsli *et al.* 2001; Rimmelé *et al.* 2003a).

The last phase (M₆) in the Massif was a retrogressive greenschist-facies metamorphism associated with exhumation of metamorphic rocks in the footwall of presently low-angle normal faults that accommodated latest Oligocene–Early Miocene orogenic collapse in western Turkey (e.g., Bozkurt and Park 1994,

1997a, 1997b, 2001; Bozkurt *et al.* 1995; Hetzel *et al.* 1995a, 1995b, 1998; Verge 1995; Hetzel and Reischmann 1996; Koçyiğit *et al.* 1999a; Bozkurt 1994, 2000, 2001a, 2001b, 2003, 2004; Bozkurt and Satır 2000; Bozkurt and Oberhänsli 2001; Gessner *et al.* 2001a, 2001b; Gökten *et al.* 2001; Işık and Tekeli 2001; Lips *et al.* 2001; Sözbilir 2001, 2002; Seyitoğlu *et al.* 2002; Whitney and Bozkurt 2002; Işık *et al.* 2003, 2004; Ring *et al.* 2003; Rimmelé *et al.* 2003a, 2003b; Bozkurt and Sözbilir 2004; Purvis and Robertson 2004; Westaway *et al.* 2004). This phase was associated with syn-kinematic granitoid intrusions (Bozkurt 1994, 2004; Bozkurt and Park 1994, 1997b, 2001; Hetzel *et al.* 1995a; Bozkurt and Oberhänsli 2001; Işık *et al.* 2004 and references therein).

1.5.1.2. Magmatism

There have been four distinct magmatic activities described in the Menderes Massif: Proterozoic, Cambrian, Triassic and Tertiary (Table 1.3; Bozkurt and Oberhänsli 2001).

The first Proterozoic magmatic activity is observed at entire Menderes Massif where orthogneisses and metagranites yield ages of 2555 to 1740 Ma. The second event is again a major magmatic activity occurred during the Precambrian–Cambrian time. The orthogneisses yield different but very close ages (~541 Ma on the average) at different parts of the massif as seen in Table 1.3. The third magmatic activity in the region is represented by metagranitoids intruding into ‘core’ schists. The ages of these are found to be ~230-240 Ma and the intrusion of them were attributed to the closure of Karakaya basin, a remnant basin of Palaeotethys (Koralay *et al.* 2001, 2004).

In the central submassif, the Turgutlu and Salihli granitoids are present in the footwall of a low-angle normal fault, which forms the boundary between the metamorphics and overlying Neogene sedimentary rocks. The age of intrusion is Burdigalian (a $^{40}\text{Ar}/^{39}\text{Ar}$ hornblende age of 19.5 ± 1.4 Ma; Hetzel *et al.* 1995a). Similarly, the metamorphic rocks in the northern submassif were intruded by the Late Oligocene–Early Miocene Eğrigöz granite. $^{40}\text{Ar}/^{39}\text{Ar}$ data indicate that the cooling age of the Eğrigöz granitoid is 20.19 ± 0.28 Ma (Işık *et al.* 2004). The intrusion of these granitoids is interpreted as syntectonic with

respect to the exhumation of the massif (Bozkurt and Oberhänsli 2001 and references therein).

Table 1.3. Magmatism in the Menderes Massif (after Bozkurt and Oberhänsli 2001)

Phase	Lithology	Location	Age (Ma)	Method	Reference
1	Metagranites and orthogneisses	Entire Menderes Massif	2555-1740	^{207}Pb - ^{206}Pb single zircon evaporation	Reischmann <i>et al.</i> (1991)
2	Weakly deformed granite	Southern Menderes Massif	546.2±1.2	^{207}Pb - ^{206}Pb single zircon evaporation	Hetzel and Reischmann (1996)
			521±8.0 to 572±7.0	^{207}Pb - ^{206}Pb single zircon evaporation	Loos and Reischmann (1999)
	Metagranites and orthogneisses	Entire Menderes Massif	528±4.3 to 541.4±2.5	^{207}Pb - ^{206}Pb single zircon evaporation	Dannat (1997)
			547.2±1	^{207}Pb - ^{206}Pb single zircon evaporation	Gessner <i>et al.</i> (2001a)
			561.5±1.8 to 570.5±2.2	^{207}Pb - ^{206}Pb single zircon evaporation	Koralay <i>et al.</i> (2004)
Weakly deformed granite	Central Submassif	541±14 to 566±9	SHRIMP U-Pb zircon	Gessner <i>et al.</i> (2004)	
		551±1.4	^{207}Pb - ^{206}Pb single zircon evaporation	Hetzel <i>et al.</i> (1998)	
3	Metagranites	Central Submassif	240.3±2.2	^{207}Pb - ^{206}Pb single zircon evaporation	Dannat (1997) Koralay <i>et al.</i> (1998)
			226.5±6.8		
4	Eğrigöz Granite	Northern Submassif	20.19±0.28	$^{40}\text{Ar}/^{39}\text{Ar}$ biotite	Işık <i>et al.</i> (2004)
	Turgutlu and Salihli Granitoids	Central Submassif	19.5±1.4	$^{40}\text{Ar}/^{39}\text{Ar}$ amphibole isochron	Hetzel <i>et al.</i> (1995a)

1.5.1.3. Deformation

The Menderes Massif has a complex deformation history, which is examined in two groups as pre-Alpine and Alpine (Table 1.4).

Pre-Alpine (D₁)

Since the traces of earlier deformational phases have been erased by the later phases, evidence for the pre-Alpine deformation in the Menderes Massif is scarce. The only evidence for D₁ is documented from the Pan-African core rocks in the southern submassif and from Derbent area in central submassif. Although the Menderes Massif has experienced a complex pre-Alpine polyphase deformation, the details about the phases are still unknown. However, the available data suggest that the pre-Alpine development of the Menderes Massif includes a Pan-African orogeny and a Permo-Triassic Cimmerian event during the closure of Karakaya basin (e.g., Akkök 1983; Koralay *et al.* 2001, 2004; Candan *et al.* 2001, Satır and Friedrichsen 1986; Şengör *et al.* 1984; Bozkurt and Oberhänsli 2001 and references therein).

Table 1.4. Deformation in the Menderes Massif (Bozkurt and Oberhänsli 2001).

Deformation phase		Kinematics	Age
Pre-Alpine (D ₁)			?
Alpine	Contractional (D ₂)	Top-to-the-N–NNE	Eocene
	Extensional (D ₃)	Top-to-the-N–NNE in the northern submassif (Bivergent in the central submassif) (Top to the S–SSW in the southern submassif)	Early Miocene
Neotectonic (D ₄)		Approximately N–S extension	Pliocene or younger (~5 Ma onwards)

Alpine-Contractional (D₂)

The entire Menderes Massif was affected and gained its 'massif' character by a D₂ contractional deformation, which was synchronous with the main Menderes metamorphism and characterized by a penetrative S₂ regional foliation and approximately N–S-trending mineral lineation (L₂). This foliation has a dome-shaped pattern on the scale of the entire massif, whereas it defines two antiforms and a synform on the scale of central submassif. N- to NNE-vergent folds, deforming the S₂ regional foliation, at micro-, meso- and mapable-scales are the other common structural elements of this deformation (Bozkurt and Oberhänsli 2001 and references therein). Structural analysis of D₂ fabrics shows a top-to-the N-NNE shear sense suggesting N-directed thrusting (Bozkurt 1994, 1995, 2001a, 2004; Hetzel *et al.* 1998; Bozkurt and Park 1999; Bozkurt and Satır 2000; Arslan *et al.* 2002; Rimmelé *et al.* 2003a, 2003b). Therefore this deformation is thought to be the result of a northward backthrusting of Lycian Nappes and consequent internal imbrication of the Menderes Massif (Bozkurt and Park 1999; Rimmelé *et al.* 2003b).

Alpine-Extensional (D₃)

D₃ deformation is an extensional deformation that accompanied orogenic collapse; the collapse has resulted in the exhumation of the metamorphic rocks of the Menderes Massif along presently low-angle normal faults, attesting to the core-complex nature of the massif (e.g., Bozkurt and Park 1994, 1997a, 1997b, 2001; Bozkurt *et al.* 1995; Hetzel *et al.* 1995a, 1995b, 1998; Verge 1995; Hetzel and Reischmann 1996; Koçyiğit *et al.* 1999a; Bozkurt 2000, 2001a, 2001b, 2003, 2004; Bozkurt and Satır 2000; Bozkurt and Oberhänsli 2001; Gessner *et al.* 2001a, 2001b; Gökten *et al.* 2001; Işık and Tekeli 2001; Lips *et al.* 2001; Sözbilir 2001, 2002; Seyitoğlu *et al.* 2002; Whitney and Bozkurt 2002; Işık *et al.* 2003, 2004; Ring *et al.* 2003; Rimmelé *et al.* 2003a, 2003b; Bozkurt and Sözbilir 2004; Purvis and Robertson 2004; Westaway *et al.* 2004).

D₃ fabrics, which are formed during retrograde metamorphic evolution at greenschist-facies conditions, are characterized by an S₃ shear-band foliation,

strongly overprinting the S_2 regional foliation where the latter is preserved in microlithons. An approximately NNE–SSW-trending mineral-stretching lineation (L_3) is always associated with S_3 foliation. The rocks of Menderes Massif apparently show one lineation due to the close parallelism between L_2 and L_3 lineations (Bozkurt and Oberhänsli 2001 and references therein).

Structural analysis of D_3 fabrics shows that they are the result of bivergent NNE–SSW-directed extension. The present day subdivision of the Menderes Massif into southern, central and northern submassifs has important implications for the kinematics of D_3 deformation: (1) top-to-the-S–SSW fabrics in the southern submassif; (2) bivergent extension in the central submassif being top-to-the-N–NNE along the southern margin of the Gediz Graben in the north and top-to-the S–SSW along the northern margin of the Büyük Menderes Graben in the south; and (3) top-to-the-N–NNE fabrics in the northern submassif. This suggests that the Menderes Massif may be composed of at least three small core complexes. The evidence from the recent studies suggest that core-complex formation and thus D_3 extensional deformation started in the Early Miocene (e.g., Bozkurt and Park 1994, 1997a, 1997b, 2001; Bozkurt *et al.* 1995; Hetzel *et al.* 1995a, 1995b, 1998; Verge 1995; Hetzel and Reischmann 1996; Koçyiğit *et al.* 1999a; Bozkurt 2000, 2001a, 2001b, 2003, 2004; Bozkurt and Satır 2000; Bozkurt and Oberhänsli 2001; Gessner *et al.* 2001a, 2001b; Gökten *et al.* 2001; Işık and Tekeli 2001; Lips *et al.* 2001; Sözbilir 2001, 2002; Seyitoğlu *et al.* 2002; Whitney and Bozkurt 2002; Işık *et al.* 2003, 2004; Ring *et al.* 2003; Rimmelé *et al.* 2003a, 2003b; Bozkurt and Sözbilir 2004; Purvis *et al.* 2004).

Neotectonic (D_4)

The last deformation (D_4) that affected the Menderes Massif was high-angle normal faulting and consequent graben formation; the massif is dissected into northern, central and southern submassifs, with the Gediz and Büyük Menderes grabens taken as dividing lines (Figure 1.5; Bozkurt and Oberhänsli 2001).

Although their age is still controversial, the grabens are relatively younger features due to the fact that the high-angle normal faults cut and displace the low-angle normal faults. Along the graben-margin-bounding normal faults, the metamorphic rocks in the footwall are dissected and elevated (Bozkurt and Sözbilir 2004 and references therein).

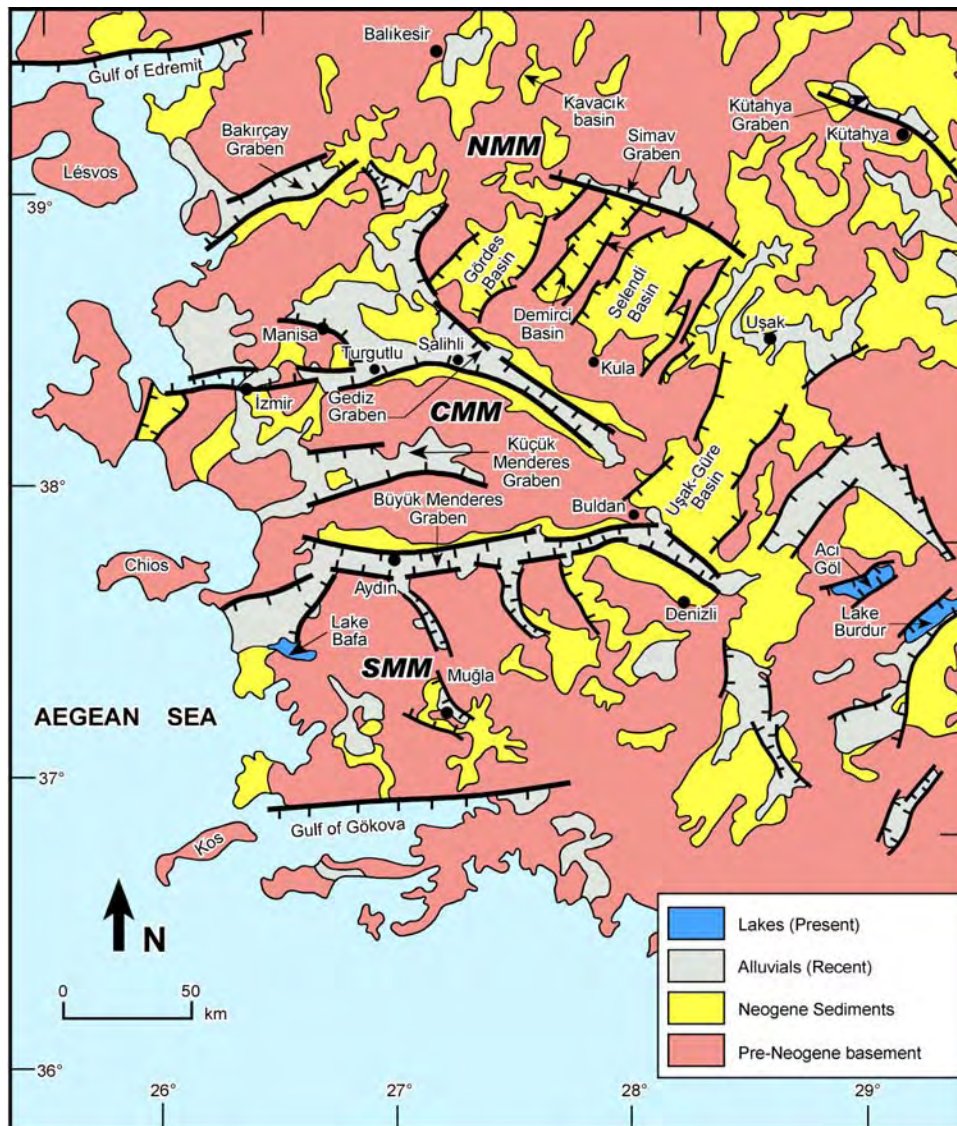


Figure 1.5. Simplified map showing major structural elements of western Anatolia and the subdivision of the Menderes Massif after neotectonic (D_4) deformation (from Bozkurt and Sözbilir 2004). CMM – central Menderes Massif, NMM – northern Menderes Massif, SMM – southern Menderes Massif.

1.5.2. Current Problems

Although western Turkey has been the subject of intense research including the tectono-metamorphic evolution and exhumation of the Menderes Massif, graben formation and basin evolution, there are still many contentious issues that concern:

(1) *age of the orthogneisses (core augen gneisses) and the nature of their contact relations with structurally overlying metasediments*: While some considers that the protolith of the augen gneisses intruded as granitoids into the metasediments during the Tertiary time (Bozkurt *et al.* 1992, 1993, 1995; Erdoğan 1992, 1993; Mittwede *et al.* 1995a, 1995b, 1997; Bozkurt and Park 1994, 1997a, 1997b, 2001; Erdoğan and Güngör 2004), others refute the cross-cutting relationships (except for the area along the eastern shore of Lake Bafa) and suggest that the granitic protolith intruded during Late Precambrian and Early Cambrian times (c. 521 and 572 Ma, averaging 550 Ma; U-Pb and Pb-Pb single zircon evaporation and SIMS methods) (e.g., Hetzel and Reischmann 1996; Dannat 1997; Loos and Reischmann 1999; Gessner *et al.* 2001a, 2004; Koralay *et al.* 2004). The conclusion that the granitic protolith for the augen gneisses was intruded during the Tertiary time is supported by: (i) intrusive relations between the 'core' rocks and the structurally overlying 'cover' schists, and (ii) the presence of weak contact metamorphism in the schists (Erdoğan 1992, 1993; Bozkurt 1996; Mittwede *et al.* 1995a, 1995b; Erdoğan and Güngör 2004). On the other hand, the documented intrusive contacts between the augen gneisses and the structurally overlying 'cover' metasediments are inferred to indicate the presence of Precambrian schists in the 'cover' rocks (Hetzel and Reischmann 1996; Loos and Reischmann 1999; Gessner *et al.* 2004). In a similar way, the available zircon ages (2555–521 Ma) are interpreted as representing a fragment of Pan-African basement in the Menderes Massif (Şengör *et al.* 1984; Satir and Friedrichsen 1986; Hetzel and Reischmann 1996; Loos and Reischmann 1999; Ring *et al.* 1999; Gessner *et al.* 2001a, 2004).

As is seen from the above discussion, there is an apparent conflict between the field relations and geochronological data. There are three attempts to address this conflict: (1) wide scatter of ages represents inherited zircon from

variety of sources (Bozkurt *et al.* 1995); (2) if the Precambrian zircon ages are correct, the Menderes Massif can be interpreted as “*mantle gneiss dome*” where the so-called Pan-African basement remobilized during the climax of main Menderes metamorphism (Bozkurt and Park 1997b); (3) there is evidence for the existence of more than one type of granitoid rocks in the so-called ‘*core*’ rocks; one being the younger, possibly Tertiary, leucocratic metagranite whereas the other being the orthogneisses (augen gneisses). The former is intrusive into both the orthogneisses and metasediments and occur all along the orthogneisses–schist contact in the southern Menderes Massif. In this view, the leucogranites are emplaced as sheet-like bodies into country rocks in the footwall of a ductile extensional shear zone, located between orthogneisses and metasediments, during Late Oligocene–Early Miocene time (Bozkurt 2004).

In a similar way, the contact relationship between the orthogneisses and the structurally overlying schists – so-called ‘*core-cover*’ contact – has been the subject of major debate among geoscientists. The proposed models fall into three categories: (1) the contact is a major unconformity (Schuiling 1962; Başarır 1970, 1975; Çağlayan *et al.* 1980; Öztürk and Koçyiğit 1983; Şengör *et al.* 1984; Konak 1985; Satır and Friedrichsen 1986; Konak *et al.* 1987); (2) there is no unconformity but the contact is essentially intrusive (Erdoğan 1992, 1993; Bozkurt *et al.* 1992, 1993, 1995; Erdoğan and Güngör 2004) and later being used as a major extensional shear zone (Bozkurt and Park 1994, 1997a, 1997b, 1999, 2001; Bozkurt *et al.* 1995); (3) the contact is a major top-to-the-S–SSW structural discontinuity. But the nature of the shear zone is also debated: a compressional shear zone (Ring *et al.* 1999; Gessner *et al.* 2001a, 2001b, 2001c, 2004; Régnier *et al.* 2003) or an extensional shear zone (Bozkurt 1994, 2004; Bozkurt and Park 1994, 1997a, 1997b, 1999, 2001; Bozkurt *et al.* 1993, 1995; Hetzel and Reischmann 1996; Bozkurt and Satır 2000; Lips *et al.* 2001; Whitney and Bozkurt 2002; Rimmelé *et al.* 2003b).

(2) *The origin of presently low-angle normal faults of the Menderes core complex*: while some authors infer that the breakaway faults initiate as low-angle structures (~30°: Hetzel *et al.* 1995a; Sözbilir and Emre 1996) others document evidence for original high-angle normal faults (48–53°) that were back-rotated to lower angles during the course of continental extension (Bozkurt

2000, 2001a, 2003; Bozkurt and Sözbilir 2004). Similarly, rolling-hinge model of Buck (1988) was also proposed for the evolution of the central Menderes Massif (Gessner *et al.* 2001a; Seyitoğlu *et al.* 2002).

(3) *The origin and timing of the continental extension*: the cause of N–S extension in western Turkey has been the subject of considerable debate and the proposed theories fall into four distinct groups: (i) *Tectonic escape model* – The Anatolian block began to extrude westward with the initiation of dextral motion along the North Anatolian Fault System commenced by late Serravalian (~12 Ma; Dewey and Şengör 1979; Şengör 1979, 1982, 1987; Şengör *et al.* 1985; Görür *et al.* 1995); (ii) *orogenic collapse model* – the start of extension is much earlier, (~18 Ma: Early–Middle Miocene) and is attributed to spreading and thinning of overthickened crust following the latest Palaeogene collision across Neotethys (Dewey 1988; Seyitoğlu and Scott 1991, 1992a, 1992b; Seyitoğlu *et al.* 1992); (iii) *Back-arc spreading model* – inception of subduction rollback process and consequent southwestward migration of the Aegean Arc caused the extension in back-arc area. But there is no consensus over the inception of rollback process where proposed ages range from 60 Ma and 5 Ma (McKenzie 1978a, 1978b; Le Pichon and Angelier 1979, 1981; Jackson and McKenzie 1988; Kissel and Laj 1988; Meulenkamp *et al.* 1988, 1994; Thomson *et al.* 1998); (iv) *episodic, two-stage graben model* – crustal extension in western Turkey is expressed by two distinct phases of extension being separated by a short-time interval of N–S crustal shortening during the late Serravalian–late Early Pliocene times (Koçyiğit *et al.* 1999a). The model favours the combined effect of two or more of the above mechanisms where an earlier phase of core complex formation during the Early–Middle Miocene orogenic collapse was superimposed by the modern phase of Plio-Quaternary extension commenced due to the westward escape of the Anatolian block (Koçyiğit *et al.* 1999a, 2000; Bozkurt 2000, 2001a, 2001b, 2002, 2003; Yılmaz *et al.* 2000; Cihan *et al.* 2003; Koçyiğit and Özacar 2003; Bozkurt and Sözbilir 2004) along with the initiation of the North Anatolian Fault System (~5 Ma: Barka and Kadinsky-Cade 1988; Westaway 1994a or ~7 Ma: Gautier *et al.* 1999; Westaway 2003).

Recent structural and isotopic evidence from extension related metamorphism and magmatism in western Turkey (Kazdağ Massif: Okay and Satır 2000) and in the Aegean islands (e.g., Avigad *et al.* 1997; Jolivet *et al.* 1998 and references therein) suggest that the Miocene extension in the Aegean was primarily related to the back-arc spreading due to the rollback of the Aegean-Cyprean subduction zone.

Also, it is now accepted that the continental extension in western Turkey is expressed by two distinct structural styles: (i) latest Oligocene–Early Miocene rapid exhumation of metamorphic core complexes in the footwall of presently low-angle ductile-brittle normal faults (detachment faults) (Bozkurt and Park 1994, 1997a, 1997b; Hetzel *et al.* 1995a, 1995b, 1998; Verge 1995; Emre 1996; Hetzel and Reischmann 1996; Emre and Sözbilir 1997; Koçyiğit *et al.* 1999a; Bozkurt 2000, 2001a, 2001b, 2004; Bozkurt and Satır 2000; Okay and Satır 2000; Bozkurt and Oberhänsli 2001; Gessner *et al.* 2001a, 2001b; Gökten *et al.* 2001; Işık and Tekeli 2001; Lips *et al.* 2001; Sözbilir 2001, 2002; Işık *et al.* 2003, 2004; Özer and Sözbilir 2003; Ring *et al.* 2003; Rimmelé *et al.* 2003b; Bozkurt and Sözbilir 2004) related to orogenic collapse and/or back-arc extension, and; (ii) late stretching of crust and consequent Plio-Quaternary E–W graben formation along high-angle normal faults (modern phase of extension) (e.g., Koçyiğit *et al.* 1999a, 1999b, 2000; Bozkurt 2000, 2001a, 2001b, 2002, 2003, 2004; Sarıca 2000; Seyitoğlu *et al.* 2000, 2002; Yılmaz *et al.* 2000; Genç *et al.* 2001; A. Gürer *et al.* 2002; F. Gürer *et al.* 2001; F. Gürer and Yılmaz 2002; Yılmaz and Karacık 2001; Sözbilir 2001, 2002; Altunel *et al.* 2003; Koçyiğit and Özacar 2003; Cihan *et al.* 2003; Özer and Sözbilir 2003; Bozkurt and Sözbilir 2004; Purvis and Robertson 2004; Westaway *et al.* 2004). There is, however, no consensus over whether the two distinct styles of extension (core-complex and rift modes) represent a single continuous extensional tectonic regime from latest Oligocene–Early Miocene to present times, or they represent two different events, separated by a hiatus.

(4) *The rates of crustal deformation:* The rate of extension in the Aegean is also controversial where proposals range between $> 60 \text{ mm a}^{-1}$ (maybe as high as 110 mm a^{-1} ; Jackson and McKenzie 1988) and $\sim 3\text{--}4 \text{ mm a}^{-1}$ (e.g.

Westaway 1994a, 1994b; Le Pichon *et al.* 1995; Straub *et al.* 1997; Reilinger *et al.* 1997; Kahle *et al.* 2000; McClusky *et al.* 2000; Lenk *et al.* 2003).

1.6. Previous Studies: the Gördes Region

Approximately E–W-trending grabens (e.g., Edremit, Bakırçay, Kütahya, Simav, Gediz, Küçük Menderes, Büyük Menderes, and Gökova grabens) and their basin-bounding active high-angle normal faults are the most prominent neotectonic features of western Anatolia (e.g. Bozkurt 2001a, 2001b, 2003 and references therein). However, in addition to these dominantly E–W-trending grabens, there are also less prominent NNE-trending basins, such as Gördes, Demirci, Selendi, and Uşak-Güre basins, located in the northern submassif to the north of the Gediz Graben (Figures 1.5 and 1.6).

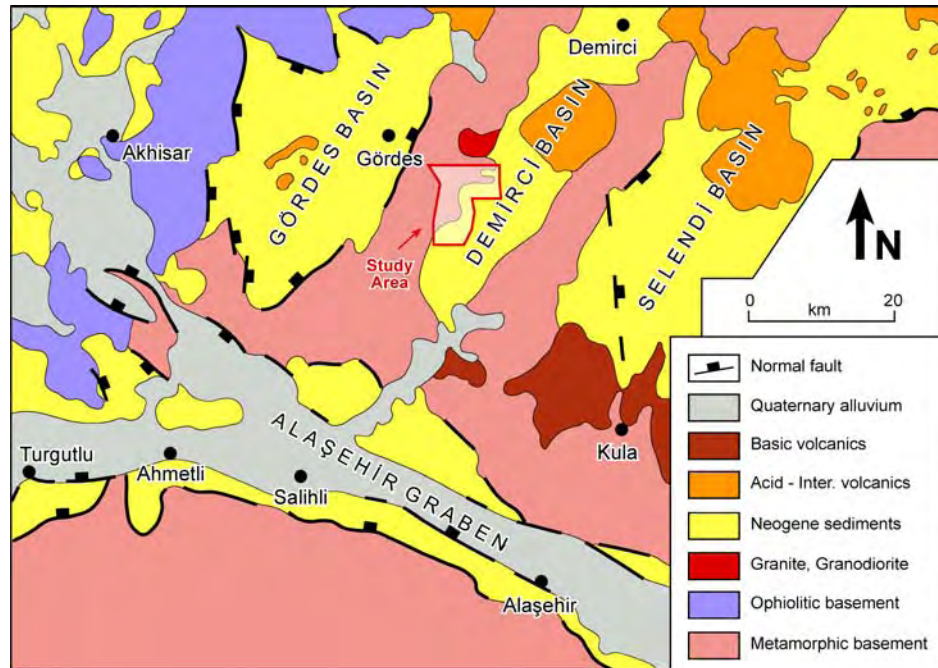


Figure 1.6. General location map of the NNE-trending basins (Gördes, Demirci, and Selendi basins) of western Anatolia (Seyitoğlu 1997).

Similar to the approximately E–W-trending grabens, relatively younger sedimentary basin fills unconformably overly the metamorphic rocks of the Menderes Massif in these NNE–SSW-trending basins. This is also the case on the area, constituting the horst between Gördes and Demirci basins, which is located on the south-east of Gördes town, where the field studies of this M.Sc. thesis were carried out.

In this region, following rock units form the main constituents: (1) metamorphic rocks of the Menderes Massif, namely, orthogneisses, schists with different mineral compositions, and migmatites; (2) pegmatoids in the form of domes and numerous tourmaline-rich dikes/veins or sills; (3) finally, very young granitic intrusions without any sign of deformation/metamorphism.

Being one of the most seismically active and rapidly extending regions in the world, western Anatolia has always attracted the attention of many geoscientists during the last three decades. The Menderes Massif – a large, crustal-scale metamorphic culmination – forms a perfect laboratory to study polydeformation, core complex formation and basin evolution. As extensional fabrics are superimposed on contractional fabrics, the Menderes Massif provides valuable information about core complex formation (Bozkurt 2001a; Bozkurt and Oberhänsli 2001 and references therein). Because of these reasons, western Anatolia including the Menderes Massif formed the subject of numerous intense research by both native and foreign scientists.

The very first workers who studied the geology of western Anatolia were Hamilton and Strickland (1841). Their study, entitled “*On the Geology of the Western parts of Asia Minor*” introduced the different rock units and documented valuable information about the geology of the area.

It was Philippson (1910-1915) who originally named the today’s Menderes Massif as “*Lydisch-Karische Massif*” and defined it as an old dome-like, central, mainly gneissic mass, broken by faulting during Alpine orogeny. The other names given to the Menderes Massif were “*Saruhan-Menteşe Massif*” (Akyol 1924 in Pamir and Erentöz 1974) and the “*West Anatolia Massif*” (Ketin 1966). The today’s commonly used term “*Menderes Massif*” was introduced into literature by Pamir (1928; in Pamir and Erentöz 1974).

The Menderes Massif has been the subject of many workers since the early 1900's, and it is still the apple of many active researchers' eyes. Similarly, the Gördes region in the northern Menderes Massif has also been studied by various geoscientists.

The first studies were carried out by geologists from the Mineral Research and Exploration Institute of Turkey (MTA). Canet and Jaoul (1946) gave general information about the geology of Manisa, Aydın, Kula and Gördes regions. Birand (1953) studied some minerals and rocks around Gördes. Bayramgil (1954) investigated the mineralogy of Gördes pegmatites whereas Egger (1960) studied the mica, feldspar and kyanite formations at Gördes pegmatite field. The information about the Neogene volcanism of the Gördes region was first given by Nebert (1961).

Ayan (1973) carried out a detailed study, for the first time, in the area at the east of Gördes. His study area includes the study area of this M.Sc. research and covers an area of about 330 km² to the east of the Gördes. Ayan prepared a detailed geological map of the area (Figure 1.7), investigated the geochemical characteristics of the magmatic rocks, particularly pegmatoids and discussed briefly the significance of migmatization and granitization events. He concluded that during the peak metamorphic conditions during Alpine deformation, migmatization took place and has resulted in the generation of granitic magma and their emplacement as domes of variable sizes.

Dağ (1989) carried out a Ph.D. study in this region and focused on the mineralogy and geochemistry of Gördes pegmatoids. Following this study, Dağ and Dora (1991) presented a major and trace element data on two different sets of pegmatoids (NE–SW- and E–W-trending) in the region, and discussed the importance of mineralogical and geochemical differences between the rocks of differently trending pegmatoid dykes/veins. They found out that the pegmatoids in Gördes area contain characteristically Na-feldspar, K-feldspar, quartz, muscovite, biotite, tourmaline and garnet as main mineralogical phases whereas E–W-trending dykes/veins contain beryl as rare constituent (Dağ and Dora 1986).

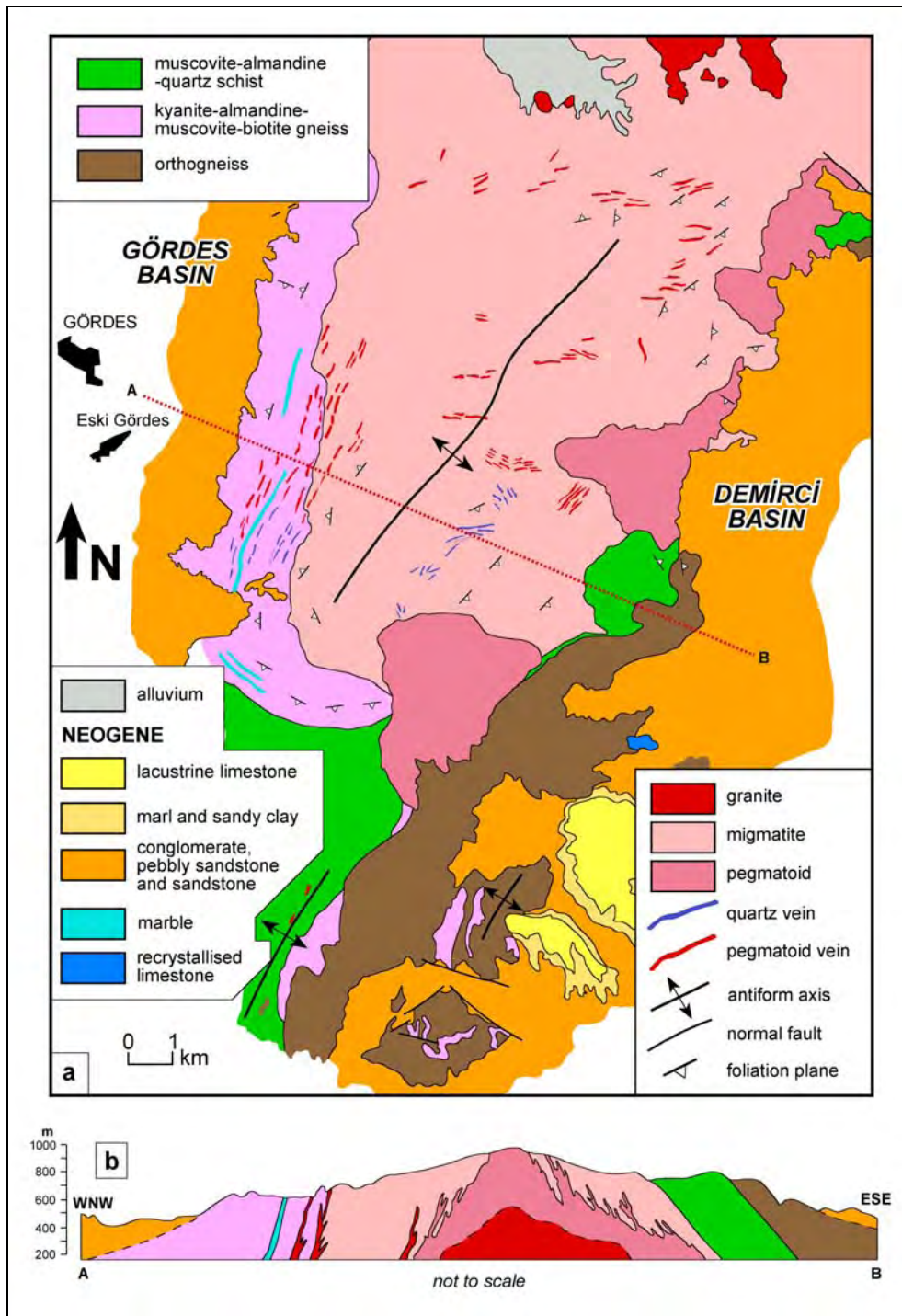


Figure 1.7. (a) Simplified geological map of the horst between Gördes and Demirci Basins and **(b)** cross-section along line A-B (Ayan 1973).

Candan (1989) also carried out a Ph.D. study on the petrography, petrology and mineralogy of the region located between Demirci and Borlu towns (Manisa). Later, Candan *et al.* (1990) studied the metamorphism and fission-track age determination of apatite crystals from Demirci-Borlu region. In this study, they concluded that the metamorphic basement in the Gördes submassif consists of the following lithologies in ascending order: sillimanite-garnet gneiss, sillimantine-garnet-kyanite schist, sillimantine-staurolite-garnet-kyanite schist, staurolite-garnet schist and garnet-mica schist. Kyanite-andalusite pegmatoids were formed in the course of the last major metamorphism giving the final stage to the Menderes Massif. The cooling ages of the apatite crystals are found to be ranging from Early Oligocene to Early Miocene.

The petrography and metamorphism of the metagabbros in the Demirci-Gördes submassif formed the subject of another study by Candan (1994). According to this latter study, the micaschists, gneissic levels, leucocratic metagranites, migmatites and acidic metavolcanics comprising the so-called core series are cut by stocks and sills of metagabbroic rocks. Although it was postulated that these metagabbros represent post-metamorphic Middle Miocene intrusions, more recent works favor for Precambrian/Cambrian igneous activity and HP metamorphism for the origin of metagabbros (Candan *et al.* 2001).

Esenli (1993a, 1993b) and Köktürk and Gümüş (1995) studied the Gördes zeolites. In these studies, the geochemical relations between chemical composition and quantity of zeolitization were examined; the data is consistent with the interpretation that all major elements were mobile. XRD and SEM analyses of volcanic and volcanoclastic rocks from Bigadiç and Gördes zeolite occurrences revealed the presence of erionite and mordenite.

The works by Seyitoğlu and Scott (1994a, 1994b) is rather concentrated on the tectonics and sedimentation of the Gördes Basin: the basin fill is represented by a 1000-m-thick Lower Miocene sedimentary succession comprising three units namely the Dağdere, Tepeköy and Kuşlukköy formations. The age of basin fill is constrained between 24.2 Ma and 16.3 Ma. The palaeocurrent directions from south to north demonstrate that the basin had a north-dipping basin floor.

One of the few structural studies on the northern Menderes Massif is carried out by Işık and Tekeli (2001), which focuses on the Simav region. During this study, they determined that late orogenic Tertiary extensional deformation is extended to the north of the Menderes Massif. The Simav metamorphic core complex of the northern Menderes Massif is unconformably overlain by a sedimentary succession older than ~15.5 Ma (Seyitoğlu 1997), which indicates that the exhumation of Simav metamorphic core complex and extension related deformation occurred before Early Miocene. They concluded that the extensional deformation in the Menderes Massif occurred at different time intervals in the southern, central and northern submassifs and the sense of shear shows opposite directions, and therefore the massif is represented by several core complexes formed at different times.

Işık *et al.* (2003) carried out a microstructural study on the northern submassif around Alaşehir and Simav detachment faults and concluded that these faults were produced by similar extensional processes. However, available radiometric age determinations along the two shear zones and thermochronological data led the authors to interpret that the Alaşehir detachment fault is younger than the Simav detachment fault and that they are the product of a multi-stage extensional process. They suggest that the Simav detachment fault represents an earlier stage of the Tertiary extensional tectonics of the Menderes Massif, while a later stage resulted in the development of the Alaşehir detachment fault.

The latest study of Işık *et al.* (2004) on the northern Menderes Massif focuses on the age determination of extensional ductile deformation and granitoid intrusion around Simav region. The timing of shear zone formation and the intrusion of syn-tectonic granitoids is constrained by $^{40}\text{Ar}/^{39}\text{Ar}$ geochronology on muscovite from mylonitic gneiss, and biotite from the Eğrigöz granitoid. The results indicate that mylonitic deformation occurred at 22.86 ± 0.47 Ma, whilst the cooling age of the granitoid is 20.19 ± 0.28 Ma. The intrusion and cooling of the Eğrigöz granitoid occurred between ~23–20 Ma. These data demonstrate that extensional deformation in the northern Menderes core complex began before Early Miocene times and represents an early stage in the Tertiary extensional tectonics of western Turkey.

Ring *et al.* (2003) studied cooling patterns and their relation to extensional faults in the Anatolide belt of western Turkey and concluded that the inferred cooling histories show a remarkably symmetric pattern across the Anatolide belt and progressed in two stages from the outer submassifs (Gördes and Çine submassifs) towards the centre of the belt, where extension is today focused. A hypothesis has been put forward, which explains cooling in these two submassifs as a consequence of Late Oligocene to Early Miocene normal faulting and thinning of a crustal-scale hanging wall consisting of the Cycladic blueschist unit, the Lycian nappes and the İzmir–Ankara zone.

The latest study on Gördes area is carried out by Bozkurt (2003) who discussed the origin of the NE-trending basins and their relation to the E–W-trending grabens in western Turkey. The stratigraphical and structural aspects of the basin fill in the E–W Gediz Graben and in the NE-trending Gördes, Demirci, Selendi and Uşak-Güre basins are reassessed there. According to this study, the Miocene configuration of different trending basins shows close similarities, and suggests that they started to develop simultaneously during the Early Miocene. Miocene sedimentation in these basins occurred in the hanging-wall of a presently low-angle, north-dipping, major normal fault (detachment fault) that bounds the Gediz Graben to the south, while the metamorphic rocks of the Menderes Massif in the footwall were progressively deformed, uplifted and exhumed. The Miocene sediments in the NE-trending basins were also deformed along broad folds with axes parallel to the basin margins. In conclusion, this paper favors a model with "*rotational accommodation faults*" at high-angle to the breakaway fault responsible of the exhumation of the Menderes Massif (initiated during Early Miocene), followed by a neotectonic extension (Pliocene) responsible of the present-day E–W grabens.

The studies carried out in the Gördes region up to now are mainly focused on the general geology of the area and on the geochemistry of some specific metamorphic and/or magmatic rock units. Some are about the geology of sedimentary fill of the Neogene basins and their tectonics. However, research on (1) the structure (deformational history) of various metamorphic and magmatic rocks and their boundary relationships; (2) the origin and evolution of migmatites and emplacement of dikes/veins and domes of pegmatoids; and (3)

the mutual relationship between migmatization/plutonism and extensional exhumation of the metamorphics is rather scarce in the Gördes area. In this regard, the present research on the structure, metamorphism and magmatism in the northern Menderes Massif fills an important gap in the literature. Although similar studies are common in central and southern submassifs of the Menderes Massif, there is almost, except for these studies concentrated on the exhumation of metamorphic rocks exposed around the Simav Graben (Işık and Tekeli 2001; Işık *et al.* 2003, 2004) no studies in the northern submassif.

As mentioned earlier, one of the main targets of this M.Sc. study is to understand the relationship between the various rocks units of Menderes Massif exposed in the study area and to discuss the geologic importance of them. While doing this, answers to problems such as the relationship between migmatitization, formation of pegmatoid domes and granite magmatism would also be discussed.

CHAPTER 2

STRATIGRAPHY

2.1. Introduction

In this chapter, the general stratigraphy of the rock units exposed on the southwest of Gördes is described. The two main purposes of this chapter are: (1) to describe the various lithologic units cropping out within the study area and its near vicinity, and (2) to identify the boundary relationships between these units. A brief review of the available literature is combined with the field observations where necessary.

As mentioned in the previous chapter, this M.Sc. study is focused on the horst between Gördes and Demirci basins, where the metamorphic rocks of the northern Menderes Massif are exposed and unconformably overlain by Neogene sedimentary basin fills at some locations. The horst is bounded by oblique-slip normal faults comprising the eastern boundary of the Gördes Basin on the west. The contact with the Demirci Basin on the east is marked by a series of steep, discontinuous en échelon oblique-slip normal faults (e.g., Yılmaz *et al.* 2000; Bozkurt 2003 and references therein). The nature of the contact relations will be discussed later in the chapter.

The rock units exposed in the study area are grouped into four categories: (1) the metamorphic rocks, including orthogneisses and metasediments comprising the northern Menderes Massif, (2) pegmatoids, (3) Neogene sedimentary rocks, and (4) Quaternary alluvial sediments (Figures 2.1 and 2.2). The characteristics of each unit will be described below in details.

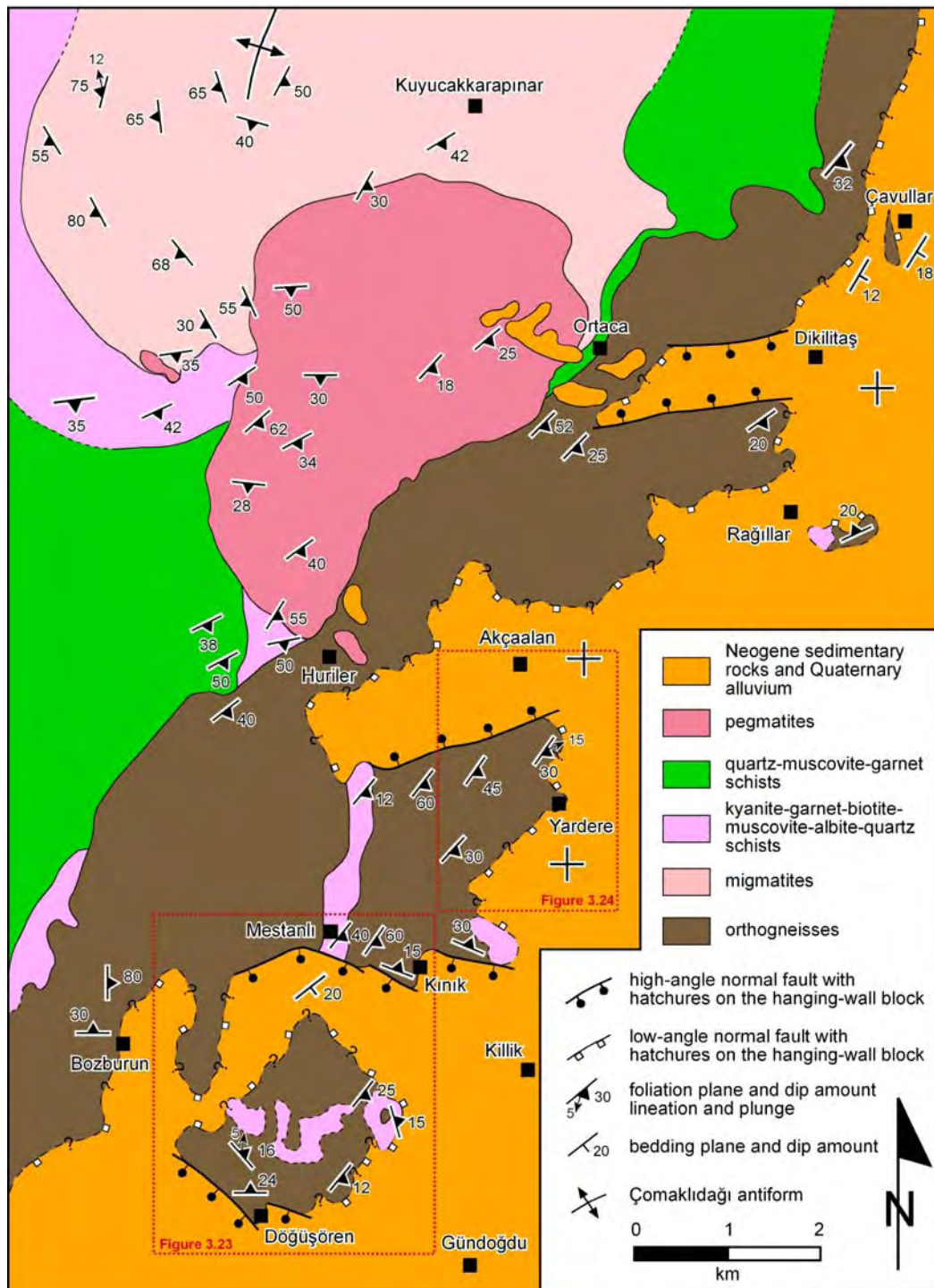


Figure 2.1. Geological map of the study area. See Figure 1.6 for location.

Age	Formation	Lithology	Description
Quat.			alluvial sediments
Late Mio.-Pliocene	Adala		lacustrine limestone
Early - Middle Miocene	Köprübaşı		marl and sandy claystone
			conglomerate, pebbly sandstone and siltstone
Eocene (?) - Miocene (?)	Menderes Massif		quartz-muscovite-garnet schists
			kyanite-garnet-biotite-muscovite-albite-quartz schists
			migmatites
			orthogneisses
Late Precambrian - Early Cambrian			orthogneisses
			pegmatites
			"core rocks"
			Metasedimentary "cover" rocks
			Neogene sedimentary rocks

Figure 2.2. Generalized columnar section of the study area.

2.2. Metamorphic Rocks

The metamorphic rocks of the northern Menderes Massif present in the study area can be categorized into two different units: (1) metagranite now in the form orthogneiss, conventionally known as augen gneiss, and (2) the metasedimentary rocks (migmatites, kyanite-garnet-biotite-muscovite-albite-quartz schists, and quartz-muscovite-garnet schists).

2.2.1. Orthogneisses

The orthogneisses, traditionally known as augen gneisses, occur in an about 1 to 4 km wide, more than 15-km-long, approximately NE–SW-trending belt in the study area; small isolated exposures cropping out beneath the Neogene sedimentary rocks are also common (Figure 2.1). The outcrops of orthogneisses are well-exposed in many localities in the study area such as west–southwest of Çavullar village, west of Yardere village, on the area between Mestanlı and Kınık villages, and north of Döğüşören village. In these localities, the contact with the metasediments is not well-exposed because of the dense vegetation cover and poor conditions of outcrops; so that it is difficult to comment on the nature of the contact. They are interpreted as deformed and dynamothermally metamorphosed granitoid in the southern and central parts of the Menderes Massif (e.g., Bozkurt *et al.* 1992, 1993, 1995; Erdoğan 1992, 1993; Bozkurt and Park 1994, 1997a, 1997b, 1999, 2001; Hetzel and Reischmann 1996; Hetzel *et al.* 1995a, 1995b, 1998; Bozkurt 1996, 2001b, 2004; Loss and Reischmann 1999; Bozkurt and Oberhänsli 2001; Gessner *et al.* 2001a, 2001b, 2004; Lips *et al.* 2001; Güngör and Erdoğan 2002; Özer and Sözbilir 2003; Erdoğan and Güngör 2004; Koralay *et al.* 2004). Similar rocks in the Gördes area is also named as “*banded gneisses*” (Ayan 1973).

The augen gneisses are usually white to dirty white or cream in colour; the colour becomes darker depending on the biotite content. The augen gneisses are variably mylonitic and display a well-developed SE-dipping, NNE–SSW-striking penetrative S_1 foliation, and a pronounced NNE–SSW-trending mineral

stretching lineation defined by preferred subparallel alignment of micas, stringers of quartz, the longest dimension of feldspar augen and tourmaline needles where present. They display a characteristic porphyroblastic texture, characterized by large megacrysts (porphyroclast or augen) of feldspars ranging from 1 or 2 cm to as much as 5 cm along their longest axes, within a more ductile fine- to medium-grained matrix of quartz, muscovite, biotite and K-feldspar which is deflected around the megacrysts (Figure 2.3a; see Chapter 3 for details). In almost all areas, mylonitic deformation is intense and has modified the feldspar porphyroclasts into asymmetric augen with recrystallized tails defining a typical stair-stepping geometry (Figure 2.3a). The size of augen/porphyroclasts is variable and becomes smaller with increasing deformation intensity (Figures 2.3b and 2.3c). Euhedral to subhedral black tourmaline is common locally and occur usually as disseminated needles being parallel/subparallel to the local mineral elongation lineation (Figure 2.4).

The orthogneisses contain many enclaves of metasediments, particularly biotite-albite-quartz schists, with variable sizes ranging from centimetres to metres; some are large enough to represent mappable units. Examples occur in areas to the east of Rağıllar, to the north of Döğüşören and to the east of Mestanlı (Figure 2.1). They usually form elongated bodies flattened in the plane of the foliation in the orthogneisses; their general trend is everywhere parallel to the local mineral stretching lineation. The foliation in the enclaves and orthogneisses are closely parallel each other. The only area, where the contact between the metasedimentary enclave and the orthogneisses is exposed well, occurs about 1 km east of Mestanlı village (Figure 2.5). The contact is rather sharp and represents an abrupt change in rock type. The exposures at topographically higher elevations to the north of Döğüşören occur as small isolated bodies on top of the orthogneisses, similar to roof pendants. The schist enclaves are rather darker because of their abundant biotite content.

Petrographically, the orthogneisses are mylonitic leucocratic coarse-grained granitoid rocks made up mainly of feldspar (both K-feldspar and plagioclase), quartz, biotite and muscovite with considerable amounts of tourmaline. Zircon, apatite and sphene form the common accessory minerals.

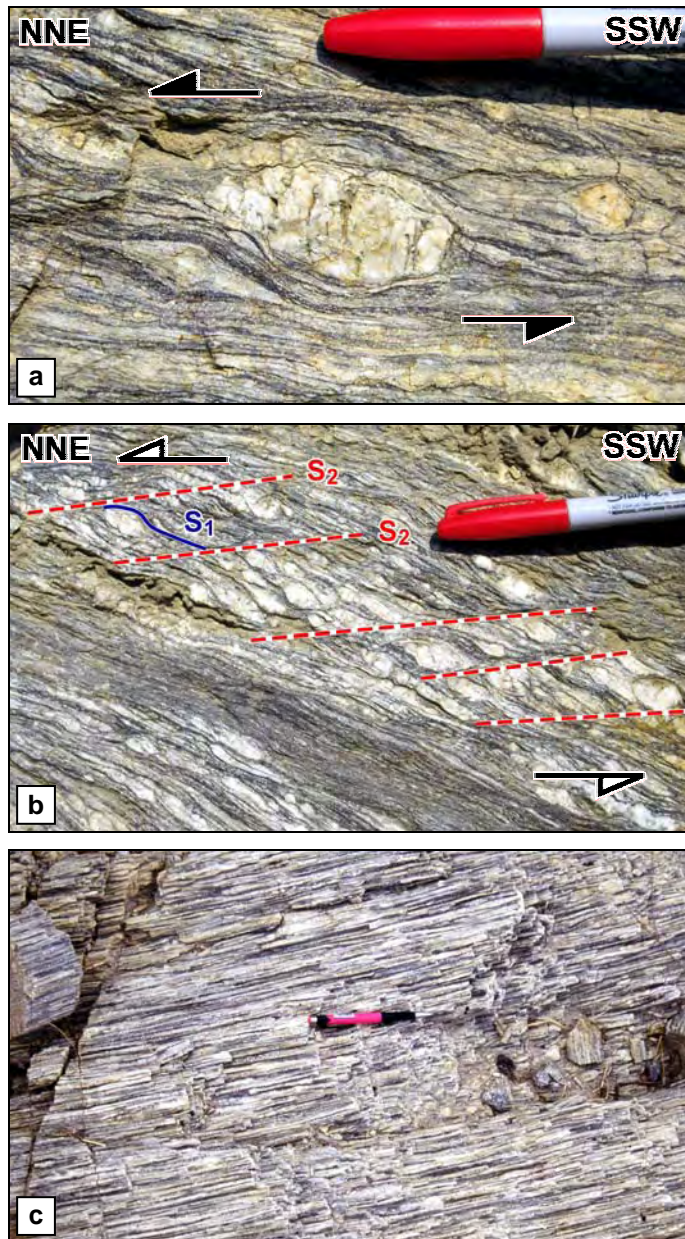


Figure 2.3. (a) A porphyroclastic texture defined by a large feldspar augen within a more ductile fine grained matrix deflected around it. The recrystallized tails define a typical σ -type porphyroclast where stair-stepping geometry defines a top-to-the-NNE deformation; (b) a relatively finer-grained texture in the orthogneisses suggesting a relatively intense deformation with respect to the example in (a). The σ -type asymmetry of feldspar porphyroclasts is consistent with a top-to-the-N-NNE deformation. The rock displays two distinct fabrics with a shear band foliation (S_2) and S_1 foliation preserved in the microlithons between adjacent shear-bands. The S_1 foliation defines an 'S' pattern where oblique-foliation curves into parallelism with S_2 foliation. The present configuration of S_2 indicates a top-to-the-N-NNE shear sense; (c) a typical ultramylonitic orthogneiss. The rock has suffered from intense deformation where the feldspars are all flattened and stretched in the plane of foliation; thus defining a texture similar to 'pencil' structure. The lineation is intense and well-pronounced. Please note that no asymmetric fabric/structure is preserved. Pencil is 15-cm long.

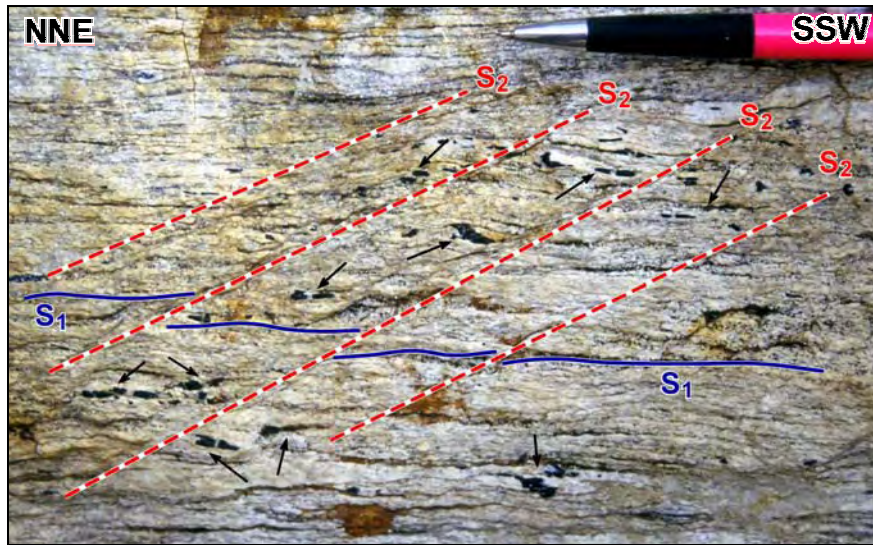


Figure 2.4. A field view from the orthogneisses displaying two distinct foliation with S_2 shear band foliation overprinting the early S_1 foliation. The geometry is consistent with top-to-the-NNE deformation. Please also note that tourmaline needles (arrowed) show close parallelism with the S_1 regional/main foliation in the rock. Part of the pencil on the figure is 10-cm long.



Figure 2.5. A view from the contact between the contact between kyanite-garnet-biotite-muscovite-albite-quartz schists (s) and orthogneisses (o). The contact shows close parallelism with foliation in both lithologies (E of Mestanlı). The hammer is 33-cm long.

They display a blastomylonitic texture with large "retort-shaped" feldspar megacrysts (porphyroclasts or augen) within a fine- to medium-grained matrix foliation of muscovite, biotite, plagioclase and K-feldspar (Figure 2.6a); the matrix foliation is seen to deflect around porphyroclasts (Figures 2.3a, 2.3b and 2.4).

Feldspars porphyroclasts are composed of K-feldspars and plagioclase grains, and usually occur as large anhedral to subhedral megacrysts with irregular grain boundaries. Feldspar megacrysts are commonly surrounded by dynamically recrystallized smaller feldspar grains, defining a typical '*core-and-mantle*' microstructure (Figures 2.6b, 2.6c). A "*core-and-mantle texture*" is used here as a purely descriptive term to describe the structure, especially common in highly deformed dynamically recrystallized rocks, in which large porphyroclasts of quartz or feldspar have abundant small sub-grains and new grains developed around their margin (Barker 1990, p. 139). The term "*porphyroclast*" is used in the sense of Passchier and Simpson (1986) who defined it as "relics of strong minerals derived from the parental rock (protolith) of the mylonite". The core feldspar grains are generally larger than the mantle and matrix grains. The widths of recrystallized mantles are very small relative to the core diameters, and the cores have highly serrated boundaries. Core grains show evidence for strained/undulatory extinction and, signs of brittle deformation with fractured and broken grains and plastic deformation with kinked grains (Figure 2.6c). K-feldspars (commonly orthoclase and occasionally microcline) are the commonest constituent and comprise the majority of the porphyroclasts in orthogneisses. Almost all K-feldspar grains are usually compact with no inclusions and show well-developed microperthitic texture and are rarely twinned on the polysynthetic law. Occasionally microclines occur as small "*patchy twinned*" crystals; they display albite-pericline twinning and "*quadrille structure*" characterized by two sets of lamellae at right angles. Myrmekitic intergrowth is ubiquitous at K-feldspar grain boundaries, particularly along the long sides of inequant grains, which faces finite-shortening direction being parallel to the S-foliation in the rock. Although it is not as common as K-feldspars, plagioclase also occurs as large porphyroclasts with

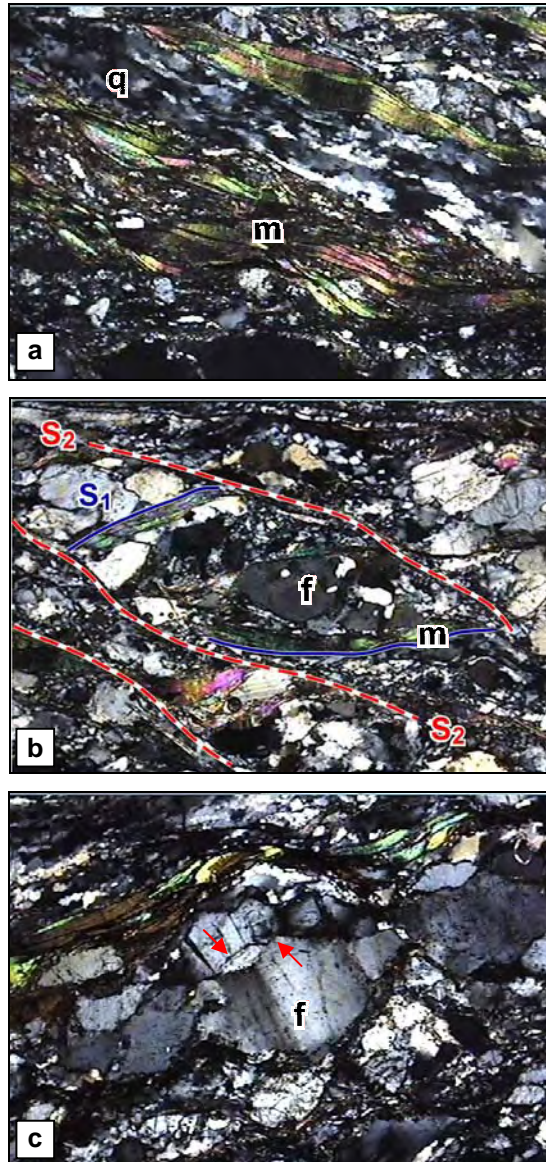


Figure 2.6. Photomicrographs of orthogneisses showing **(a)** compositional S_1 foliation defined by parallel alignment of biotite, muscovite and quartz minerals. The quartz grains in P-domain are elongated and display sutured grain boundaries. Most show undulatory extinction, showing continuum of deformation following their crystallization. The fabrics are consistent with deformational mechanisms of grain boundary migration and intracrystalline deformation. Note that long axes of mica laths (m) and elongate quartz-grains (q) define the main S_1 foliation in the sample. **(b)** Typical core-and-mantle structure defined by large feldspar cores surrounded by small subgrains and dynamically recrystallized new grains around their margins. Note that the sample display two sets of foliations with S_2 overprinting S_1 foliation. S_1 is defined by S-shaped mica laths (m) where as S_2 is marked by intense granulation and oxidation. **(c)** An elongated core feldspar grain (f) showing kinking surrounded by small recrystallized grains (core-and-mantle structure). The core grain is broken by microfractures (arrowed) along which dynamic recrystallization of quartz and feldspar has taken place. This suggests brittle-ductile conditions of deformation. The host feldspar grain is deformed by subgrain rotation as well. Fold of each view is 1.5 mm.

variable sizes usually smaller than that of K-feldspar grain in the same section. The majority of plagioclase twins obey the albite twin law and twinning on the combined Calsbad-albite laws is very rare. In some plagioclase grains, albite twinning is associated with pericline law twinning, suggesting a mechanical origin.

Quartz occurs as either large anhedral to subhedral porphyroclasts or elongated ribbons of newly dynamically recrystallized aggregates. The large grains/megacrysts define a typical “*core-and-mantle microstructure*” with brittlely deformed/broken core grains surrounded by subgrains and/or dynamically recrystallized smaller new grains. Evidence of strain is manifested by ubiquitous undulatory extinction in quartz. Myrmekitic intergrowth of quartz with plagioclase feldspar along the long sides of the K-feldspar megacrysts occurs characteristically in many of the thin-sections. Intense mylonitization of the rock is expressed by the common granulation and dynamic recrystallization of feldspars and quartz grains. Both feldspars and quartz also occur as small matrix grains.

Micas, both biotite and muscovite, occur as subidioblastic laths and show remarkable parallelism, defining the main foliation in almost all of the thin-sections (Figure 2.6a). Most are preserved in the matrix with their long axes and (001) surfaces aligned parallel to the foliation. The matrix grains display evidence for intense deformation with fine-grained material. Some micas occur as larger pre-tectonic porphyroclasts and show evidence of deformation in the form of fractured, broken and kinked grains aligned in a direction parallel to the S-surface but oblique to the C-planes, or aligned with their (001) surfaces parallel to the main foliation. Biotites are characterized by buff to dark brown pleochroism, oxidation, and complete replacement by Fe-oxide.

The augen gneisses contain abundant blue-black *tourmaline*, which is widely distributed but locally absent. The presence of black tourmaline indicates the importance of boron-rich fluids in the late stage crystallization of granitic protolith. Under the microscope, the high relief, slate blue colour and pleochroism, occasionally second order interference colours and zoning are very characteristic. It usually occurs as broken, anhedral grains.

Zircon is usually present as short prismatic crystals, often found as inclusions in biotites. *Apatite* is the commonest accessory mineral and is usually

found with, and surrounded, by biotite and, rarely, with tourmaline. It usually occurs as tabular crystals.

A minor proportion of the biotite is replaced by chlorite and iron-oxide whereas feldspars by sericite or kaolinite. Rarely, sphene is developed from biotite. Chlorite occurs as a minor alteration product of biotite and usually develops along the (001) cleavage.

During the last decade, the age and origin of the core augen gneisses and their contact relations with structurally overlying schists has been the subject of considerable debate. Most previous workers suggested a sedimentary protolith for augen gneisses (Schuiling 1962; Başarır 1970, 1975; Öztürk and Koçyiğit 1983; Şengör *et al.* 1984; Satır and Friedrichsen 1986). Satır and Friedrichsen (1986) suggested that the sedimentation of the protoliths of the augen gneisses began ~750 Ma ago based on a Rb/Sr whole rock isochron. Some early workers had also suggested a granitic protolith for augen gneisses (de Graciansky 1965; Konak 1985; Konak *et al.* 1987) and the later geochemical studies of Bozkurt *et al.* (1992, 1993, 1995) also showed out that the protoliths are granitoid rocks. Today it is commonly accepted that the protoliths of augen gneisses were calc-alkaline, peraluminous, S-type, late-to post-tectonic, tourmaline-bearing two-mica leucogranites (Bozkurt *et al.* 1995). There are two interpretations about the age of granitic protoliths: (1) The first considers that the protolith of the augen gneisses intruded as granitoids into the metasediments during the Tertiary time (Bozkurt *et al.* 1992, 1993, 1995; Erdoğan 1992, 1993; Mittwede *et al.* 1995a, 1995b, 1997; Bozkurt and Park 1994, 1997a, 1997b, 2001). Observation of intrusive contact relations between the 'core' rocks and the structurally overlying 'cover' schists, the presence of weak contact metamorphism in the 'cover' schists around Kayabükü (Bozkurt 1996) and Kargıcak (Mittwede *et al.* 1995a, 1997) villages and in the Mesozoic carbonates along the eastern shore of Lake Bafa (Erdoğan 1992, 1993; Erdoğan and Güngör 2004), and the age of the oldest unconformable sediments (21 ± 0.4 Ma; Becker-Platen *et al.* 1977) are the main supports for this interpretation. (2) The second interpretation, based on geochronological data (U-Pb and Pb-Pb single zircon evaporation methods), is that the granitic protolith intruded during Late Precambrian and Early Cambrian times (c. 521 and 572 Ma, averaging 550 Ma) (e.g., Hetzel and Reischmann 1996; Dannat 1997; Loos and

Reischmann 1999; Gessner *et al.* 2001a, 2004; Koralay *et al.* 2004). This idea refutes the cross-cutting relationships, except for the area along the eastern shore of Lake Bafa. It has been further suggested that the documented intrusive contacts indicate the presence of Precambrian metasediments in the 'cover' schists although no evidence was provided (Hetzl and Reischmann 1996). Wide-scatter of zircon U-Pb ages in the range of 2555–521 Ma suggest that the augen gneisses represent a fragment of Pan-African basement in the Menderes Massif (Şengör *et al.* 1984; Satir and Friedrichsen 1986; Hetzel and Reischmann 1996; Loos and Reischmann 1999; Ring *et al.* 1999; Gessner *et al.* 2001a, 2004; Koralay *et al.* 2004).

This apparent conflict between the field and geochronological data may be explained in two ways: (1) zircons are resistant minerals and could survive even high-grade metamorphism such that the wide scatter of ages would mean that the zircons were inherited from a variety of sources and therefore zircon ages not necessarily give correct intrusion ages (Bozkurt *et al.* 1995); (2) if the Precambrian zircon ages are correct, then the documented intrusive contacts would mean the remobilization of Pan-African basement during the climax of the Eocene the main Menderes metamorphism, and the granitic melt was then emplaced concordantly into the structurally overlying schists. Therefore, the Massif would be interpreted as a "mantle gneiss dome" (Bozkurt and Park 1997b). Following its remobilization, the granite was progressively uplifted – relative to the schists comprising the hanging-wall – along a major extensional shear zone and converted into mylonitic augen gneisses (Bozkurt and Park 1994, 1997a, 1997b).

However, the recent field studies in the southern Menderes Massif around Yatağan (Muğla) by Bozkurt (2004) shows that none of the above models address the apparent conflict satisfactorily as there is evidence for the existence of more than one type of granitoid rocks in the so-called 'core' of the southern Menderes Massif: one being the younger, possibly Tertiary, leucocratic metagranite whereas the other being the orthogneisses where the former is intrusive into the latter and the structurally overlying 'cover' schists.

Since the origin of the augen gneisses is controversial, the contact relationship between the augen gneisses and metasedimentary rocks (see below for details) is also controversial. The contact is considered as a major

unconformity by various authors who suggest a sedimentary protolith for augen gneisses (Schuiling 1962; Şengör *et al.* 1984; Satır and Friedrichsen 1986; Konak *et al.* 1987). A metaconglomerate cropping out locally at the base of the metasedimentary rocks and made of quartzite, granite and tourmalinite pebbles has been interpreted as a basal conglomerate, which supports the idea of an unconformity (Konak *et al.* 1987). Other authors claimed that the 'core–cover' contact is mainly intrusive and that the protoliths of the augen gneiss unit are younger granitoids (Cenozoic in age), this contact later being reactivated as a major shear zone (Bozkurt and Park 1994, 1997a; Bozkurt *et al.* 1995). Another interpretation is that the 'core–cover' contact is tectonic: it has been described as an Alpine extensional shear zone allowing exhumation of 'core' rocks during top-to-the-south shearing in the southern Menderes Massif and along the northern margin of the Büyük Menderes graben (Bozkurt and Park 1994, 1997a, 1997b, 1999, 2001; Hetzel and Reischmann 1996; Bozkurt and Satır 2000; Lips *et al.* 2001; Özer and Sözbilir 2003; Rimmelé *et al.* 2003a, 2003b; Bozkurt 2004) or as a thrust fault along which the schist sequence was emplaced on top of the augen gneiss unit, either during top-to-the-south Alpine nappe stacking resulting from the collision between Sakarya block and Menderes–Tauride platform (Ring *et al.* 1999, 2003; Gessner *et al.* 2001, 2004), either during top-to-the-north Alpine contractional deformation, later being reactivated during top-to-the-south Alpine extensional deformation (Bozkurt 2001b, 2004; Bozkurt and Oberhänsli 2001; Lips *et al.* 2001; Özer and Sözbilir 2003).

As mentioned previously, the contact between the orthogneisses and the metasediments is not well-exposed due to the dense vegetation cover and poor conditions of outcrops in the study area. The only area, where the contact is exposed well occurs about 1 km east of Mestanlı village (Figure 2.5). There, the metasedimentary rocks are present as an enclave within the orthogneisses, and the contact is rather sharp representing an abrupt change in rock type. From the structural point of view, the orthogneisses overlie the metasediments (see foliation pattern in Figure 2.1). This suggests that the orthogneisses are structurally above the metasediments and that the contact may represent a tectonic feature. The metamorphic grade in the augen gneisses is relatively higher than that of the schists below (see Chapter 4). This, in turn, indicates that

the contact, if tectonic, is a typical thrust/reverse fault which may be attributed to the internal imbrication and stacking of Menderes Massif during Eocene deformation (see Chapter 4). Unfortunately, the contact is not well-exposed. Where the contact is observed, it is difficult to test its nature as the evidence available is very limited.

2.2.2. Metasediments

The metasediments form the other rock association in the study area and comprises a conformable sequence of migmatites, kyanite-garnet-biotite-muscovite-albite-quartz schists and quartz-muscovite-garnet schists with intercalated marbles/recrystallized carbonates at different structural levels within the sequence. They are structurally overlain by the orthogneisses where the main foliation in both types of rocks shows remarkable parallelism. The sequence is deformed into a regional-scale, NE-trending antiformal structure with migmatites forming the core, so that the metamorphic grade diminishes from core towards the limbs (Figures 2.1 and 2.2).

2.2.2.1. Migmatites

Migmatites cover large areas on the northern parts of the study area; they comprise the structurally lowermost section of the metasediments and are in direct contact with pegmatoid dome (Figure 2.7a). The network of approximately E-W- and NE-trending tourmaline-rich pegmatoid and quartz dykes (sometimes sills) are common features observed in this lithology (Figure 2.8a). Both the migmatites and pegmatites are present as a dome shaped mixture, which is generated from partially molten and diapirically risen crust (see Chapter 4 for details).

Migmatites display, in general, conformable boundary relationships with the structurally overlying metasediments but cross-cutting relationships with the pegmatoids are evident (Figures 2.7 and 2.8). The unit is conformably overlain by

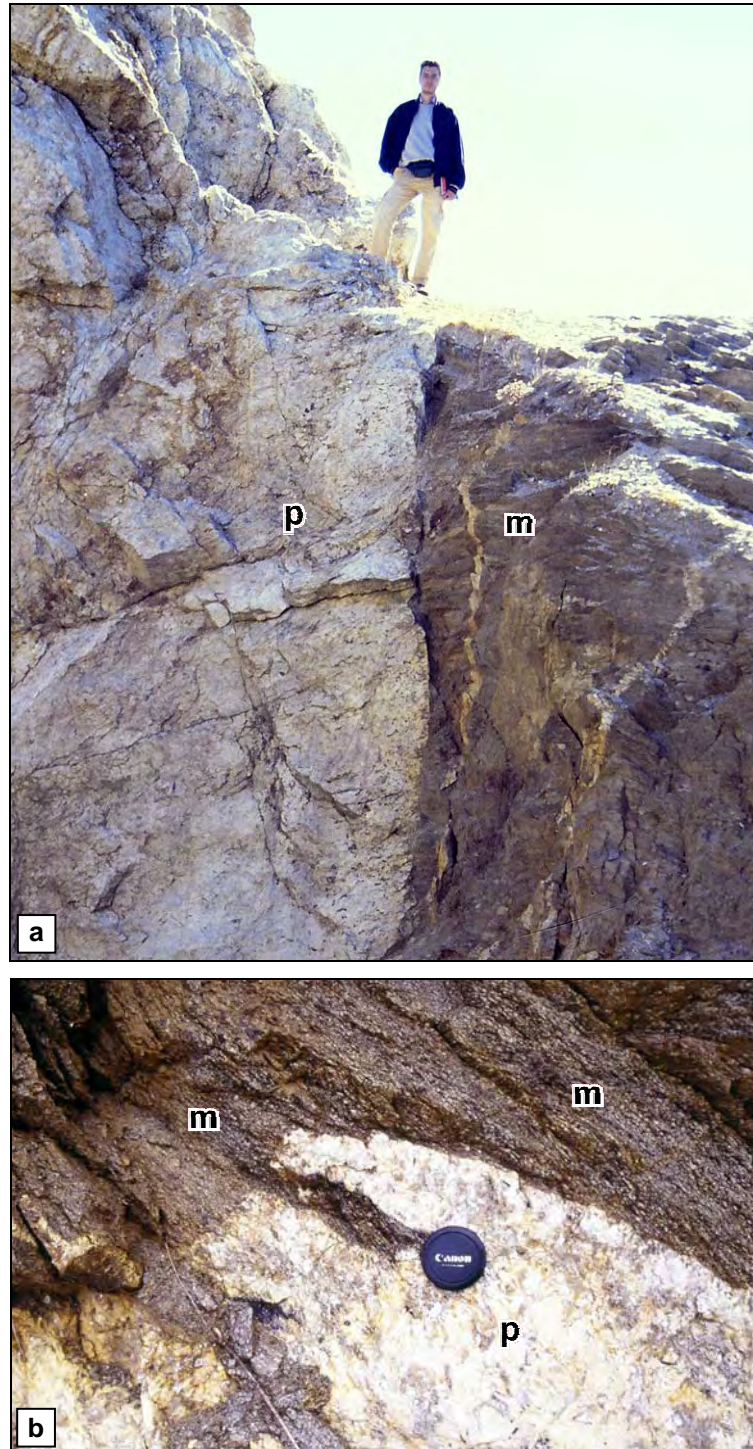


Figure 2.7. (a) Field view showing the direct contact of migmatites (m) with the pegmatoid dome (p). The pegmatoids has a sharp contact cutting the regional foliation of migmatites. Note thin pegmatite dikes cutting the main foliation in the migmatites. The dikes have a general trend being parallel to the contact. Scale is 175 cm high; **(b)** a close-up view the contact between pegmatoids (p) and migmatites (m). Camera lens cap has a diameter of 5 cm.

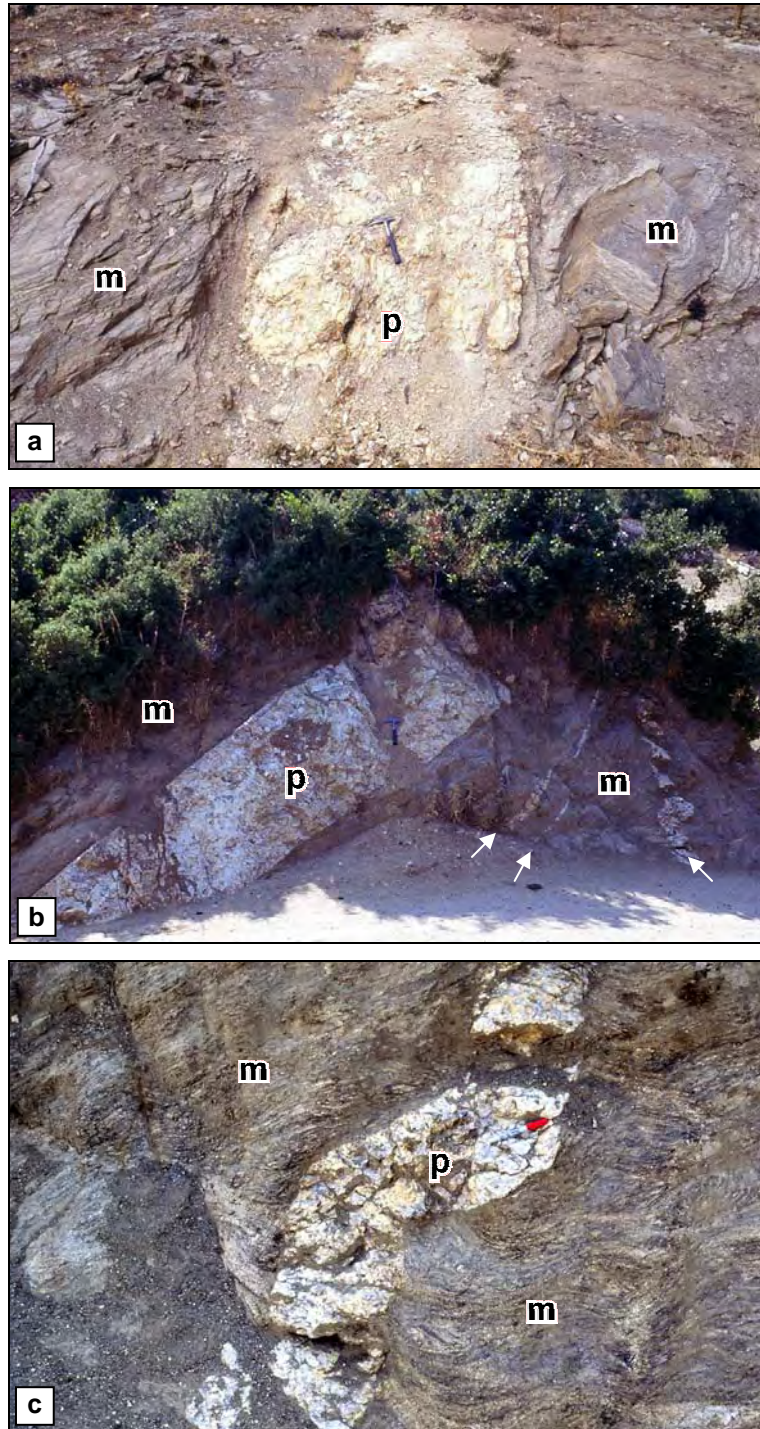


Figure 2.8. Different field views from pegmatites (p) intruding into the migmatites (m) discordantly **(a)** or concordantly **(b)** as dikes or both as dikes and sills **(c)**. Note that the primary foliation planes on migmatites do not continue in the pegmatites and there is a deflection on the foliation pattern near pegmatite contacts suggesting forcible emplacement. In (b) there are three more parallel thin dikes of pegmatites (arrowed). Hammer in (a) and (b) is 33-cm long, and pen in c is 15 cm long.

the kyanite-garnet-biotite-muscovite-albite-quartz schists in the west and quartz-muscovite-garnet schists in the east. The contact with the pegmatoid dome is well exposed at a number of localities where it is sharp, and the pegmatoids are intrusive into migmatites with nice cross-cutting relationships exposed locally (Figures 2.7 and 2.8). It is difficult to comment on the nature of contact relationships with the other lithologies of metasediments but it is interpreted as structurally conformable and gradational with respect to the metamorphic grade.

Here the term "*migmatite*" is used for a megascopically composite rock consisting of two or more petrographically different parts, one of which is the country rock generally in a more or less metamorphic stage, the other is of pegmatitic, aplitic, granitic or generally plutonic appearance (Mehnert 1968). According to Johannes (1983), the term "country rock" is not appropriate because the metamorphic portions of migmatites are not country rocks but original. Johannes (1983) defined the migmatites as composite rocks consisting partly of gneiss or schist and partly of portions having a plutonic appearance.

According to Mehnert (1968), migmatites can be divided into two main parts, the "palaesome" and "neosome" (Figure 2.9). The "palaesome" is described as the unaltered or only slightly altered parent rock of the migmatite and "neosome" as the newly formed part of a migmatite (Mehnert 1968). The neosome is divided into the dark "melanosome" containing mainly dark (mafic)

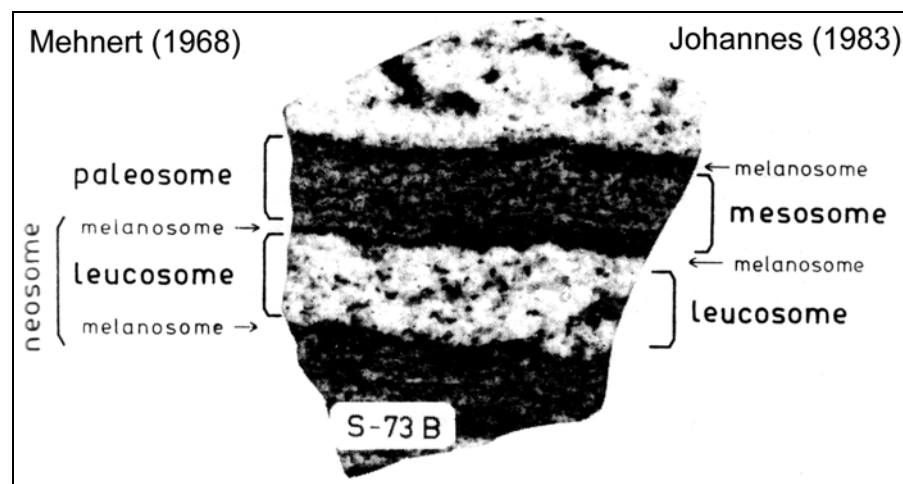


Figure 2.9. A hand specimen of migmatite showing nomenclature used by Mehnert 1968 and Johannes 1983 (from Johannes 1983).

minerals, such as biotite, hornblende, etc., and the light plutonic “leucosome” containing more light minerals (quartz and/or feldspar). Johannes (1983) propose the terms “mesosome”, instead of “palaeosome” of Mehnert, for the gneissic or schistose portions of a migmatite, and with Menhert, “leucosome” for the leucocratic plutonic part and “melanosome” for the dark selvage rich in mafic minerals.

The migmatites in the study area are typical stromatic migmatites, composed of leucocratic layers of dirty white coloured pegmatitic/magmatic appearance (leucosomes/neosome) and darker (dark green or locally light green) layers of gneisses (mesosome/palaeosome; Figure 2.10a). The leucosomes are entirely concordant with the main foliation in pelitic parts. The schistose portion (*melanosome* or *restite*) at the margins of the leucosomes are unusually dark in colour having been depleted in light coloured minerals during the processes of migmatization.

The rock displays a distinct pervasive foliation and an invariably associated strong lepidoblastic fabric due to the approximately parallel alignment of mica flakes. Locally, well-developed gneissose texture is also characteristic and is represented by the alternation of dark mica-rich and lighter quartz-rich bands on a scale of 2–3 millimetres to 1–2 centimetres (Figure 2.10a). The widespread occurrence of F_1 minor folds deforming the main foliation in the rocks is a common feature of the migmatites (Figure 2.10b, see Chapter 3 for details). The granitic layers are boudinaged locally and form isolated, asymmetric lenses within the pelitic parts of the migmatites (Figure 2.10c).

Petrographically, the schistose portion is made up mainly of plagioclase, quartz, orthoclase, biotite, and muscovite whereas zircon, apatite, and magnetite form accessory minerals (Figures 2.11a-b). At some horizons, they contain garnet and/or kyanite as porphyroblasts up to 0.5 cm in diameter within a fine-grained matrix of mica (mainly biotite and muscovite) and quartz (Figures 2.11c-f, 2.12a-b). *Garnets* are present as pre-tectonic crystals and they usually occur in association with biotites. Chloritization is extensive along fractures through garnet and in most cases the empty spaces are filled with quartz grains.

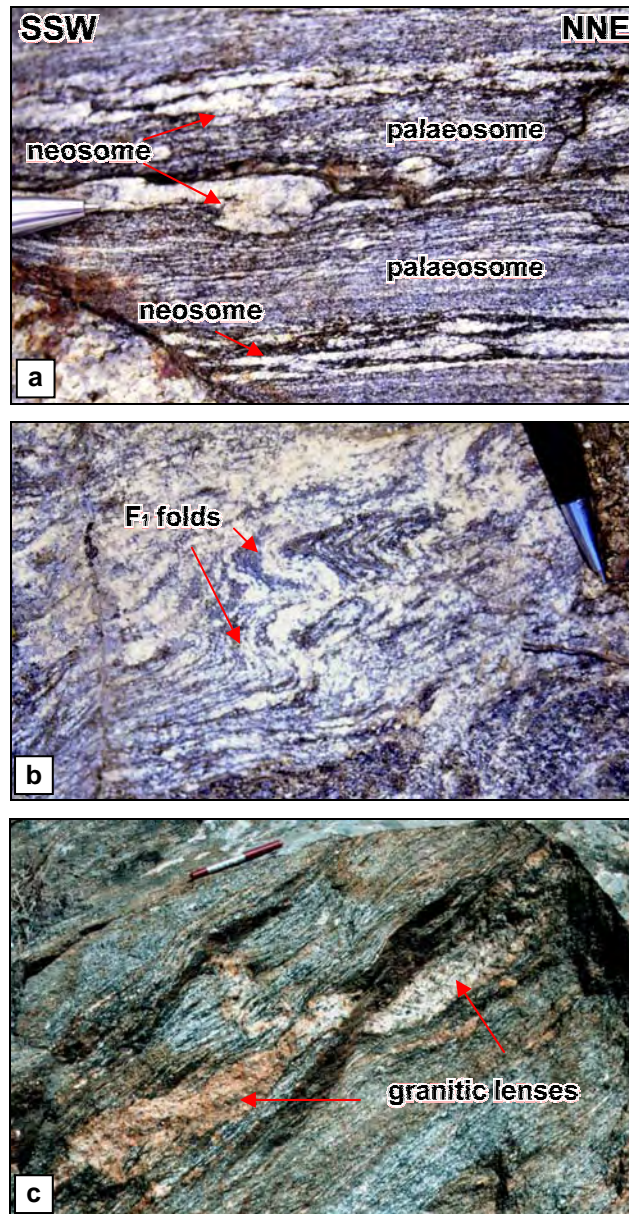


Figure 2.10. (a) Typical field view of migmatites with alternating dark (palaeosome) and light (neosome) layers (Tip of the pen is 2 cm). The leucocratic layer in the middle is deformed along an intrafolial asymmetric fold suggesting a top-to-the-NNE deformation. Please also note that a small granitic body on the lower left corner is intrusive into the migmatites with a sharp contact where regional S_1 foliation abruptly terminates against it. The granitic body is associated with a thin melanosome parallel to the contact, suggesting that this body is a part of migmatization and partial melting story of the migmatites. **(b)** F_1 minor folding developed on migmatites (Part of the pen is 5 cm long). The paleosome and leucosomes define the typical migmatitic texture where thickening in the fold hinges but thinning in the limbs are evident. **(c)** Isolated granitic lenses in the form of boudins within the migmatites (Pen is 14 cm long). Please note that the granitic lenses passes both concordant and discordant relations with the main foliation in the migmatites. The interfingering nature of the contact is suggestive of spatial and temporal relations between migmatization and granitic magma generation.

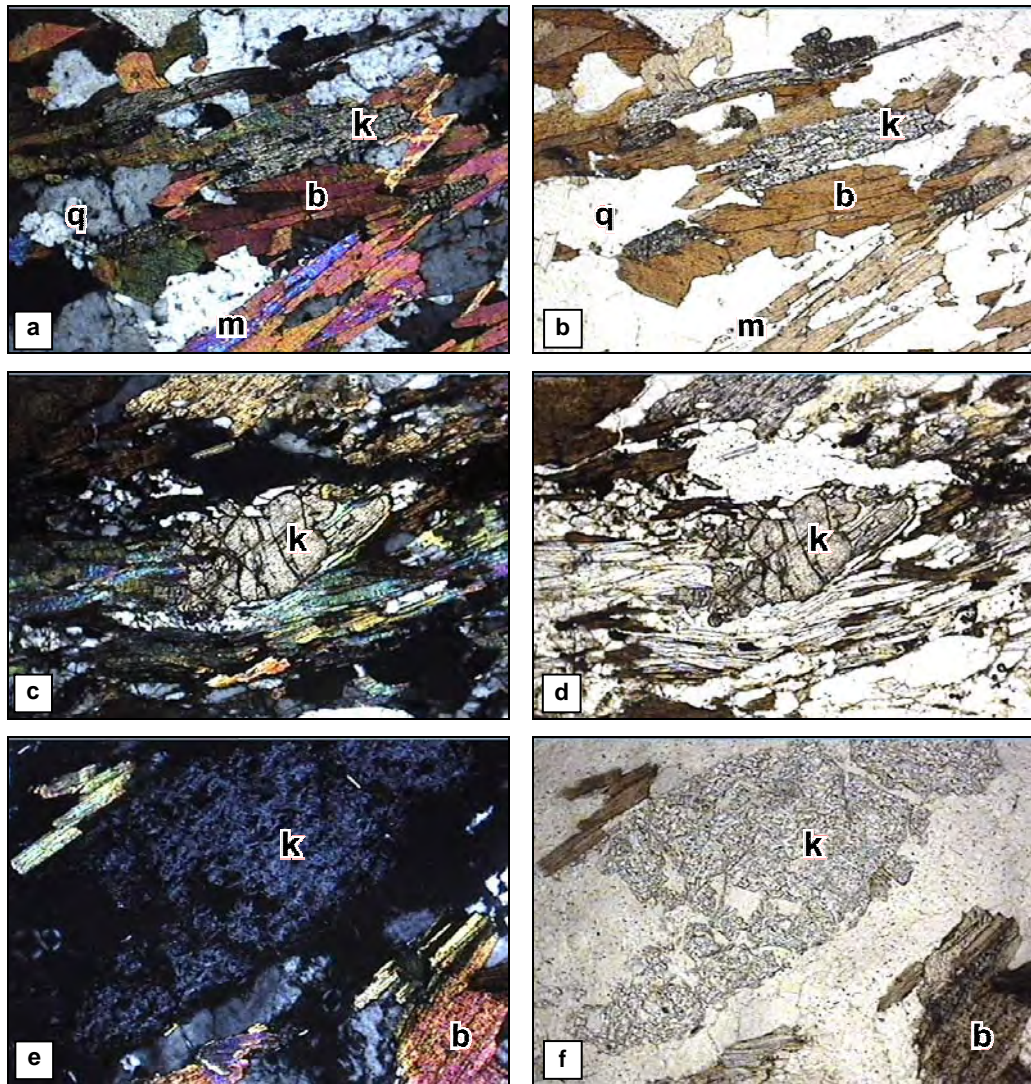


Figure 2.11. Photomicrographs from migmatites showing **(a)** alignment of biotites (b), muscovites (m), quartz (q) and kyanites (k) parallel to the main foliation (S_1), **(b)** is the same view of (a) under plane polarized light; **(c)** kyanite porphyroblast (k) within a fine-grained matrix of mica (mainly biotite and muscovite) and quartz; **(d)** is the same view of (c) under plane polarized light; **(e)** close-up of a sporadically occurring kyanite (k) surrounded by biotites (b); **(f)** is the same view of (e) under plane polarized light. Fold of each view is 1.5 mm.

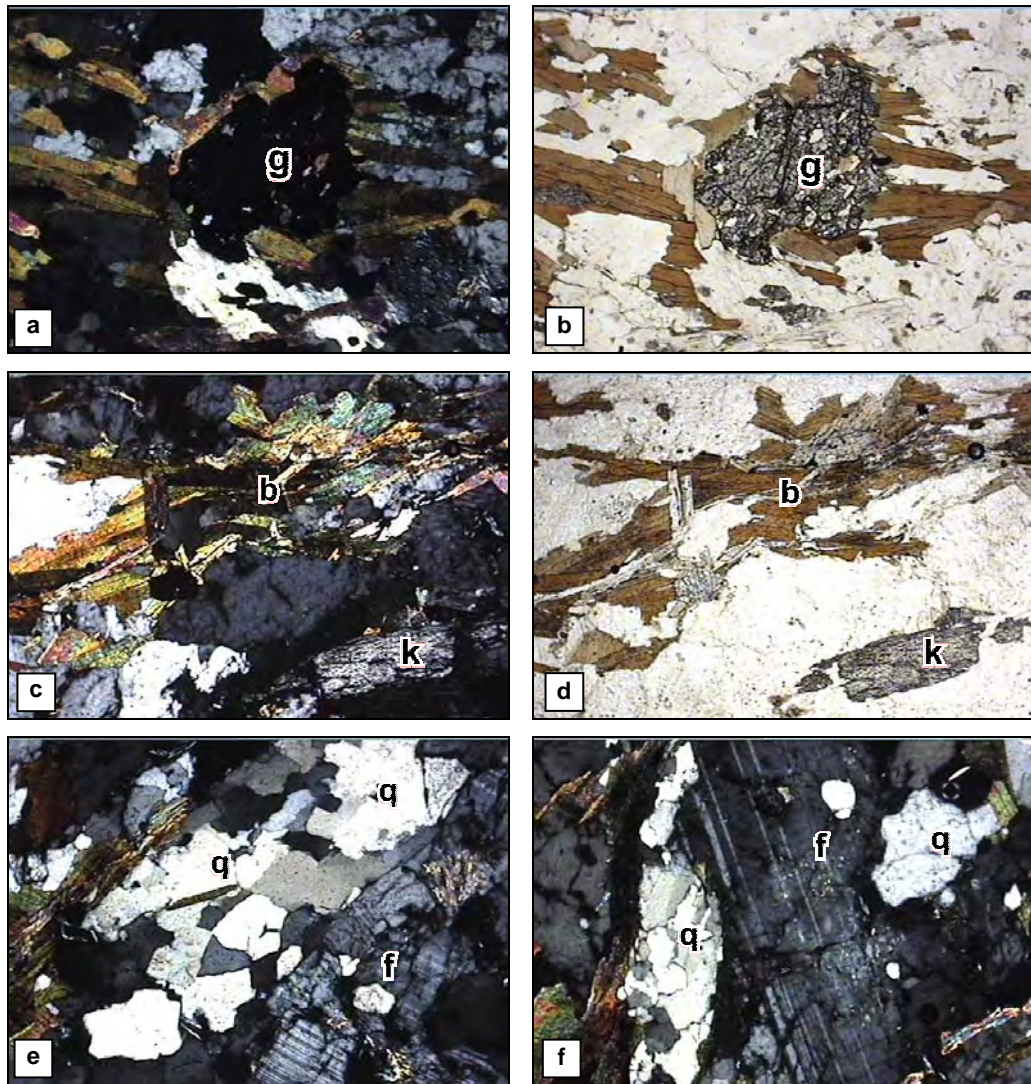


Figure 2.12. Photomicrographs from migmatites showing **(a)** a pre-tectonic garnet porphyroblast (g) and the biotite-, muscovite-, quartz-rich matrix wrapping around it; **(b)** is the same view of (a) under plane polarized light; **(c)** compositional main foliation (S_1) defined mainly by the biotites (b). An elongate kyanite (k) crystal is present and oriented parallel to the main foliation with its long axes. **(d)** is the same view of (c) under plane polarized light; **(e)** and **(f)** quartz grains (q) with straight grain boundaries showing a tendency of defining a polygonal texture and feldspar grains (f) deformed by deformation band, lamella and tapering twins. Fold of each view is 1.5 mm.

In some cases ghost garnet is also evident. *Biotite* is the characteristic mica with typical reddish birefringence and brownish pleochroism. They define the main foliation in the rock (Figure 2.12c-d). *Quartz* grains have straight grain boundaries and show a tendency of defining a polygonal texture (Figure 2.12e). *Feldspar* grains are deformed with deformation band, lamella and tapering twins (Figure 2.12e-f). They also have straight grain boundaries where the long axes of grains are parallel to the main foliation. In quartz, some larger grains show pronounced undulatory extinction. *Kyanite* mineral is evident in the migmatites and its amount increases towards the pegmatite contacts.

2.2.2.2. Kyanite-Garnet-Biotite-Muscovite-Albite-Quartz Schists

The schists are mostly exposed on the north-western parts of the study area (Figure 2.1). These rock units cover significant amount of area on the western flank of the Çomaklıdağı anticline shown on the geological map, outside the study area. They are also present as small exposures in the southern parts of the study area, at places such as west of Huriler, east of Rağıllar, west of Bozburun and east of Mestanlı. In Mestanlı, the schists occur as relatively thin, NE-trending belt within the orthogneisses (Figure 2.1). Similarly, they form small and patchy outcrops on top of the orthogneisses in the area to the north of Döğüşören (Figure 2.1). In almost all outcrops, the kyanite-garnet-biotite-muscovite-albite-quartz schists form conformable contacts with the migmatites, quartz-muscovite-garnet schists and orthogneisses where the main foliation in these rocks shows distinct parallelism. The contact with the pegmatites is sharp and show cross-cutting relationships (Figure 2.13).

The schists comprise a sequence of intercalated fine- to medium-grained pelite/semipelite and marble/recrystallized limestones. There are transitional boundaries between each of the individual lithologies. They also contain many small, concordant veins of quartz and dikes of pegmatoid (Figure 2.13).

These schists are characteristically grey to dark green in colour and display a distinct foliation and a well-developed lepidoblastic texture defined by the parallel alignment of micas. The lineation is penetrative and pronounced

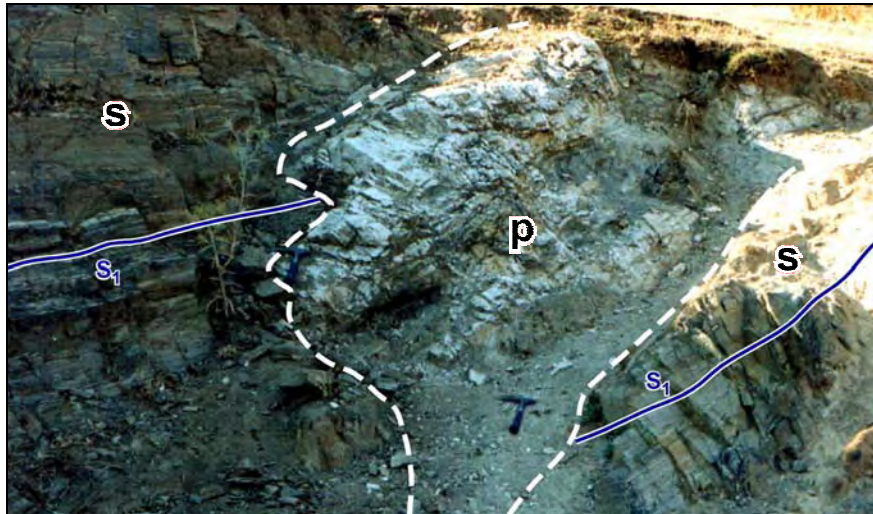


Figure 2.13. A pegmatite dike (p) intruded into kyanite-garnet-biotite-muscovite-albite-quartz schists (s) near Mestanlı. Please note that the main regional foliation S_1 do not continue in the pegmatites and terminates abruptly against it. The hammer is 33-cm long.

throughout the study area. Locally, they have brownish-buff colour due to extensive oxidation associated with garnets and/or biotite. The pelitic schists frequently enclose beds, lenses and layers of highly strained, well-foliated, dark grey marble/recrystallized marbles. At some localities, the two lithologies rapidly alternate. The marbles retain their original medium to thick bedding and display well-developed foliation, approximately parallel to bedding plane, which is defined usually by concentrations of micas. They show extensive boudinage and folds of similar and isoclinal styles.

Petrographically, these schists contain quartz, plagioclase (albite), orthoclase, biotite and muscovite as essential minerals whereas zircon, apatite, rutile, and magnetite form accessories. Micas, mainly *muscovites*, form long elongated flakes defining the main foliation in the rock (Figure 2.14a, b). The foliation is also defined by alternating quartz-rich and phyllosilicate-rich domains where quartz rich domains are characterized by dynamically recrystallized quartz grains with sutured boundaries (Figure 2.14c). Kyanite and garnet occur sporadically (Figures 2.14e-f, 2.15a-f). Where garnet is present, the rock possesses a porphyroblastic texture with large garnet porphyroblasts within a fine-grained

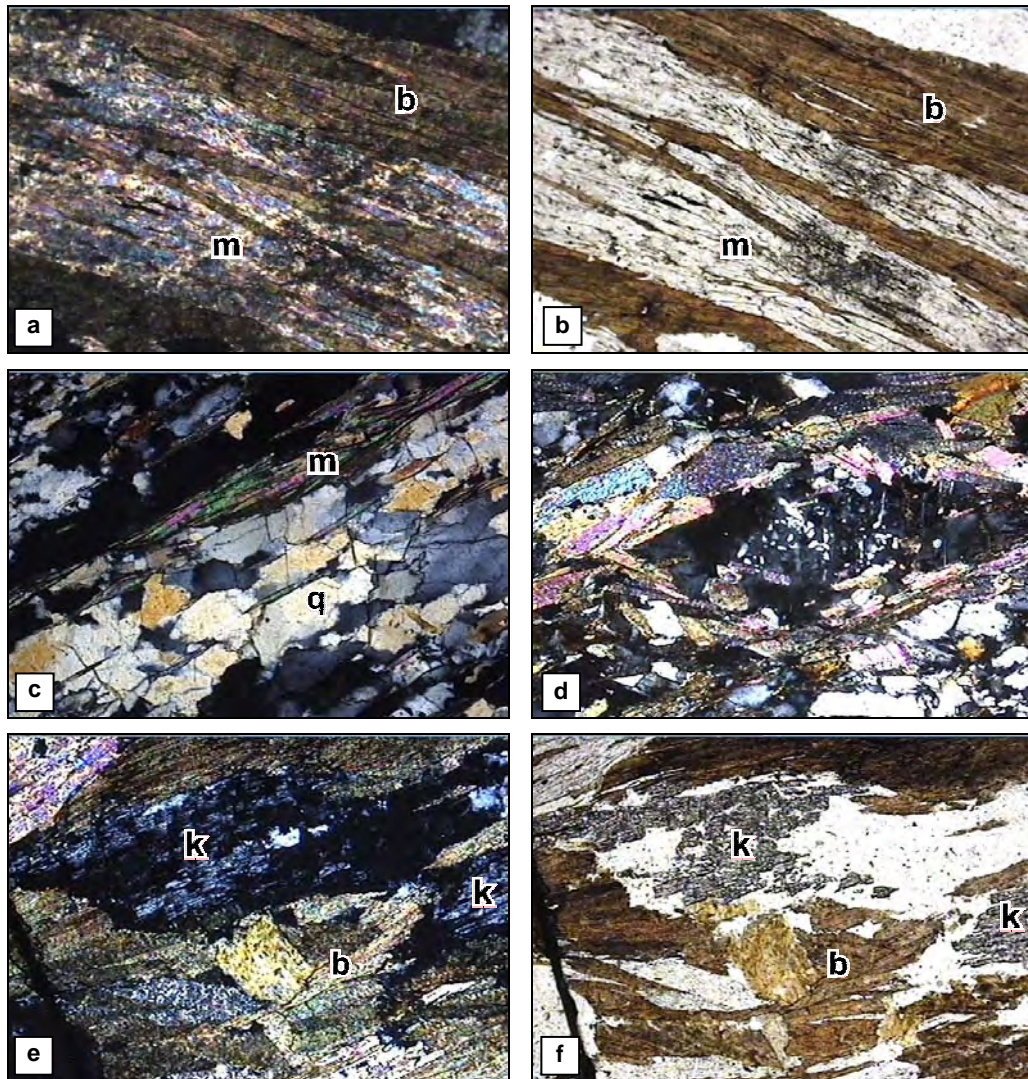


Figure 2.14. Photomicrographs from kyanite-garnet-biotite-muscovite-albite-quartz schists: **(a)** main compositional foliation (S_1), defined by parallel alignment of biotite (b) and muscovite (m) micas; **(b)** same view of (a) under plane polarized light; **(c)** foliation is also defined by dynamically recrystallized quartz (q) grains with sutured boundaries. Note that the quartz grains have a tendency to have straight grain boundaries with polygonal texture, suggesting relatively high temperature conditions of deformation. **(d)** A quartz grain showing graphitic texture surrounded by micas; **(e)** a sporadically occurring kyanite (k) surrounded by biotites (b); **(f)** same view of (e) under plane polarized light. Fold of each view is 1.5 mm.

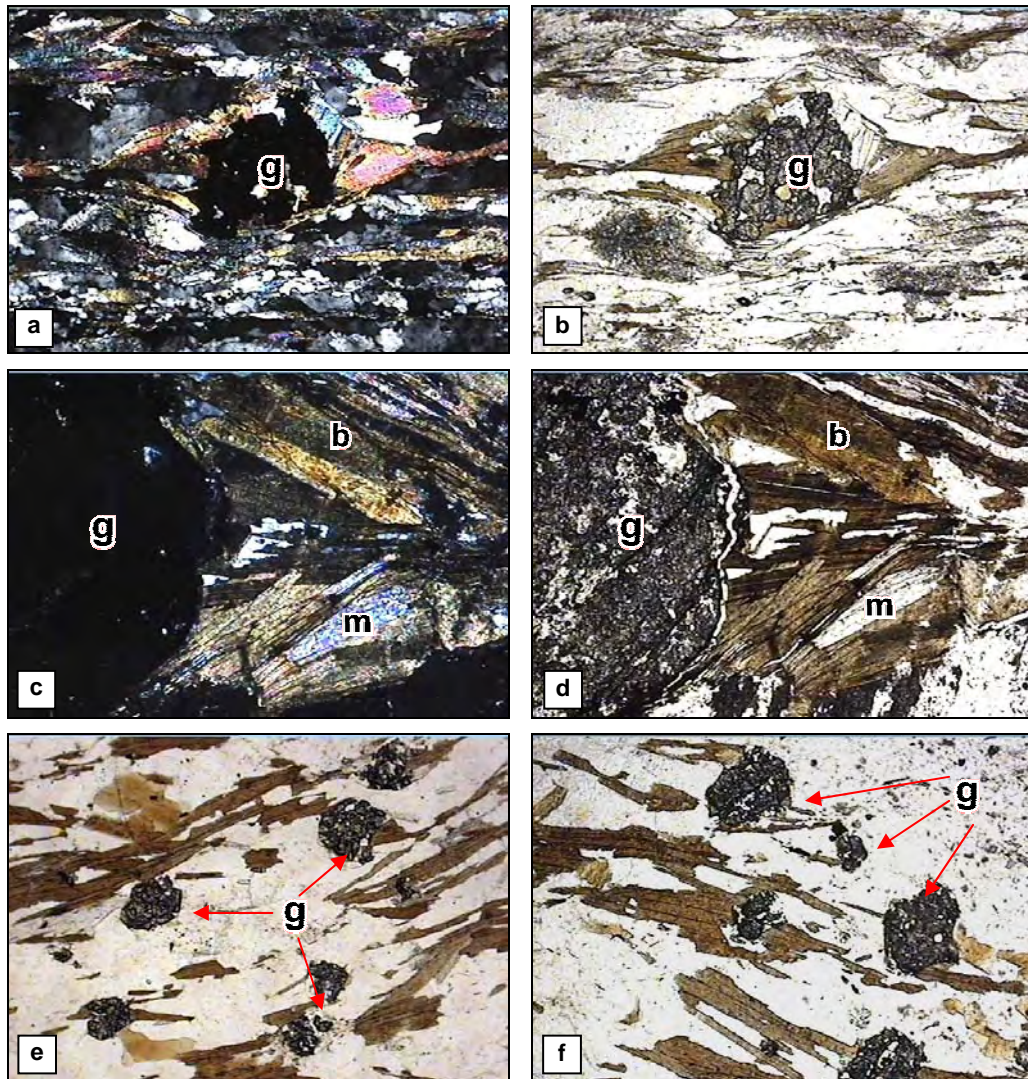


Figure 2.15. Photomicrographs from kyanite-garnet-biotite-muscovite-albite-quartz schists showing sporadically occurring garnet porphyroclasts. **(a)** a pre-tectonic garnet porphyroclast (g) and the biotite-, muscovite-, quartz-rich matrix wrapping around it; **(b)** same view of (a) under plane polarized light; **(c)** a detailed view showing a garnet porphyroclast (g) and adjacent biotites (b) and muscovites (m) wrapping around it; **(d)** same view of (c) under plane polarized light; **(e)** and **(f)** shows general sporadic appearance of some garnet crystals (g) in the rock. Fold of each view is 1.5 mm.

micaceous matrix which seems to wrap around the porphyroblasts (Figures 2.15a-d). *Garnets* occur as anhedral crystals devoid of any inclusion and their sizes may reach up to a few mm. Where *quartz* occurs, their growth is controlled by mica flakes and they also show deformation with undulatory extinction. Some of the quartz grains show graphitic texture (Figure 2.14d). There are *feldspars* showing undulatory extinction and they are usually surrounded by a muscovite-rich matrix. They also show banding, kinking and tapering deformation twinning. Some of the *albite* crystals are elongated in the plane of foliation where the twinning is parallel to foliation itself. There are some rhomb-shaped albite crystals oriented oblique to the main foliation and in these cases twinning is oblique to the foliation as well.

2.2.2.3. Quartz-Muscovite-Garnet Schists

Quartz-muscovite-garnet schists crop out within the western and northwestern half of the study area. Excellent exposures of the type lithology occur to the west of Huriler and Çavullar (Figure 2.1). They vary in colour from dirty white to white and display a distinct foliation and a well-developed lepidoblastic texture defined by the parallel alignment of muscovites. In most of their exposures, they have a monotonous speckled "salt and pepper" and shiny appearance due to the random distribution of muscovite flakes. This lithology is typically represented by fine- to medium-grained psammite which is generally interbedded with very schistose, medium- to dark-green semipelites/pelites. The schists display clearly conformable (gradational) boundary relationships with the underlying migmatites and kyanite-garnet-biotite-muscovite-albite-quartz schists whereas the contact with pegmatoids and orthogneisses is sharp; discordant with pegmatoids but concordant with orthogneisses when the regional pattern of S_1 foliation is considered.

Petrographically, in addition to quartz and muscovite these schists also include sporadic garnet and tourmaline whereas zircon, monazite, magnetite and rutile form accessories (Figure 2.16).

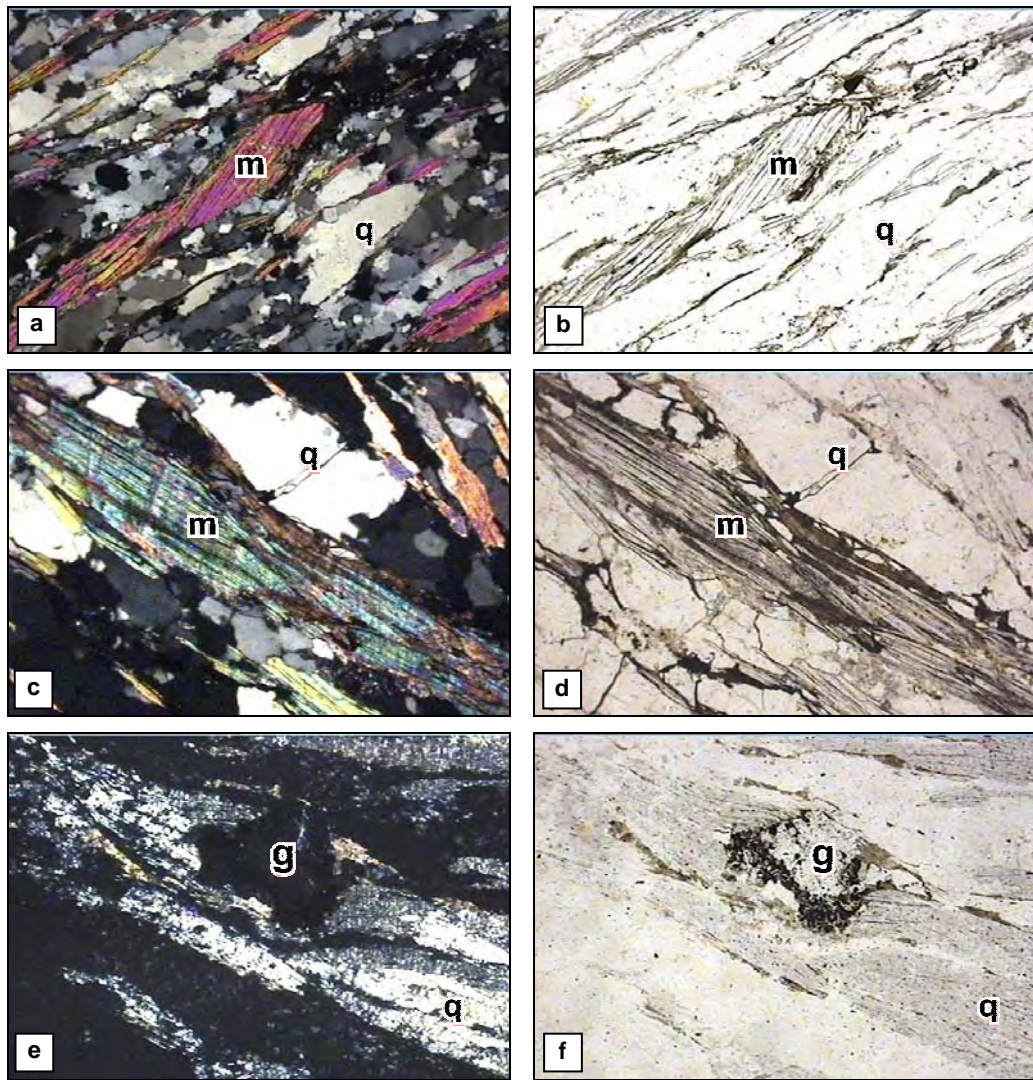


Figure 2.16. (a,c) Photomicrographs showing well developed S_1 foliation defined by parallel alignment of muscovite micas (m) and quartz (q) on quartz-muscovite-garnet schists. (b, d) are same views of (a) and (c) under plane polarized light. (e) A remnant of a garnet porphyroblast (g) within a fabric made up of quartz. (f) Same view of (e) under plane polarized light. Fold of each view is 1.5 mm.

2.3. Pegmatites

Pegmatites form one of the most important and common lithologic association in the study area. They occur as a large dome (with a diameter of several kilometers) intrusive into other metamorphic lithologies (Figure 2.1). Small isolated exposures cutting across the main foliation in the metasediments and the orthogneisses are also common throughout the study area (Figures 2.7, 2.8, 2.13) Approximately NE- and E–W-trending tourmaline-rich pegmatite dikes and/or sills are also common features. The thickness of these tabular bodies vary between 10–20 cm to about 5 metres. The NE-trending pegmatite dikes are particularly common around the contact with the migmatites and kyanite-garnet-biotite-muscovite-albite-quartz schists. When moved from northwest to southeast in the study area, both the thickness and the intensity of the pegmatite dikes increases. The dikes are usually discordant and cut the regional foliation in the metamorphic rocks hosting them (Figure 2.8a; but there are examples that show close parallelism to the foliation; Figure 2.8b), when moved further southwest towards the central parts of the study area, they start to appear as individual big dome shaped blocks with diameters of several meters (Figure 2.17a). The dome is elongated with longest axis trending in NE-direction.

The outcrops of pegmatites are well-exposed in the northern half of the study area. In these localities, the contact with the metasediments is not well-exposed because of the dense vegetation cover and poor conditions of outcrops but the cross-cutting relationships are observed locally at many locations and this is also evident from the map pattern (Figures 2.1).

Pegmatites form typical land forms where their outcrops form boulders, inselbergs, and all-slopes topography. They form numerous and widely distributed positive relief with *boulder*- a more-or-less rounded mass standing either in isolation on bald hill crests or in groups residual on valley floors and hill slopes. In most cases, pegmatoids form lone isolated hills with steep flanks that stand abruptly from the surrounding plains known as *inselbergs* (Twidale 1982; Figure 2.17a). Some are bald, steep-sided domical hills with bare rock exposed over

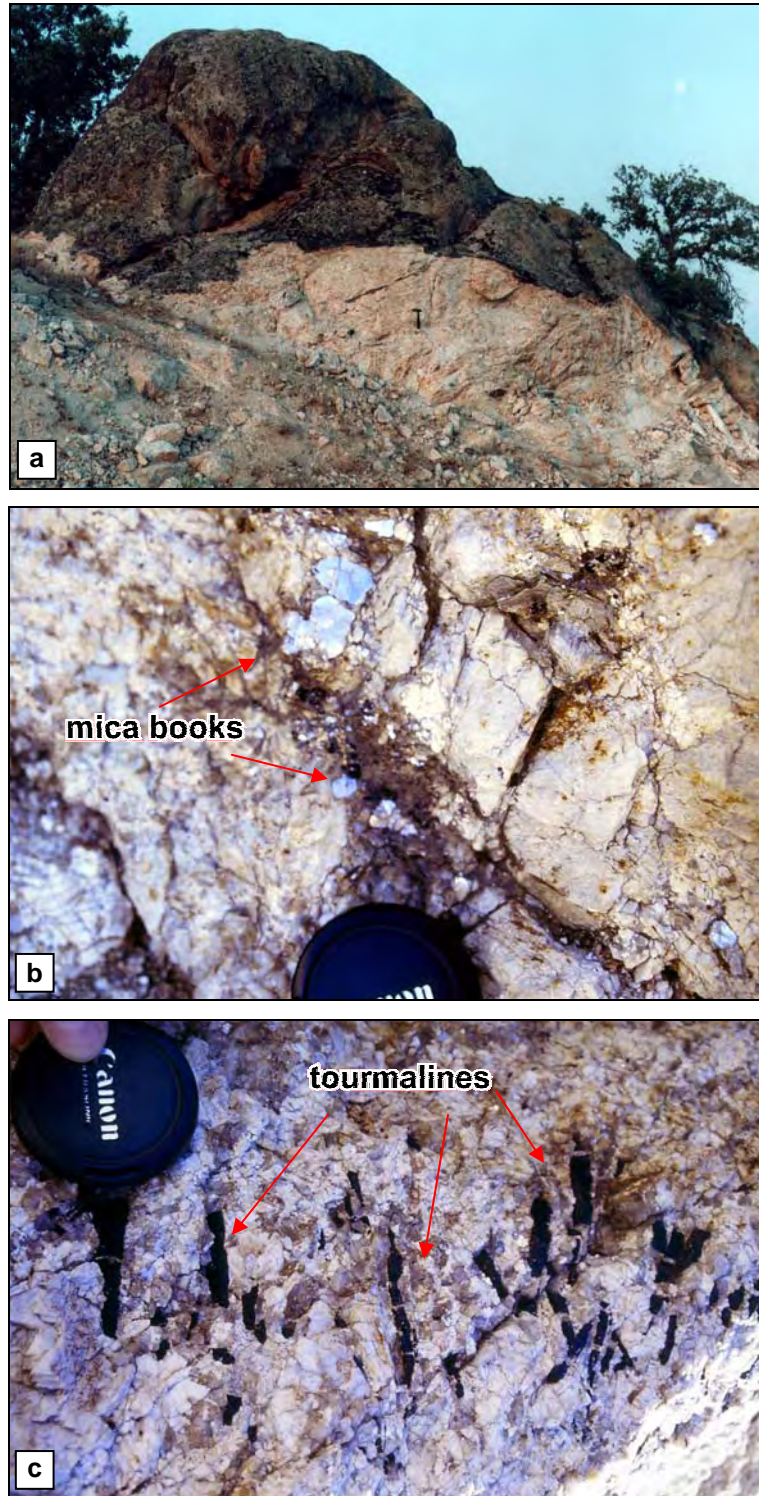


Figure 2.17. (a) Typical dome shaped isolated pegmatite body known as '*inselberg*' on the study area (hammer is 33-cm long); (b) large mica books present on pegmatites; (c) black tourmalines occurring as long blades aligned in NE-direction, parallel to the general trend of dykes. Camera lens cap has a diameter of 5 cm.

most of the surface. These are known as *Bornhardt* (Willis 1934, 1936; Twidale 1982). Some of these isolated hills are made up of block- or boulder-strewn residuals known to as *nubbies* (Twidale 1982).

The rock is usually white to dirty white or cream in colour; usually show no penetrative planar and/or linear fabrics and can be considered as relatively undeformed and metamorphosed. They are typically composed of feldspar, muscovite, quartz and tourmaline. The sizes of feldspars are variable ranging from a few millimetres to a few centimetres. In many cases, the rock is characterized by the presence of large white mica porphyroblasts or books (Figure 2.17b). Black tourmaline is abundant and usually occurs as long blades aligned in NE-direction, parallel to the general trend of dykes (Figure 2.17c). Tourmaline becomes abundant and concentrated around the pegmatoid margins.

Petrographically, the pegmatites consist of feldspar (both K-feldspar and plagioclase), quartz, and muscovite with considerable amounts of tourmaline (Figure 2.18a-c). Zircon, apatite and sphene form the common accessory minerals. Feldspars porphyroclasts are composed of K-feldspars and plagioclase grains, and usually occur as large anhedral to subhedral megacrysts with irregular grain boundaries. Feldspar megacrysts (Figure 2.19a-c) show evidence for deformation with undulatory extinction and, signs of brittle deformation with fractured and broken grains. K-feldspars (commonly orthoclase) are the commonest constituent and comprise the majority of the porphyroclasts showing microperthitic texture. Plagioclase also occurs as large porphyroclasts with variable sizes. The majority of plagioclase twins obey the albite twin law and twinning on the combined Carlsbad-albite laws is very rare. Quartz also occurs as large anhedral to subhedral grains (Figure 2.20a-c). Muscovite occurs as large subidioblastic grains. They contain abundant blue-black tourmaline, suggesting the presence of boron-rich fluids in the late stage crystallization of granitic protolith. Under the microscope, the high relief, slate blue colour and pleochroism. According to Dağ and Dora (1991), E-W trending dykes also contain beryl.

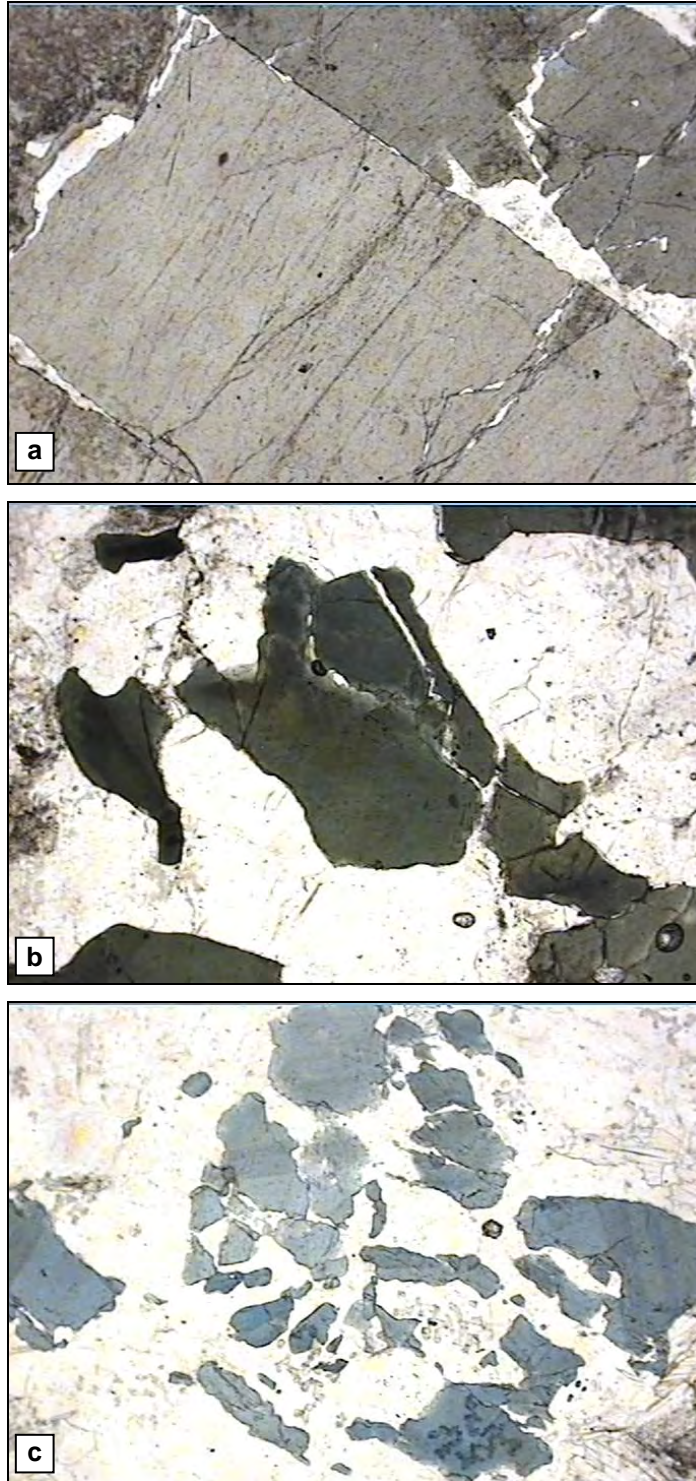


Figure 2.18. Photomicrographs showing different appearances of tourmaline crystals in pegmatites under plane polarized light. **(a)** A big tourmaline crystal showing a grey pleochroism; **(b, c)** tourmaline crystals showing a green pleochroism and a typical blue coloured shorelite pleochroism. Fold of each view is 1.5 mm.

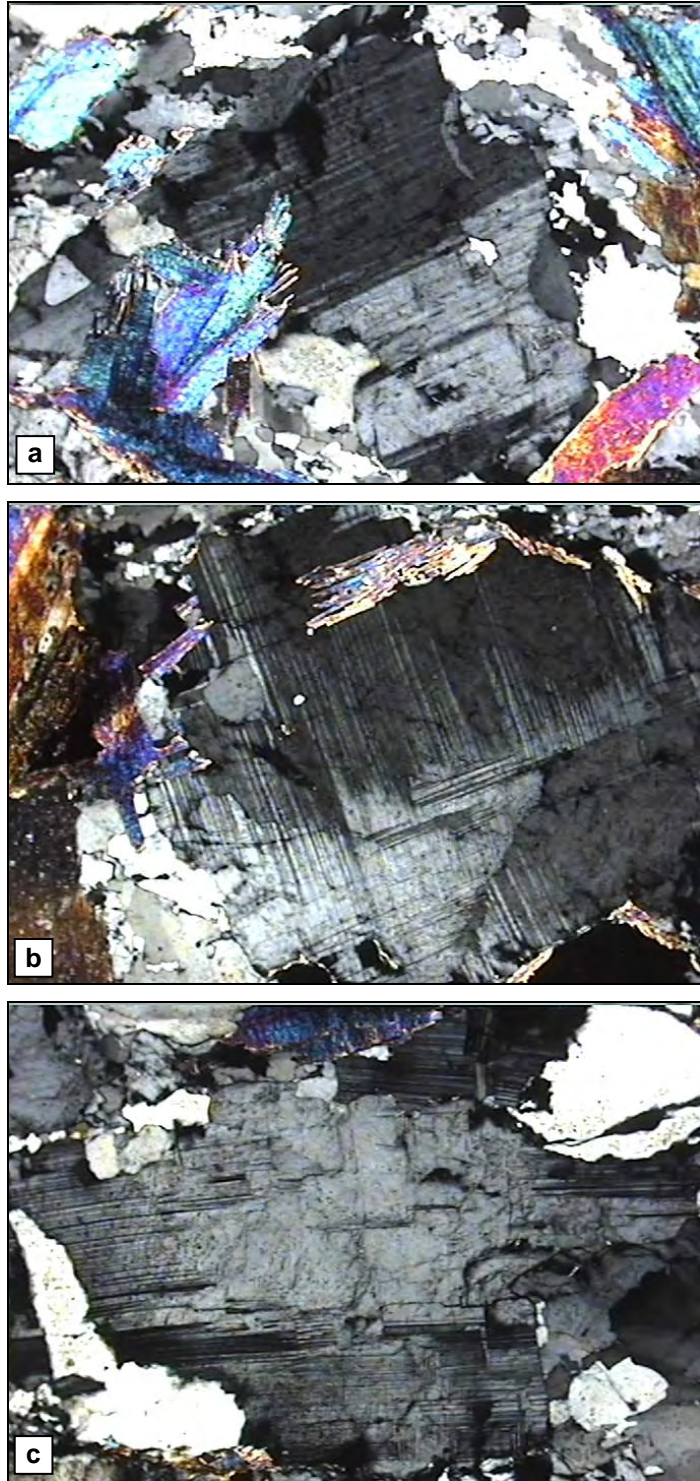


Figure 2.19. Photomicrographs illustrating different appearances of deformation twins in feldspar plagioclases in pegmatites. Note that none of the microphotos display a defined foliation. The tapering twins suggest that feldspars experienced intracrystalline deformation at some degree. Carlsbad twinning in **(a)** and kinking in **(b)** is evident. Fold of each view is 1.5 mm.

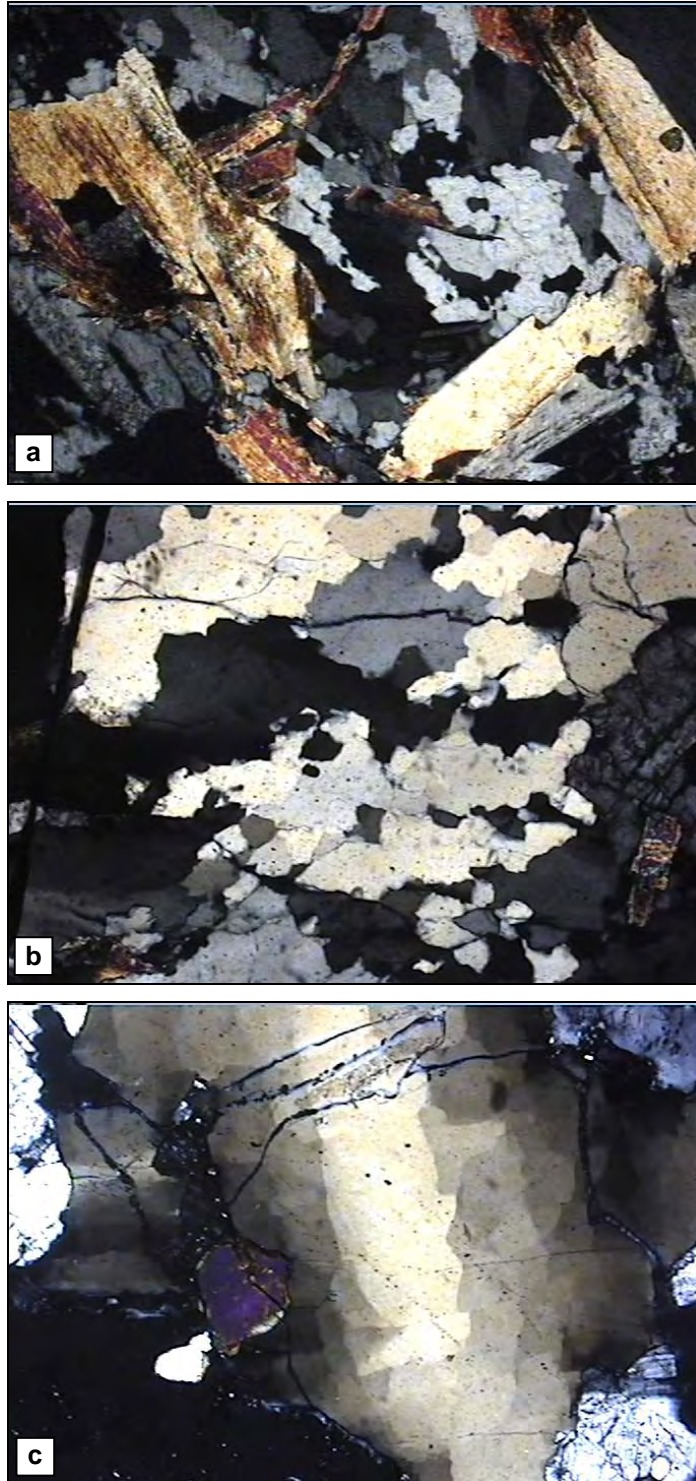


Figure 2.20. Photomicrographs showing different appearances of quartz crystals in pegmatites. **(a,b)** Large anhedral to subhedral quartz grains; **(c)** a quartz crystal showing undulatory extinction suggesting that quartz has experienced intracrystalline deformation, like in feldspars. Fold of each view is 1.5 mm.

2.4. Neogene Sedimentary Rocks

The Neogene sedimentary rocks, covering large areas on the eastern side of the study area, unconformably overly metamorphic units of the Menderes Massif. The sedimentary rocks in the region can be grouped into two as fluvial clastic rocks and the rocks with lacustrine origin.

The fluvial clastic rocks make up the most important sedimentary unit since they cover the largest area in the study area. This unit is made up of a generally fining-upward sequence of conglomerates with large pebbles (boulder conglomerates), poorly consolidated sandstones, and sandy claystones and siltstones (Figure 2.21a). The conglomerates are typical poorly sorted basal conglomerates including gneiss and schist fragments of variable sizes (from a few centimetres to a few meters; (Figure 2.21b). The bedding planes of these units are clearly observable. They generally occur as horizontal layers or they show a gentle dip of at most 20° towards SE, and contain syn-sedimentary structures such as slumps in some localities (Figure 2.21c)

During the field studies, the location where (i) these fluvial sedimentary units are exposed well, (ii) the accessibility and conditions for taking a measured section is suitable, and (iii) the relationship between the sedimentary rocks and the basement metamorphic rocks can be well observed, is chosen as the outcrops just at the south of Çavullar village. The details of the rock units cropping out there are given in Figure 2.22. In this locality, the sedimentary units are placed unconformably on top of a presently low-angle fault surface, details of which will be discussed in Chapter 4. Here, the typical fining upward is demonstrated well with the sedimentary sequence starting with a greenish grey coloured poorly sorted basal conglomerate with large gneiss blocks within a fine-grained clayey matrix (Figure 2.22). As moved upwards in the sequence, the size of fragments originated from basement rocks significantly decrease. The more than 330-cm-thick basal conglomerates pass into green coloured clays and then pinkish grey coloured sandstones and sandy claystones. After an about 200-cm-thick conglomerate layer with medium sized gneiss particles within a sandy matrix, another horizon of sandstone, siltstone, and claystone

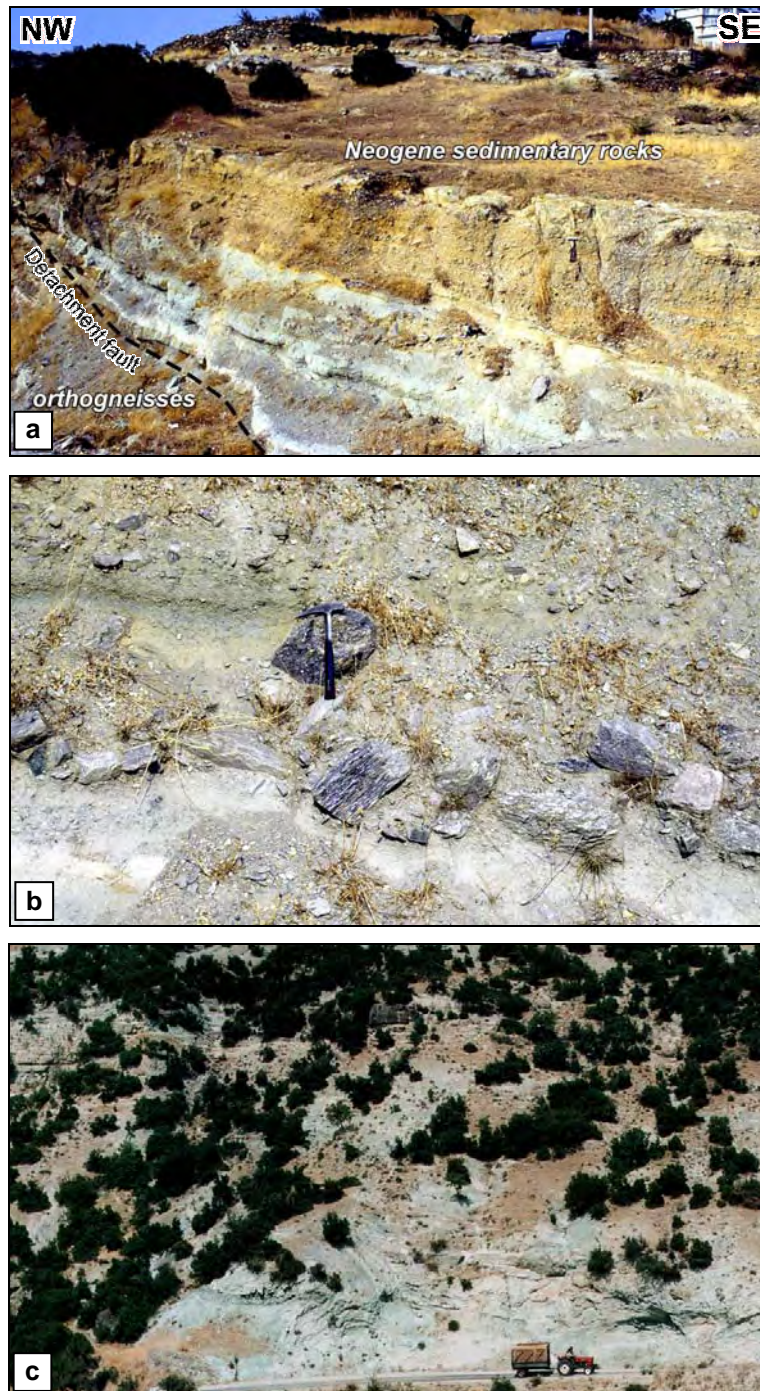


Figure 2.21. (a) General appearance of the Neogene sedimentary rocks exposed at Çavullar. There is a gentle dip towards southeast. Hammer is 33-cm long. **(b)** Close-up field view of the conglomerate with large, angular gneiss fragments at Çavullar. Hammer is 33-cm long. **(c)** Syn-sedimentary structures in the Neogene sedimentary rocks (NE of Çavullar; tractor and trailer is 5-m long).

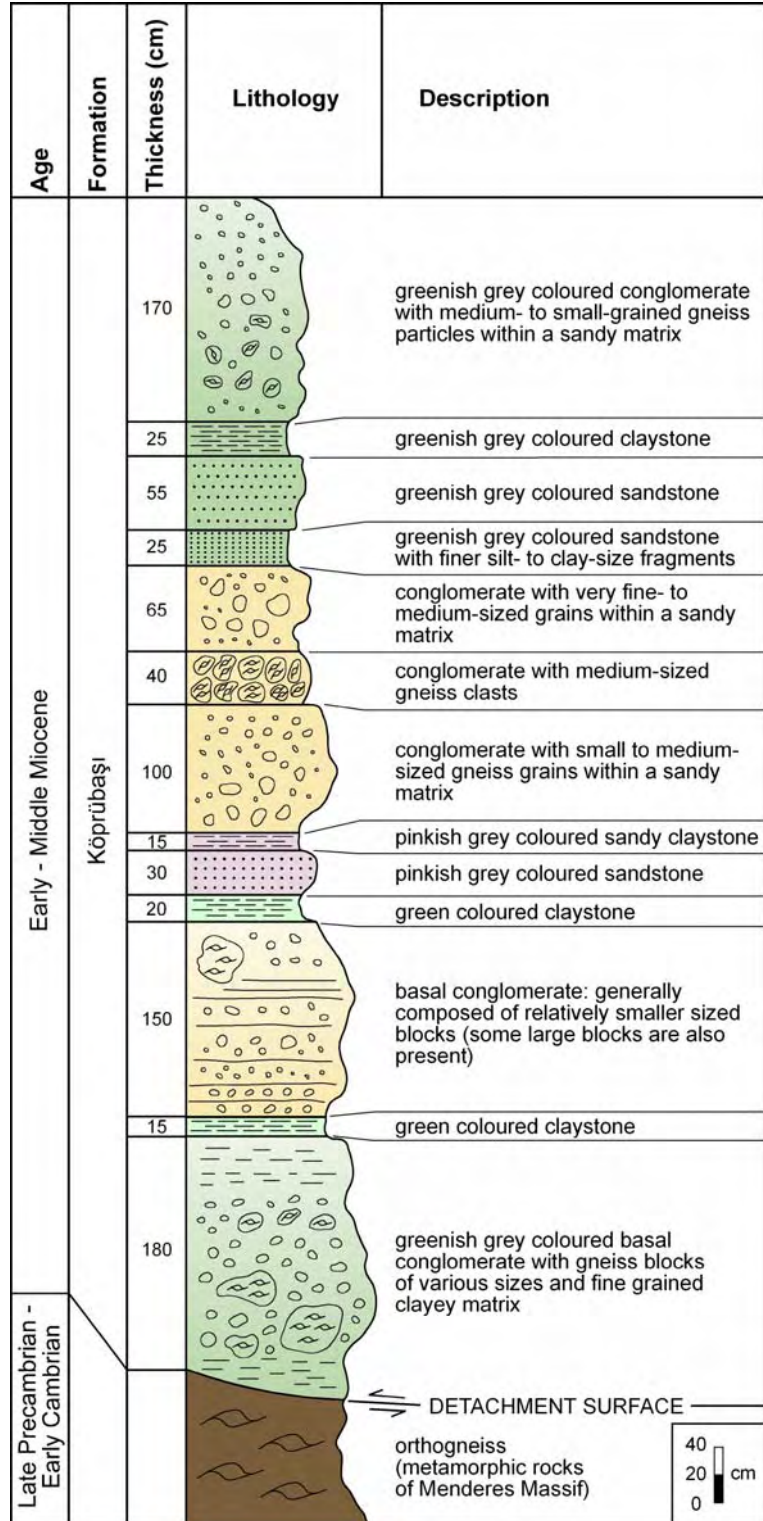


Figure 2.22. Measured columnar section of the sedimentary sequence exposed near Çavullar village.

alternations is present. This, in turn, is followed by a 170-cm-thick greenish grey coloured conglomerate with small grained gneiss particles in a sandy matrix.

The other group of Neogene sedimentary rocks with lacustrine origin is present on the eastern parts of Akçaalan and Yardere villages. These rocks of Late Miocene age are made up of marls and sandy claystones, and the overlying lacustrine limestones. According to Ayan (1973), these units were deposited with the initiation of lacustrine conditions after a decrease in the fluvial activity in the region. The units just above the fluvial conglomerates, sandstones and siltstones are greenish coloured marls, sandy and silty marls with layers of chert and tuff. These lithologies are essentially horizontal with thickness reaching 50–100 m (Ayan 1973). The uppermost portions of the Neogene sedimentary units in the study area are composed of light yellow, white, and grey coloured lacustrine limestones.

As mentioned previously, the study area of this research lies on the horst between Demirci and Gördes basins, and the Neogene sedimentary rocks described above, cropping out on the study area, makes up some part of the Lower–Middle Miocene continental clastic rocks constituting the Demirci Basin fill. The stratigraphy of the Demirci Basin has been well documented recently by Yılmaz *et al.* (2000). It starts with a cobble (up to 1 m in diameter) and pebble conglomerate unit (50–300 m thick) with subrounded to subangular clasts, derived from underlying metamorphic rocks of the Menderes Massif (Borlu Formation). These internally chaotic, poorly sorted clastic rocks are interpreted as debris flows and alluvial fan deposits formed in association with elevations of the adjacent fault blocks. These units pass laterally into a well-bedded sandstone-siltstone alternation (Köprübaşı Formation) and then to the marls and shales (Demirci Formation; Figure 2.24). The Köprübaşı Formation is characterized by a typical volcano-sedimentary sequence made of ash-fall tuff horizons alternating with clastic rocks, latite-dacite lavas and flow-lahar breccias (Okçular volcanics). Volcanics become dominant upwards in the stratigraphical section and towards the volcanic centers in the north. The age of the volcanic rocks are found to be 18–14 Ma. As seen in Figure 2.23, the Köprübaşı Formation also includes some conglomerate layers in its lower levels in the southern parts of the Demirci Basin. The volcano-sedimentary association of

Early–Middle Miocene age is overlain disconformably by the Upper Miocene–Lower Pliocene limestones of the Adala Formation. In some places, the formation rests directly on the metamorphic rocks.

According to this information, the fluvial clastic rocks comprising the most important sedimentary unit in the study area is interpreted to be a part of the lowest levels of the Köprübaşı Formation. It is suggested here that the marls, sandy and silty marls, and layers with chert and tuff, which overly the fluvial clastics, belong to the middle and upper portions of Köprübaşı Formation (Figure 2.23), and the lacustrine limestone unconformably overlying all the units makes up the Adala Formation in the study area.

Age	Formation	Thickness	Lithology	Description
Late Mio. - Plio.	Adala	35 m		Lacustrine limestone
—Discontinuity—				
Early - Middle Miocene	Demirci	>75 m		Laminated mudstone and shale
	Köprübaşı	1000 m		Lacustrine mudstone, marl
				Tuff Conglomerate, sandstone, siltstone and mudstone
—Transitional contact—				
	Borlu	~200 m		Lacustrine limestone Fluvial sandstone Boulders-conglomerate
Late Olig. - Early Mio.				Metamorphic rocks of Menderes Massif

Figure 2.23. Stratigraphical summary column of the Demirci Basin (from Yılmaz *et al.* 2000).

The contact between these sedimentary rocks and the metamorphics are of two types: (1) neotectonic high-angle normal faults generated due to N–S extension prevailing in western Anatolia, and (2) presently low-angle normal faults generated during the Early Miocene exhumation of the Menderes Massif. The metamorphics and sedimentary rocks are observed to be juxtaposed along either of these two fault types within the whole study area (see Chapter 3, Sections 3.4.1 and 3.5 for detailed information).

2.5. Quaternary Alluvial Sediments

The alluvial sediments being deposited presently within the study area include poorly sorted sediments (block, cobble, boulder, pebble, sand, silt, clay) deposited along the alluvial fans, stream and river plains and valleys. Their grain size ranges from a few centimeters to a few meters (Figure 2.24).

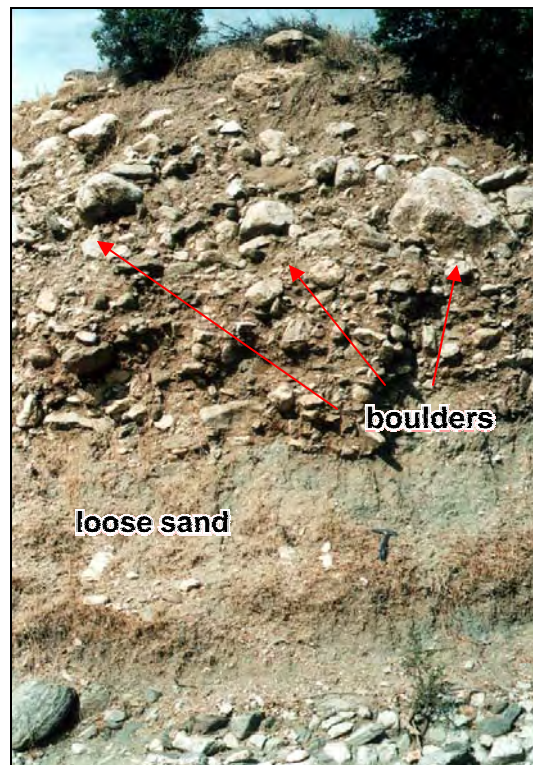


Figure 2.24. Quaternary alluvial sediments in the study area made up of loose sand-size material and fragments of various metamorphic rocks. Hammer is 33-cm long.

CHAPTER 3

STRUCTURAL GEOLOGY

3.1. Introduction

In this chapter, detailed information about both macro- and micro-scale geological structures observed and investigated during the field and laboratory studies is given. The main targets of this chapter are: (1) to establish the number and sequence of deformation that the rocks of Menderes Massif have experienced, (2) to describe the structures formed during each phase and finally (3) to discuss the kinematic and tectonic significance of these structures.

3.2. Deformational Phases

Field observations, statistical analysis of field measurements, and microstructural analysis have been used to determine the number of fabric generations (deformational phases), the kinematics (shear sense) during each phase, the mechanisms responsible for the deformation and relative timing of deformation and coeval metamorphism. The evidence which lead to the understanding of the deformational phases are structures such as foliation planes, lineations and certain types of shear sense indicators observable both on the field and under the microscope. The word "*foliation*" is used as a general term to describe any homogeneously distributed planar feature that occurs penetratively in a body of rock, and defined by the preferred orientation or parallel alignment of platy and tabular minerals or aggregates in the given rock, or to denote the compositional banding defined by the concentration of particular minerals such as biotite and leucocratic minerals such as quartz and feldspar. The "*lineation*" term defines any linear feature that occurs penetratively in a rock body and denotes preferred alignment of elongate minerals such as

amphibole, quartz or micas, and the linear alignment of elongate clusters of grains of particular minerals such as quartz and micas.

On the rocks of the northern Menderes Massif in the study area, three distinct phases of Alpine deformation have been identified: (1) top-to-the-N–NNE contraction (D_1 deformation), (2) top-to-the-N–NNE extension (D_2 deformation), and (3) late brittle normal faulting (D_3 deformation). There is no evidence for the presence of pre-Alpine fabrics either because (1) these rocks have not suffered from any pre-Alpine deformation and/or metamorphism; (2) the traces of earlier deformation(s)/fabric(s) have been destroyed by subsequent Alpine events or (3) it is not possible to distinguish these deformations by field and/or microscopic studies.

3.3. D_1 Deformation

D_1 deformation is developed within the metamorphic rocks of the study area including the metasediments and the orthogneisses and is characterized by a penetratively developed, distinct regional foliation, S_1 ; it is penetrative in almost all lithologies and is invariably associated with mineral stretching lineation, L_1 . Both the foliation and lineation are visible on both hand specimen and thin section under the polarizing microscope (Figures 2.3, 2.4, 2.6a, 2.11e-f, 2.14a-c, 2.16a-d, 3.1, and 3.2).

S_1 foliation in the metasediments developed parallel or subparallel to the original layering/bedding (S_0) defined by compositional layering and subparallel mica and quartz preferred orientation. This phenomenon is much more clear in the psammitic schists and in areas where the pelitic/semipelitic schists are intercalated with carbonates. The S_1 foliation is mostly defined by the parallel alignment of micas (Figures 2.11e-f, 2.14a-c, 2.16a-d, 3.1, and 3.2c-h). It is therefore well developed in pelitic to semipelitic lithologies but less obvious in psammites and carbonates. The approximately NE–SW-trending S_1 foliation is mostly moderately dipping to the SE or NW due to the effect of later NNE–SSW-trending F_2 folding and D_3 normal faulting. The field measurements showed out that schists present on the western and eastern limbs of the anticline (see the section 3.4.2 on ' F_2

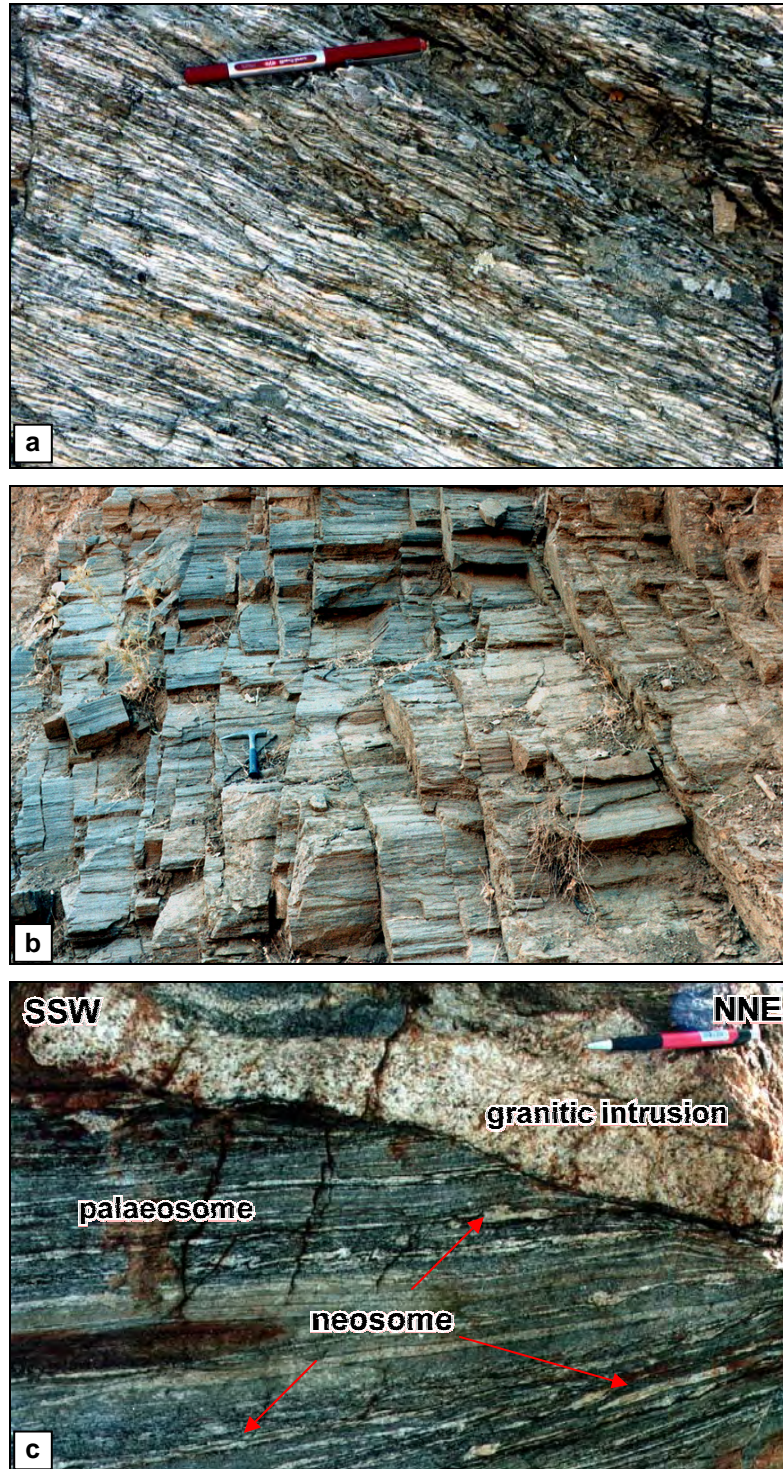


Figure 3.1. Typical field views from the main regional foliation (S_1) developed on **(a)** orthogneisses (pen is 14-cm long); **(b)** kyanite-garnet-biotite-muscovite-albite-quartz schists (hammer is 33-cm long); and **(c)** migmatites composed of alternating dark (palaeosome) and light (neosome) layers and a granitic intrusion (pen is 15-cm long). The asymmetric fold deforming a leucosome layer in (c) indicates a top-to-the-NNE deformation. Note the abrupt termination of S_1 foliation against tabular granitic intrusion.

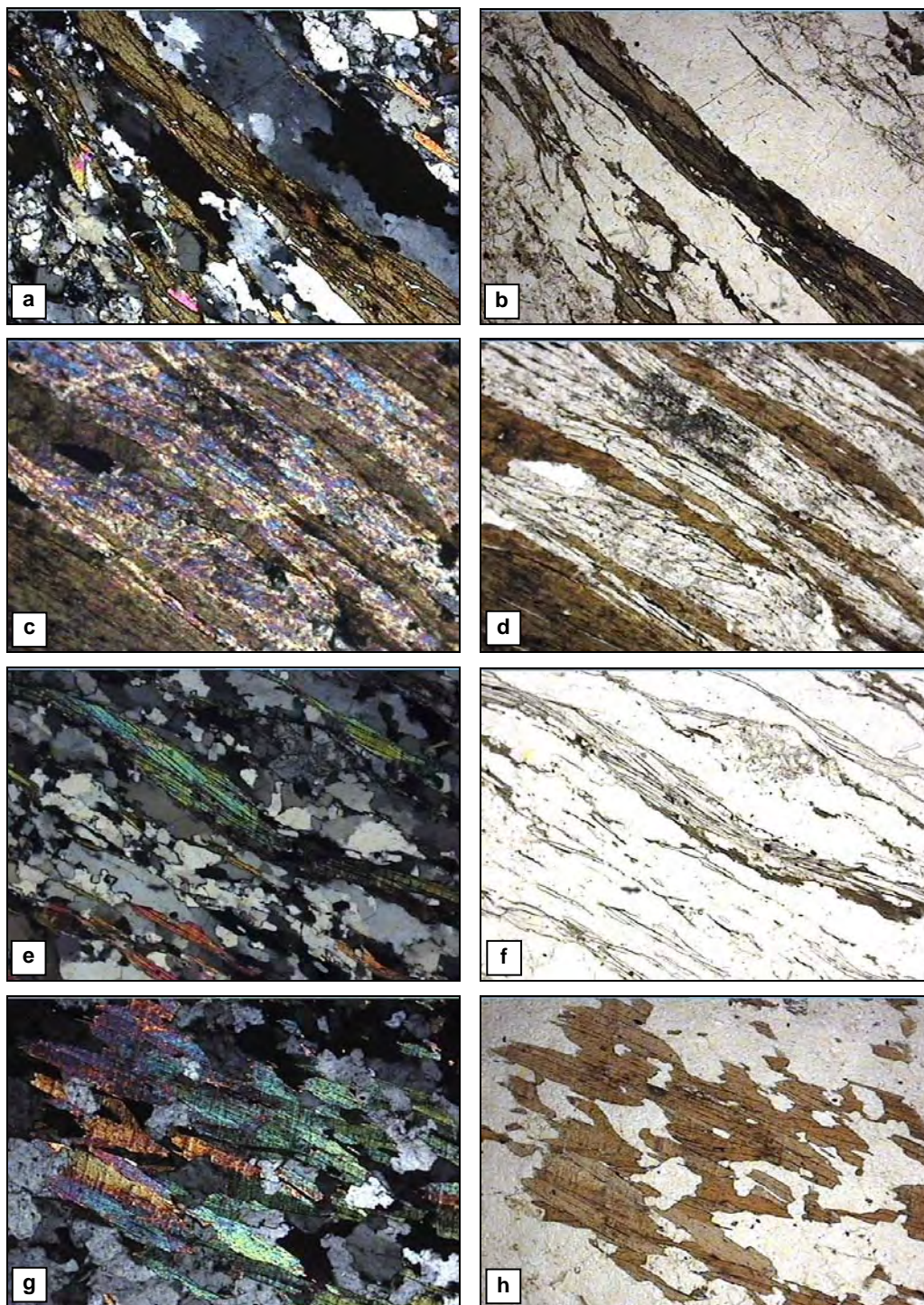


Figure 3.2. Photomicrographs showing the main foliation defined by parallel alignment of biotites, muscovites and quartz on orthogneisses **(a)**, kyanite-garnet-biotite-muscovite-albite-quartz schists **(c)**, quartz-muscovite-garnet schists **(e)**, and migmatites **(g)**. **(b,d,f,h)** are the same views of (a), (c), (e), and (g) under plane polarized light, respectively. Fold of each view is 1.5 mm.

Folding) have the following average attitudes respectively: 025°N/61°NW and 039°/50°SE. The general trend of S_1 foliation is seen generally to be constant throughout the study area, except for a number of localities, particularly at the hinge zone of F_2 fold where foliation strikes in ENE–WSW and dips to the south (Figure 2.1). The migmatites are characterized by compositional foliation defined by the alternating layers of dirty white coloured leucosomes and dark green gneisses (mesosome/ palaeosome; Figure 2.10a, 3.1c, 3.2g-h). Being affected by F_2 folding, the foliation planes of the migmatites on the western limb of the fold show a NNW–SSE (~321°N) trend and a mean dip of 56° towards SW and the ones on the eastern limb show a NE–SW trend (055°N) with a mean dip of 37° towards SE. There may be abrupt changes on the attitude of the foliation planes near the pegmatitic intrusions. Stereograms of the foliation planes in the schists and migmatites were prepared from 135 measurements plotted and contoured on the Schmidt net, lower hemisphere projection (Figure 3.3a-d).

Compositional foliation is also developed in semipelitic and psammitic schists and is marked by widely spaced concentrations of phyllosilicate-rich (muscovite and/or biotite) and quartz-rich domains (P- and Q-rich domains, respectively) where the domain boundary trends parallel to the foliation. Petrographically, the foliation is defined mostly by the preferred alignment of flakes or long stringers of mica (both muscovite and biotite) and elongate quartz grains; it wraps around porphyroblasts of garnet and kyanite where developed. The (001) surfaces micas show remarkable parallelism with the S_1 foliation

The L_1 mineral elongation/stretching lineation in the metasediments is often contained within the S_1 foliation in the metasediments and is defined mostly by the preferred parallel alignment of mostly micas and elongate quartz grains. It is approximately NNE–SSW-trending and has a moderate plunge. Due to being affected by later F_2 folding, the plunge of lineation is both towards south and north (Figure 3.3e-f). As is seen from this diagram, mean plunge of lineation is approximately 26° to NE or SW.

The orthogneisses in the study area are typical L–S tectonites containing a penetrative and well-pronounced foliation invariably associated with a pronounced pervasive NNE–SSW-trending mineral elongation/stretching

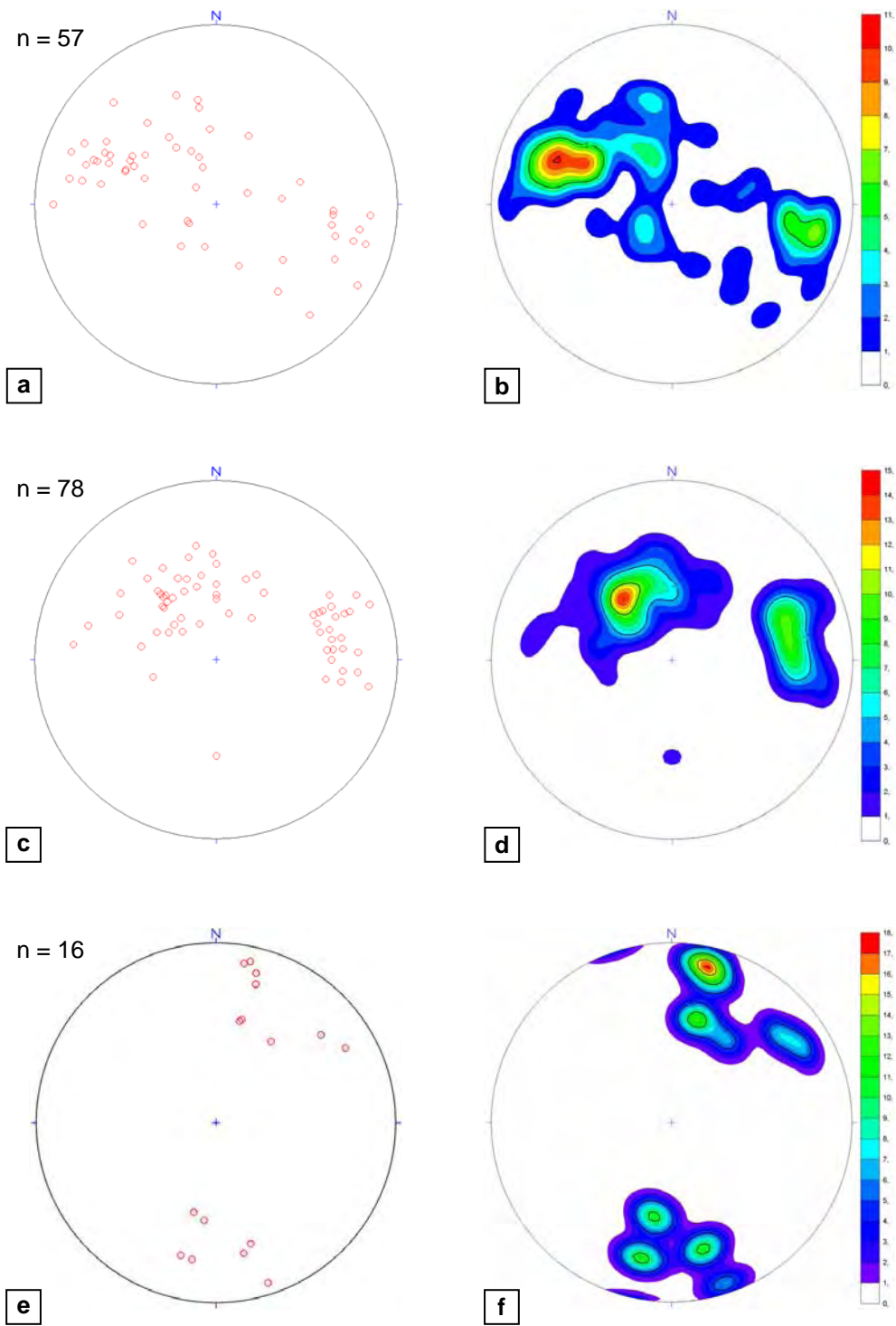


Figure 3.3. Lower hemisphere stereonet (Schmidtt net) projections and contour plots of poles to regional S_1 foliation on schists (**a, b**), on migmatites (**c, d**); and L_1 lineations from metasediments (**e, f**).

lineation where dip and plunge amounts are usually around 42° and 18° , respectively (Figure 3.4). Both features are visible in the field, in hand specimen and in thin section under the polarized microscope. At localities where deformation is intense, these structures become relatively penetrative and more pronounced. In areas of high strain, the augen gneisses are transformed into ultramylonites with intense deformation (Figure 2.3c) where the stretched and elongated feldspar grains and quartz ribbons defines a pronounced mineral elongation lineation. The foliation is defined by flattened quartz aggregates and platy minerals, such as muscovite and biotite (Figures 2.3, 2.4, 2.6a, 3.1a, and 3.2a-b). In general the rock is characterized by a blastomylonitic texture, both in hand specimen and under the microscope, where the S_1 foliation is seen to deflect around the large retort-shaped feldspar porphyroclasts or augen (Figure 2.3a).

Figure 3.4a shows a stereogram of the S_1 foliation where 121 poles have been plotted and contoured on a Schmidt net, lower hemisphere projection. The S_1 foliation of gneisses has a general NE–SW trend and a moderate SE dip on the whole area (the average attitude: $037^\circ\text{N}/42^\circ\text{SE}$; Figure 3.4a-b). However, there are some changes on the strike, dip and dip direction of the foliation at several localities, such as south of Kınık, the poles to which appear on the southern side of the stereogram on Figure 3.4a. They are attributed to the later effect of F_2 folding and D_3 brittle normal faulting.

Petrographically, the foliation in the orthogneisses is defined by the preferred parallel alignment of micas and quartz ribbons. The orthogneisses characteristically display a northeast-plunging mineral elongation/stretching lineation contained in the plane of the S_1 foliation (Figure 3.4c-d). It is primarily defined by the sub-parallel alignment of the longest dimensions of feldspar augen (recrystallized tails of feldspar porphyroclasts), stretched stringers of quartz grains, and smeared-out micas. Within the study area, the lineation is generally remarkably systematic in orientation. A contoured diagram of lineations prepared from 10 measurements shows a mean trend of approximately NE–SW ($\sim 053^\circ\text{N}$) and plunge of about 18° towards NE (Figure 3.4c-d).

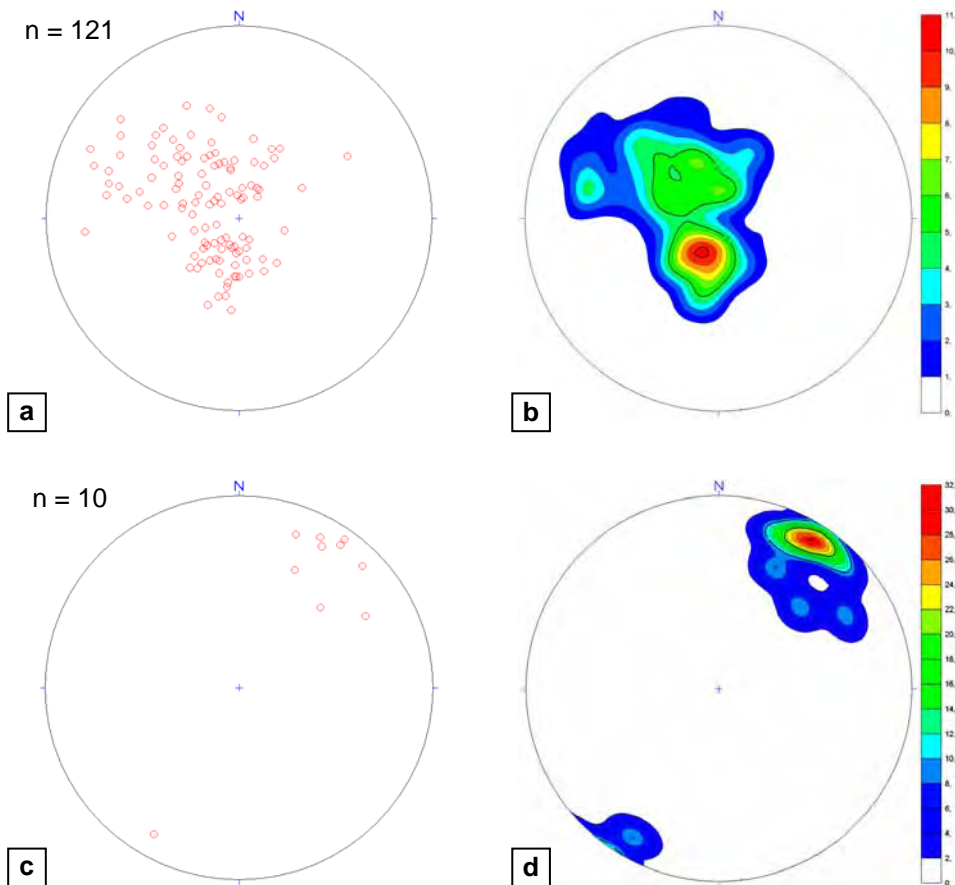


Figure 3.4. Lower hemisphere stereonet (Schmidth net) projections and contour plots of poles to regional S_1 foliation (**a, b**) and L_1 lineations in the orthogneisses. (**c, d**).

The foliation in the orthogneisses becomes very crude or unrecognizable in structurally higher rocks that are usually brecciated. The foliation in the mylonites strikes approximately parallel with the direction of the stretching lineation.

The exposures of these orthogneisses display subtle variations in the intensity of deformation. In the structurally lower exposures, the augen gneisses show relatively slight mylonitization characterized by more brittle deformation, jointing and minor faulting, with larger feldspar porphyroclasts reaching up to 5 cm in diameter along their longest axes. The orthogneisses display various kinematic indicators, including asymmetric feldspar porphyroclasts, S-C relationships, and asymmetric quartz grain-shape foliation.

3.3.1. F₁ Folding

The S₁ main foliation in the metasediments, particularly the migmatites, defines mesoscopic/outcrop-scale folds with axes almost parallel with the associated mineral elongation lineation; they are interpreted as synchronous with the shearing. The foliation generally dips around 30° but is more steeply dipping where it is affected by folding.

Folding of S₁ regional foliation occurs through the different lithologies of the metasediments. F₁ folds (Figures 2.10b and 3.5) are common and well-observed in carbonates alternating with pelitic rocks or in carbonate-rich lithologies or in migmatites. They occur as rootless intrafolial structures and vary from tight to isoclinal in style. The thickening along the hinges but thinning in the limbs is common feature of F₁ folds (Figure 2.10b). The size of mesostructures is variable from a few centimetres to tens of metres in wavelength. Where carbonates dominate, F₁ folding is commonly associated with boudin formation, indicating a component of subhorizontal extension parallel in the plane of, and compression perpendicular, to S₁ foliation. The common development of intrafolial folds suggests that, following its generation, S₁ foliation is deformed into folds during the later increments of the D₁ shearing movements.

3.3.2. Microstructural Features of Deformed Grains in Orthogneisses

It is common to all that there is no mineral changes or nor new mineral and/or mineral paragenesis formation during the deformation and metamorphism of granitic rocks because these rocks contain minerals that are relatively stable over large portions of P–T space. The study of both naturally and/or experimentally deformed granitic rocks show that characteristic microstructural changes occur in the constituent minerals, particularly in feldspars, micas, and quartz which are very useful tools in the estimation of metamorphic conditions associated with the deformation. Therefore, microstructural analysis of feldspars, micas and quartz in the orthogneisses has been carried out in order to assess the metamorphic

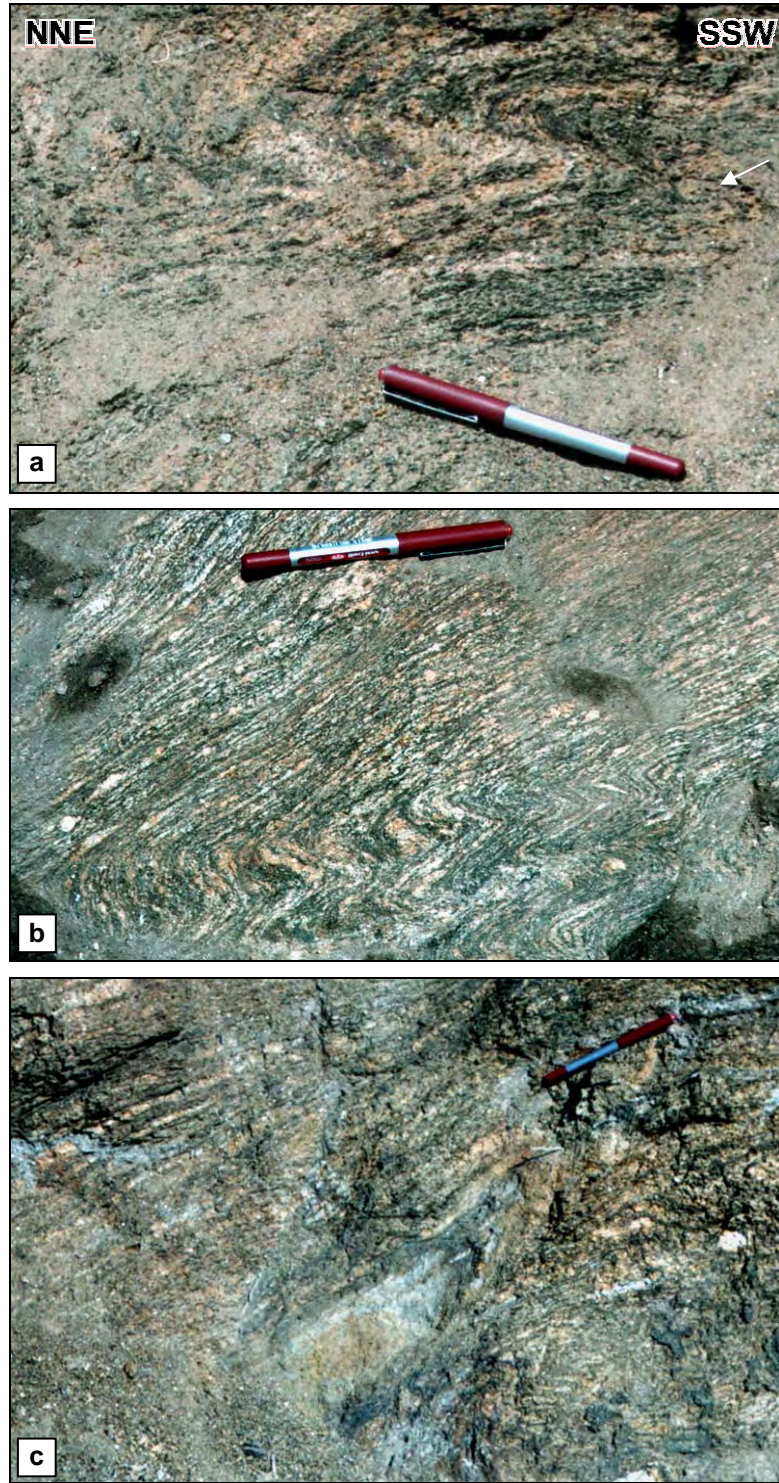


Figure 3.5. Different field views from F_1 folding in migmatites. Pen is 14-cm long. Note a relatively brittle thrust in (a) (arrowed) deforming and offsetting the limbs of an asymmetric clockwise (S-) folds in the migmatites. The geometry of fault and the fold suggest a top-to-the-NNE deformation.

conditions prevailed during their deformation (D_1 deformation) into orthogneisses. A brief account of these observations is given below.

The most common deformational feature observed in feldspars is the development of typical '*core-and-mantle*' microstructure (cf. White 1975), characterized by a rim/mantle of subgrains and dynamically recrystallized new grains enveloping a large feldspar porphyroclasts with highly serrated grain boundaries (Figures 2.6b-c, 3.6a). The core grains show evidence for little internal deformation other than minor fracturing relative to the fine-grained foliated matrix of quartz, feldspar and micas, suggesting that the grain size reduction and subgrain formation occurred through continued fracturing and separation of broken fragments. Pronounced irregular undulatory extinction is ubiquitous in all core grains (Figures 3.6b). The subgrains are easy to recognize because of their relatively larger grain size and comparable misorientation whereas new grains have a tendency to show parallelism to the S-foliation inferred from the direction and sense of shear in the thin-sections. The misorientation is consistent with progressive rotation of subgrains with respect to the host core grain. In relatively high strain zones, the core feldspar grains are partially mantled by new grains and subgrains where new grains tend to spread along the matrix foliation away from the host grain as asymmetric tails, thus producing a typical σ_a porphyroclasts with recrystallized asymmetric tails (cf. Passchier and Simpson 1986; Figure 3.6c). This feature is a common phenomenon of orthogneisses and characteristic feature observed in the field. The observation of both the subgrains and new grains in the mantle around larger core porphyroclasts suggest recovery processes of subgrain rotation and dynamic recrystallization through grain-boundary migration in the feldspars porphyroclasts within '*core-and-mantle*' microstructure. Subgrain rotation as well as grain-boundary migration suggest that both climb- and recrystallization-accommodated dislocation creep were operating in the same sample (cf. Passchier and Trouw 1996). Here the term '*Subgrain rotation*' means that misorientation of the subgrains, indicated by variation in the shade of grey under polars in the microscope, increases progressively from the core of the grain toward the mantle, where there is little or no distinction between recrystallized grains and highly

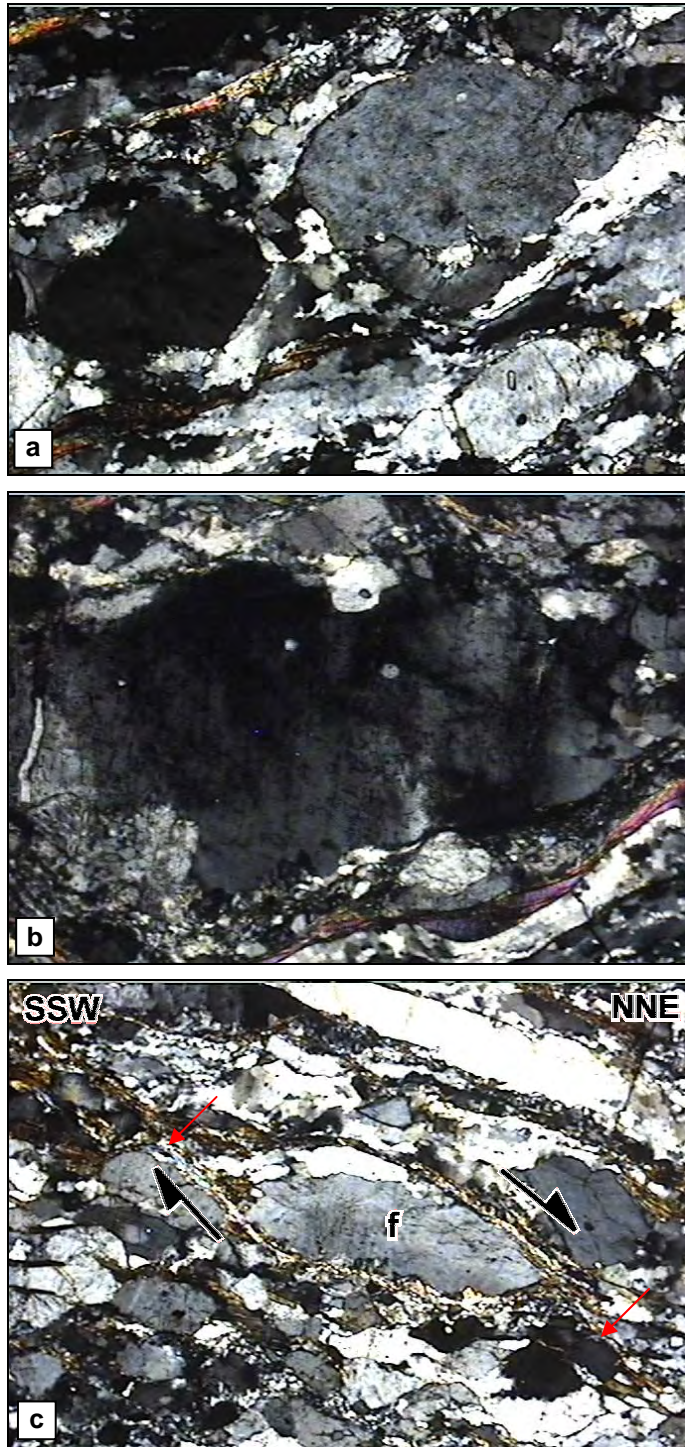


Figure 3.6. Photomicrographs from orthogneisses showing (a) typical core-and-mantle structure defined by large feldspar cores surrounded by small subgrains and dynamically recrystallized new grains around their margins; (b) undulatory extinction of feldspar grains; (c) a typical feldspar porphyroblast (f) defining a core-and-mantle microstructure where recrystallized tails (arrowed) define a stair-step geometry and a σ_a -type porphyroblast indicating a top-to-the-NNE deformation. Fold of each view is 1.5 mm.

misoriented subgrains. '*Dynamic recrystallization/syn-tectonic recrystallization*' is a process by which new crystals form from old grains during the deformation processes. '*Boundary migration recrystallization*' is recrystallization by means of the migration of a grain boundary separating highly strained from unstrained crystal of the same mineral (Twiss and Moores 1992). '*Dislocation*' is a line of defects in a crystal, produced during growth or deformation, and which is thermodynamically unstable (Barker 1990; p. 134). '*Creep*' means continuous, usually slow, deformation of a rock or individual crystal resulting from relatively low stress acting over a long period of time (Barker 1990; p. 133). The serrated grain boundaries of adjacent feldspar grains are also consistent with dynamic recrystallization through grain boundary migration (cf. Tullis and Yund 1980).

Deformation bands and kink bands are common particularly in plagioclases whereas polysynthetic twins occur in some of the matrix K-feldspars (Figures 2.6c, 3.7a-b, 3.8). Although the majority of twins in plagioclases obey the albite twin law, there are many examples of mechanical twinning obeying pericline-law twinning (cf. Smith 1974; Jensen and Starkey 1985; Smith and Brown 1988). Most of the deformation twins have narrow thin needle-shaped geometry and taper to a point or end abruptly within the host grain. The abundance of microkinks and mechanical twins indicates deformation by cataclastic flow and significant amount of twinning and dislocation-climb in feldspars (cf. Tullis and Yund 1987; Pryer 1993)

The most important textural feature of feldspars is ubiquitous development of *myrmekite* – a symplectic intergrowth of vermicular quartz and plagioclase resulting from the retrograde replacement of K-feldspar – on K-feldspar grain boundaries, mostly notably on the long sides of inequant grains parallel to the foliation direction which invariably face maximum finite shortening direction (Z) whereas there is no evidence of such intergrowths on the two sides of the K-feldspar porphyroclast facing the maximum finite elongation direction (X) in the foliation but there are some subgrains and recrystallized new grains (Figure 3.7c). Myrmekitic intergrowths are attributed to the deformation of an incompletely crystallized magma (Hibbard 1979, 1987) or to the imposed stress and consequent concentrations of elastic strain energy, and strain hardening along the K-feldspar grain boundaries some considerable time after crystallization of the magma was

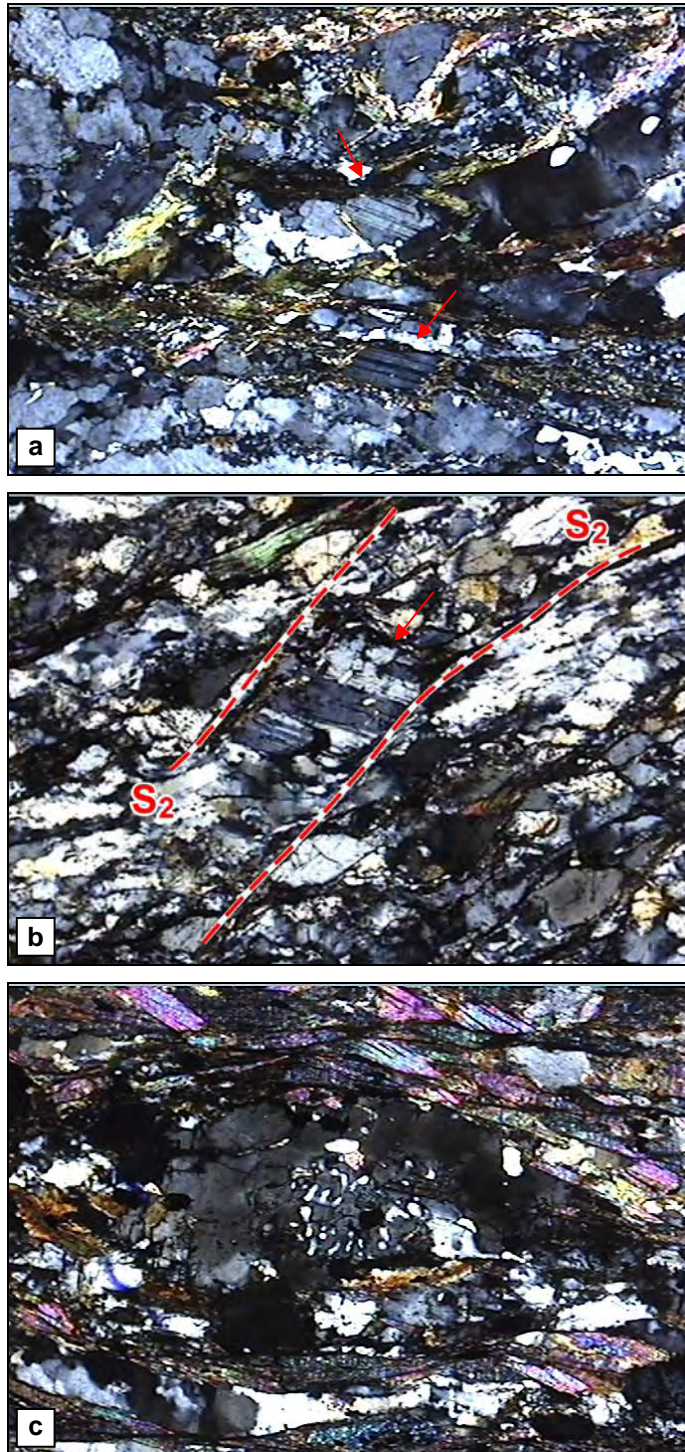


Figure 3.7. Photomicrographs from orthogneisses showing different appearances of deformation twins in feldspars (arrowed) (a,b) and myrmekitic intergrowth of vermicular quartz and plagioclase (c). Please note the development of S₂ foliation in (b) suggesting top-to-NNE deformation. Fold of each view is 1.5 mm.

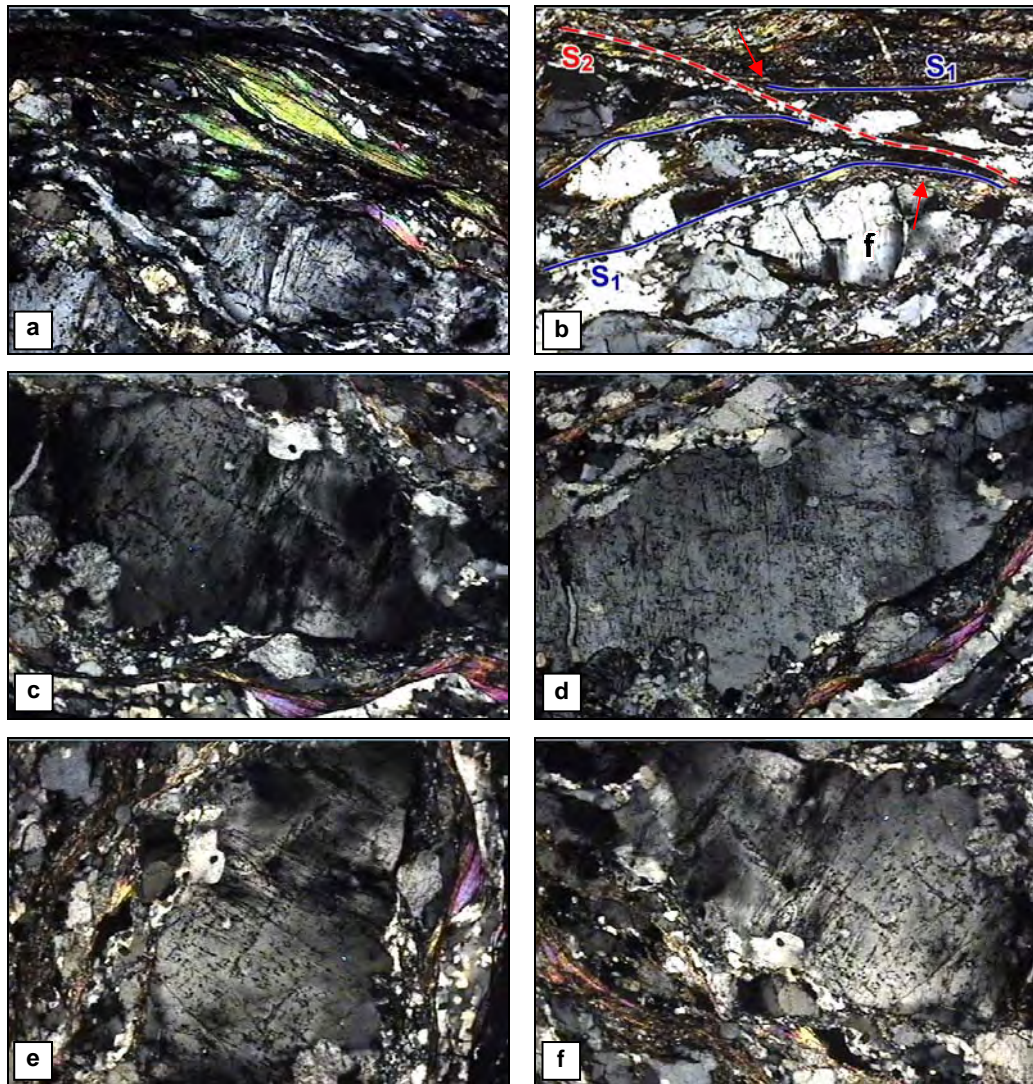


Figure 3.8. Photomicrographs from orthogneisses showing different appearances of deformation twins in feldspars. Please note the brittle fracturing and subgrain formation (f) in (b). The section possesses two sets of foliation. The S_1 foliation is defined by micas and elongated quartz grains. S_2 foliation is represented by a weak fabric where dynamically recrystallized quartz grains define the fabric. Note how S_1 curves into parallelism with S_2 (arrowed). Undulatory extinction is pronounced in all microphotos. Fold of each view is 1.5 mm.

complete (Simpson 1985; Simpson and Wintsch 1989). The former hypothesis requires myrmekitic intergrowths to concentrate around the feldspar porphyroclasts, particularly at their relatively low-pressure sites. However, the myrmekitic intergrowths under discussion are clearly concentrated on the high strain sites of the K-feldspars, thus supporting the strain-related myrmekite formation.

Similar to feldspars the deformation of quartz grains or porphyroclasts in the orthogneisses commonly resulted in the development of typical '*core-and-mantle*' microstructure where broken/fractured, highly strained quartz porphyroclasts in the core is surrounded by a marginal zone composed of subgrains and dynamically recrystallized new fine-grained aggregates (Figure 3.9a). The core grains exhibit undulose extinction, deformation bands and lamellae (Figure 3.9a). The size of subgrains in the mantle decreases away from the large porphyroclasts into new grains developed around them. Quartz also occurs in ribbons of dynamically recrystallized elongate rectangular grains with serrated grain boundaries, similar to the Type 4 quartz ribbons of Boullier and Bouchez (1978; Figure 3.9b). The quartz ribbons are readily recognizable in the field and they show remarkable parallelism with the main foliation of the rock defined by the mica laths. In such cases, the rock exhibits a gneissic foliation of alternating quartz-rich and mica-rich domains where the size and growth of quartz is controlled/determined by the micas. In some thin-sections, the newly recrystallized elongate quartz grains show preferred orientation with their long axis oblique or at a low angle to the main foliation of the rock (c-foliation). Some of the matrix grains show high temperature plasticity with polygonal grains. The features associated with quartz deformation suggest non-coaxial, crystal-plastic deformation where highly serrated crystal boundaries indicate higher mobility and migration of the grain boundaries (cf. Passchier and Trouw 1996). The presence of serrated grain boundaries (Figure 3.9c) also suggests that the new grain recrystallization is associated with primary dynamic recrystallization via strain hardening (White 1977; Twiss and Moores 1992). The common observation of undulose extinction in both new recrystallized grains and subgrains of feldspars and quartz suggest early stages of subgrain development and continuum of deformation following their formation.

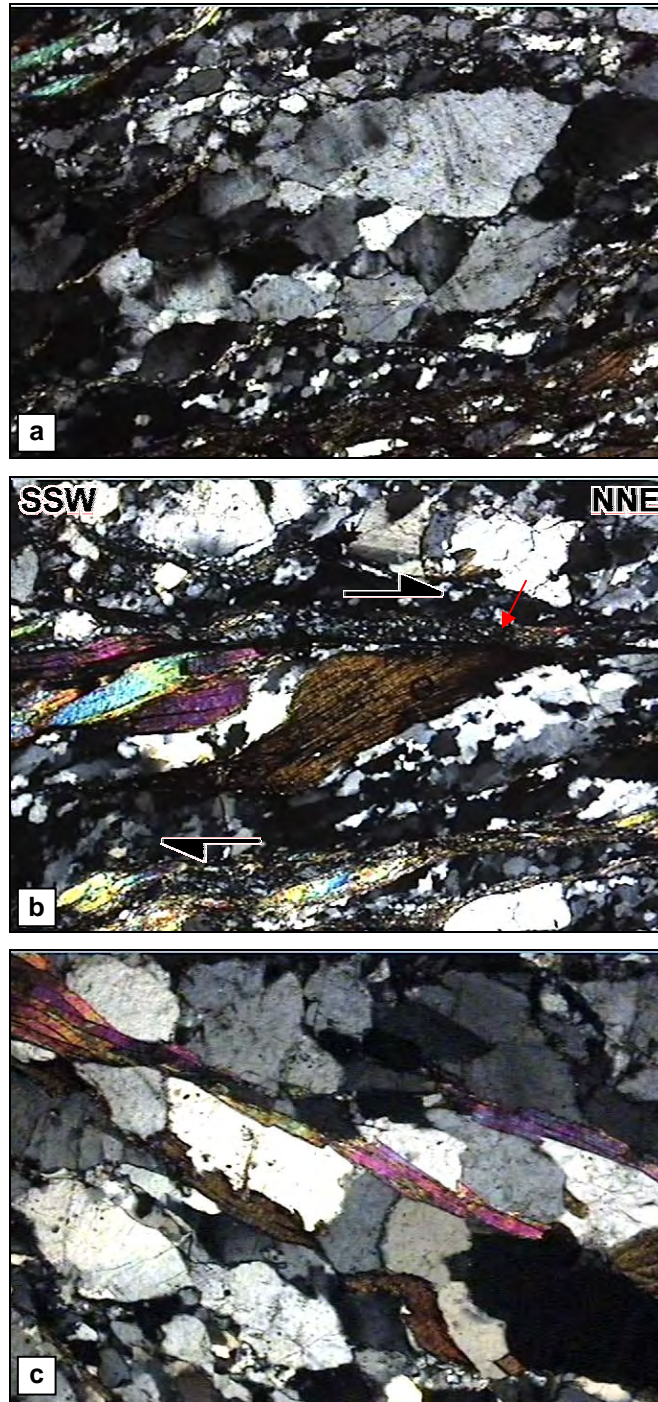


Figure 3.9. Photomicrographs from orthogneisses showing **(a)** quartz sub-grains in the core surrounded by dynamically recrystallized fine-grained aggregates; **(b)** a biotite porphyroblast defining a mica-fish structure. Dynamically recrystallized elongate quartz grains define an oblique-grain shape foliation, typical to Type 4 ribbon structure. Note intense granulation along C-surfaces (arrowed). The asymmetry of 'mica-fish' and oblique grain shape foliation defined by quartz grains indicate a top-to-the-NNE shearing; **(c)** serrated grain boundaries on quartz. Note how shape and size of quartz is controlled by mica blades. Fold of each view is 1.5 mm.

Most of the mica grains, both muscovite and biotite, in the mylonitic orthogneisses are recrystallized or mechanically rotated minerals and they show preferred parallelism to the S_1 main foliation of the rock. Larger biotite occurs as porphyroclasts oriented with their (001) surfaces at an angle to the S_1 foliation facing the incremental shortening direction (Figure 3.9b). Evidence of strain such as undulatory extinction, bending and kinking, particularly in biotite grains is very common. Some exhibit signs of brittle deformation with broken or even displaced grains. The structures associated with micas are consistent with internal deformation by bend-gliding, kinking and fracturing.

3.3.3. Shear-sense Indicators

The use of shear criteria to determine the movement sense of shear zones was critical to this study. Movement senses were determined at both the outcrop scale and under the microscope using oriented samples. The vergence and asymmetry of intrafolial folds (Figures 2.10b and 3.5a), the asymmetry of feldspar porphyroblasts (Figures 2.3a-b, and 3.6a), C' -foliation, spiral-shaped inclusion trails in garnet porphyroblasts, S-C foliation, mica-fish (Figure 3.9b), oblique-grain shape fabrics (Figure 3.9b), all suggest an unambiguous non-coaxial deformation during the D_1 deformation and a shear sense of upper levels moving up to the NNE (Figures 3.10, 3.11 and 3.12).

3.4. D_2 Deformation

D_2 deformation is expressed by the widespread development of mylonitic S_2 foliation invariably associated with NNE–SSW-trending mineral elongation/stretching lineation (L_2). S_2 fabrics are developed within the metamorphic rocks of the study area, but they are well-expressed in the orthogneisses overprinting the regional S_1 foliation (Figures 2.3a-b, 3.7a, 3.8a, 3.10, 3.13, 3.14). The S_2 foliation shows progressive increase in pervasiveness up structural section towards the contact with the overlying Neogene sediments.

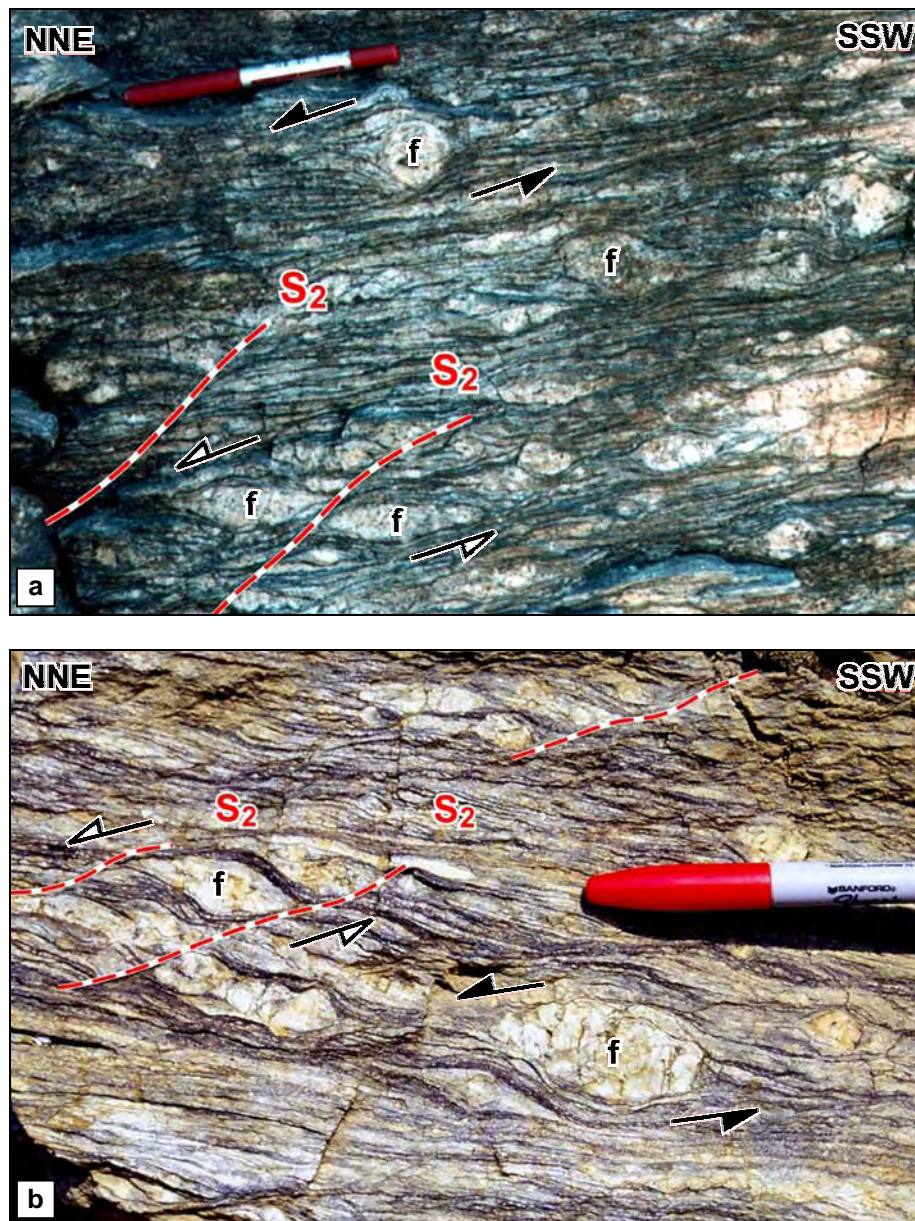


Figure 3.10. The main regional foliation (S_1) on the orthogneisses near Döğüşören (a) and Çavullar (b) villages. The σ -type feldspar porphyroclasts (f) indicate a top-to-the-N-NNE motion. Note how ductile foliation wraps around the porphyroclasts. Smaller feldspar porphyroclasts are elongated in the plane of foliation. Quartz ribbons are evident. Pen is 14 cm long. Please also note that S_2 foliation is overprinting the S_1 suggesting a top-to-the-NNE shearing.

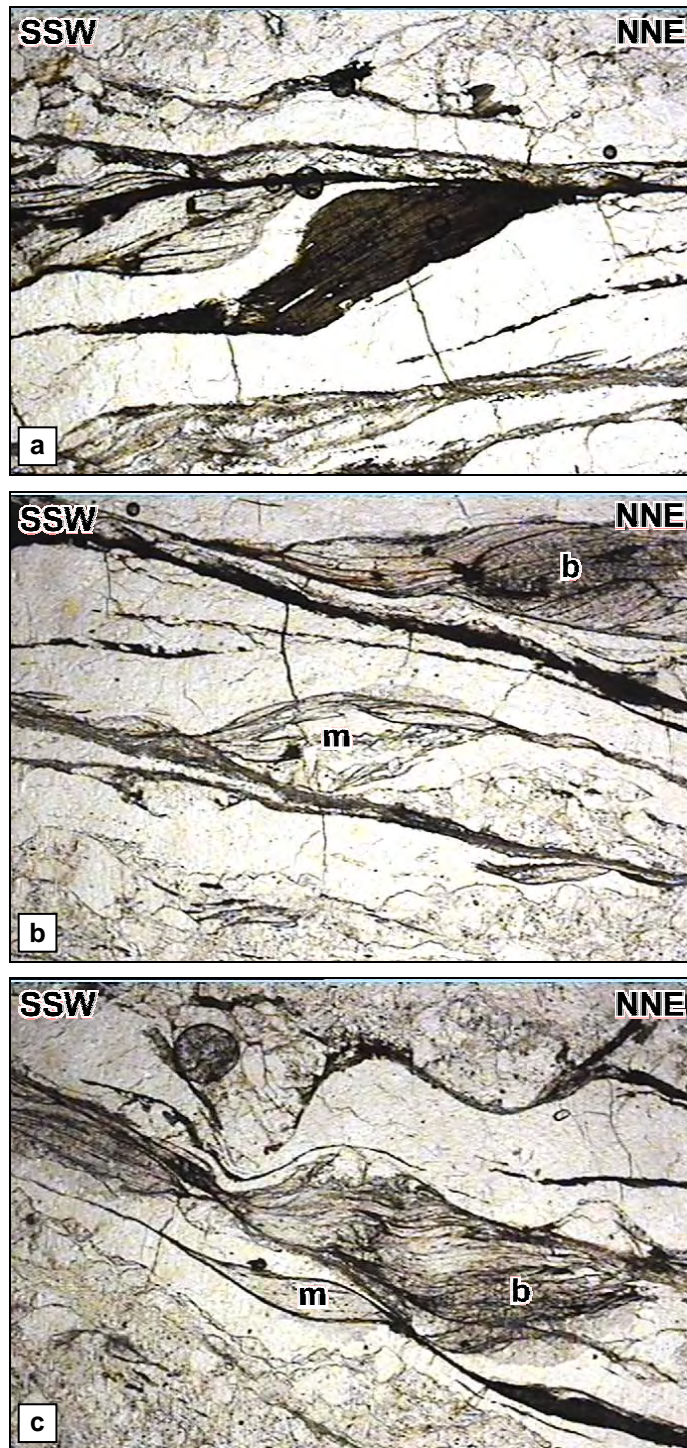


Figure 3.11. Photomicrographs from orthogneisses showing various shear sense indicators. **(a)** A large biotite porphyroblast defining a well-developed mica-fish structure indicating a top-to-the-NNE shear sense (same view of Figure 3.9b under plane polarized light); **(b, c)** mica-fish structures defined by muscovite porphyroblasts indicating a top-to-the-NNE movement. Please note how stretched mica (m) defines a stair-stepping geometry (typical to σ_a -type porphyroblasts). Fold of each view is 1.5 mm.

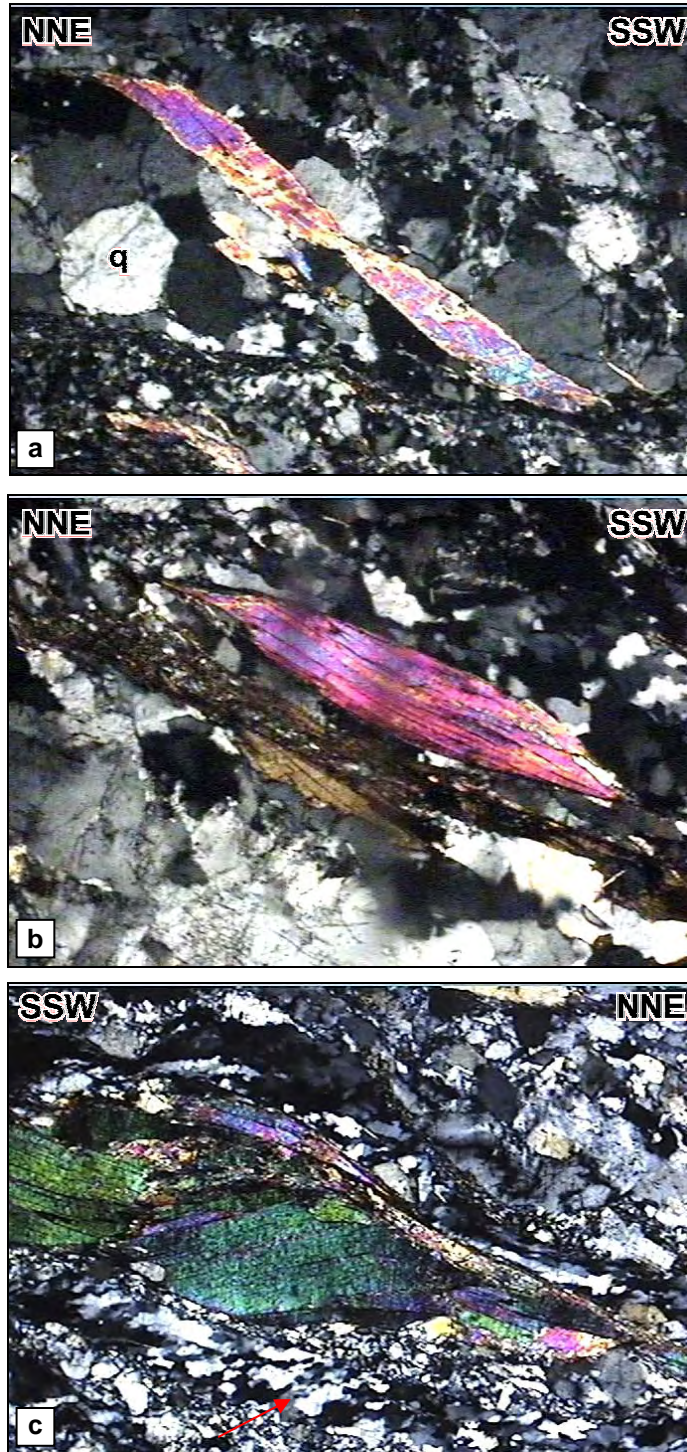


Figure 3.12. Photomicrographs from orthogneisses showing muscovite minerals, defining well-developed mica-fish structures indicating a top-to-the-NNE deformation, in a matrix composed mainly of quartz. Note polygonal quartz grains (q) in (a) suggesting relatively high-temperature conditions of deformation. In (c) elongate quartz grains define a typical grain-shape foliation with their long axis being parallel to each other (arrowed). Fold of each view is 1.5 mm.

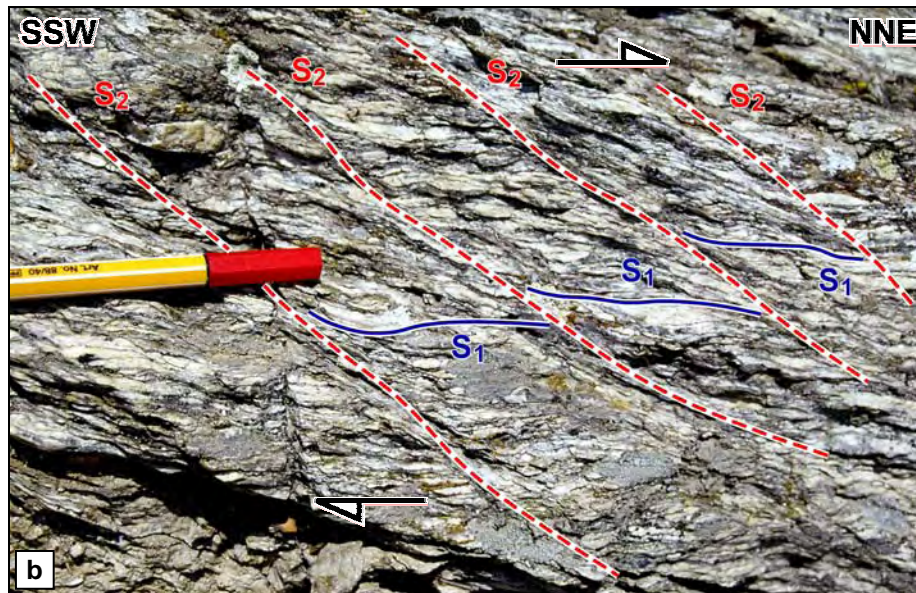
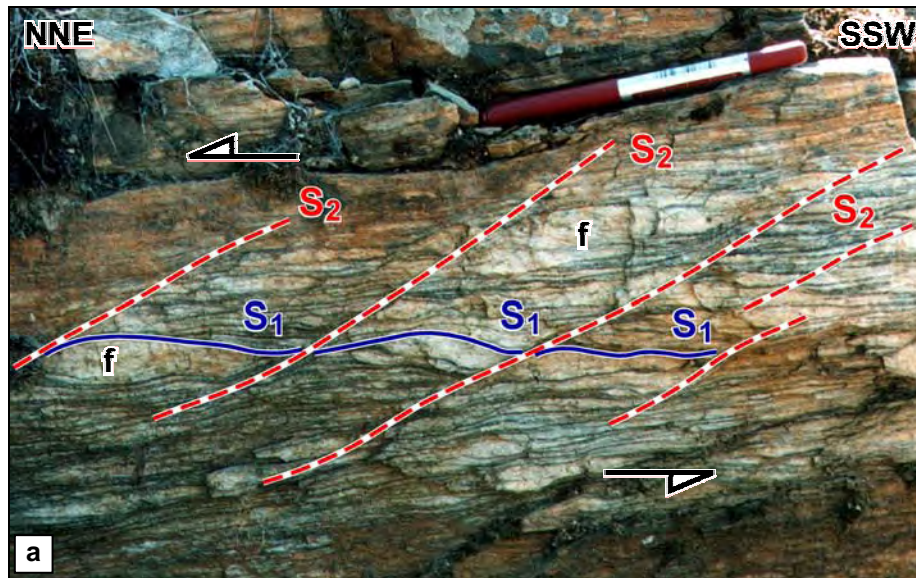


Figure 3.13. (a) The S_2 foliation (from upper right to lower left) overprinting the main regional foliation (S_1) on the orthogneisses near Doğuşören village. Typical C'-type shear band foliation indicating a top-to-the-NNE shearing is clearly observable. Please also note how S_1 foliation is intense and defined by preferred parallel alignment of flattened feldspar porphyroclasts (f), quartz ribbons and micas. Pen is 14-cm long. **(b)** The S_2 foliation (from upper left to lower right) overprinting the main regional foliation (S_1) on the orthogneisses near Yardere village. Part of the pen is 8-cm long. Note how S_1 foliation curves into parallelism with S_2 foliation.

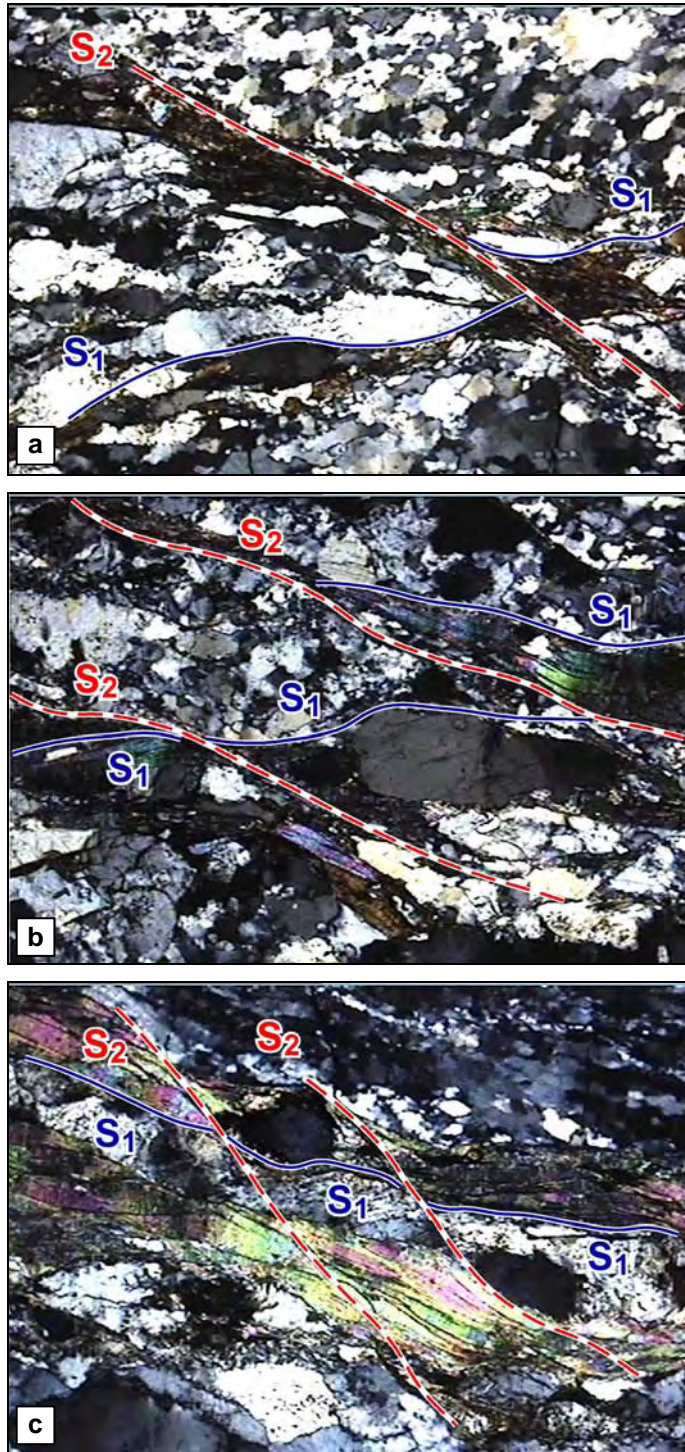


Figure 3.14. Photomicrographs from orthogneisses showing the primary main regional foliation (S_1) defined by parallel alignment of quartz, micas and elongated feldspar, and the secondary foliation (S_2) overprinting the first one. Please note that in (a) and (b) S_2 foliation strongly overprints S_1 and the quartz-rich domains defining the S_1 abruptly ends near the micas defining S_2 , and that in (c). The S_2 foliation is weaker than in (a) and (b). Chlorite replacement along S_2 is evident in (a). Fold of each view is 1.5 mm.

S_2 fabrics are represented by a well-developed shear band foliation strongly overprinting the earlier S_1 foliation. Where the shear band foliation is pervasive the S_1 foliation is preserved as curved or inclined foliation in microlithons/domains between adjacent parallel shear bands (Figures 2.3b, 2.4a, 3.8a, 3.13, and 3.14).

The S_2 foliation has a general trend of NW–SE ($\sim 134^\circ\text{N}$) and the average dip is approximately 36° towards NE. Figure 3.15 shows a stereogram of the S_2 foliation where 21 poles have been plotted and contoured on a Schmidt net, lower hemisphere projection. It also shows a uniformity of dip, with moderate-gentle dip values, and a concentration of dips at around 36°N . The present-day configuration of shear bands suggests a non-coaxial flow with a down-dip sense of shear, top-to-the-NNE; this direction is parallel to the local mineral stretching lineation. The retrograde metamorphic reactions under (?) greenschist facies conditions is common along shear band foliations and expressed by the development of retrogressive chlorite replacing biotite.

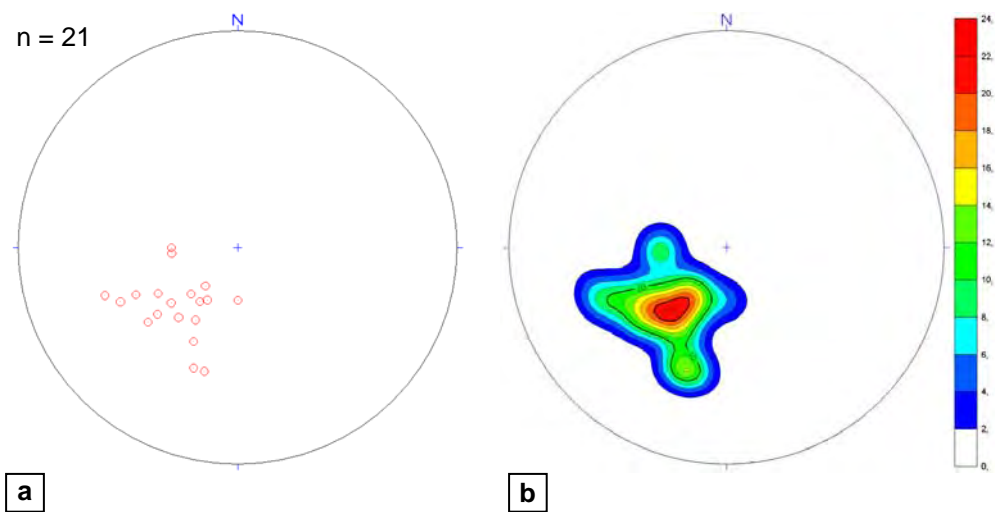


Figure 3.15. Lower hemisphere stereonet (Schmidt net) projections **(a)** and contour plot of poles to S_2 foliation on orthogneisses **(b)**.

3.4.1. Detachment Faulting

The nature of the upper contact of the metamorphic rocks with Neogene sediments in the present area is largely obscured because: (i) the contact is poorly exposed or covered by dense vegetation or (ii) simply the metamorphic rocks are unconformably overlain by the youngest representatives of the Neogene sediments. There is only one locality where the upper contact of the orthogneisses with the Neogene sediments is observed. In this locality to the southwest of Çavullar (Figure 2.1) the metamorphic rocks are separated from the overlying Neogene sediments by an approximately E–W-trending, north-dipping presently low-angle normal fault (Figures 2.21, 3.16, 3.17). The footwall rocks show evidence for brittle deformation with brecciation and iron-oxide development where the regional S_1 foliation and S_2 shear band foliation are destroyed (Figure 3.17). The rock is characterized by relatively extensive development of fractures filled with iron oxide. Although it is poorly exposed and preserved because of extensive weathering, the contact between the brecciated rocks and the underlying mylonitic orthogneisses is interpreted as gradual, suggesting the progressiveness of deformation from ductile to brittle conditions. The fault plane is ornamented by the extensive development of slip-lineations approximately parallel to the general trend of the local mineral stretching lineation in the footwall rocks, indicating the genetic relationships between the fault and the underlying mylonites.

3.4.2. F_2 Folding

The S_1 foliation in the metamorphics of the study area is later deformed by a mapable-scale F_2 fold trending in a NNE–SSW direction approximately parallel to the mineral elongation lineation (Figure 2.1). The S_1 foliation is generally approximately NE–SW trending and uniformly developed throughout the study area. Figure 3.18 shows a stereogram of the S_1 foliations where 135 poles have been plotted and contoured on a Schmidt net, lower hemisphere projection. It shows the variation in dip direction produced by the F_2 folding, with generally moderate dip values, and a concentration of dips at around 58°SE and 43°NW .



Figure 3.16. The presently low-angle fault comprising the boundary between orthogneisses and Neogene sedimentary rocks near Çavullar.

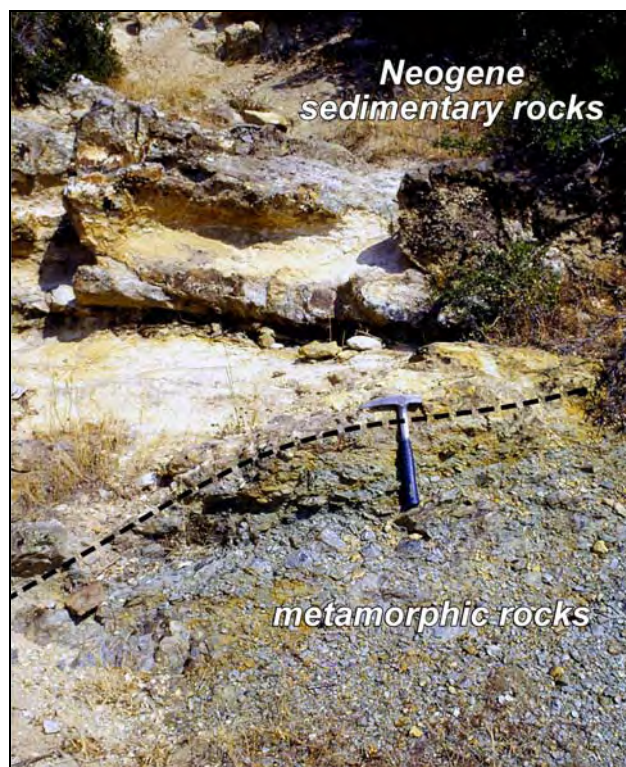


Figure 3.17. Close-up view of the metamorphic-sedimentary rock contact where the footwall rocks show evidence for brittle deformation with brecciation and iron-oxide development. The regional S_1 foliation and S_2 shear band foliation are destroyed. Hammer is 33-cm long.

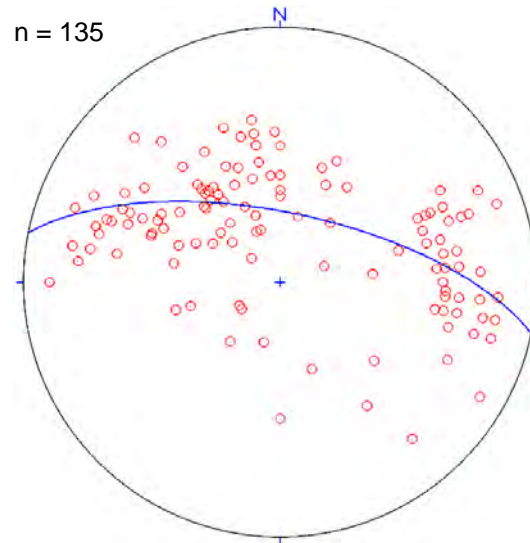


Figure 3.18. Lower hemisphere stereonet (Schmidh net) projections of poles to foliations on migmatites and schists. Best fit great circle to poles is π -griddle.

The general trend of this fold indicates approximately WNW–ESE-directed compression, which is perpendicular to the general direction of NNE-trending extension in the study area.

Although the strike, dip and dip direction of the foliation are variable at several localities, the distribution of poles to the foliation planes of schists and migmatites (Figure 3.18) clearly reflect the presence of an anticline located on the NW of the study area; it is here named as Çomaklıdağı anticline. The poles to foliation planes of schists (Figure 3.3a) are concentrated on the W and E quadrants of the northern half of the stereonet, indicating a NE–SW trending fold axis and SE and NE dipping limbs of the anticline. The poles to foliation planes of migmatites (Figure 3.3c) display dense concentration on the NW quadrant and the eastern side of the stereogram after being deformed by a NE-trending and SE-plunging anticline. In Figure 3.18, the poles to foliation planes of schists and migmatites are displayed together and the best fit great circle passing from the pole distributions (π -griddle) is plotted. The attitude of π -griddle is found to be $281^{\circ}\text{N}/68^{\circ}\text{NE}$. Therefore the attitude of the hinge line is calculated as $22^{\circ}/192^{\circ}$, which proves the presence of NNE–SSW-trending, SW-plunging asymmetrical anticline on the northwestern parts of the study area.

3.5. D₃ Deformation

The last deformation phase affected the study area and indeed the whole western Anatolia is the neotectonic brittle high-angle normal faulting (D₃) during the modern phase of N-S extension. The faults formed during this deformation generally define the boundaries between the Neogene sedimentary rocks of the Gördes and Demirci basins, and the metamorphic rocks of the Menderes Massif within the study area. The localities where the Neogene sediments are cut and displaced by normal faults and put into direct contact with the metamorphics include the following regions: the area between Kınık and Mestanlı villages, northern areas of Yardere village and western parts of the Dikilitaş village. The field observations at these localities will be summarized below.

3.5.1. Kınık-Mestanlı Area

The region between Kınık and Mestanlı villages on the south of the area is an ideal location to investigate the boundary relationships between the sedimentary basin fills and the metamorphic rocks exposed in the area. There, the contact between the sedimentary units of Demirci Basin and the orthogneisses is an oblique-slip normal fault formed during the regional neotectonic (D₃) deformation which affected whole western Anatolia (see Chapter 1 for details). On the road from Kınık to Mestanlı village, the fault plane itself, slip-lineations, and other related structures are well-exposed (Figures 3.19a-c, 3.20). This is the best location to collect fault-slip data and to study the kinematics of D₃ normal faulting within the study area.

During the field studies, numerous slip measurements were taken from this fault plane. The collected data is summarized in Table 3.1. As seen in Table 3.1, the fault slip data can be categorized in two different sets: (1) the fault planes with rake angles more than 45° (between 50° and 70°) and (2) the ones with rake angles less than 45° (between 35° and 40°) (Table 3.1). The average

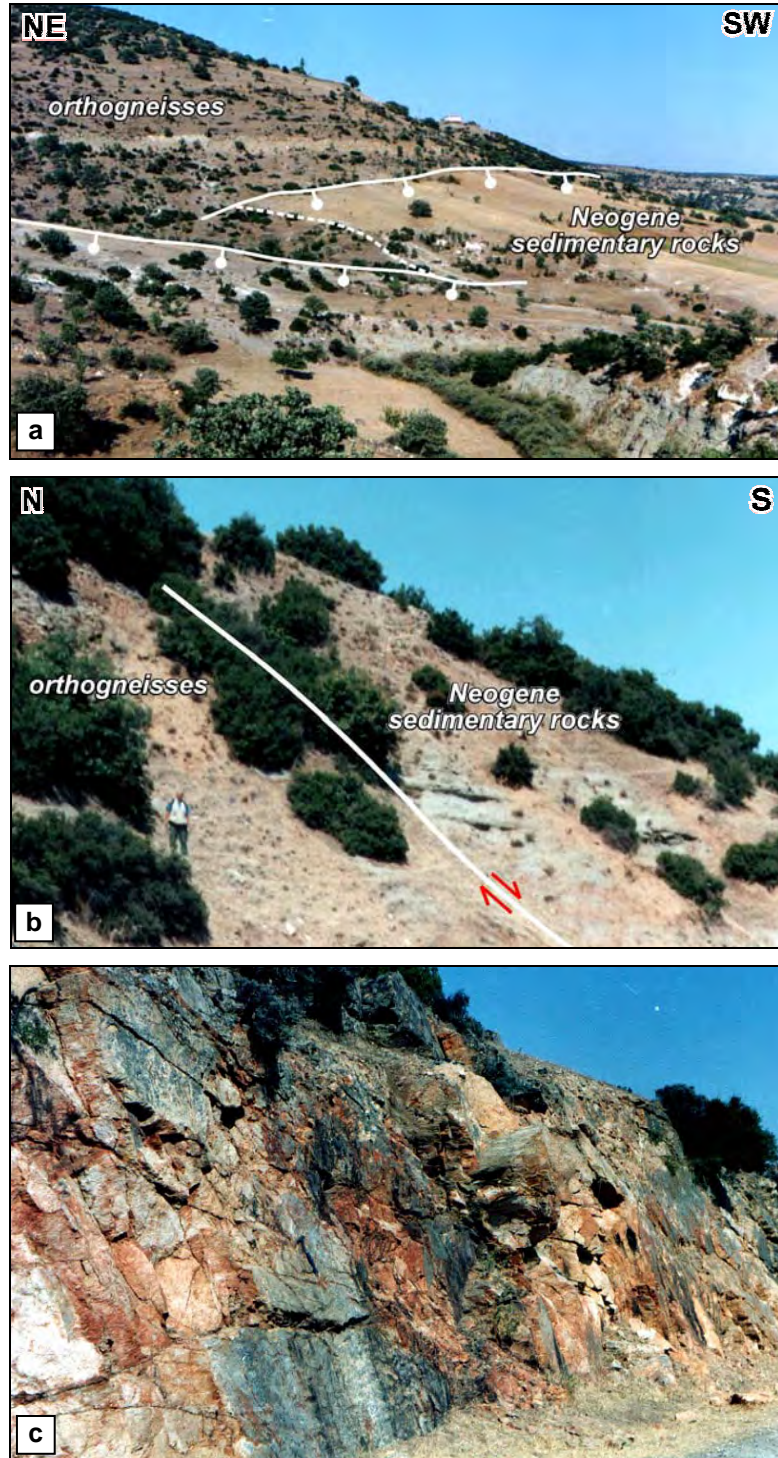


Figure 3.19. General views of the faulted contact between orthogneisses and Neogene sedimentary rocks from the area between Kınık and Mestanlı **(a)** and east of Kınık **(b)**. Note how bedding in the Neogene sediments terminates against the orthogneisses along the fault plane; the juxtaposition is pronounced. Scale is 170 cm high. **(c)** General view of the fault plane exposed between Kınık and Mestanlı villages. Hammer is 33-cm long.

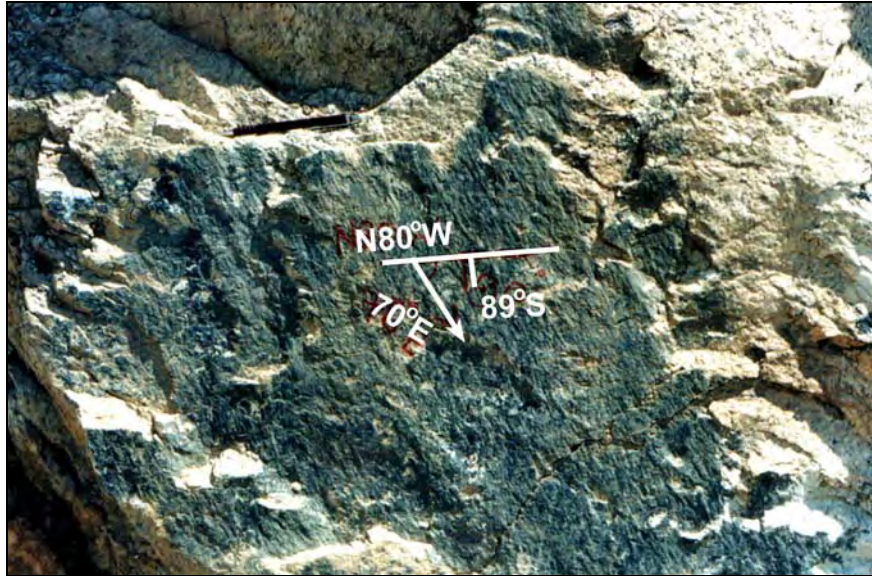


Figure 3.20. Close-up view of the fault plane and slip lineations on the same fault plane. Pencil is 14-cm long.

Table 3.1. Selected fault plane measurements from Kınık–Mestanlı area.

Strike (°N)	Dip amount (°SW)	Rake (°E)	Sense	Principal stress axes	ϕ
280	89	70	Normal + Left Lateral		
290	88	55	Normal + Left Lateral		
295	88	53	Normal + Left Lateral	$\sigma_1 = 61^\circ/034^\circ$	0.983
300	69	50	Normal + Left Lateral	$\sigma_2 = 14^\circ/277^\circ$	
310	68	57	Normal + Left Lateral	$\sigma_3 = 25^\circ/180^\circ$	
300	63	52	Normal + Left Lateral		
Mean: 296	78	56	Normal + Left Lateral		
305	70	40	Left Lateral + Normal	$\sigma_1 = 18^\circ/091^\circ$	0.510
300	65	35	Left Lateral + Normal	$\sigma_2 = 56^\circ/332^\circ$	
300	89	40	Left Lateral + Normal	$\sigma_3 = 27^\circ/191^\circ$	
305	67	35	Left Lateral + Normal		
Mean: 303	73	38	Left Lateral + Normal		

attitude (strike and the dip amount and direction) of the measured fault planes is WNW–ESE (~299°N) and 76° SW.

In order to determine the kinematic framework of faulting during this latest extensional period, the fault kinematic analysis using the data from striated fault planes of the high-angle normal fault in Kınık–Mestanlı area (Table 3.1) is performed. The fault slip data are analyzed, using the stress inversion method of Angelier (1984, 1991). The inverse analysis of fault-slip data allows the determination of stress orientations from measurements of fault slip data (the orientation and sense of slip along numerous faults: e.g., Angelier 1984, 1991).

The method is based on the assumption that the rigid block displacement is independent and that the stria on a fault plane is parallel to the maximum resolved shear stress (τ) applied on this fault (Carey and Brunier 1974; Carey 1979; Angelier 1984; Lisle 1987; Means 1987). All inversion results include the orientation (plunge and azimuth) of the principal stress axes as well as the 'stress ratio (φ)' [$\varphi = (\sigma_2 - \sigma_1) / (\sigma_3 - \sigma_1)$], a linear quantity describing relative stress magnitudes. The stress axes σ_1 , σ_2 , and σ_3 correspond to maximum intermediate, and minimum principal stress axes, respectively (see Angelier 1984 for the details of stress inversion procedure).

The analysis is carried separately for the two different sets of fault data and the computed results are tabulated in Table 3.1. For the higher rake faults the calculated σ_1 trends in 034° and plunges steeply at 61°, whereas σ_2 , and σ_3 axes have average attitudes of 14°/277° and 25°/180°, respectively (Table 3.1, Figure 3.21). Computed results of fault slip data define a N–S extension which is conformable with the present day configuration of western Turkey. When the fault planes with lower rake values are concerned the calculated principal stress axes have the following attitudes: $\sigma_1 = 18^\circ/091^\circ$, $\sigma_2 = 56^\circ/332^\circ$ and $\sigma_3 = 27^\circ/191^\circ$ (Table 3.1, Figure 3.22). The data is rather consistent with an approximately E–W-trending compression during faulting.

As seen in Figure 3.23, when moved from the area between Kınık and Mestanlı, where Neogene sedimentary rocks and metamorphic rocks are bounded by a normal fault, towards southernmost parts of the study area, the

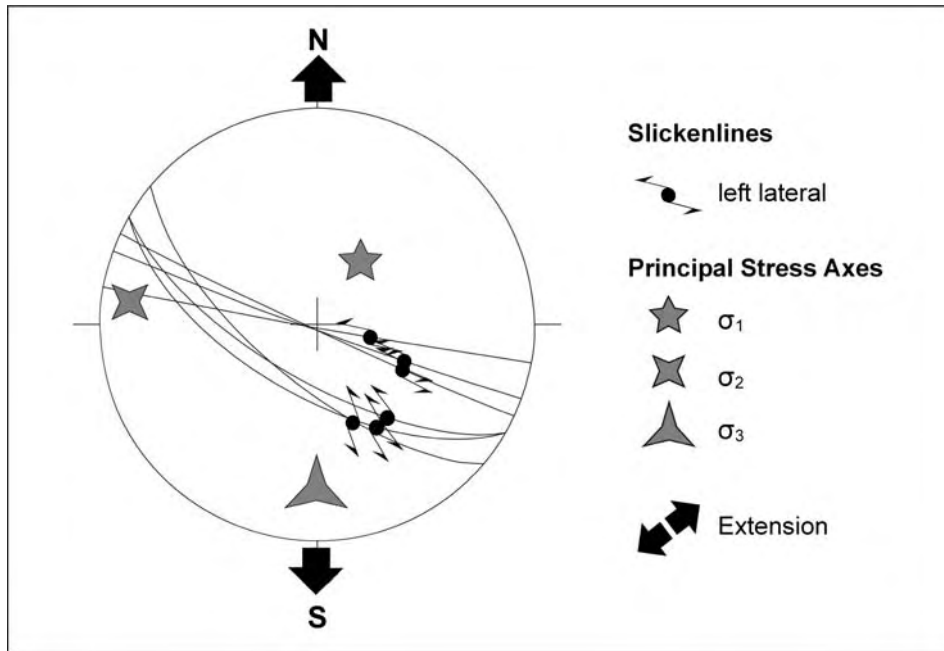


Figure 3.21. Schmidth lower hemisphere equal-area projections of fault slip data with higher rake angles from Kınık–Mestanlı area. Great circles are fault surfaces, the arrows are slickensides (see Table 3.1 for details).

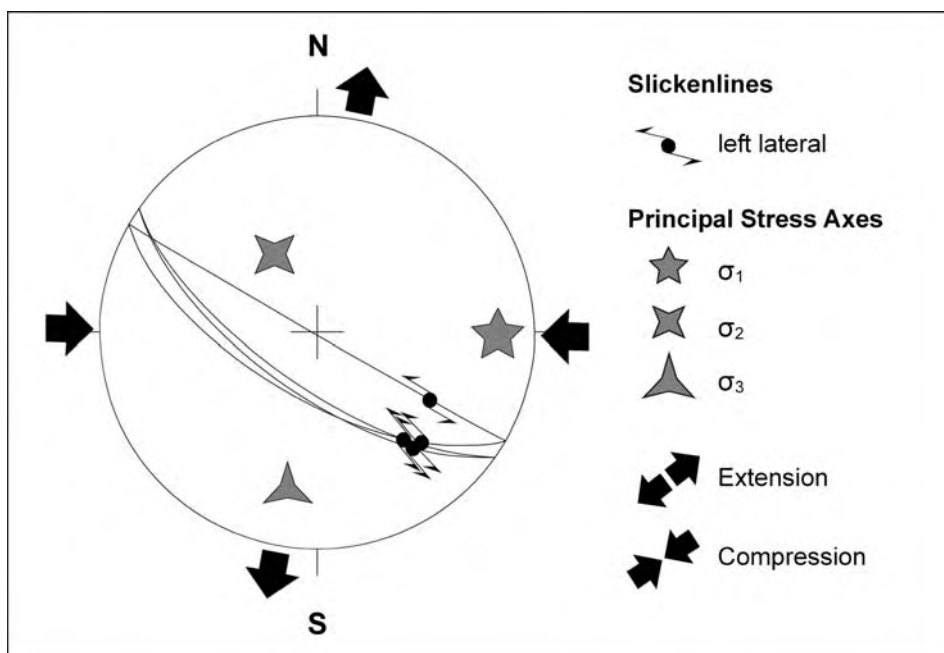


Figure 3.22. Schmidth lower hemisphere equal-area projections of fault slip data with lower rake angles from Kınık–Mestanlı area. Great circles are fault surfaces, the arrows are slickensides (see Table 3.1 for details).

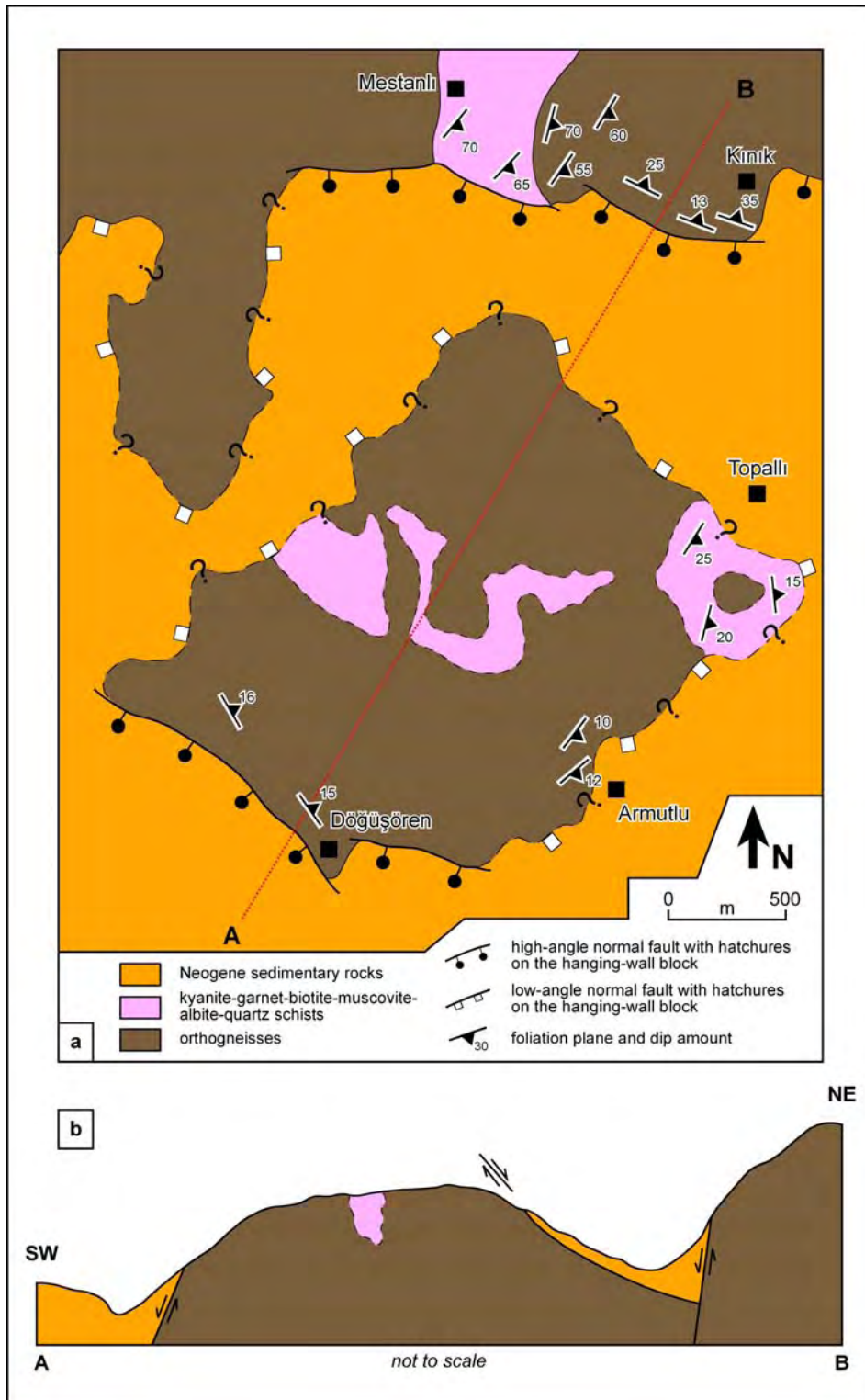


Figure 3.23. (a) Geological map of Kınık and surroundings; **(b)** cross-section along line A-B.

metamorphic rocks crop out again on the region between Topallı, Armutlu and Döğüşören villages. Although, it could not be possible to observe and examine any fault plane, the field observations reflect that the boundary relationship between the Neogene sedimentary rocks and the metamorphic rocks is possibly a (normal) fault at the southernmost parts of this area, namely, near Döğüşören and Armutlu villages. However, near Topallı village, there is no evidence for the contact between Neogene sediments and the metamorphics being a high-angle fault, but it may be a presently low-angle fault or an unconformity. Therefore, the current situation in the southern parts of the study area is speculated to be as shown in Figure 3.23.

3.5.2. Yardere Area

In the whole study area, the boundary relationships between Neogene sedimentary basin fill and the Menderes Massif metamorphic rocks are of two types. The first type is high-angle normal faulting due to regional D_3 faulting as explained in the previous section. The second contact type is a presently low-angle normal fault (detachment fault) which was presumably active prior to the deposition of youngest representation of sedimentary fill. These different boundary types can be observed in several locations within the study area; Yardere village forms one of the type localities where such boundary relations are observed.

As seen on the geological map of the study area (Figure 2.1) and the detailed geological map of the Yardere region (Figure 3.24), on the northern parts of the village, orthogneisses are in direct contact with Neogene sedimentary rocks of Demirci Basin. The boundary between these two units is a normal fault exposed on the north of Çatal Tepe which is situated just on the northeast of Yardere (Figure 3.26). The morphology of the area and the field relationship between the rock units clearly demonstrate the presence of this fault. The fault has a general E–W trend between NW of Gazlı Mahallesi and E of Çatal Tepe, but no fault plane is preserved.

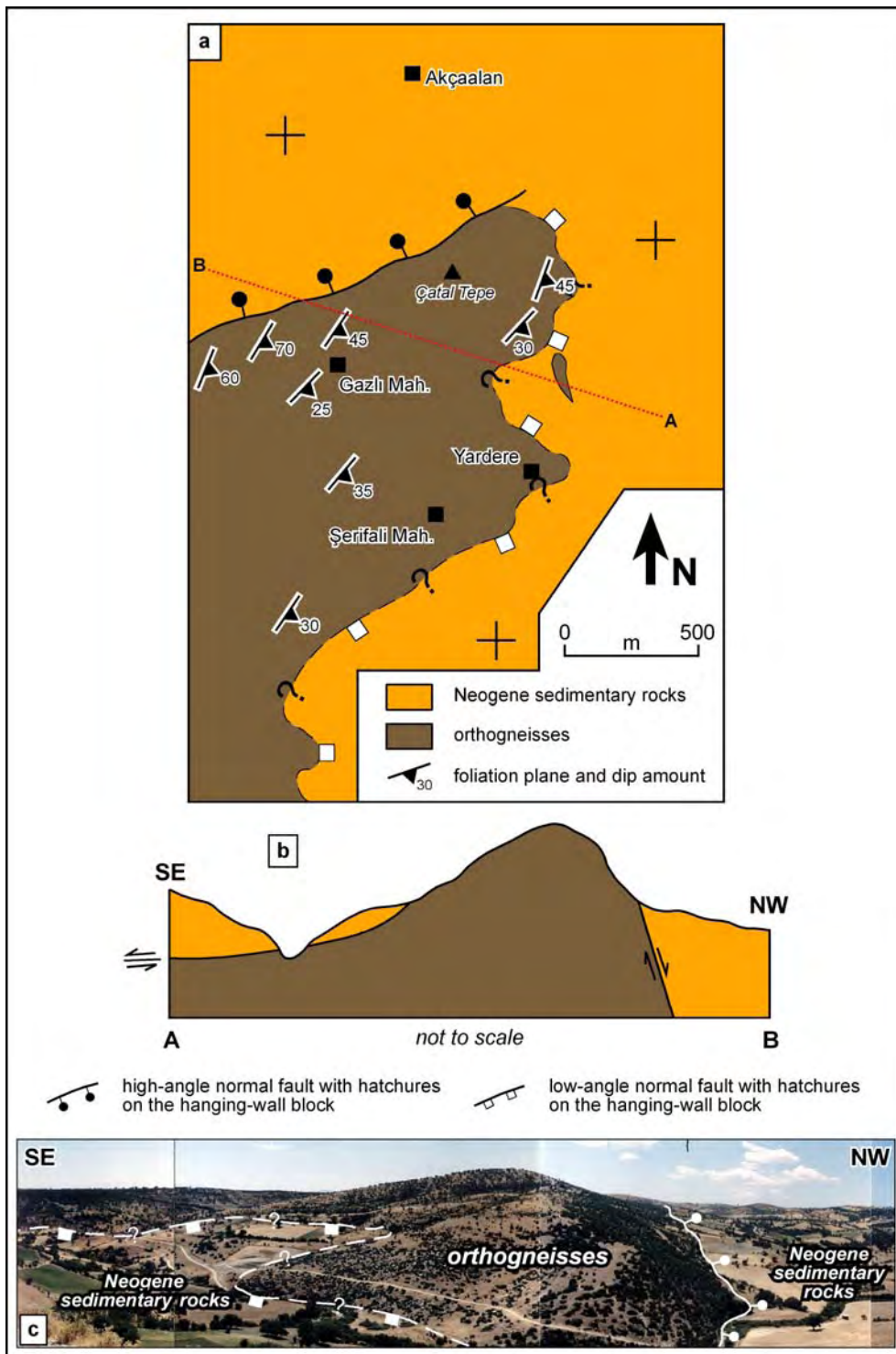


Figure 3.24. (a) Detailed geological map of Yardere region and surroundings; (b) cross-section along line A-B; (c) photograph along line A-B.

Just on the northeast of Yardere, on the southern parts of the normal fault and Çatal Tepe, the contact between the Neogene sediments and the metamorphics is interpreted as a low-angle fault surface. As moved from Çatal Tepe towards southeast in the downslope direction (Figure 3.24a), the orthogneisses present on the topographically higher parts pass into Neogene sediments on the topographically lower parts and there is not a dramatic change in the slope, as present in the north.

Inside the deeper parts of the valley, which is eroded by the stream flowing from the east of Çatal Tepe towards south in approximately N–S direction, the sedimentary units first pass into basal conglomerate with large angular gneiss fragments, and in the very deep parts of the valley, the orthogneisses are exposed.

Under the light of these observations, the geologic relationship between the rock units present on the Yardere village and surroundings are concluded to be as presented on the Figure 3.24. It is very clear that these sediments post-date the arrival of orthogneisses to surface as they contain large fragments derived from them. But, these sediments form the youngest representation of Demirci Basin that onlap the faulted margins. In this respect, the contact is a typical nonconformity which developed on top of a presently-low angle normal fault operating during the early stages of basin fill sedimentation. Another to say, the fault was synchronous with the older basin fill – while the metamorphic rocks were deformed in the footwall, sediments were deposited on the hangingwall.

3.5.3. Dikilitaş Area

Another locality where the boundary between Neogene sedimentary rocks and the orthogneisses is a high-angle normal fault is Dikilitaş region. The contacts on both the northwestern and southwestern sides of Dikilitaş are fault contacts (Figure 2.1). The fault plane itself is not exposed but the second order minor mesofaults are common in the region (Figure 3.25) from which numerous slip measurements were taken.



Figure 3.25. A close-up view of an exposed small-scale fault plane near Dikilitaş. Pencil is 14-cm long.

The collected data is summarized in Table 3.2. According to these measurements, the general trend and the dip of the fault are found to be NW–SE ($\sim 296^\circ\text{N}$) and 69° NE on the average, respectively. The rake measurements vary between 70° and 85° from W (average: 76° ; Figure 3.26; Table 3.2).

Similar to the Kınık–Mestanlı fault, the slip data of this fault are also analyzed using the stress inversion method of Angelier (1984, 1991), details of which are given in the related section. Computed results of fault slip data define again a nearly N–S extension. The calculated σ_1 has a trend of 228° and a dip of 66° , whereas σ_2 and σ_3 axes have the following attitudes, respectively: $18^\circ/091^\circ$ and $15^\circ/356^\circ$, respectively (Table 3.2, Figure 3.26).

These results suggest that the southern Dikilitaş fault is an oblique-slip normal fault with a minor left-lateral strike-slip component. The average rake angle of slickenlines is found to be 76° , which also means that the normal component is dominant. These data once again prove that the high-angle normal faults are formed due to N–S extension which reflects the present day configuration of western Turkey.

Table 3.2. Fault plane measurements from Dikilitaş area.

Strike (°N)	Dip amount (°N)	Rake (°W)	Sense	Principal stress axes	ϕ
245	55	70	Normal + Left Lateral	$\sigma_1=66^\circ/228^\circ$ $\sigma_2=18^\circ/091^\circ$ $\sigma_3=15^\circ/356^\circ$	0.226
305	89	72	Normal + Left Lateral		
315	65	85	Normal + Left Lateral		
320	65	75	Normal + Left Lateral		
Mean: 296	69	76	Normal + Left Lateral		

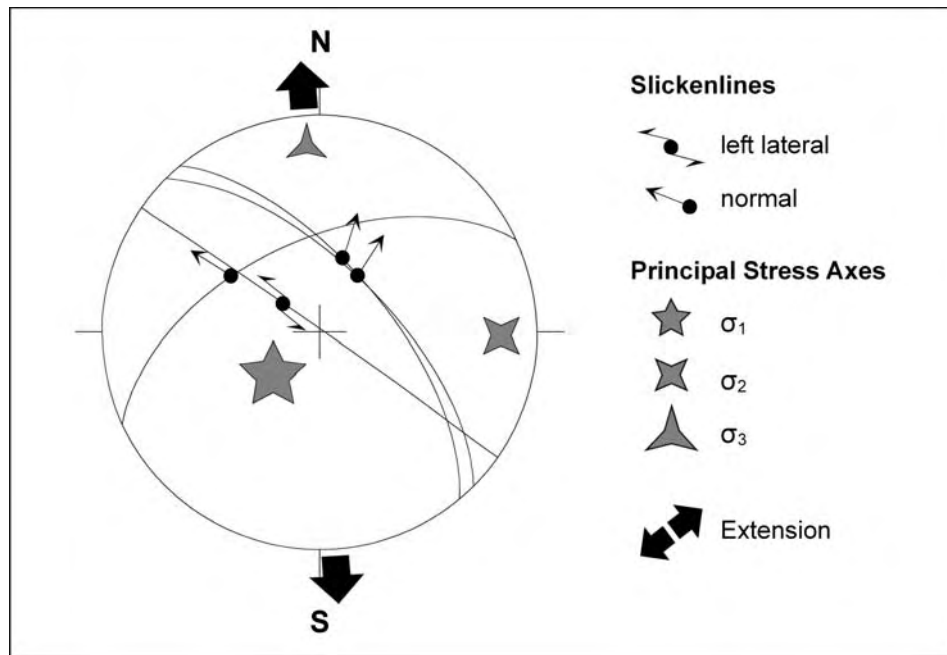


Figure 3.26. Schmidtt lower hemisphere equal-area projections of fault slip data from the southern Dikilitaş Fault. Great circles are fault surfaces, the arrows are slickensides (see Table 3.2 for details).

CHAPTER 4

DISCUSSION AND CONCLUSION

4.1. Introduction

The aims of this chapter are (1) to establish the sequence of metamorphism in relation to the different deformational stages within the study area, (2) to discuss the metamorphic grade during each phase; (3) to discuss the origin of migmatization and its relation to pegmatite formation; (4) to discuss the tectonic setting of each deformational and associated metamorphic phase; (5) to examine the relationship between migmatization, magmatism and exhumation of the metamorphic rocks and finally (6) to interpret the sequence of phases in terms of the geotectonic evolution of western Turkey.

4.2. Metamorphism

Both the field and petrographic studies of the metamorphic rocks of the study area have shown that these rocks have experienced, at least, two-distinct phases of metamorphic event associated with a top-to-the-NNE contractional and then a top-to-the-NNE extensional deformation during the exhumation of the metamorphic rocks: M_1 and M_2 metamorphism, respectively.

4.2.1. M_1 Metamorphism

The first phase of metamorphism is a more regional event and pervasive throughout the metamorphic rocks of the study area. It is associated with S_1 regional foliation both in the metasediments and orthogneisses. The field, petrographic, and textural evidence from the metasediments and microstructures

of deformed grains in the orthogneisses are used to estimate the metamorphic conditions prevailed during M_1 metamorphism; the data are all consistent in indicating that the M_1 metamorphism reached upper amphibolite facies conditions with associated partial anatexis. Evidence from the metasediments can be summarized as follows:

(1) The determination of metamorphic grade prevailed during the M_1 metamorphism is largely based on the use of the index minerals. On the other hand, it is also realized that the precise determination of metamorphic grade using the index minerals of the Barrovian zonal assemblages is impossible particularly when aluminosilicate minerals such as staurolite, kyanite and sillimanite are absent. There are examples worldwide that these minerals are absent although the pressure and temperature conditions would favour their growth; in such cases the absence of these minerals are attributed to the composition of protolith rocks where semipelitic and/or calcsilicate rocks have unsuitable composition for aluminosilicate minerals to form (Winchester 1972, 1974; Yardley 1989, p.67).

The mineral assemblage observed within the pelitic and semipelitic schists is typical with biotite + muscovite + quartz + feldspar + garnet + kyanite. The presence of garnet and kyanite within these rocks suggests metamorphic conditions of at maximum, middle–upper amphibolite facies (e.g., Turner 1981; p. 209; Yardley 1989; Powell *et al.* 1981; Bozkurt 1994, 1996; Bozkurt and Park 1999). The sporadic occurrence of garnet and kyanite in the metasediments is thought to be related to the composition of the protolith rocks. Although it is not observed in this research, fibrolitic sillimanite has been recorded in the metasediments of the study area (Ayan 1973; Candan 1989) conforming that M_1 metamorphism reached upper amphibolite facies conditions.

(2) The presence of stromatic migmatites with local granitic leucosomes developed parallel to the regional S_1 foliation strongly suggests that partial anatexis took place during peak M_1 metamorphism (MMM) and that the M_1 metamorphism have reached upper amphibolite sillimanite zone (cf. Yardley 1989).

(3) The microscopic fabric within the metasediments also provides valuable information relating to the grade of metamorphism. The banded compositional foliation or segregation into phyllosilicate- and quartz-rich domains in the

semipelitic schists is a diagnostic feature of high-grade metamorphic rocks similar to the gneissose banding in the migmatites.

All the available mineralogical, field and textural evidence suggests that the metasediments of the study area have been subjected to a regional Barrovian type metamorphism which reached upper amphibolite facies conditions with partial anatexis.

The effects of the M_1 on the orthogneisses are difficult to assess because there is almost no change in the mineralogical content of the granitic protolith and no new characteristic mineral(s) form during their metamorphism. This is because that the granitic rocks contain minerals that are relatively stable over large portions of P-T space. Despite of these difficulties, the detailed study of microstructural changes particularly in feldspars, micas, and quartz are very useful tools in the estimation of metamorphic conditions associated with their deformation. In the following lines, the evidence of the metamorphic conditions prevailed during D_1 deformation of orthogneisses is summarized below.

(1) *Feldspars*: In areas of relatively slow-strain, feldspars display typical "core-and-mantle" structure, characterized by a larger feldspar core mantled by fine recrystallized grains. On the other hand, in areas of intense deformation, most of the feldspar porphyroclasts are deformed and flattened in the plane of foliation; in such areas orthogneisses exhibit a gneissose texture characterized by alternating mica-rich and feldspar-rich domains/bands. Microscopically, the flattened feldspars are composed mostly of dynamically recrystallized new grains and relatively less subgrains. Characteristic occurrence of deformation twins, undulatory extinction, deformation bands, kink bands and albite twinning in association with pericline-law twinning form evidence of strain in feldspars. Ubiquitous formation of myrmekite along the long sides of inequant K-feldspar grains which invariably face the maximum finite shortening direction form the other characteristic feature of the feldspars in the orthogneisses. These microstructures indicates that feldspars behave in both plastic and brittle fashion, since grain size reduction occurs through grain boundary migration and/or subgrain rotation and also through fracturing (e.g., Debat *et al.* 1978; Tullis 1978; Berthè *et al.* 1979; Watts and Williams 1979; Kerrick *et al.* 1980; Vidal *et al.* 1980; White *et al.* 1980; Simpson 1981, 1985; Hanmer 1982a, 1982b; Tullis *et al.* 1982; Tullis 1983; White

and White 1983; Olsen and Kohlstedt 1985; Tullis and Yund 1985; Gapais 1989a, 1989b; Simpson and Wintsch 1989; Pryer 1993). The metamorphic significance of various microstructures developed in the feldspars can be summarized as:

- (a) The kink bands in plagioclases suggest low temperature plasticity and deformation conditions at middle to upper greenschist facies (cf. Simpson 1985).
- (b) Deformation twins, undulatory extinction, deformation bands and kink bands all indicate temperature conditions of probably between 300 and 400°C (White 1975; Boullier 1980; Pryer 1993).
- (c) Dynamic recrystallization through either subgrain rotation or grain boundary migration suggests minimum temperature conditions of 400°–500°C (Marshall and Wilson 1976; Wilson 1980; Simpson and Wintsch 1989).
- (d) Recovery by dynamic recrystallization in feldspars takes place at temperatures greater than 550°C (cf. Olsen and Kohlstedt 1985).
- (e) Strain-related myrmekite formation along long axes of inequant K-feldspar porphyroclasts that face the maximum finite shortening direction suggests minimum metamorphic conditions of epidote-amphibolite facies (400°–500°C) (Simpson 1985; Simpson and Wintsch 1989).
- (f) Complete recrystallization of feldspars, particularly plagioclases, and the deformation of feldspars in plastic fashion indicate temperature conditions in excess of 530°–600°C during their deformation which is broadly consistent with upper amphibolite facies (Sturt 1969; Boullier and Gueguen 1975; Boissière and Vauchez 1979; Jensen and Starky 1985).
- (g) Cataclastic failure of feldspar can be correlated with the change from lower amphibolite to upper greenschist facies conditions, between 450°–500°C (Pryer 1993).
- (h) Randomly oriented fracturing in feldspars and cataclastic failure of quartz indicate temperatures below 300°C (Pryer 1993).

(2) *Quartz*: Deformation of quartz commonly results in the development of "core-and-mantle" structure and mostly "type 4" quartz ribbons (cf. Boullier and Bouchez 1978) of elongated, preferably oriented, newly recrystallized, quartz aggregates suggesting primary dynamic recrystallization. Undulatory extinction, deformation bands and lamellae are the strain-related features associated with quartz suggesting dynamic recrystallization at minimum temperatures between 250° and 300°C (Tullis 1978). On the other hand, larger grains size (exceeding 100 microns) indicates much higher metamorphic conditions at epidote-amphibolite facies or even higher (Twiss 1977; Simpson 1985; Etheridge and Wilkie 1981). Similarly, the "type-4" quartz ribbons indicate that deformation has reached at least epidote-amphibolite facies conditions (cf. Boullier and Bouchez 1978).

(3) *Micas*: Most of the micas (both biotite and muscovite) show complete recrystallization with their (001) planes defining the regional S_1 foliation whereas larger porphyroclasts, especially biotite, underwent deformation by bend-gliding and kinking. Kink-band formation in biotite and complete recrystallization in micas suggest deformation at minimum of upper greenschist to epidote-amphibolite facies conditions (Simpson 1985).

In a conclusion, the microstructures of deformed grains in the orthogneisses in the study area are broadly consistent with fabric development under temperatures greater than 550°C (e.g., Sturt 1969; Boullier and Gueguen 1975; White 1975; Twiss 1977; Bossière and Vauchex 1979; Boullier and Bouchez 1978; Tullis 1978; Debat *et al.* 1978; Berthè *et al.* 1979; Watts and Williams 1979; Kerrich *et al.* 1980; Vidal *et al.* 1980; White *et al.* 1980; Etheridge and Wilkie 1981; Simpson 1981, 1985; Hanmer 1982a, 1982b; Tullis *et al.* 1982; Tullis 1983; White and White 1983; Jensen and Starky 1985; Olsen and Kohlstedt 1985; Tullis and Yund 1985; Gapais 1989a, 1989b; Simpson and Wintsch 1989; Pryer 1993). The frequent occurrence of homogeneously flattened feldspar grains are consistent with metamorphic conditions at upper amphibolite facies (or even granulite facies) conditions (Tullis and Yund 1985). However, the presence of abundant resistant retort-shape feldspar porphyroclasts in the mylonitic orthogneisses suggests that both plagioclase and K-feldspar are relatively strong and resistant to ductile

deformation and that greenschist to lower amphibolite facies metamorphism during their deformation (cf. White 1975; Tullis and Yund 1985).

This event is correlated with the Eocene main Menderes metamorphism (MMM) affecting the whole Menderes Massif. This event is a regional HT/MP Barrovian-type metamorphism which reached upper-amphibolite-facies conditions with local anatexis melting in the structurally lowest units and greenschist grade in the structurally highest lithologies (Şengör *et al.* 1984; Satır and Friedrichsen 1986; Bozkurt 1994, 1995, 2004; Hetzel *et al.* 1998; Bozkurt and Park 1999; Hetzel and Reischmann 1996; Ring *et al.* 1999, 2001b, 2003; Bozkurt and Satır 2000; Bozkurt 2001a; Lips *et al.* 2001; Whitney and Bozkurt 2002; Régnier *et al.* 2003; Rimmelé *et al.* 2003a, 2003b). The information about this metamorphic phase is given in Chapter 1 (see Section 1.4.1.1) and its significance with the kinematics of associated D_1 deformation will be discussed in Section 4.3.1.

4.2.2. M_2 Metamorphism

A post- M_1 phase of retrograde metamorphism can be recognized in the rocks of the study area; it is termed M_2 metamorphism and associated with the development of S_2 shear band foliation overprinting the earlier S_1 foliation. Along S_2 foliation retrogressive processes are characteristic; it is expressed by the development of retrogressive chlorite replacing biotite. In the metasediments, sporadic development of chlorite can also be attributed to this phase. Retrogressive processes suggest metamorphic reactions under (?) greenschist facies conditions.

In addition to pervasive ductile deformation microstructures, the deformed grains in the orthogneisses exhibit evidence for brittle deformation through fracturing of feldspars and quartz grains, suggesting temperatures below 300°C (Pryer 1993). The brittle deformation fabrics/microstructures become dominant towards the structurally upper parts of the orthogneisses with overlying Neogene sediments. The brittle fabrics are attributed to decreasing metamorphic grade during exhumation as a function of depth where D_1 fabrics developed under upper amphibolite facies conditions have suffered cataclastic deformation under low

greenschist facies conditions. This, in turn, may reflect the transition of deformation from ductile to brittle during exhumation.

The retrogressive M_2 metamorphism is therefore characterized by replacement textures developed under the conditions of declining temperature and pressure, presumably during the uplift of the metamorphic complex. The latter effect of D_2 deformation and associated M_2 metamorphism overprinting the early D_1/M_1 fabrics are consistent with the extensional exhumation of metamorphic rocks.

As a summary, the petrographic, textural, microstructural and field evidence all reveal two major metamorphic events in the study area. The first is a regional Barrovian type metamorphism (M_1) which reached upper amphibolite facies conditions. During peak M_1 , crustal anatexis occurred and a granitic melt was produced. A second localized metamorphism (M_2) took place during the exhumation of the metamorphic rocks in an extensional shear zone at presumably greenschist facies conditions during declining temperature and pressure associated with the uplift of the massif.

4.3. Deformation

Both the field and microstructural studies of the metamorphic rocks of the study area have shown that these rocks have experienced, at least, three-distinct phases of deformation associated with metamorphism: (1) a top-to-the-NNE D_1 deformation, (2) a top-to-the-N-NNE D_2 deformation, and late (3) brittle normal faulting (D_3 deformation).

4.3.1. D_1 Deformation

The effect of deformation (D_1) and associated M_1 metamorphism is commonly observed within the metamorphic rocks of the study area and is expressed by the penetrative pervasive regional foliation (S_1) and invariably associated approximately NNE-trending mineral elongation/stretching lineation (L_1) that lies in the plane of the foliation. Asymmetric micro- and meso-folds (F_1) with

axial plane foliation parallel to S_1 are common structures associated with these rocks; they are particularly common in the migmatites. Various kinematic indicators are all consistent with a top-to-the-NNE sense of movement during this phase. The sense is consistent with the results of kinematic analysis in other parts of the Menderes Massif (Bozkurt 1994, 1996, 2000, 2001a, 2001b, 2004; Bozkurt and Park 1999; Bozkurt and Satır 2000; Hetzel *et al.* 1995a, 1995b, 1998; Bozkurt and Oberhänsli 2001; Gessner *et al.* 2001a, 2001b; 2004; Gökten *et al.* 2001; Işık and Tekeli 2001; Lips *et al.* 2001; Arslan *et al.* 2002; Whitney and Bozkurt 2002; Işık *et al.* 2003, 2004; Erdoğan and Güngör 2004). The other important point realized from the structural analysis the massif is that the mineral elongation lineation trends approximately N–S and does not change its orientation across the lithological contacts throughout the Menderes Massif. These observations suggests that the mineral lineation and associated penetrative regional foliation and top-N deformation is a common phenomenon and are all genetically related.

This phase of deformation was synchronous with M_1 regional Barrovian type metamorphism (main Menderes metamorphism, MMM) that reached upper amphibolite facies conditions. The progressive increase of metamorphic grade towards the structurally lower parts of the massif observed in other parts of the Menderes Massif is consistent with a tectonic burial mechanism for the origin of MMM (e.g., Şengör and Yılmaz 1981; Şengör *et al.* 1984; Satır and Friedrichsen 1986; Bozkurt 1994, 1996; Hetzel *et al.* 1998; Bozkurt and Park 1999; Ring *et al.* 1999, 2002, 2003; Bozkurt and Satır 2000; Whitney and Bozkurt 2002; Régnier *et al.* 2003; Rimmelé *et al.* 2003a, 2003b). This event is biostratigraphically constrained between Early Eocene (the age of the youngest known metamorphosed sediment) and Early Oligocene (the age of the oldest known unconformable unmetamorphosed sediments) (Şengör and Yılmaz 1981; Şengör *et al.* 1984; Okay 2001, 2002; Özer *et al.* 2001; Özer and Sözbilir 2003). This is in excellent agreement available radiometric ages (Satır and Friedrichsen 1986; Bozkurt and Satır 2000; Lips *et al.* 2001). More information about the age of MMM is given in Section 1.4.1.1.

The top-to-the-NNE deformation associated with M_1 metamorphism is an important observation and its significance with respect to the origin and evolution of the main Menderes metamorphism needs to be discussed. The main Menderes

metamorphism has long been attributed to the burial of the Menderes Massif area beneath the southward advancing Lycian Nappes (Şengör and Yılmaz 1981; Şengör *et al.* 1984b; Satır and Friedrichsen 1986; Collins and Robertson 1998, 1999, 2003). On the other hand, the unambiguous documentation of approximately top-to-the-N deformation associated with the main Menderes metamorphism from the southern Menderes Massif questioned this long standing hypothesis so that the MMM is attributed to the northward back-thrusting of Lycian nappes over the Menderes Massif (Bozkurt 1994, 1995; Bozkurt and Park 1999). This view was later supported by other structural studies in other parts of the Menderes Masif (Hetzl *et al.* 1999; Bozkurt 2000, 2001a; Arslan *et al.* 2002; Rimmelé *et al.* 2003a, 2003b). It is important to note that this hypothesis does not rule out the model that originates the Lycian Nappes from the İzmir-Ankara Neotethyan suture and transports it southward over the Menderes Massif area (Gutnic *et al.* 1979; Şengör and Yılmaz 1981; Şengör *et al.* 1984; Collins and Robertson 1997, 1998, 1999, 2003; Çelik and Delaloye 2003). The recent documentation of carpholites from the metasediments of the southern Menderes Massif and Lycian nappes suggests an Alpine HP event and can be considered to be the result of deep burial (> 30 km) of the Menderes Massif area beneath the southward moving Lycian Nappes (Oberhänsli *et al.* 2001; Rimmelé *et al.* 2003a, 2003b).

In conclusion, the top-to-the-NNE D_1 deformation and associated upper amphibolite facies M_1 metamorphism is the result of a contractional deformation within a crustal-scale shear zone formed in response to the northward backthrusting of Lycian Nappes following their final emplacement to present-day location (Bozkurt 1994, 1995, 1996; Bozkurt and Park 1999; Rimmelé *et al.* 2003b).

4.3.2. F_1 Folding

The widespread occurrence of F_1 folds encountered in migmatites is one of the most diagnostic structural elements formed during the D_1 deformation and can be attributed to the bending and buckling produced by shear movements. The

folding of migmatitic leucosomes may suggest that leucosomes may (1) pre-date the folds, (2) form syn-tectonically or (3) form post-tectonically by selective reconstitution of layers of appropriate composition (cf. Mehnert 1968). The style of folding observed in the migmatites – thickened crests and thinned limbs in these folds – may suggest that mobilization and deformation were simultaneous processes and that the folding has originated during the main act of mobilization rather than before or after.

4.3.3. D₂ Deformation

The D₂ deformation is expressed by the widespread development of S₂ shear band foliation and L₂ mineral elongation/stretching lineation. The present-day configuration of shear bands is consistent with a non-coaxial flow during a top-to-the-NNE shearing. This phase was associated with M₂ retrogressive metamorphism possibly at (?) greenschist facies conditions. The microstructures of deformed grains in the orthogneisses are broadly consistent with fabrics developed under greenschist facies conditions at temperatures below 300°C (Pryer 1993). The S₂ foliation is well expressed and best preserved in the orthogneisses. The detailed fieldwork and microstructural studies of deformed grains in the orthogneisses demonstrate that the metamorphic rocks of the study area has been affected by both ductile and brittle deformation mechanisms. The progressiveness of deformation through first ductile then brittle mechanisms is expressed just beneath a low-angle normal fault exposed in Çavullar area (Figure 2.1). There the footwall rocks exhibit a typical structural sequence with low-grade mylonites that grades structurally upward into cataclastic rocks (breccia), manifesting a brittle deformation. The breccia is clearly superposed onto the mylonitic orthogneisses which possess two distinct fabrics with a S₂ shear band foliation and curved and/or inclined S₁ foliation in microlithons/domains preserved between parallel shear bands (Figures 3.10b, 3.16, 3.17). The hanging-wall rocks are represented by cobble conglomerates composed mainly of variably-sized fragments derived from the underlying orthogneisses. The lack of any deformation

in the conglomerates and the presence of footwall rocks suggest that the rocks postdate the activity along the normal fault.

The structural sequence observed in the footwall rocks of the low-angle normal fault suggests that the ductile and brittle deformations were product of a single continuous deformation and reflects ductile-brittle continuum of deformation during which the metamorphic rocks experienced progressive mylonitization through cataclasis (brecciation) under conditions of decreasing temperature and pressure. This phenomenon is consistent with a deformation in an extensional shear zone in the footwall of which initially ductilely deformed metamorphic rocks begin to deform in brittle fashion through gradually decreasing temperature and pressure conditions. Eventually the footwall rocks are exposed at the surface if the shear zone continues operating (cf. Lister and Davis 1989).

Similar structures, presently low-angle normal faults, separating an essentially non-mylonitic upper plate from underlying variably mylonitic metamorphic and igneous rocks are found in different parts of the western Turkey (the southern Menderes Massif: Bozkurt 1994, 1995, 1996, 2004; Bozkurt and Park 1994, 1997a, 1997b, 1999, 2002; Hetzel and Reischmann 1996; Bozkurt and Satır 2000; Bozkurt and Oberhänsli 2001; Lips *et al.* 2001; Whitney and Bozkurt 2002; Rimmelé *et al.* 2003a, 2003b; the central Menderes Massif, along the southern margin of the Gediz Graben and northern margin of the Büyük Menderes Graben: Hetzel *et al.* 1995a, 1995b, 1998; Emre 1996; Emre and Sözbilir 1997; Koçyiğit *et al.* 1999a, 1999b; Seyitoğlu *et al.* 2000, 2001; Bozkurt 2001a, 2003; Bozkurt and Oberhänsli 2001; Lips *et al.* 2001; Gessner *et al.* 2001a, 2001b; Gökten *et al.* 20001; Sözbilir 2001, 2002; Işık *et al.* 2003; Özer and Sözbilir 2003; Ring *et al.* 2003; Bozkurt and Sözbilir 2004; the northern Menderes Massif: Verge 1995; Işık and Tekeli 2001; Işık *et al.* 2003, 2004; and the Kazdağ Massif: Okay and Satır 2000) and in the Aegean islands (e.g., Lister *et al.* 1984; Wijbrans and McDougall 1986, 1988; Avigad and Garfunkel 1989; Buick and Holland 1989; Gautier *et al.* 1990; Urai *et al.* 1990; Buick 1991a, 1991b; Faure *et al.* 1991; Lee and Lister 1992; Gautier *et al.* 1993; Gautier and Brunn 1994; Jolivet *et al.* 1994, 1996; Vandenberg and Lister 1996; Avigad *et al.* 1997; Keay *et al.* 2001; Pe-Piper *et al.* 1997, 2002; Pe-Piper 2000; Avigad *et al.* 2001; Jolivet 2001; Ring *et al.* 2001a, 2001b; Trotet *et al.* 2001a, 2001b; Altherr and Siebel 2002; Hejl *et al.*

2002; Liati *et al.* 2002; Rawling and Lister 2002; Ring and Reischmann 2002; Rosenbaum *et al.* 2002; Jolivet *et al.* 2003 Koukouvelas and Kokkalas 2003; Ring and Layer 2003; Schmadicke and Will 2003; Ring *et al.* 2003).

The top-to-the-NNE sense of shearing along retrogressive low-grade S_2 shear band foliation together with the present north-dip of the presently low-angle normal fault and the progressive deformation from ductile to brittle in the footwall rocks demonstrate that the D_2 deformation occurred in a top-to-the-NNE extensional shear zone, located between the metamorphic rocks and the structurally overlying Neogene sediments during the exhumation of the Menderes Massif and that the shear zone was active at greenschist-facies conditions. The low-angle normal fault gives a very small exposure, covering an area of less than 1 km², but the size of the fault is too small and cannot explain the formation and exhumation of the metamorphic rocks in the northern Menderes Massif, thus pending a regional-scale structure in the region. It seems that a regional-scale fault has existed in the northern Menderes Massif and in the study area between the metamorphic rocks and the Neogene basins but it has been eroded away following the exhumation of the metamorphic rocks. The erosional remnants of the structure are preserved here and there in the massif and can readily be observed locally, as in Çavullar area (Figure 2.1).

It is here speculated that the low-angle normal fault observed in the study area forms erosional remnant and/or preserved part of a larger-scale fault located on the northern side of the E–W-trending Simav Graben where Işık and Tekeli (2001) introduced a low-angle normal fault (named the Simav detachment fault). This fault separates the so-called mylonitic core rocks of the Menderes Massif in the footwall from the brittely deformed allochthonous schists, marbles, ophiolitic rocks and Neogene sediments of the Akdağ Basin in the hanging-wall. The footwall rocks are also intruded by two syn-extensional granitoid rocks known as Eğrigöz and Koyunoba granitoids. Both the metamorphic rocks and granitoids have experienced progressive ductile-brittle deformation during a top-to-the-NNE shearing associated during the uplift and cooling of the footwall rocks (Işık and Tekeli 2001; Işık *et al.* 2003, 2004). The volcanic rocks in the Neogene basin yielded K–Ar whole rock ages of 15.3±0.3 to 15.8±0.3 Ma (Ercan *et al.* 1997) whereas ⁴⁰Ar/³⁹Ar muscovite ages from the footwall mylonites and Eğrigöz

granitoids are 22.86 ± 0.47 Ma and 20.19 ± 0.28 Ma, respectively (Işık *et al.* 2004). The data indicates that ductile deformation in the extensional shear zone commenced in Early Miocene. The age of volcanic sediments in the Akdere basin together with the isotopic data from the footwall rocks suggests that the emplacement of Eğrigöz granitoid and the exhumation of the metamorphics have occurred between 20–15 Ma (Işık *et al.* 2004). Işık *et al.* (2003) speculated that the Simav detachment represents an earlier stage of extensional tectonics of Menderes Massif and affected larger areas including the central Menderes Massif (see *figure 10* in Işık *et al.* 2003). In this model, the presently low-angle normal faults along the southern margin of the Gediz Graben and northern margin of the Büyük Menderes Graben formed as high-angle normal faults after the Simav detachment fault became inactive at 15 Ma ago.

In conclusion, the northern Menderes Massif is a typical core complex made up of middle-lower crustal high-grade metamorphic and magmatic rocks, exhumed in the footwall of presently low-angle normal fault. The constituent rocks are unroofed during extension that followed crustal thickening due the Palaeogene continental collision between the Sakarya continent in the north and Anatolide-Tauride platform in the south across the Neotethys.

4.3.4. F₂ Folding

A regional-scale F₂ fold with a NNE–SSW-trending axis is observed within the study area. It is an open fold that refolds the earlier S₁ regional foliation in the metamorphic rocks of the study area (Figure 2.1). The general trend of this fold is consistent with an approximately WNW–ESE-directed compression, which is perpendicular to the general direction of NNE-trending extension in the study area.

The NNE–SSW-trending folds are not only confined to the metamorphic rocks of the northern Menderes Massif but similar structures have been mapped in the NE-trending basins to the north of the Gediz Graben (Bozkurt 2003 and references therein). Folds of mappable scale clearly deform the Miocene basin fill in almost all NE-trending basins including the Gördes, Demirci, Selendi,

Uşak-Güre basins and Kavacık basins (Bozkuş 1996; Seyitoğlu 1997; Yılmaz *et al.* 2000; Bozkurt 2003). Similarly, the folded nature of sediments of Early to early Middle Miocene age in the Uşak-Güre basin in areas close to the northern margin of the Gediz Graben has been documented by Westaway *et al.* (2003). Moreover, Bozkurt and Park (1997a) demonstrated the existence of stretching lineation parallel folds in the orthogneisses of the southern Menderes Massif in the footwall of a south-facing extensional shear zone where these structures are interpreted as the result of an approximately E–W-directed compression that accompanied the extensional ductile deformation. These observations confirm that the NE-trending folds are not local structures but occur in almost all NE-trending basins and in the Menderes Massif and that the folding in the metamorphic rocks and the Miocene sediments of the NE-trending basins are genetically related. The folds do not occur in the Pliocene or younger sediments, thus conforming a Miocene age for the timing of folding.

Folds with axes parallel to the NNE-trending mineral stretching lineation in the metamorphic rocks and to the basin margins of the NE-trending basins have important bearing on the evolution of the extensional tectonics in western Turkey. The general trend of these folds indicates horizontal shortening in a WNW–ESE direction at a high angle to the mineral stretching lineation and extension direction and to general trend of NE-trending basins. The folds are interpreted as the result of a deviation from plane strain deformation on a regional scale due to an extra component of WNW–sub-horizontal shortening during the development of the top-to-the-NNE shear zone.

It is therefore concluded that extensional ductile deformation in western Turkey was accompanied and/or alternated with an approximately E–W-directed horizontal shortening perpendicular to the stretching direction during the later stages of extensional shear zone deformation (Bozkurt 2003). Similar observations have also been made in central Aegean region (Cyclades; Avigad *et al.* 2001 and references therein).

4.3.5. D₃ Deformation

The high-angle (63–89°) faults of diverse size form the other conspicuous feature of the study area and form the boundaries between various rock associations of the study area (Figure 2.1). The faults brought the Neogene sediments in contact with the metamorphic rocks, suggesting that faulting must postdate the Neogene sedimentation. In general, these structures are degraded by erosion but there are localities where fault planes can be observed. In such localities, the fault plane-related features such as slickenlines and tension cracks characteristically occur on the fault planes. Otherwise the faults are inferred on the basis of their topographic expression and juxtaposition of various Neogene sedimentary associations with the metamorphic rocks.

The fault kinematic analysis using slip-data define two distinct phases of brittle deformation along high-angle oblique-slip faults with a dominant sinistral faulting and normal faulting. The computed results of sinistral slip data is consistent with a roughly horizontal σ_1 trending in 091° and plunging 18° that suggests an approximately E–W compression. On the other hand, the computed results of slip data from the faults with distinct normal motion in Kınık-Mestanlı and Dikilitaş areas suggest steeply plunging σ_1 (61° and 66°, respectively), and are consistent with approximately N–S extension.

Although it is clear that there are two distinct phases of deformation occurred along the high-angle normal faults, there is no overwhelming field data to comment on the relative timing of these motions; that is overprinting relations have not been observed anywhere in the study area. On the other hand, it is speculated, based on the regional correlations and nature of neotectonic deformation in western Turkey, that normal motion postdates the sinistral motion.

The E–W-directed compression suggested by sinistral strike-slip motion is consistent with the inferences about the origin and significance of F₂ folding in the study area. This, in turn, suggests that the fault was operating as a sinistral strike-slip fault under approximately E–W compression during the later stages of top-to-the-NNE ductile-brittle extension along presently low-angle fault and that approximately E–W sub-horizontal shortening accompanied the shear zone

deformation during its later stages. The fault was then reactivated during modern phase of N–S extensional tectonics prevailing in western Turkey since the latest Miocene–Pliocene time.

The similarity between the trend of the normal faults exposed within the study area and those bounding the margins of approximately E–W-trending grabens, such as Gediz, Simav, Bakırçay and Büyük Menderes grabens, suggest that these structures may be of the same age, Pliocene (~5 Ma) or younger. The slip analysis of graben-bounding faults is also consistent with approximately N–S extension derived from fault-slip data obtained along the Büyük Menderes and Gediz grabens (e.g., Bozkurt 2000, 2003; Sözbilir 2001, 2002; Bozkurt and Sözbilir 2004).

4.4. Significance of D₂ and D₃ Deformations

The results of present study suggests that the rocks of the study area has experienced two distinct phases of extension: (1) rapid exhumation of metamorphic rocks and associated pegmatoids in the footwall of presently low-angle ductile-brittle normal fault located to the north of E–W-trending Simav Graben commenced by the Early Miocene time; and (2) late stretching of crust and consequent E–W normal faulting along Plio-Quaternary high-angle faults. This is consistent with the previous studies in the Menderes and Kazdağ massifs and E–W-trending grabens of western Turkey that the Neogene extension in western Turkey has expressed itself in two distinct structural styles (Bozkurt 1994, 1995, 2000, 2001a, 2001b, 2002, 2003, 2004; Bozkurt and Park 1994, 1997a, 1997b, 1999, 2002; Hetzel *et al.* 1995a, 1995b, 1998; Verge 1995; Emre 1996; Hetzel and Reischmann 1996; Emre and Sözbilir 1997; Koçyiğit *et al.* 1999a, 1999b, 2000; Bozkurt and Satır 2000; Okay and Satır 2000; Sarıca 2000; Seyitoğlu *et al.* 2000, 2001; Yılmaz *et al.* 2000; Bozkurt and Oberhänsli 2001; F. Gürer *et al.* 2001, 2002; Genç *et al.* 2001; Gessner *et al.* 2001a, 2001b, 2001c, 2004; Gökten *et al.* 2001; Işık and Tekeli 2001; Lips *et al.* 2001; Sözbilir 2001, 2002; Yılmaz and Karacık 2001; A. Gürer *et al.* 2002; Koçyiğit and Özacar 2003; Cihan *et al.* 2003; Işık *et al.* 2003, 2004; Özer and Sözbilir

2003; Ring *et al.* 2003; Bozkurt and Sözbilir 2004). In these studies the early phase of N–S extension is thought to be related to orogenic collapse and/or back-arc extension commenced by the latest Oligocene–Early Miocene time whereas later phase is attributed to E–W modern graben formation due to by the combined effect of tectonic escape and subduction rollback processes along the Aegean-Cyprean subduction zone.

Despite of the consensus over the two distinct styles (core-complex and rift modes) of Neogene extension in western Turkey, there is still on-going debate about the continuum of the two phases. There are claims that two distinct styles of extension represent a single continuous extensional tectonic regime from latest Oligocene–Early Miocene to present times (e.g., Seyitoğlu *et al.* 2000, 2001; Işık *et al.* 2003, 2004 and references therein) others documents evidence for two different events, separated by a hiatus (e.g., Koçyiğit *et al.* 1999a; Bozkurt 2000, 2001, 2003, 2004; Bozkurt and Sözbilir 2004 and references therein).

The relationships between the D₂ fabrics and D₃ high-angle normal faults in study area clearly demonstrate that ductile-brittle detachment faulting and related fabrics are cut and displaced by high-angle faulting in the study area (Figures 3.16 and 3.17). The Neogene sediments (thought to be deposited in the hanging-wall of presently low-angle normal faults) are brought into contact with metamorphic rocks along these structures. More importantly, the youngest lithologies of Neogene sediments have also been affected by high-angle faulting. In addition, the low-angle normal fault exposed in Çavullar area occurs in the footwall of the high-angle normal faults. As the low-angle normal fault forms the boundary between mylonitic metamorphic rocks and structurally overlying Neogene sediments in the study area where Neogene sediments onlap the fault. These sediments form the youngest lithologies of the Neogene sediments in the Demirci and Gördes basins and they unconformably overlie the syn-extensional basin fill which is deformed into approximately NNE–SSW-trending anticlines or synclines (Bozkurt 2003 and references therein). In this case, the low-angle normal fault must be buried beneath the basin-fill which lies in the hanging-wall of the high-angle normal faults. The observations given above suggests that the low-angle normal fault is cut and displaced by the high

angle normal faults, thus suggesting that they cannot be the part of the single deformation which necessitates the steeper faults merge into the presently gently dipping detachment fault. More, the unconformable relationships between the tilted and folded syn-extensional sediments and younger, possibly Pliocene, undeformed sediments that onlap the low-angle normal fault suggests short-term hiatus and precludes a close genetic link between earlier low-angle and later high-angle faults. Furthermore, the time gap between these faults requires different mechanisms for each.

The results of this work is therefore consistent with episodic two-stage extension model proposed for the Gediz and Büyük Menderes grabens (e.g., Koçyiğit *et al.* 1999a, 2000; Bozkurt 2000, 2002, 2003; Yılmaz *et al.* 2000; Bozkurt and Sözbilir 2004) and for the formation of Menderes and Kazdağ core-complexes (e.g., Bozkurt 2001b, 2003, 2004; Okay and Satır 2000, respectively). The first event began by the Early Miocene (e.g., Bozkurt and Park 1994, 1997a, 1997b; Hetzel *et al.* 1995a, 1998; Seyitoğlu and Scott 1996; Bozkurt 2000, 2003, 2001a, 2004; Seyitoğlu *et al.* 2000, 2002; Işık *et al.* 2003, 2004; Bozkurt and Sözbilir 2004) while the second phase commenced by ~5 Ma (e.g. Koçyiğit *et al.* 1999a; Bozkurt 2000, 2001a, 2001b, 2002, 2003, 2004; Yılmaz *et al.* 2000; Bozkurt and Sözbilir 2004) and is the result of combined effect of the initiation of dextral motion along the North Anatolian Fault System (~5 Ma: e.g. Barka and Kadinsky-Cade 1988; Westaway 1994a; Armijo *et al.* 1999 or ~7 Ma: Gautier *et al.* 1999; Westaway *et al.* 2003) and the southward pull of the Anatolian plate along Aegean-Cyprean subduction zone.

4.5. Migmatization, Partial Anatexis and Intrusion of Pegmatoids

The migmatites form the major lithological units of the metasediments in the study area. They are typical stromatic migmatites and composed of leucocratic (dirty white) magmatic layers (leucosomes) and dark green layers of gneisses. The leucosomes are concordant with the main foliation and are deformed by F_1 minor folds. The formation of granitic magma and the emplacement of pegmatoids in the form of dykes, sills and domes took place during or after this phase.

Although migmatites are commonly regarded as suggesting partial to complete anatexis associated with high-grade metamorphism slightly above the sillimanite isograd (Winkler 1976), the origin of stromatic structure and migmatites has been the subject of controversy for years. The proposed hypotheses fall into four distinct categories: (1) igneous intrusion; (2) metasomatism; (3) partial melting (anatexis); or (4) metamorphic segregation (e.g., Michel-Lévy 1893; Holmquist 1907; Wegman 1935; Scheumann 1937; Tuttle and Bowens 1958; Von Platen 1965; Kretz 1966; White 1966; Mehnert 1968; Misch 1968; Carmichael *et al.* 1974; Hedge 1972; Winkler 1974, 1976; Pitcher and Berger 1972; Yardley 1978; England and Molnar 1993; Allen *et al.* 1998; Andresen *et al.* 1998; Bagdassarov and Dorfman 1998; Baker 1998; Benn *et al.* 1998; Clemens 1998, 2003; Cruden 1998; Hodges 1998; Weinberg and Searle 1998; Chappell *et al.* 2000; Chappell and White 2001; Clemens and Watkins 2001; Kriegsman 2001; Brown *et al.* 2003; Johannes *et al.* 2003; Johnson *et al.* 2003; Sheppard *et al.* 2003; Skår and Pedersen 2003; White *et al.* 2003 and references therein). According to some, stromatic structures may result from either "*lit-part-lit*"- injection of foreign magma by splitting up the planes of the foliation of the palaeosome (Michel-Lévy 1893; Pitcher and Berger 1972) or from metasomatic transformation of schists by migrating fluids (Yardley 1978). Other claimed that "*metamorphic segregation*" – a process of solution and re-precipitation of minerals via a fluid phase – play an important role in the generation of migmatites (White 1966; Mehnert 1968; Misch 1968; Yardley 1978). On the other hand, as in the case of many natural and experimental examples, migmatites and granitic melts may be products of partial melting (anatexis) of water-saturated metasediments due to very high temperatures of the sillimanite zone metamorphism (Tuttle and Bowens 1958; Von Platen 1965; Mehnert 1968; Carmichael *et al.* 1974; Winkler 1974, 1976).

Forceful *lit-part-lit* injection of granitic melt requires cross-cutting relationships between leucosomes and dark mica-rich layers and brecciation in the paleosome layers. On the other hand, the migmatites in the study area are characterized by foliation-parallel leucosomes with no brecciation observed around them. Similarly, the migmatites and schists in the study area have comparable mineralogy. The lack of cross-cutting relations and brecciation around the leucosome layers and similar mineralogy of migmatites and schists (presumed

protolith) therefore indicate that the introduction of foreign mineral/material into the system by igneous injection or by metasomatism are not a possible mechanism for the formation of the migmatites. This, in turn, suggests that partial melting or metamorphic segregation are likely mechanisms responsible for migmatization in the present area. However, metamorphic segregation is a process which cannot explain the formation of the huge volumes of migmatites and granitic rocks which occur in the northern Menderes Massif.

It is therefore concluded that partial anatexis (possibly during the latest stages of the M_1 metamorphism or during the early stages of the extensional deformation) was the main mechanism for the formation of both the migmatites and the granitic magma in the study area. The anatectic partial melting caused widespread silicic volcanism and granitic plutonism in the later Miocene throughout western Anatolia and in the Aegean Islands (e.g., Borsi *et al.* 1972; Egger 1974; İzdar 1975; Besang *et al.* 1977; Bingöl 1977; Ataman and Bingöl 1978; Dürr *et al.* 1978; Andrissen *et al.* 1979; Altherr *et al.* 1979, 1982; Fytikas *et al.* 1979; Kaya and Savaşçın 1981; Şengör and Yılmaz 1981; Bingöl *et al.* 1982; Innocenti *et al.* 1982, 1984; Keller 1983; Ercan *et al.* 1985, 1986, 1987; Schliestedt *et al.* 1987; Del Moro *et al.* 1988; Wijbrans and McDougall 1986, 1988; Henjes-Kunst *et al.* 1988; Yılmaz 1989; Zimmermann *et al.* 1989; Buick and Holland 1989; Buick 1991a, 1991b; Faure *et al.* 1991; Jones *et al.* 1991; Kolocotroni and Dixon 1991; Reischmann *et al.* 1991; Boronkay and Doutsos 1994; Seyitoğlu and Scott 1991, 1992a, 1992b; Hetzel *et al.* 1995a; Pe-Piper *et al.* 1997, 2002; Pe-Piper 2000; Okay and Satır 2000; Delaloye and Bingöl 2000; Keay *et al.* 2001; Yılmaz *et al.* 2001; Altherr and Siebel 2002; Koukouvelas and Kokkalas 2003; Tomaschek *et al.* 2003; Bozkurt 2004; Erdoğan and Güngör 2004).

4.6. Relationships among Migmatization, Crustal Melting, Extension, and Intrusion

Although it is now commonly accepted that migmatization, crustal melting, continental extensional deformation and magma emplacement are closely related processes, it is still not clearly understood whether crustal

melting preceded extension and was therefore a contributing force for collapse/extension or whether melting was a response of extension. It is because crustal melting may occur during heating or decompression, and there may be a positive feedback between melting and extension (Hodges 1998) and decompression in general (England and Molnar 1993). There are claims that the emplacement of magmatic bodies in thickened continental crust may promote lateral (Royden 1996; McKenzie *et al.* 2000) and vertical (Teyssier and Whitney 2002) crustal flow and eventual orogenic collapse. Similarly, intrusion of magmas may result in strain localisation in the footwall of major low-angle normal faults by modifying the initial thermal and mechanical properties of the continental lithosphere (e.g., Lynch and Morgan 1987; Chèry *et al.* 1989; Lister and Baldwin 1993; Parsons and Thompson 1993; Tommasi *et al.* 1994; Hill *et al.* 1995; Brown and Solar 1998; Geoffroy 1998, 2001; Morley 1999a, 1999b; Simpson 1999; Callot *et al.* 2001, 2002; Ebinger and Casey 2001; Corti *et al.* 2003; Ziegler and Cloetingh 2004 and references therein). The research until today has shown that the intimate dynamic and temporal relationship among migmatization, crustal melting, extension and intrusion is crucial in interpreting the structural evolution of the continental extensional terranes and metamorphic core complex formation. To identify and document the relationships/interactions among migmatization, crustal melting, extension and intrusion, it is necessary to determine the timing of magmatic and metamorphic events in the metamorphic terranes through thermochronology and high-precision geochronology. In fact, evaluation and understanding of the dynamic relationship between crustal melting, extension and intrusion requires a multidisciplinary approach and usually involves integration of detailed field-based structural, petrographic, thermobarometric (P–T paths), geochronological (zircon and monazite U–Pb SHRIMP dating) and thermochronological (hornblende, mica and biotite $^{40}\text{Ar}/^{39}\text{Ar}$ dating) analysis of metamorphic terranes. This study will provide information about the timing as well as the rates and duration of high-temperature processes during the tectonic evolution of orogenic crust.

The available literature on the evolution of extensional tectonics and core complex formation in western Turkey demonstrate evidence for granitic magmatism/intrusion broadly synchronous with mylonitic deformation in the

footwall of presently low-angle normal faults in different parts of the Menderes Massif (southern Menderes Massif: Bozkurt and Park 1994, 1997a, 1997b, 2002; Bozkurt 2004; central Menderes Massif: Hetzel *et al.* 1995a, 1998; Bozkurt 2001b, 2003; Gessner *et al.* 2001b; Işık *et al.* 2003; northern Menderes Massif: Işık and Tekeli 2001; Işık *et al.* 2003, 2004) and in the Kazdağ Massif (Okay and Satır 2000). The syn-extensional granites display evidence for both ductile and brittle deformation, suggesting that these rocks have suffered from extensional deformation following their emplacement into the country rocks. These observations suggest a spatial and temporal relationship between the igneous activity and extensional exhumation in the Menderes Massif, i.e. the core complex formation coincides in space and time with the plutonic activity.

The pegmatoid rocks show weak evidence for deformation following their generation. In such areas it was not possible to observe penetrative fabrics but rather more brittle structures occur. Such features are readily recognized in the feldspars of the pegmatoids domes where deformation banding, deformation twins, undulatory extinction, and grain-scale fractures form the evidence of deformation. The outcrop pattern of the pegmatoid domes is characteristic as they are elongated with long axes being parallel to the local mineral stretching lineation in the study area. These data suggests that pegmatoid domes have experienced some amount of deformation following their crystallization and/or during crystallization. The field relations of migmatization suggest that there is magma emplacement following partial melting during peak M_1 metamorphism. But it is yet not known if the granitic/pegmatitic melt was produced during partial melting at peak M_1 and it has the same composition with migmatites. Another to say, it is not known if the partial melting produced vast amount of melt to explain the pegmatitic domes in the study area. The answer to this question requires detailed geochemical analysis of migmatites and pegmatites and geochronologic studies. Although the relative timing of melt generation with respect to M_1 metamorphism and D_2 extensional tectonics is not established, the intrusion of pegmatoids must have occurred after D_1 deformation / M_1 metamorphism because where observed pegmatoids display cross-cutting relations with the S_1 regional foliation both in the schists and migmatites.

As there is not detailed geochronological, thermochronological and P–T studies carried out in the metamorphic rocks and pegmatoids of the study area, it is very difficult to assess the relationships among migmatization, magma generation/crustal anatexis, extension and intrusion. Nevertheless, the following scenario can be speculated. The granitic melt was produced either by (1) high temperatures during the peak M_1 metamorphism which was accompanied by a pressure reduction due to the uplift and unroofing of the Menderes Massif by removal of nappes over the massif area or (2) the thinning of the crust during this extensional collapse of the orogenically overthickened crust which gave rise to crustal anatexis at depth (pressure-release melting or adiabatic decompression; Wilson 1989). But the emplacement of the granitic material (the pegmatoid domes) must have taken place in the footwall of presently low-angle normal fault that accompanied the collapse of the orogen. There is no evidence of contact metamorphism in the country rocks – schists, migmatites and orthogneisses – observed along the contacts, indicating that the country rocks were at elevated temperatures during the emplacement of pegmatoids. It is very clear that both the partial melting during peak M_1 and extensional D_2 deformation might have contributed to the melt generation in the northern Menderes Massif but the interplay between the two processes is not known. Final exhumation of both the pegmatoids and country rocks have taken place in the footwall of low-angle normal fault through progressive ductile and brittle deformation.

4.7. Is the Horst Between Gördes and Demirci Basins A Gneissic Dome?

Gneiss domes are common constituents of orogenic core zones and occur worldwide in orogens ranging in age from Archean through Cenozoic and in tectonic settings from wide (hundreds to thousands of kilometers) collisional orogens to narrow (tens of kilometers) shear belts. Having an elongated shape and usually being aligned parallel to the trend of the orogen, they are characterized by a core of migmatites/plutons surrounded by high-grade metasedimentary rocks (cf. Teyssier and Whitney 2002 and references therein). The origin of gneiss domes has been debated for more than 50 years, but there is no general agreement on how they form. Their origin has been ascribed to

several different mechanisms such as diapirism, crustal shortening, and/or extension (Teyssier and Whitney 2002). According to these authors, many gneiss domes record positive feedback between decompression and partial melting of orogenic middle crust and the driving force for the formation of gneiss domes might be the instability that is created by this feedback between decompression and partial melting. The decreasing buoyancy associated with increasing melt fraction drives further decompression at near-isothermal conditions as the partially molten crust rises diapirically. This combination of processes may explain the generation and retention of large volumes of crustally derived melt recorded in many deep-seated migmatite terranes and inferred for active orogens. In exhumed orogens, the signature of the rapid ascent of partially molten crust is a gneiss dome cored by migmatite and/or granite.

Teyssier and Whitney (2002) review the effectiveness of different decompression mechanisms for creating conditions for partial melting, and propose that ascent of hot orogenic crust creates low-density, low-viscosity regions that rise sufficiently fast and retain enough melt to maintain near-isothermal conditions. This combination of decompression and partial melting may account for the ubiquitous occurrence of gneiss domes in orogens. It is suggested that once decompression is initiated by denudation, thinning, and/or diapirism, buoyancy-driven ascent is the most effective mechanism for generating large volumes of partial melt and for rapidly transferring deep crust toward the surface. The signature of this process is domal structures cored by high-grade rocks, including migmatites that contain evidence for near-isothermal decompression and dehydration melting.

By definition, the rocks of the northern Menderes Massif on the horst between Gördes and Demirci Basins resemble a typical gneiss dome characterized by core of migmatites and pegmatoid domes surrounded by high-grade schists. The pegmatoids have elongated shape being aligned parallel to the local mineral stretching lineation. The presence of migmatites in association with pegmatitic domes suggests that crustal melting occurred either: (1) during prograde heating by water-saturated melting and dehydration melting to very high temperature (>800°C) in the middle part of thickened crust, or (2) during

some decompression at more moderate temperatures (725°–800°C). Partial melting might have also been triggered by decompression driven by crustal thinning. Nevertheless, partial melting weakened the crust and facilitated orogenic collapse and crustal thinning. The subsequent extension resulted in fast exhumation of domes cored by migmatites and pegmatoids.

4.8. Geologic History

A working hypothesis for the tectono-metamorphic evolution of the Menderes Massif in the study area summarized four distinct stages:

(1) Crustal shortening and suturing of the İzmir-Ankara zone during which the rocks of Lycian Nappes were southerly transported over the Menderes Massif area (Şengör and Yılmaz 1984; Şengör *et al.* 1984; Collins and Robertson 1998; Gessner *et al.* 2001c; Ring *et al.* 2003). This deformation resulted in the deep burial of Menderes Massif rocks with depths exceeding 30 km and caused HP-metamorphism (Rimmelé *et al.* 2003).

(2) Subsequent to HP-metamorphism, the rocks of the Lycian nappes and the Menderes Massif were affected by folding, thrusting and internal imbrication of the metasediments and orthogneisses within a crustal-scale top-to-the-N–NNE contractional shear zone (D₁ deformation). This event is attributed to the northward back-thrusting of Lycian Nappes (Bozkurt 1994, 1995; Bozkurt and Park 1999; Rimmelé *et al.* 2003b) during which the contact between Lycian Nappe and Menderes Massif was reactivated as a top-to-the-N–NNE contractional (thrust) shear zone. The available palaeontological (age of the youngest sediments in the Lycian Nappes and the Menderes Massif) and geochronological data is consistent with a Middle Eocene–Early Oligocene age for the top–N deformation, which was contemporaneous with the Eocene main Menderes metamorphism (M₁ metamorphism). The metamorphic conditions reached upper amphibolite facies conditions. Migmatites and high-grade schists formed during this phase.

(3) Following the Alpine contractional deformation, a top-to-the-N–NNE (D₂ deformation) normal/extensional shear zone developed along the boundary

with the metamorphic rocks and Neogene sediments, most probably during latest Oligocene–Early Miocene extensional collapse of the orogen in western Turkey. Extensional fabrics superimposed on earlier contractional foliation at presumably greenschist facies conditions (M_2 metamorphism). Partial melting occurred during later stages of prograde M_1 metamorphism or was triggered by decompression driven by crustal thinning. The exhumation of high-grade metamorphic rocks and pegmatoids occurred in the footwall of the extensional shear zones.

(4) Subsequent final exhumation (to the surface) occurred by brittle normal faulting under near-surface conditions during the neotectonic extension and consequent graben formation that commenced during the Pliocene (c. 5 or 7 Ma) in western Turkey (e.g., Koçyiğit *et al.* 1999a; Bozkurt 2000, 2001a, 2002, 2003; Sarıca 2000; Yılmaz *et al.* 2000; Genç *et al.* 2001; F. Gürer *et al.* 2001; A. Gürer *et al.* 2002; F. Gürer and Yılmaz 2002; Sözbilir 2001, 2002; Yılmaz and Karacık 2001; England 2003; Bozkurt and Sözbilir 2004).

4.9. Conclusions

Under the light of the discussions given above and information gathered from field and laboratory studies presented in foregoing chapters, the followings are concluded.

(1) Keeping in mind that the rocks may have in fact more complex pre-Alpine metamorphism and deformation histories, it is concluded that the metamorphic rocks of the northern Menderes Massif have experienced at least three distinct phases of metamorphism and deformation during Alpine events.

(2) The first deformational phase (D_1) is the top-to-the-N-NNE contractional deformation occurred along north-directed back thrusting of Lycian Nappes and consequent internal imbrication of Menderes Massif during the Palaeocene-Eocene closure of Neotethys. This deformation was synchronous with the Main Menderes metamorphism (M_1) which reached upper-amphibolite facies conditions. The main regional foliation (S_1) and mineral stretching lineation (L_1) have developed during D_1 and M_1 . Syn-tectonically developed F_1 minor folds are other structural imprints of this phase. Partial anatexis during the

latest stage of the M_1 metamorphism was the main mechanism for the formation of both the migmatites and the granitic magma in the study area.

(3) The second deformational phase, top-to-the-N-NNE extension (D_2) and coeval retrograde metamorphism in greenschist facies conditions took place during Early Miocene spreading and thinning of the previously overthickened crust. The secondary foliation (S_2), overprinting S_1 , and the secondary lineation (L_2), mainly parallel to L_1 , have developed during this phase.

(4) The presently low-angle normal faults were originated during this period and the formation of these faults was coeval with sedimentation. That means, while the sedimentation was continuing, extension and normal faulting were also active and the Menderes Massif metamorphics were exhumed and became juxtaposed with the Miocene sediments along the footwall of presently low-angle normal faults.

(5) F_2 major folds developed during this phase lead to the conclusion that extensional ductile deformation in western Turkey was accompanied and/or alternated with an approximately E–W-directed horizontal shortening perpendicular to the stretching direction during the later stages of extensional shear zone evolution.

(6) Although the relative timing of melt generation with respect to M_1 metamorphism and D_2 extensional tectonics is not unambiguously established, the cross-cutting relations with the S_1 regional foliation both in the schists and migmatites, and weak evidence for deformation on pegmatites lead to the conclusion that the intrusion of pegmatoids occurred after and/or during very late increments of the D_1 deformation / M_1 metamorphism.

(7) The latest deformation phase (D_3) that affected the Menderes Massif is Pliocene-Pleistocene high-angle normal faulting and consequent graben formation due to N-S extension of whole western Anatolia. All the E–W grabens dissecting the Massif into northern, central and southern submassifs were formed during this phase.

(8) The high-angle normal faults clearly cut and displace the low-angle normal faults leading to a conclusion that the high-angle normal faults are much younger structures than the low-angle normal faults. The time gap between the formations of these faults requires two different mechanisms for each phase.

(9) By definition, the rocks of the northern Menderes Massif on the horst between Gördes and Demirci basins resemble a typical gneiss dome characterized by core of migmatites and pegmatoid domes surrounded by high-grade metamorphic rocks.

REFERENCES

- Akdeniz, N., Konak, N., 1979, Simav, Emet, Tavşanlı, Dursunbey, Demirci, Kütahya Dolaylarının Jeolojisi, *Mineral Research and Exploration Institute (MTA) of Turkey Report*, **6547**, Ankara, [in Turkish].
- Akkök, R., 1983, Structural and metamorphic evolution of the northern part of the Menderes Massif: new data from the Derbent area and their implication for the tectonics of the massif, *Journal of Geology*, **91**, 342-350.
- Allen, C.M., Williams, I.S., Stephens, C.J., Fielding, C.R., 1998, Granite genesis and basin formation in an extensional setting: the magmatic history of the northernmost New England Orogen, *Australian Journal of Earth Sciences*, **45**, 875-888.
- Altherr, R., Kreuzer, H., Wendt, I., Enz, H., Wagner, A., Keller, J., Harre, W., Hohndorf, A., 1982, A late Oligocene/early Miocene high temperature belt in the Attic-Cycladic Crystalline Complex (Se Pelagonian, Greece), *Geologisches Jahrbuch*, **E23**, 97-164.
- Altherr, R., Schliestedt, M., Okrusch, M., 1979, Geochronology of high-pressure rocks on Sifnos (Cyclades, Greece), *Contributions to Mineralogy and Petrology*, **70**, 245-255.
- Altherr, R., Siebel, W., 2002, I-type plutonism in a continental back-arc setting: Miocene granitoids and monzonites from the central Aegean Sea, Greece, *Contributions to Mineralogy and Petrology*, **143**, 397-415.
- Altunel, E., Stewart, I.S., Piccardi, L., Barka, A.A., 2003, Earthquake faulting at ancient Cnidus, SW Turkey, *Turkish Journal of Earth Sciences*, **12**, 137-152.
- Andresen, A., Hartz H.H., Vold, J., 1998, A late orogenic extensional origin for the infracrustal gneiss domes of the East Greenland Caledonides (72-74°N), *Tectonophysics*, **285**, 353-369.
- Andriessen, P.A.M., Boelrijk, N.A.I.M., Herbeda, E.H., 1979, Dating the events of metamorphism and granitic magmatism in the Alpine orogen of Naxos (Cyclades, Greece), *Contributions to Mineralogy and Petrology*, **69**, 215-225.
- Angelier, J., 1984, Tectonic analysis of fault slip data sets, *Journal of Geophysical Research*, **80**, 5835-5848.
- Angelier, J., 1991, Inversion of field data in fault tectonics to obtain regional stress. III: A new rapid direct inversion method by analytical means, *Geophysical Journal International*, **103**, 363-376.
- Armijo, R., Meyer, B., Hubert, A., Barka, A.A., 1999, Westward propagation of the North Anatolian fault into the northern Aegean: timing and kinematics, *Geology*, **27**, 267-270.
- Armijo, R., Tapponnier, P., Mercier, J., 1986, Quaternary extension in southern Tibet: field observations and tectonic implications, *Journal of Geophysical Research*, **91**, 13803-13872.
- Arslan, A., Erdoğan, B., Güngör, T., 2002, Transport direction of Lycian Nappes studied by kinematic indicators in Milas region, *Abstract of First International Symposium of the Faculty of Mines (İTÜ) on Earth Sciences and Engineering*, İstanbul, Turkey, p. 109.
- Artemjev, M.E., Artyushkov, E.V., 1971, Structure and isostasy of the Baikal rift and the mechanism of rifting, *Journal of Geophysical Research*, **78**, 7675-7708.
- Ataman, G., Bingöl, E., 1978, Searches on chemical composition of plutonic, volcanic and metamorphic rocks of west Anatolia, *Yerbilimleri*, **4**, 28-42.
- Avigad, D., Garfunkel, Z., 1989, Low-angle faults above and below a blueschist belt – Tinos Island, Cyclades, Greece, *Terra Nova*, **1**, 182-187.

- Avigad, D., Garfunkel, Z., Jolivet, L., Azañòn, J.M., 1997, Back arc extension and denudation of Mediterranean eclogites, *Tectonics*, **16**, 924-941.
- Avigad, D., Ziv, A., Garfunkel, Z., 2001, Ductile and brittle shortening, extension-parallel folds and maintenance of crustal thickness in the central Aegean (Cyclades, Greece), *Tectonics*, **20**, 277-287.
- Axen, G.J., Taylor, W.J., Bartley, J.M., 1993, Space-time patterns and tectonic controls of Tertiary extension and magmatism in the Great Basin of the western United States, *Geological Society of America Bulletin*, **195**, 56-76.
- Ayan, M., 1973, Gördes Migmatites, *Bulletin of Mineral Research and Exploration Institute (MTA) of Turkey*, **65**, 132-155.
- Bagdassarov, N., Dorfman, A., 1998, Granite rheology: magma flow and melt migration, *Journal of the Geological Society, London*, **155**, 863-872.
- Baker, D.R., 1998, Granitic melt viscosity and dike formation, *Journal of Structural Geology*, **20**, 1395-1404.
- Barka, A.A., Kadinsky-Cade, K., 1988, Strike-slip fault geometry in Turkey and its influence on earthquake activity, *Tectonics*, **7**, 663-684.
- Barker, A.J., 1990, *Introduction to Metamorphic Textures and Microstructures*, Blackie & Son Ltd., Glasgow, 170 p.
- Başarır, E., 1970, Bafa Gölü Doğusunda Kalan Menderes Masifi Güney Kanadının Jeolojisi ve Petrografisi, *Ege University Publications*, **102**, İzmir, [in Turkish with English Abstract].
- Başarır, E., 1975, Çine Güneyindeki Metamorfittlerin Petrografisi ve Bireysel İndex Minerallerin Doku İçerisindeki Gelişimleri, *Ph.D. Thesis*, Ege University, İzmir, [in Turkish with English Abstract].
- Bayramgil, O., 1954, Mineralogy of Gördes Pegmatites, *Geological Bulletin of Turkey*, **5(1-2)**, 54-56.
- Becker-Platen, J.D., Benda, L., Steffens, F., 1977, Litho-und biostratigraphische deutung radiometrischer Alterbestirnmungen aus dem Jungtertiar der Turkei, *Geologisches Jahrbuch*, **B25**, 139-167
- Behrendt, J.C., LeMasurier, W.E., Cooper, A.K., Tessensohn, F., Tre'hu, A., Damaske, D., 1991, Geophysical studies of the West Antarctic Rift System, *Tectonics*, **10**, 1257-1273.
- Benn, K., Ham, N.M., Pignotta, G.S., 1998, Emplacement and deformation of granites during transpression: magnetic fabrics of the Archean Sparrow pluton, Slave Province, Canada, *Journal of Structural Geology*, **20**, 1247-1259.
- Berthè, D., Choukroune, P., Jegouzo, P., 1979, Orthogneisses, mylonite and non coaxial deformation of granites: the example of the south Armorican shear zone, *Journal of Structural Geology*, **1**, 31-42.
- Besang, C., Eckhart, F.J., Harre, W., Kreuzer, H., Müller, P., 1977, Radiometrische Alterbestimmungen an neogenen Eruptivgesteinen der Turkei, *Geologisches Jahrbuch, Reihe B, Regional Geologie Ausland*, **25**, 3-36.
- Bingöl, E., 1977, Geology and petrology of Muratdağı region, *Bulletin of the Geological Society of Turkey*, **20**, 13-67.
- Bingöl, E., Delaloye, M., Ataman, G., 1982, Granitic intrusions in western Anatolia: a contribution to the geodynamic study of this area, *Eclogae Geologicae Helvetica*, **75**, 437-446.
- Birand, Ş.A., 1953, Some attractive minerals and rocks around Gördes, *Geological Bulletin of Turkey*, **4(2)**, 33-36.
- Boissière, G., Vauchez, A., 1979, Deformation naturelle par cisaillement ductile d'un granite de Grande Kabylie (Algerie), *Tectonophysics*, **51**, 57-81.
- Bonatti, E., 1985, Punctiform initiation of seafloor spreading in the Red Sea during transition from a continental to an oceanic rift, *Nature*, **316**, 33-37.

- Boronkay, K., Doutsos, T., 1994, Transpression and transtension within different structural levels in the central Aegean region, *Journal of Structural Geology*, **16**, 1555-1573.
- Borsi, S., Ferrara, G., Innocenti, F., Mazzuoli, R., 1972, Geochronology and petrology of recent volcanics in the eastern Aegean Sea (West Anatolia and Lesbos Island), *Bulletin of Volcanology*, **36**, 473-496.
- Boullier, A.M., 1980, A preliminary study on the behaviour of brittle minerals in a ductile matrix: example of zircons and feldspars, *Journal of Structural Geology*, **2**, 211-217.
- Boullier, A.M., Bouchez, J., 1978, Le quartz en rubans dans les mylonites, *Societe Geologique de France Bulletin*, **20**, 253-262.
- Boullier, A.M., Gueguen, Y., 1975, SP-mylonites: origin of some mylonites by superplastic flow, *Contributions to Mineralogy and Petrology*, **50**, 93-104.
- Bozkurt, E., 1994, *Effects of Tertiary Extension in the Southern Menderes Massif, Western Turkey*, Ph.D. thesis, Keele University, UK, 295 p.
- Bozkurt, E., 1995, Deformation during main Menderes metamorphism (MMM) and its tectonic significance: evidence from Southern Menderes Massif, western Turkey, *EUG VIII, Strasbourg, 9-13 April, Terra Abstracts*, **7**, 176.
- Bozkurt, E., 1996, Metamorphism in the Palaeozoic schists of the Southern Menderes Massif: field, petrographic, textural and fabric data from Selimiye (Milas-Muğla) area, *Turkish Journal of Earth Sciences*, **5**, 105-121.
- Bozkurt, E., 2000, Timing of Extension on the Büyük Menderes Graben, Western Turkey and its tectonic implications, In: Bozkurt, E., Winchester, J.A., Piper, J.D.A. (eds), *Tectonics and Magmatism in Turkey and the Surrounding Area*, Geological Society, London, Special Publications, **173**, 385-403.
- Bozkurt, E., 2001a, Late Alpine evolution of the central Menderes Massif, western Anatolia, Turkey, *International Journal of Earth Sciences*, **89**, 728-744.
- Bozkurt, E., 2001b, Neotectonics of Turkey – a synthesis, *Geodinamica Acta*, **12**, 3-30.
- Bozkurt, E., 2002, Discussion on the extensional folding in the Alaşehir (Gediz) Graben, western Turkey, *Journal of the Geological Society, London*, **159**, 105-109.
- Bozkurt, E., 2003, Origin of NE-trending basins in western Turkey, *Geodinamica Acta*, **16**, 61-81.
- Bozkurt, E., 2004, Granitoid rocks of the Southern Menderes Massif (southwest Turkey): field evidence for Tertiary magmatism in an extensional shear zone, *International Journal of Earth Sciences*, **93**, 52-71.
- Bozkurt, E., Oberhänsli, R., 2001, Menderes Masif (Western Turkey): structural, metamorphic and magmatic evolution – a synthesis, *International Journal of Earth Sciences*, **89**, 679-708.
- Bozkurt, E., Park, R.G., 1994, Southern Menderes Massif: an incipient metamorphic core complex in western Anatolia, Turkey, *Journal of the Geological Society, London*, **151**, 213-216.
- Bozkurt, E., Park, R.G., 1997a, Microstructures of deformed grains in the augen gneisses of Southern Menderes Massif and their tectonic significance, western Turkey, *Geologische Rundschau*, **86**, 101-119.
- Bozkurt, E., Park, R.G., 1997b, Evolution of a mid-Tertiary extensional shear zone in the Southern Menderes Massif, western Turkey, *Bulletin of Geological Society of France*, **168**, 3-14.
- Bozkurt, E., Park, R.G., 1999, The structure of the Palaeozoic schists in the southern Menderes Massif, western Turkey, a new approach to the origin of the main Menderes metamorphism and its relation the Lycian Nappes, *Geodinamica Acta*, **12**, 25-42.
- Bozkurt, E., Park, R.G., 2001, Discussion on the evolution of the Southern Menderes Massif in SW Turkey as revealed by zircon dating, *Journal of the Geological Society, London*, **158**, 393-395.

- Bozkurt, E., Park, R.G., Winchester, J.A., 1992, Evidence against the core/cover concept in the southern sector of the Menderes Massif, *International Workshop: Work in Progress on the Geology of Turkey, Keele University, Keele, 9-10 April 1992, Abstracts*, p22.
- Bozkurt, E., Park, R.G., Winchester, J.A., 1993, Evidence against the core/cover interpretation of the southern sector of the Menderes Massif, west Turkey, *Terra Nova*, **5**, 445-451.
- Bozkurt, E., Satır, M., 2000, The southern Menderes Massif (western Turkey): geochronology and exhumation history, *Geological Journal*, **35**, 285-296.
- Bozkurt, E., Sözbilir, H., 2004, Tectonic evolution of the Gediz Graben: field evidence for an episodic, two-stage extension in western Turkey, *Geological Magazine*, **141**, 63-79.
- Bozkurt, E., Winchester, J.A., Park, R.G., 1995, Geochemistry and tectonic significance of augen gneisses from the southern Menderes Massif (west Turkey), *Geological Magazine*, **132**, 287-301.
- Bozkuş, C., 1996, Kavacık (Dursunbey-Balıkesir) Neojen grabenin stratigrafisi ve tektoniği, *Turkish Journal of Earth Sciences*, **5**, 161-170 [in Turkish with English abstract].
- Brown, M. Solar, G.S., 1998, Shear-zone systems and melts: feedback relations and self-organization in orogenic belts, *Journal of Structural Geology*, **20**, 211-227.
- Brown, P.E., Dempster, T.J., Hutton, D.H.W., 2003, Extensional tectonics and mafic plutons in the Ketilidian rapakivi granite suite of South Greenland, *Lithos*, **67**, 1-13.
- Brun, J.P., Sokoutis, D., Van Den Driessche, J., 1994, Analogue modeling of detachment fault systems and core complexes, *Geology*, **22**, 319-322.
- Brun, J.P., Van Den Driessche, J., 1994, Extensional gneiss domes and detachment fault systems: structure and kinematics, *Bulletin de la Société Géologique de France*, **165**, 519-530.
- Brunn, J.H., de Graciansky, P.C., Gutnic, M., Juteau, T., Lefevre, R., Marcoux, J., Monod, O., Poisson, A., 1970, Structures majeures et correlations stratigraphiques dans les Taurides occidentales, *Le Bulletin de la Societe Geologique de la France*, **12**, 515-556.
- Buck, W.R., 1988, Flexural rotation of normal faults, *Tectonics*, **7**, 959-973.
- Buck, W.R., 1991, Modes of continental lithospheric extension, *Journal of Geophysical Research*, **96**, 20161-20178.
- Buick, I.S., 1991a, The late Alpine evolution of an extensional shear zone, Naxos, Greece, *Journal of the Geological Society, London*, **148**, 93-103.
- Buick, I.S., 1991b, Mylonite fabric development on Naxos, Greece, *Journal of Structural Geology*, **13**, 643-655.
- Buick, I.S., Holland, T.J.B., 1989, The P-T-t path associated with crustal extension, Naxos, Cyclades, Greece, In: Daly, J.S., Cliff, R.A., Yardley, B.W.D. (eds), Evolution of metamorphic belts, *Geological Society of London Special Publications*, pp365-369.
- Burchfiel, B.C., Zhiliang, C., Hodges, K.V., Yuping, L., Royden, L., Changrong, D., Jiene, X., 1992, *The South Tibetan Detachment System, Himalayan Orogen: Extension Contemporaneous with and Parallel to Shortening in a Collisional Mountain Belt*, Geological Society of America Special Publications, **269**, 41 p.
- Çağlayan, M.A., Öztürk, E.M., Öztürk, Z., Sav, H., Akat, U., 1980, Menderes Masifi güneyine ait bulgular ve yapısal yorum, *Geological Engineering, Turkey*, **10**, 9-19 [in Turkish with English Abstract].
- Callot, J.P., Geoffroy, L., Brun, J.P., 2002, Development of volcanic margins: three-dimensional laboratory models, *Tectonics*, **21**, 1052 (doi: 10.1029/2001TC901019).
- Callot, J.P., Grigne, C., Geoffroy, L., Brun, J.P., 2001, Development of volcanic margins: two-dimensional laboratory models, *Tectonics*, **20**, 148-159.

- Candan, O., 1989, *Petrography, Petrology and Minerology of the Region Located Between Demirci-Borlu Towns (Northern Flank of the Menderes Massif)*, Dokuz Eylul University, Graduate School of Natural and Applied Sciences, Research Papers, NO. FBE/JEO-89-AR-057, Izmir-Turkey.
- Candan, O., 1994, Petrography and metamorphism of the metagabbros at the northern part of Alaşehir; Demirci-Gördes submassif, Menderes Massif, *Bulletin of the Geological Society of Turkey*, **37/1**, 29-40.
- Candan, O., Dora O.Ö., Oberhänsli, R., Çetinkaplan, M., Partzsch, J.H., Warkus, F.C., Dürr, S., 2001, Pan-African high-pressure metamorphism in the Precambrian basement of the Menderes Massif, western Anatolia, Turkey, *International Journal of Earth Sciences*, **89**, 793-811.
- Candan, O., Dora, O.Ö., Oberhänsli, R., Oelsner, F.C., Dürr, S.T., 1997, Blueschist relics in the Mesozoic series of the Menderes Massif and correlation with Samos Island, Cyclades, *Schweiz Mineralogische und Petrographische Mitteilungen*, **77**, 95-99.
- Candan, O., Helvacı, C., Böhler, G., Walder, G., Mark, T.D., 1990, Metamorphism and fission-track age determination of apatite crystals from Demirci-Borlu region, Gördes submassif of the Menderes Massif, western Turkey, *Mineral Research and Exploration Institute (MTA) of Turkey Bulletin*, **111**, 65-74.
- Canet, J., Jaoul, P., 1946, About the geology of Manisa-Aydın-Kula-Gördes region, *Mineral Research and Exploration Institute (MTA) of Turkey Report*, **2068**.
- Carey, E., 1979, Recherche des directions principales de contraintes associées au jeu d'une population de failles, *Revue des Geologie Dynamique Géographique et Physique*, **21**, 57-66.
- Carey, E., Brunier, B., 1974, Analyse théorique et numérique d'une modèle mécanique élémentaire appliqué a l'étude d'une population des failles, *Comptes Rendus de l'Académie des Sciences, Paris, Serie D*, **279**, 891-894.
- Carmichael, I.S.E., Turner, F.J., Verghoogen, J.R., 1974, *Igneous Petrology*, McGraw-Hill Book Company, New York, 739 p.
- Çelik, O.F., Delaloye, M.F., 2003, Origin of metamorphic soles and their post-kinematic mafic dyke swarms in the Antalya and Lycian ophiolites, SW Turkey, *Geological Journal*, **38**, 235-256.
- Chappell, B.W., White A.J.R., 2001, Two contrasting granite types: 25 years later, *Australian Journal of Earth Sciences*, **48**, 489-499.
- Chappell, B.W., White, A.J.R., Williams, I.S., 2000, Lachlan Fold Belt granites revisited: high- and low-temperature granites and their implications, *Australian Journal of Earth Sciences*, **47**, 123-138.
- Chéry, J., 2001, Core complex mechanics: from the Gulf of Corinth to the Snake Range, *Geology*, **29**, 439-442.
- Chéry, J., Daignières, M., Lucazeau, F., Vilotte, J.P., 1989, Strain localization in rift zones (case of thermally softened lithosphere): a finite element approach, *Bulletin de la Société Géologique de France*, **8**, 437-443.
- Cihan, M., Saraç, G., Gökçe, O., 2003, Insights into biaxial extensional tectonics: an example from the Sandıklı Graben, west Anatolia Turkey, *Geological Journal*, **38**, 47-66.
- Clemens, J.D., 1998, Observations on the origins and ascent mechanisms of granitic magmas, *Journal of the Geological Society, London*, **155**, 843-851.
- Clemens, J.D., 2003, S-type granitic magmas - petrogenetic issues, models and evidence, *Earth-Science Reviews*, **61**, 1-18.
- Clemens, J.D., Watkins, J.M., 2001, The fluid regime of high-temperature metamorphism during granitoid magma genesis, *Contributions to Mineralogy and Petrology*, **140**, 600-606.
- Collins, A.S., Robertson, A.H.F., 1997, Lycian mélange, southwest Turkey: an emplaced Cretaceous accretionary complex, *Geology*, **25**, 255-258.

- Collins, A.S., Robertson, A.H.F., 1998, Processes of Late Cretaceous to Late Miocene episodic thrust-sheet translation in the Lycian Taurides, SW Turkey, *Journal of the Geological Society, London*, **155**, 759-772.
- Collins, A.S., Robertson, A.H.F., 1999, Evolution of the Lycian Allocthon, western Turkey, as a north-facing Late Paleozoic to Mesozoic rift and passive continental margin, *Geological Journal*, **34**, 107-138.
- Collins, A.S., Robertson, A.H.F., 2003, Kinematic evidence for late Mesozoic–Miocene emplacement of the Lycian Allocthon over the western Anatolide, belt, SW Turkey, *Geological Journal*, **38**, 295-310.
- Coney, P.J., 1980, Cordilleran metamorphic core complexes: an overview. In: Crittenden, M.D., Coney, P.J., Davis, G.H. (eds), *Cordilleran Metamorphic Core Complexes*, Geological Society of America Memoir, **153**, 7-31.
- Corti, G., Bonini, M., Conticelli, S., Innocenti, F., Manetti, P., Sokoutis, D., 2003, Analogue modelling of continental extension: a review focused on the relations between the patterns of deformation and the presence of magma, *Earth-Science Reviews*, **63**, 169-247.
- Crittenden, M.D., Coney, P.J., Davis, G.H. (eds.), 1980, *Cordilleran Metamorphic Core Complexes*, Geological Society of America Memoir, **153**, 490 p.
- Cruden, A.R. 1998, On the emplacement of tabular granites, *Journal of the Geological Society, London*, **155**, 853-862.
- Dağ, N., 1989, *Mineralogy and Geochemistry of Gördes Pegmatoids*, Ph.D. Thesis, Dokuz Eylül University, İzmir, 142 p.
- Dağ, N., Dora, O. Ö., 1986, Gördes beryls, *Journal of Ege University*
- Dağ, N., Dora, O.Ö., 1991, Gördes (Menderes Massif) pegmatoids, *Bulletin of the Geological Society of Turkey*, **34/1**, 1-8.
- Dannat, C., 1997., *Geochemie, Geochronologie und ND-Sr-Isotopie der granitoiden Kerngneise des Menderes Massivs, SW Türkei*, Ph.D. Thesis, Johannes Gutenberg Universität, Mainz, 120 p.
- De Graciansky, P.C., 1965, Menderes Masifi güney kıyısı boyunca görülen metamorfizma hakkında açıklamalar, *General Directorate of Mineral Research and Exploration of Turkey Bulletin*, **64**, 88-121 [in Turkish with English Abstract].
- De Graciansky, P.C., 1972, Reserches géologiques dans le Taurus Lycien occidental, *Thèse, University de Paris-Sud, Orsay*, 570 p.
- Debat, P., Soula, J.C., Kubin, L., Vidal, J.L., 1978, Optical studies of natural deformation microstructures in feldspars (gneiss and pegmatites from Occitania, Southern France), *Lithos*, **11**, 133-145.
- Del Moro, A., Innocenti, F., Kyriakopoulos, C., Manetti, P., Papadopoulos, P., 1988, Tertiary granitoids from Thrace (Northern Greece) Sr isotopic and petrochemical data, *Neues Jahrbuch fuer Mineralogie, Geologie und Palaeontologie*, **159**, 113-135.
- Delaloye, M., Bingöl, E., 2000, Granitoids from Western and Northwestern Anatolia: Geochemistry and modeling of geodynamic evolution, *International Geology Review*, **42**, 241-268.
- Dewey, J.F., 1988, Extensional collapse of orogens, *Tectonics*, **7**, 1123-1139.
- Dewey, J.F., Şengör, A.M.C., 1979, Aegean and surrounding regions: complex multiple and continuum tectonics in a convergent zone, *Geological Society of America Bulletin*, **90**, 84-92.
- Dora, O.Ö., Candan, O., Kaya, O., Koralay, E., Dürr, S., 2001, Revision of “Leptite-gneisses” in the Menderes Massif: a supracrustal metasedimentary origin, *International Journal of Earth Sciences*, **89**, 836-851.
- Dürr, S., Altherr, R., Keller, J., Okrusch, M., Seidel, E., 1978, The median Aegean crystalline belt: stratigraphy, structure, metamorphism and magmatism, In: Closs, H., Roeder, D.R., Schmidt, K. (eds), *Alps, Apennines, Hellenides*, Schweizerbart, Stuttgart, 455-477.

- Ebinger, C.J., Casey, M., 2001, Continental break-up in magmatic provinces: an Ethiopian example, *Geology*, **29**, 527-530.
- Egger, A., 1960, Mica, Feldspar and Kyanite Formations at Gördes (Manisa) Pegmatite Field, *Mineral Research and Exploration Institute (MTA) of Turkey Report*, **2759**.
- Egger, A., 1974, *Mineral Exploration in Two Areas*, UNESCO Tech. Rep. 4, Up/UN/TUR-72-004, New York, NY.
- Emre, T., 1996, Geology and tectonics of Gediz graben, *Turkish Journal of Earth Sciences*, **5**, 171-185 [in Turkish with English abstract].
- Emre, T., Sözbilir, H., 1997, Field evidence for metamorphic core complex, detachment faulting and accommodation faults in the Gediz and Büyük Menderes grabens, western Anatolia, *International Earth Sciences Colloquium on Aegean Regions 1995 Proceedings*, **1**, 73-93
- England, P., 2003, The alignment of Earthquake T-axes with the principal axes of geodetic strain in the Aegean region, *Turkish Journal of Earth Sciences*, **12**, 47-54.
- England, P.C., 1983, Constraints on extension of continental lithosphere, *Journal of Geophysical Research*, **88**, 1145-1152.
- England, P.C., Molnar, P., 1993, The interpretation of inverted metamorphic isograds using simple physical calculations, *Tectonics*, **12**, 145-157.
- Ercan, T, Satır, M., Kreuzer, H., Türkecan, A., Günay, E., Çevikbaş, A., Ateş, M., Can, B., 1985, Interpretation of new chemical, isotopic and radiometric data on Cenozoic volcanics of western Anatolia, *Bulletin of the Geological Society of Turkey*, **28**, 121-136.
- Ercan, T, Satır, M., Kreuzer, H., Türkecan, A., Günay, E., Çevikbaş, A., Ateş, M., 1987, Characteristic features of the Tertiary aged pseudobasalts of Manisa-Balıkesir area, *Geological Engineering, Turkey*, **30/31**, 31-42.
- Ercan, T, Türkecan, A., Can, B., Günay, E., Çevikbaş, A., Ateş, M., 1986, The geology of Ayvalık area and petrology of volcanic rocks, *Geological Engineering, Turkey*, **27**, 19-30.
- Ercan, T., Satır, M., Sevin, D., Türkecan, A., 1997, Interpretation radiometric age data on Tertiary–Quaternary volcanic rocks Anatolia, *Bulletin of Mineral Research and Exploration Institute (MTA) of Turkey*, **119**, 103-112 [in Turkish with English abstract].
- Erdoğan, B., 1990, Stratigraphy and tectonic evolution of İzmir – Ankara zone between İzmir and Seferihisar, *Turkish Association of Petroleum Geologists Bulletin*, **2/1**, 1-20 [in Turkish with English abstract].
- Erdoğan, B., 1992, Problem of core-mantle boundary of Menderes Massif, *Geosound*, **20**, 314-315.
- Erdoğan, B., 1993, Menderes Masifinin kuzey kanadının stratigrafisi ve çekirdek-örtü ilişkisi, *Abstracts of the Geological Congress of Turkey, Ankara, Turkey*, p. 56.
- Erdoğan, B., Güngör, T., 2004, The Problem of the Core-Cover Boundary of the Menderes Massif and an Emplacement Mechanism for Regionally Extensive Gneissic Granites, Western Anatolia (Turkey), *Turkish Journal of Earth Sciences*, **13**, 15-36.
- Esenli, F., 1993a, The chemical changes during zeolitisation (heulandite-clinoptilolite-type) of the acidic tuffs in the Gördes Neogene basin, *Bulletin of the Geological Society of Turkey*, **36/2**, 37-44.
- Esenli, F., 1993b, Quantitative analyses of heulandites-clinoptilolites in zeolite-bearing tuffs from Gördes region, *Geological Engineering, Turkey*, **1993**, 42-49.
- Etheridge, M.A., Wilkie, J.C., 1981, An assessment of dynamically recrystallized grain size as a palaeopiezometer in quartz-bearing mylonite zones, *Tectonophysics*, **78**, 475-508.
- Faure, M., Bonneau, M., Pons, J., 1991, Ductile deformation and syntectonic granite emplacement during the Late Miocene extension of the Aegean (Greece), *Le Bulletin de la Societe Geologique de la France*, **162**, 3-11.

- Fytikas, M., Giuliani, O., Innocenti, F., Manetti, P., Mazzuoli, R., Peccerillo, A., Villari, L., 1979, Neogene volcanism of the northern and central Aegean region, *Annals Geologiques*, **30**, 106-129.
- Gans, P.B., 1987, An open-system, two-layer crustal stretching model for the eastern Great Basin, *Tectonics*, **6**, 1-12.
- Gans, P.B., 1997, Large-magnitude Oligo-Miocene extension in the southern Sonora: implications for the tectonic evolution of northwest Mexico, *Tectonics*, **16**, 388–408.
- Gans, P.B., Bohrsen, W.A., 1998, Suppression of volcanism during rapid extension in the Basin and Range Province, United States, *Science*, **279**, 66–68.
- Gans, P.B., Mahood, G.A., Scherner, E., 1989, *Synextensional Magmatism in the Basin and Range Province: A Case Study from the Eastern Great Basin*, Geological Society of America Special Paper, **233**, 53 p.
- Gapais, D., 1989a, Shear structures within deformed granites: mechanical and thermal indicators, *Geology*, **17**, 1144-1147.
- Gapais, D., 1989b, Structures mecanismes de deformation et analyse cinematique, *Mem. Doc. Centre Armoricaïn d'Etude Struct. Socles*, **28**, 1-366.
- Gautier, P., Brun, J.P., 1994, Ductile crust exhumation and extensional detachments in the central Aegean (Cyclades and Evvia islands), *Geodinamica Acta*, **7**, 57-85.
- Gautier, P., Ballèvre, M., Brun, J.P., Jolivet, L., 1990, Cinématique de l'extension ductile a Naxos et Paros (Cyclades), *Comptes Rendus de l'Académie des Sciences Paris, Serie II*, **310**, 147-153.
- Gautier, P., Brun, J.P., Jolivet, J., 1993, Structure and kinematics of Upper Cenozoic extensional detachment on Naxos and Paros (Cyclades islands, Greece), *Tectonics*, **12**, 1180-1194.
- Gautier, P., Brun, J.P., Moriceau, R., Sokoutis, D., Martinod, J., Jolivet, L., 1999, Timing, kinematics and cause of Aegean extension: a scenario based on a comparison with simple analogue experiments, *Tectonophysics*, **315**, 31-72.
- Genç, Ş.C., Altunkaynak, Ş., Karacık, Z. Yazman, M., Yılmaz, Y., 2001, The Çubukdağ graben, south of İzmir: its tectonic significance in the Neogene geological evolution of the western Anatolia, *Geodinamica Acta*, **14**, 45-56.
- Geoffroy, L., 1998, Diapirism and intraplate extension – cause or consequence, *Comptes Rendus de l'Academie des Sciences, Serie II: Sciences de la Terre et des Planets*, **326**, 267-273.
- Geoffroy, L., 2001, The structure of volcanic margins: some problematics from the North Atlantic/Labrador-Baffin System, *Marine and Petroleum Geology*, **18**, 463-469.
- Gessner, G., Ring, U., Passchier, C.W., Güngör, T., 2001c, How to resist subduction: Eocene post-high pressure emplacement of the Cycladic blueschists unit onto the Menderes nappes, Anatolide belt, western Turkey, *Journal of Geological Society, London*, **158**, 769-780.
- Gessner, K., Collins, A.S., Ring, U., Güngör, T., 2004, Structural and thermal history of poly-orogenic basement: U–Pb geochronology of granitoid rocks in the southern Menderes Massif, Western Turkey, *Journal of the Geological Society, London*, **161**, 93-101.
- Gessner, K., Piazzolo, S., Güngör, T., Ring, U., Kröner, A., Passchier, C.W., 2001b, Tectonic significance of deformation patterns in granitoid rocks of the Menderes nappes, Anatolide belt, southwest Turkey, *International Journal of Earth Sciences*, **89**, 766-780.
- Gessner, K., Ring, U., Christopher, J., Hetzel, R., Passchier, C.W., Güngör, T., 2001a, An active bivergent rolling-hinge detachment system: central Menderes metamorphic core complex in western Turkey, *Geology*, **29**, 611-614.
- Glazner, A.F., Bartley, J.M., 1984, Timing and tectonic setting of the Tertiary low-angle normal faulting and associated magmatism in the southwestern United States, *Tectonics*, **3**, 385-396.

- Gökten, E., Havzaoğlu, Ş., Şan, Ö., 2001, Tertiary evolution of the central Menderes Massif based on structural investigations of metamorphics and sedimentary cover rocks between Salihli and Kiraz (western Turkey), *International Journal of Earth Sciences*, **89**, 745-756.
- Göncüoğlu, M.C., Dirik, K., Kozlu, H., 1996-1997, Pre-Alpine and Alpine terranes in Turkey: explanatory notes to the terrane map of Turkey, *Annales Geologiques des Pays Helleniques*, **37**, 515-536.
- Görür, N., Şengör, A. M. C., Sakıncı, M., Tüysüz, O., Akkök, R., Yiğitbaş, E., Oktay, F. Y., Barka, A. A., Sarıca, N., Ecevitöğlu, B., Demirbağ, E., Ersoy, Ş., Algan, O., Güneysu, C., Akyol, A., 1995, Rift formation in the Gökova region, southwest Anatolia: implications for the opening of the Aegean Sea, *Geological Magazine*, **132**, 637-650.
- Güngör, T., Erdoğan, B., 2002, Tectonic significance of mafic volcanic rocks in a Mesozoic sequence of the Menderes Massif, West Turkey, *International Journal of Earth Sciences*, **91**, 386-397.
- Gürer, A., Pinçe, A., Gürer, Ö.F., İlkışık, O.M., 2002, Resistivity distribution in the Gediz Graben and its implications for crustal structure, *Turkish Journal of Earth Sciences*, **11**, 15-26.
- Gürer, F.Ö., Bozcu, M., Yılmaz, K., Yılmaz, Y., 2001, Neogene basin development around Söke-Kuşadası (western Anatolia) and its bearing on tectonic development of the Aegean region, *Geodinamica Acta*, **14**, 57-70.
- Gürer, Ö.F., Yılmaz, Y., 2002, Geology of the Ören and surrounding regions, SW Turkey, *Turkish Journal of Earth Sciences*, **11**, 2-18.
- Gutnic M, Monod O, Poisson A, Dumon J.F., 1979, Géologie des Taurides Occidentales (Turquie), *Mémoire de la Societe Geologique de la France*, **137**, 1-112.
- Hamilton, W., 1987, Crustal extension in the Basin and Range Province, southwestern United States, In: Coward, M.P., Dewey, J.F. & Hancock, P.L. (eds), *Continental Extensional Tectonics*, Geological Society Special Publications, London, **28**, 155-176.
- Hamilton, W.J., Strickland, H.E., 1841, On the geology of the western parts of Asia minor, *Transactions of Geological Society, London*, **2**, 1-40.
- Hanmer, S.K., 1982a, Vein array as kinematic indicators as in kinked anisotropic materials, *Journal of Structural Geology*, **4**, 151-160.
- Hanmer, S.K., 1982b, Microstructure and geochemistry of plagioclase and microcline in naturally deformed granite, *Journal of Structural Geology*, **4**, 197-213.
- Hardcastle, K.C., Hills, I.S., 1991, Brute3 and Select - Quickbasic 4 programs for determination of stress tensor configurations and separation of heterogeneous populations of fault-slip data, *Computers and Geosciences*, **17**, 23-43.
- Hedge, C.E., 1972, *Source of Leucosomes of Migmatites in the Front Range, Colorado*, Geological Society of America Memorials, **35**, 65-72.
- Hejl, E., Riedl, H., Weingartner, H., 2002, Post-plutonic unroofing and morphogenesis of the Attic-Cycladic complex (Aegea, Greece), *Tectonophysics*, **349**, 37-56.
- Henjes-Kunst, F., Altherr, R., Kreuzer, H., Hansen, B.T., 1988, Disturbed U-Th-Pb systematics of young zircons and uranorthorites: the case of the Miocene Aegean granitoids, Greece, *Chemical Geology (Isotope Geosciences Section)*, **73**, 125-145.
- Hetzel, R., Passchier, C.W., Ring, U., Dora, O.Ö., 1995a, Bivergent extension in orogenic belts: the Menderes Massif (southwestern Turkey), *Geology*, **23**, 455-458.
- Hetzel, R., Reischmann, T., 1996, Intrusion age of Pan-African augen gneisses in the southern Menderes Massif and the age of cooling after Alpine ductile extensional deformation, *Geological Magazine*, **133**, 565-572.
- Hetzel, R., Ring, U., Akal, C., Troesch, M., 1995b, Miocene NNE-directed extensional unroofing in the Menderes Massif, southwestern Turkey, *Journal of Geological Society, London*, **152**, 639-654.

- Hetzl, R., Romer, R.L., Candan, O., Passchier, C.W., 1998, Geology of the Bozdağ area, central Menderes Massif, SW Turkey: Pan-African basement and Alpine deformation, *Geologische Rundschau*, **87**, 394-406.
- Hibard, M.J., 1979, Myrmekite as a marker between preaqueous and postaqueous phase saturation in granitic systems, *Geological Society of America Bulletin*, **90**, 1047-1062.
- Hibard, M.J., 1987, Deformation of incompletely recrystallized magma systems: granitic gneisses and their tectonic implications, *Journal of Geology*, **85**, 543-561.
- Hill, E.J., Baldwin, S.L., Lister, G.S., 1992, Unroofing of active metamorphic core complexes in the D'Entrecasteaux Islands, Papua New Guinea, *Geology*, **20**, 907-910.
- Hill, E.J., Baldwin, S.L., Lister, G.S., 1995, Magmatism as an essential driving force for formation of active metamorphic core complexes in eastern Papua New Guinea, *Journal of Geophysical Research*, **100**, 10441-10451.
- Hodges, K.V., 1998, The thermodynamics of Himalayan orogenesis, In: Treloar, P.J., O'Brien, P.J. (eds), What drives metamorphism and metamorphic reactions?, *Geological Society of London Special Publications*, **138**, 7-22.
- Holmquist, P.J., 1907, Adergneisbildung und magmatische Assimilation im Grundgebirge Schwedens, *Geologiska Föreningens I Stockholm Förhandlingar*, **29**, 313-354.
- Hutton, D.H.W., Dempster, T.J., Brown, P.E., Becker, S.D., 1990, A new mechanism of granitic emplacement: intrusion in active extensional shear zones, *Nature*, **343**, 452-455.
- Illies, J.H., Greiner, G., 1978, Rhinegraben and the Alpine system, *Geological Society of America Bulletin*, **89**, 770-782.
- Innocenti, F., Kolios, N., Manneti, P., Mazzuoli, R., Peccerillo, G., Rita, F., Villaria, L., 1984, Evolution and geodynamic significance of the Tertiary orogenic volcanism in Northeastern Greece, *Bulletin of Volcanology*, **47**, 25-37.
- Innocenti, F., Kolios, N., Manneti, P., Rita, F., Villari, L., 1982, Acid and basic Late NEogene volcanism in central Aegean Sea: its nature and geotectonic significance, *Bulletin of Volcanology*, **45**, 87-97.
- Işık, V., Seyitoğlu, G., Çemen, İ., 2003, Ductile-brittle transition along the Alasehir detachment fault and its structural relationship with the Simav detachment fault, Menderes Massif, western Turkey, *Tectonophysics*, **374**, 1-18.
- Işık, V., Tekeli, O., 2001, Late orogenic crustal extension in the northern Menderes Massif (western Turkey): evidence for metamorphic core complex formation, *International Journal of Earth Sciences*, **89**, 757-765.
- Işık, V., Tekeli, O., Seyitoğlu, G., 2004, The $^{40}\text{Ar}/^{39}\text{Ar}$ age of extensional ductile deformation and granitoid intrusions in the northern Menderes core complex: implications for the initiation of extensional tectonics in western Turkey, *Journal of Asian Earth Sciences*, **23**, 555-566.
- İzdar, E., 1975, *Geotectonic evolution of western Anatolia and comparison with the units of Aegean Sea and its surroundings*, Faculty of Science Publication, Ege University, **8**, 59 p.
- Jackson, J., McKenzie, D., 1988, The relationship between plate motions and seismic moment tensors and rates of active deformation in the Mediterranean and Middle East, *Geophysical Journal*, **93**, 45-73.
- Jackson, J.A., 1994, The Aegean deformation, *Annual Review of Geophysics*, **22**, 239-272.
- Jensen, L.N., Starkey, J., 1985, Plagioclase microfabrics in a ductile shear zone from the Jotun Nappe, Italy, *Journal of Structural Geology*, **98**, 65-79.
- Johannes, W., 1983, On the origin of layered migmatites, In: Atherton, M.P., Gribble, C.D. (eds), *Migmatites, Melting and Metamorphism*, Shiva Geology Series, Shiva, Nantwich, UK, pp. 234-248.

- Johannes, W., Ehlers, C., Kriegsman, L.A., 2003, The link between migmatites and S-type granites in the Turku area, southern Finland, *Lithos*, **68**, 69-90.
- Johnson, S.E., Fletcher, J.M., Fanning, C.M., 2003, Structure, emplacement and lateral expansion of the San Jose Tonalite pluton, Peninsular Ranges batholith, Baja California, Mexico, *Journal of Structural Geology*, **25**, 1933-1957.
- Jolivet, L., 2001, A comparison of geodetic and finite strain pattern in the Aegean, geodynamic implications, *Earth and Planetary Science Letters*, **187**, 95-104.
- Jolivet, L., Brun, J.P., Gautier, P., Lallemand, S., Patriat, M., 1994, 3D-Kinematics of extension in the Aegean region from the early Miocene to the present, insights from the ductile crust, *Le Bulletin de la Societe Geologique de la France*, **165**, 195-209.
- Jolivet, L., Faccenna, C., Goffe, B., Burov, E., Agard, P., 2003, Subduction tectonics and exhumation of high-pressure metamorphic rocks in the Mediterranean orogens, *American Journal of Science*, **303**, 353-409.
- Jolivet, L., Faccenna, C., Goffé, B., Mattei, M., Rossetti, F., Brunet, C., Storti, F., Funicello, R., Cadet, J.P., d'Agostino, N., Parra, T., 1998, Midcrustal shear zones in postorogenic extension: example from the northern Tyrrhenian Sea, *Journal of Geophysical Research*, **103**, 12123-12160.
- Jolivet, L., Goffé, B., Monié, P., Truffert, Luxey, C., Patriat, M., Bonneau, M., 1996, Miocene detachment in Crete and exhumation P-T-t paths of high-pressure metamorphics, *Geologie Rundschau*, **87**, 394-406.
- Jones, C.E., Tarney, J., Baker, J., 1991, Emplacement mechanisms and petrogenesis of Tertiary granitoids, Rhodope Massif, N. Greece, *Terra Abstracts*, **3**, p. 40.
- Kahle, H.G., Cocard, M., Peter, Y., Geiger, A., Reilinger, R., Barka, A., Veis, G., 2000, GPS-derived strain rate field within the boundary zones of the Eurasian, African, and Arabian Plates, *Journal of Geophysical Research*, **105**, 23353-23370.
- Kaya, O., Savaşçın, Y., 1981, Petrologic significance of the Miocene volcanic rocks in Menemen, west Anatolia, *Aegean Earth Science*, **1**, 45-48.
- Keay, S., Lister, G., Buick, I., 2001, The timing of partial melting, Barrovian metamorphism and granite intrusion in the Naxos metamorphic core complex, Cyclades, Aegean Sea, Greece, *Tectonophysics*, **342**, 275-312.
- Keller, J., 1983, Potassic volcanism of the Mediterranean area, *Journal of Volcanology and Geothermal Research*, **18**, 321-335.
- Kerrich, R., Allison, I., Barnett, R.L., Moss, S., Starkey, J., 1980, Microstructural and chemical transformations accompanying deformation of granite in a shear zone at Mieville, Switzerland; with implications for stress carron cracking and superplastic flow, *Contributions to Mineralogy and Petrology*, **73**, 221-242.
- Ketin, İ., 1966, Tectonic units of Anatolia (Asia minor), *Bulletin of Mineral Research and Exploration Institute (MTA) of Turkey*, **66**, 22-34.
- King, G., Ellis, M., 1990, The origin of large local uplift in extensional regions, *Nature*, **348**, 689-693.
- Kissel, C., Laj, C., 1988, Tertiary geodynamical evolution of the Aegean arc: a paleomagnetic reconstruction, *Tectonophysics*, **146**, 183-201.
- Koçyiğit, A., Özacar, A., 2003, Extensional neotectonic regime through the NE edge of the Outer Isparta Angle, SW Turkey: new evidence field and seismic data, *Turkish Journal of Earth Sciences*, **12**, 67-90.
- Koçyiğit, A., Ünay, E., Saraç, G., 2000, Episodic graben formation and extensional neotectonic regime in west Central Anatolia and the Isparta angle: a case study in the Akşehir-Afyon Graben, Turkey, In: Bozkurt, E., Winchester, J.A., Piper, J.D.A (eds), *Tectonics and Magmatism in Turkey and the Surrounding Area*, Geological Society, London, Special Publications, **173**, 405-421.
- Koçyiğit, A., Yusufoglu, H., Bozkurt, E., 1999a, Evidence from the Gediz graben for episodic two-stage extension in western Turkey, *Journal of the Geological Society, London*, **156**, 605-616.

- Koçyiğit, A., Yusufoglu, H., Bozkurt, E., 1999b, Reply to 'Discussion on evidence from the Gediz graben for episodic two-stage extension in western Turkey', *Journal of the Geological Society, London*, **156**, 1240-1242.
- Köktürk, U., Gümüş, A., 1995, Fibrous minerals within Bigadiç and Gördes zeolites, *Geosound*, **26**, 33-45.
- Kolocotroni, C.N., Dixon, J.E., 1991, The emplacement and generation of I-type granites during extension. The Oligocene Vrontou Pluton, NE Greece, *Terra Abstracts*, **3**, 40-41.
- Konak, N., 1985, A discussion on the core-cover relationships on the basis of recent observations (Menderes Massif), *Abstract of Geological Congress of Turkey, Ankara*, p. 33.
- Konak, N., Akdeniz, N., Öztürk, E.M., 1987, *Geology of the south of Menderes Massif: Correlation of Variscan and pre-Variscan events of the Alpine Mediterranean Mountain belt*, Guide book for the field excursion along western Anatolia, Turkey, IGCP Project No. 5, 42-53.
- Koralay, E., Dora, O.Ö., Chen, F., Satir, M., Candan, O., 2004, Geochemistry and Geochronology of Orthogneisses in the Derbent (Ağşehir) Area, Eastern Part of the Ödemiş-Kiraz Submassif, Menderes Massif: Pan-African Magmatic Activity, *Turkish Journal of Earth Sciences*, **13**, 37-61.
- Koralay, E., Satir, M., Dora O.Ö., 1998, Geochronologic evidence of Triassic and Precambrian magmatism in the Menderes Massif, west Turkey, *Third International Turkish Geology Symposium Abstracts*, p. 285
- Koralay, R., Satir, M., Dora, O.Ö., 2001, Geochemical and geochronological evidence for Early Triassic calc-alkaline magmatism in the Menderes Massif, western Turkey, *International Journal of Earth Sciences*, **89**, 822-835.
- Koukouvelas, I.K., Kokkalas, S., 2003, Emplacement of the Miocene west Naxos pluton (Aegean Sea, Greece): a structural study, *Geological Magazine*, **140**, 45-61.
- Kretz, R., 1966, Grain-size distribution for certain metamorphic minerals in relation to nucleation and growth, *Journal of Geology*, **74**, 147-173.
- Kriegsman, L.M., 2001, Partial melting, partial melt extraction and partial back reaction in anatexitic migmatites, *Lithos*, **56**, 75-96.
- Le Pichon, X., Angelier, J., 1979, The Aegean arc and trench system: a key to the neotectonic evolution of the eastern Mediterranean area, *Tectonophysics*, **60**, 1-42.
- Le Pichon, X., Angelier, J., 1981, The Aegean Sea, *Philosophical Transactions of Royal Society, London Serie A*, **300**, 357-372.
- Le Pichon, X., Chamot-Rooke, C., Lallemand, S., Noomen, R., Veis, G., 1995, Geodetic determination of the kinematics of Central Greece with respect to Europe: implications for Eastern Mediterranean tectonics, *Journal of Geophysical Research*, **100**, 12675-12690.
- Lee, J., Lister, G.S., 1992, Late Miocene ductile extension and detachment faulting, Mykonos, Greece, *Geology*, **20**, 121-124.
- Lenk, O., Türkez, A., Ergintav, S., Kurt, A.I., Belgen, A., 2003, Monitoring the kinematics of Anatolia using permanent GPS network stations, *Turkish Journal of Earth Sciences*, **12**, 55-66.
- Liati, A., Gebauer, D., Wysoczanski, R., 2002, U-Pb SHRIMP-dating of zircon domains from UHP garnet-rich mafic rocks and late pegmatoids in the Rhodope zone (N Greece); evidence for Early Cretaceous crystallization and Late Cretaceous metamorphism, *Chemical Geology*, **184**, 281-299.
- Lips, A.L.W., Cassard, D., Sözbilir, H., Yılmaz, H., 2001, Multistage exhumation of the Menderes Massif, western Anatolia (Turkey), *International Journal of Earth Sciences*, **89**, 781-792.
- Lisle, R.J., 1987, Principle stress orientations from faults: an additional constraints, *Annales Tectonica*, **1**, 155-158.
- Lister, G.S., Baldwin, S.L., 1993, Plutonism and the origin of metamorphic core complexes, *Geology*, **21**, 607-610.

- Lister, G.S., Banga, G., Geenstra, A., 1984, Metamorphic core complexes of Cordilleran type in the Cyclades, Aegean Sea, Greece, *Geology*, **12**, 221-225.
- Lister, G.S., Davis, A.D., 1989, The origin of metamorphic core complexes and detachment faults formed during Tertiary continental extension in the northern Colorado River region, U.S.A., *Journal of Structural Geology*, **11**, 65-94.
- Lister, G.S., Etheridge, M.A., Symonds P.A., 1986, Detachment faulting and the evolution of passive continental margins, *Geology*, **14**, 246-250.
- Loos, S., Reischmann, T., 1999, The evolution of the southern Menderes Massif in SW Turkey as revealed by zircon datings, *Journal of the Geological Society, London*, **156**, 1021-1030.
- Lynch, H.D., Morgan, P., 1987, The tensile strength of the lithosphere and the localisation of extension, In: Coward, M.P., Dewey, J.F., Hancock, P.L. (eds), *Continental Extensional Tectonics*, Geological Society Special Publications, **28**, 53-65.
- Mantovani, E., Viti, M., Babbucci, D., Tamburelli, C., Albarello, D., 2001, Back arc extension: which driving mechanism?, In: Jessell, M. W., 2001, General Contributions, *Journal of the Virtual Explorer*, **3**, 17-45.
- Marshall, D.B., Wilson, C.J.L., 1976, Recrystallization and peristerite formation in albite, *Contributions to Mineralogy and Petrology*, **57**, 55-69.
- McClusky, S., Balassanian, S., Barka, A.A., Demir, C., Ergintav, S., Georgiev, I., Gürkan, O., Hamburger, M., Hurst, K., Kahle, H.G., Kastens, K., Kekelidze, G., King, R., Kotzev, V., Lenk, O., Mahmoud, S., Mishin, A., Nadariya, M., Ouzounis, A., Paradissis, D., Peter, Y., Prilepin, M., Reilinger, R.E., Sanlı, İ., Seeger, H., Tealeb, A., Toksöz, M.N., Veis, G., 2000, Global Positioning System constraints on plate kinematics and dynamics in the Eastern Mediterranean and Caucasus, *Journal of Geophysical Research*, **105**, 5695-5720.
- McKenzie, D., Nimmo, F., Jackson, J.A., Gans, P.B., Miller, E.L., 2000, Characteristics and consequences of flow in the lower crust, *Journal of Geophysical Research*, **105**, 11029-11046.
- McKenzie, D.P., 1978a, Some remarks on the development of sedimentary basins, *Earth and Planetary Science Letters*, **40**, 25-32.
- McKenzie, D.P., 1978b, Active tectonics of the Alpine-Himalayan belt: the Aegean Sea and surrounding regions, *Geophysical Journal of Royal Astronomical Society*, **55**, 217-254.
- Means, W.D., 1987, A newly recognized type of slickenside striation, *Journal of Structural Geology*, **9**, 585-590.
- Mehnert, K.R., 1968, *Migmatites and the Origin of Granitic Rocks*, Elsevier, Amsterdam, 393 p.
- Ménard, G., Molnar, P., 1988, Collapse of a Hercynian Tibetan Plateau into a Late Paleozoic European Basin and Range province, *Nature*, **334**, 235-237.
- Merle, O., Michon, L., 2001, The formation of the West European rift: a new model as exemplified by the Massif Central area, *Bulletin de la Société Géologique de France*, **172**, 213-221.
- Meulenkamp, J.E., Van Der Zwaan, G.J., Van Wamel, W.A., 1994, On Late Miocene to recent vertical motions in the Cretan segment of the Hellenic arc, *Tectonophysics*, **234**, 53-72.
- Meulenkamp, J.E., Wortel, W.J.R., Van Wamel, W.A., Spakman, W., Hoogerduyn Strating, E., 1988, On the Hellenic subduction zone and geodynamic evolution of Crete in the late Middle Miocene, *Tectonophysics*, **146**, 203-215.
- Michel-Levy, A., 1893, Contribution a l'étude du granite de Flamanville et des granites Français en general, *Service de la Carte Géologique de la France Bulletin*, **5**, 317 p.
- Misch, P., 1968, Plagioclase compositions and non-anatectic origin of migmatitic gneisses in northern Cascade mountains of Washington state, *Contributions to Mineralogy and Petrology*, **17**, 1-70.

- Mittwede, S.K., Karamanderesi, İ.H., Helvacı, C., 1995a, *Tourmaline-rich Rocks of the Southern Part of the Menderes Massif, Southwestern Turkey*, International Earth Sciences Colloquium on the Aegean Region 1995 Excursion Guide, Dokuz Eylül University, Department of Geological Engineering, İzmir, 25 p.
- Mittwede, S.K., Sinclair, W.D., Helvacı, C., Karamanderesi, İ.H., 1997, Quartz-tourmaline nodules in leucocratic metagranite, southern flank of the Menderes Massif, SW Turkey. *Tourmaline '97, International Symposium on Tourmaline Abstract Volume*, Czech Republic, 57-58.
- Mittwede, S.K., Sinclair, W.D., Karamanderesi, İ.H., Helvacı, C., 1995b, Geochemistry of quartz-tourmaline nodules from Irmadan (Muğla-Yatağan), Türkiye, *Abstracts of the Second International Turkish Geology Workshop*, September 6–8, 1995, Sivas, Turkey, p. 74.
- Morgan, P., Seager, W.R., Golombek, M.P., 1986, Cenozoic mechanical and tectonics evolution of the Rio Grande Rift, *Journal of Geophysical Research*, **91**, 6263–6276.
- Morley, C.K., 1999a, Aspects of transfer zone geometry and evolution in East African Rifts. In: Morley, C.K. (ed), *Geoscience of Rift Systems – Evolution of East Africa*, American Association of Petroleum Geologists Studies in Geology, **44**, 161-171.
- Morley, C.K., 1999b, Marked along-strike variations in dip of normal faults—the Lokichar fault, N. Kenya rift: a possible cause for metamorphic core complexes, *Journal of Structural Geology*, **21**, 479-492.
- Nebert, K., 1961, Information about the Neogene volcanism of the Gördes region, *Bulletin of Mineral Research and Exploration Institute (MTA) of Turkey*, **57**, 50-54.
- Newton, R. C., 1987, Petrologic aspects of Precambrian granulite facies terrains bearing on their origins. In: Kröner, A. (ed), *Proterozoic Lithospheric Evolution*, American Geophysics Union Geodynamics Series, **17**, 11-26.
- Oberhänsli, R., Monie, P., Candan, O., Warkus, F.C., Partzsch, J.H., Dora, O.Ö., 1998, The age of blueschist metamorphism in the Mesozoic cover series of the Menderes Massif, *Schweiz Mineralogische und Petrographische Mitteilungen*, **78**, 309-316.
- Oberhänsli, R., Partzsch, J., Candan, O., Çetinkaplan, M., 2001, First occurrence of Fe-Mg-caroholite documenting high-pressure metamorphism in metasediments of the Lycian Nappes, SW Turkey, *International Journal of Earth Sciences*, **89**, 867-873.
- Okay, A.İ., 1980a, Sodic amphiboles as oxygen fugacity indicators in metamorphism, *Geology*, **88**, 225-232.
- Okay, A.İ., 1980b, Mineralogy, petrology and phase relations of glaucophane-lawsonite zone blueschists from the Tavşanlı region, northwest Turkey, *Contribution to Mineralogy and Petrology*, **72**, 243-255.
- Okay, A.İ., 1984a, Distribution and characteristics of the northwest Turkish blueschists, In: Dixon, J.E., Robertson, A.H.F. (eds), *The Geological Evolution of the Eastern Mediterranean*, Geological Society, London, Special Publications, **17**, 455-466.
- Okay, A.İ., 1984b, Kuzeybatı Anadolu'da yer alan metamorfik kuşaklar [in Turkish with English Abstract], In: *Ketin Symposium, Geological Society of Turkey Publications*, 83-92.
- Okay, A.İ., 1986, High-pressure/low temperature metamorphic rocks of Turkey, *Geological Society of America Memoir*, **164**, 333-347.
- Okay, A.İ., 1989, Tectonic units and sutures in the Pontides, northern Turkey. In: Şengör, A.M.C. (ed), *Tectonic Evolution of the Tethyan Region*, Kluwer, Dordrecht, 109-116.
- Okay, A.İ., 2001, Stratigraphic and metamorphic inversions in the central Menderes Massif: a new structural model, *International Journal of Earth Sciences*, **89**, 709-727.
- Okay, A.İ., 2002, Reply: Stratigraphic and metamorphic inversions in the central Menderes Massif: A new structural model, *International Journal of Earth Sciences*, **91**, 173-178.
- Okay, A.İ., Harris, N.B.W., Kelley S.P., 1998, Exhumation of blueschists along a Tethyan suture in northwest Turkey, *Tectonophysics*, **285**, 272-299.

- Okay, A.İ., Satır, M., 2000, Coeval plutonism and metamorphism in a latest Oligocene metamorphic core complex in northwest Turkey, *Geological Magazine*, **137**, 495-516.
- Okay, A.İ., Siyako, M., 1993, The new position of the İzmir-Ankara Neo-Tethyan suture between İzmir and Balıkesir. In: Turgut, S. (ed), *Tectonics and Hydrocarbon Potential of Anatolia and Surrounding Regions*, Proceedings Ozan Sungurlu Symposium, 333-355.
- Okay, A.İ., Tüysüz, O., 1999, Tethyan sutures of northern Turkey, In: Durand, B., Jolivet, L., Horvath, D., Serrane, M. (eds), *The Mediterranean Basins: Tertiary Extension within the Alpine Orogen*, Geological Society, London, Special Publications, **156**, 475-515.
- Okrusch, M., Richter, P., Katsikatsos, G., 1985, High-pressure rocks of Samos, Greece, In: Dixon, J.E., Robertson, A.H.F. (eds), *The Geological Evolution of the Eastern Mediterranean*, Geological Society, London, Special Publications, **17**, 529-536.
- Olsen, T.S., Kohlstedt, D.L., 1985, Natural deformation and recrystallization of some intermediate plagioclase feldspars, *Tectonophysics*, **111**, 107-131.
- Özcan, A., Göncüoğlu, M.C., Turan, N., Uysal, S., Şentürk, K., Işık, A., 1988, Late Palaeozoic evolution of the Kütahya-Bolkardağ belt, *METU Journal of Pure and Applied Sciences*, **21**, 211-220
- Özer, S., Sözbilir, H., 2003, Presence and tectonic significance of Cretaceous rudist species in the so-called Permo-Carboniferous Göktepe Formation, central Menderes Massif, western Turkey, *International Journal of Earth Sciences*, **92**, 397-404.
- Özer, S., Sözbilir, H., Özkar, İ., Toker, V., Sarı, B., 2001, Stratigraphy of Upper Cretaceous–Palaeogene sequences in the southern and eastern Menderes Massif (western Turkey), *International Journal of Earth Sciences*, **89**, 852–866.
- Özkaya, İ., 1982, Origin and tectonic setting of some melange units in Turkey, *Journal of Geology*, **90**, 269-278.
- Özkaya, İ., 1990, Origin of allochthons in the Lycian belt, southwest Turkey, *Tectonophysics*, **177**, 367-379.
- Özkaya, İ., 1991, Evolution of a Tertiary volcanogenic trough in SW Turkey—the Alakaya Basin of the Lycian Belt, *Geologische Rundschau*, **80**, 657-668.
- Öztürk, A., Koçyiğit, A., 1983, Menderes grubu kayalarının temel-örtü ilişkisine yapısal bir yaklaşım (Selimiye-Muğla), *Bulletin of the Geological Society of Turkey*, **26**, 99-106, [in Turkish with English Abstract].
- Pamir, H.N., Erentöz, C., 1974, 1:500000 scale geological map of Turkey, İzmir sheet and explanatory book, *Mineral Research and Exploration Institute (MTA) of Turkey Publications*.
- Parsons, T., 1995, The Basin and Range Province, In: Olsen, K.H. (ed), *Continental Rifts: Evolution, Structure, Tectonics*, Developments in Geotectonics, **25**, 277-324.
- Parsons, T., Thompson, G.A., 1993, Does magmatism influence low-angle normal faulting?, *Geology*, **21**, 247-250.
- Passchier, C.W., Myers, J.S., Kröner, A., 1990, *Field Geology of High-Grade Gneiss Terrains*, Springer-Verlag, Berlin, 150 p.
- Passchier, C.W., Simpson, C., 1986, Porphyroclast systems as kinematic indicators, *Journal of Structural Geology*, **8**, 831-843.
- Passchier, C.W., Trouw, R.A.J., 1996, *Microtectonics*, Springer-Verlag, Berlin, 289p.
- Pe-Piper, G., 2000, Origin of S-type granites coeval with I-type granites in the Hellenic subduction system, Miocene of Naxos, Greece, *European Journal of Mineralogy*, **12**, 859-875.
- Pe-Piper, G., Kotopouli, C.N., Piper, D.J.W., 1997, Granitoid rocks of Naxos, Greece: regional geology and petrology, *Geological Journal*, **32**, 153-171.
- Pe-Piper, G., Piper, D.J.W., Matarangas, D., 2002, Regional implications of geochemistry and style of emplacement of Miocene I-type diorite and granite, Delos, Cyclades, Greece, *Lithos*, **60**, 47-66.

- Phillipson, A., (1910-1915), Reisen und forschungen im westlichen Kleinasien, *Pet. Geogr. Mitt. Erg. Hefte, Gotha*, **167, 172, 177, 180, 183**, 6 sheets, 1/300000.
- Pitcher, W.S., Berger, A.R., 1972, *The Geology of Donegal*, Wiley, New York, 435 p.
- Poisson, A., 1977, Recherches géologiques dans les Taurides occidentales (Turquie), *Thesis, University de Paris-Sud, Orsay*, 795 p.
- Powell, D., Baird, A.W., Charnley, N.R., Jordan, P.J., 1981, The metamorphic environment of the Sgurr Beag Slide; a major crustal displacement zone in Proterozoic Moine rocks of Scotland, *Journal of the Geological Society, London*, **136**, 661-673.
- Prodehl, C., Fuchs, K., Mechie, J., 1997, Seismic-refraction studies of the Afro-Arabian rift system – a brief review, *Tectonophysics*, **278**, 1-13.
- Pryer, L.L., 1993, Microstructures in feldspars from a major crustal thrust zone: the Grenville front, Ontario, Canada, *Journal of Structural Geology*, **15**, 21-36.
- Purvis, M., Robertson, A.H.F., 2004, Sedimentary-tectonic evolution of the Alaşehir Graben system in its regional Mediterranean context, *Tectonophysics*, [in press].
- Purvis, M., Robertson, A.H.F., Pringle, M., 2004, Ar⁴⁰-Ar³⁹ dating of biotite and sanidine in tuffaceous sediments and related intrusive rocks. Implications for the Early Miocene evolution of the Gördes and Selendi basins, W Turkey, *Geodinamica Acta*, [in press].
- Rawling, T.J., Lister, G.S., 2002, Large-scale structure of the eclogite-blueschist belt of New Caledonia, *Journal of Structural Geology*, **24**, 1239-1258.
- Régnier, J.L., Ring, U., Passchier, C.W., Gessner, K., Güngör, T., 2003, Contrasting metamorphic evolution of metasedimentary rocks from the Çine and Selimiye nappes in the Anatolide belt, western Turkey, *Journal of Metamorphic Geology*, **21**, 699-721.
- Reilinger, R.E., McClusky, S.C., Oral, M.B., King, W., Toksöz, M.N., 1997, Global Positioning System measurements of present-day crustal movements in the Arabian-Africa-Eurasia plate collision zone, *Journal of Geophysical Research*, **102**, 9983-9999.
- Reischmann, T., Kröner, A., Todt, W., Dürr, S., Şengör, A.M.C., 1991, Episodes of crustal growth in the Menderes Massif, W Turkey, inferred from zircon dating, *Terra Abstracts*, **3**, 34.
- Rimmelé, G., Jolivet, L., Oberhänsli, R., Goffé, B., 2003a, Deformation history of the high-pressure Lycian Nappes and implications for tectonic evolution of SW Turkey, *Tectonics*, **22**, 1007-1029.
- Rimmelé, G., Oberhänsli, R., Goffé, B., Jolivet, L., Candan, O., Çetinkaplan, M., 2003b, First evidence of high-pressure metamorphism in the 'Cover Series' of the southern Menderes Massif, Tectonic and metamorphic implications for the evolution of the SW Turkey, *Lithos*, **71**, 19-46.
- Ring, U., Brachert, T. C., Fassoulas, C., 2001a, Middle Miocene graben development in Crete and its possible relation to large-scale detachment faults, *Terra Nova*, **13**, 297-304.
- Ring, U., Gessner, K., Güngör, T., Passchier, C.W., 1999, The Menderes Massif of western Turkey and the Cycladic Massif in the Aegean – do they really correlate?, *Journal of Geological Society, London*, **156**, 3-6.
- Ring, U., Johnson, C., Hetzel, R., Gessner, K., 2003, Tectonic denudation of a Late Cretaceous-Tertiary collisional belt: regionally symmetric cooling patterns and their relation to extensional faults in the Anatolide belt of western Turkey, *Geological Magazine*, **140**, 421-441.
- Ring, U., Layer, P. W., Reischmann, T., 2001b, Miocene high-pressure metamorphism in the Cyclades and Crete, Aegean Sea, Greece: Evidence for large-magnitude displacement on the Cretan detachment, *Geology*, **29**, 395-398.
- Ring, U., Layer, P.W., 2003, High-pressure metamorphism in the Aegean, eastern Mediterranean: sequential accretion from the Late Cretaceous until the Miocene to Recent, *Tectonics*, **22**, art no. 1022, 23 p.

- Ring, U., Reischmann, T., 2002, The weak and superfast Cretan detachment, Greece: Exhumation at subduction rates in extrusion wedges. *Journal of the Geological Society, London*, **159**, 225-228.
- Rosenbaum, G., Avigad, D., Sánchez-Gómez, M., 2002, Coaxial flattening at deep levels of orogenic belts: evidence from blueschists and eclogites on Syros and Sifnos (Cyclades, Greece), *Journal of Structural Geology*, **24**, 1451-1462.
- Rosendahl, B.L., 1987, Architecture of continental rifts with special reference to east Africa, *Annual Reviews of Earth and Planetary Sciences*, **15**, 445-503.
- Royden, L., 1996, Coupling and decoupling of crust and mantle in convergent orogens: Implications for strain partitioning in the crust, *Journal of Geophysical Research-Solid Earth*, **101**, 17679-17705.
- Sarıca, N., 2000, The Plio-Pleistocene age of Büyük Menderes and Gediz grabens and their tectonic significance on N-S extensional tectonics in west Anatolia: Mammalian evidence from the continental deposits, *Geological Journal*, **35**, 1-24.
- Satır, M., Friedrichsen, H., 1986, The origin and evolution of the Menderes Massif, W-Turkey: A rubidium/strontium and oxygen isotope study, *Geologische Rundschau*, **75**, 703-714.
- Scheumann, K.H., 1937, Matatexis und metablastesis, *Tschermaks Mineralogische und Petrographische Mitteilungen*, **48**, 402-412.
- Schliestedt, M., Altherr, R., Matthews, A., 1987, Evolution of the Cycladic crystalline complex: petrology, isotope, geochemistry and geochronology, In: Helgeson, H.C., Schilling, R.D. (eds), *Chemical Transport in Metasomatism*, 76-94.
- Schmadicke, E., Will, T.M., 2003, Pressure-temperature evolution of blueschist facies rocks from Sifnos, Greece, and implications for the exhumation of high-pressure rocks in the Central Aegean, *Journal of Metamorphic Geology*, **21**, 799-811.
- Schuling, R.D., 1962, On the petrology, age and structure of the Menderes migmatite complex (SW Turkey), *Mineral Research and Exploration Institute (MTA) of Turkey Bulletin*, **58**, 71-84.
- Sederholm, J.J., 1913, Die Entstehung der migmatitischen Gesteine, *Geologische Rundschau*, **4**, 174-185.
- Seyitoğlu, G., 1997, Late Cenozoic tectono-sedimentary development of the Selendi and Uşak-Güre basins: a contribution to the discussion on the development of east-west and north trending basins in western Turkey, *Geological Magazine*, **134**, 163-175.
- Seyitoğlu, G., Çemen, İ., Tekeli, O., 2000, Extensional folding in the Alaşehir Gediz graben, western Turkey, *Journal of the Geological Society, London*, **157**, 1097-1100.
- Seyitoğlu, G., Scott, B.C., 1991, Late Cenozoic crustal extension and basin formation in west Turkey, *Geological Magazine*, **128**, 155-166.
- Seyitoğlu, G., Scott, B.C., 1992a, The age of the Büyük Menderes Graben (west Turkey) and its tectonic implications, *Geological Magazine*, **129**, 239-242.
- Seyitoğlu, G., Scott, B.C., 1992b, Late Cenozoic volcanic evolution of the northeastern Aegean region, *Journal of Volcanology and Geothermal Research*, **54**, 157-176.
- Seyitoğlu, G., Scott, B.C., 1994a, Late Cenozoic basin development in west Turkey: Gördes basin tectonics and sedimentation, *Geological Magazine*, **131**, 631-637.
- Seyitoğlu, G., Scott, B.C., 1994b, Neogene palynological and isotopic age data from Gördes Basin, West Turkey, *Newsletters Stratigraphy*, **31**, 133-142.
- Seyitoğlu, G., Scott, B.C., 1996, The age of the Alaşehir graben (west Turkey) and its tectonic implications, *Geological Journal*, **31**, 1-11.
- Seyitoğlu, G., Scott, B.C., Rundle, C.C., 1992, Timing of Cenozoic extensional tectonics in west Turkey, *Journal of Geological Society, London*, **149**, 533-538.
- Seyitoğlu, G., Tekeli, O., Çemen, İ., Şen, Ş., Işık, V., 2002, The role of the flexural rotation/rolling hinge model in the tectonic evolution of the Alaşehir graben, western Turkey, *Geological Magazine*, **139**, 15-26.

- Sheppard, S., Occhipinti, S.A., Tyler, I.M., 2003, The relationship between tectonism and composition of granitoid magmas, Yarlarweelor Gneiss Complex, Western Australia, *Lithos*, **66**, 133-154.
- Sherlock, S., Kelley, S.P., Inger, S., Harris, N., Okay, A.İ., 1999, ^{40}Ar - ^{39}Ar and Rb-Sr geochronology of high-pressure metamorphism and exhumation history of the Tavşanlı Zone, NW Turkey, *Contribution to Mineralogy and Petrology*, **137**, 46-58.
- Simpson, C., 1981, *Ductile Shear Zones; a Mechanism of rock Deformation in the Orthogneisses of the Maggia Nappe, Switzerland*, Ph. D. Thesis, ETH, Zürich, Switzerland, 265 p.
- Simpson, C., 1985, Deformation of granitic rocks across the brittle-ductile transition, *Journal of Structural Geology*, **7**, 503-511.
- Simpson, C., 1999, Introduction: The influence of granite emplacement on tectonics, In: Simpson, C. (ed), *The Influence of Granite Emplacement on Tectonics*, *Tectonophysics*, **312**, vii-viii.
- Simpson, C., Wintsch, R.P., 1989, Evidence for deformation induced K-feldspar replacement by myrmekite, *Journal of Metamorphic Geology*, **7**, 261-275.
- Skår, O., Pedersen, R.B., 2003, Relations between granitoid magmatism and migmatization: U-Pb geochronological evidence from the Western Gneiss Complex, Norway, *Journal of the Geological Society, London*, **160**, 935-946.
- Smith, J.V., 1974, *Feldspar Minerals, Volume 2*, Springer, New York.
- Smith, J.V., Brown, W.L., 1988, *Feldspar Minerals, Volume 1*, Springer, New York.
- Sokoutis, D., Brun, J.-P., Van Den Driessche, J., Pavlides, S., 1993, A major Oligo-Miocene detachment in southern Rhodope controlling north Aegean extension, *Journal of Geological Society, London*, **150**, 243-246.
- Sözbilir, H., 2001, Geometry of macroscopic structures with their relations to the extensional tectonics: field evidence from the Gediz detachment, western Turkey, *Turkish Journal of Earth Sciences*, **10**, 51-67.
- Sözbilir, H., 2002., Geometry and origin of folding in the Neogene sediments of the Gediz graben, western Anatolia, Turkey, *Geodinamica Acta*, **15**, 277-288.
- Sözbilir, H., Emre, T., 1996, Menderes Masifi'nin Neotektonik evriminde oluşan supradetachment havzalar ve rift havzaları, 49. *Türkiye Jeoloji Kurultayı, Panel of the Menderes Massif, Abstract Book*, **30**, Ankara.
- Steckler, M.S., Berthelot, F., Lybris, N., LePichon, X., 1988, Subsidence of the Gulf of Suez: implications for rifting and plate kinematics, *Tectonophysics*, **153**, 249-270.
- Straub, C.S., Kahle, H.G., Schindler, C., 1997, GPS and geological estimates of the tectonic activity in the Marmara Sea region, NW Anatolia, *Journal of Geophysical Research*, **102**, 27587-27601.
- Sturt, B.A., 1969, Wrench fault deformation and annealing recrystallization during almandine amphibolite facies regional metamorphism, *Journal of Geology*, **77**, 319-332.
- Şengör, A.M.C., 1979, The North Anatolian Transform Fault: its age, offset and tectonic significance, *Journal of the Geological Society, London*, **136**, 269-282.
- Şengör, A.M.C., 1982, Ege'nin neotektonik evrimini yöneten etkenler, In: Erol, O., Oygür, V. (eds), *Batı Anadolu'nun Genç Tektoniği ve Volkanizması Paneli*, Congress of the Geological Society of Turkey-1982, 59-72.
- Şengör, A.M.C., 1987, Cross-faults and differential stretching of hanging walls in regions of low-angle normal faulting: examples from western Turkey. In: Coward, M.P., Dewey, J.F., Hancock, P.L. (eds), *Continental Extensional Tectonics*, Geological Society, London, Special Publications, **28**, 575-589.
- Şengör, A.M.C., Görür, N., Şaroğlu, F., 1985, Strike-slip faulting and related basin formation in zones of tectonic escape: Turkey as a case study. In: Biddle, K., Christie-Blick, N. (eds), *Strike-Slip Deformation, Basin Formation and Sedimentation*, Society of Economic Paleontologists and Mineralogists, Special Publications, **37**, 227-264.

- Şengör, A.M.C., Satır, M., Akkök, R., 1984, Timing of tectonic events in the Menderes Massif, western Turkey: implications for tectonic evolution and evidence for Pan-African basement in Turkey, *Tectonics*, **3**, 693-707.
- Şengör, A.M.C., Yılmaz, Y., 1981, Tethyan evolution of Turkey: a plate tectonic approach, *Tectonophysics*, **75**, 181-241
- Teyssier, C., Whitney D. L., 2002, Gneiss domes and orogeny, *Geology*, **30**, 1139-1142.
- Thomson, S.N., Stöckhert, B., Brix, M.R., 1998, Thermochronology of the high-pressure metamorphic rocks of Crete, Greece: implications for the speed of tectonic processes, *Geology*, **26**, 259-262.
- Tomaschek, F., Kennedy, A.K., Villa, I.M., 2003, Zircons from Syros, Cyclades, Greece - Recrystallization and mobilization of zircon during high-pressure metamorphism, *Journal of Petrology*, **44**, 1977-2002.
- Tommasi, A., Vauchez, A., Fernandes, L.A.D., Porcher, C.C., 1994, Magma assisted strain localization in an orogen-parallel transcurrent shear zone of southern Brazil, *Tectonics*, **13**, 421-437.
- Trotet, F., Jolivet, L., Vidal, O., 2001a, Tectono-metamorphic evolution of Syros and Sifnos islands (Cyclades, Greece), *Tectonophysics*, **338**, 179-206.
- Trotet, F., Jolivet, L., Vidal, O., 2001b, Exhumation of syros and Sifnos metamorphic rocks (Cyclades, Greece). New constraints on the P-T paths, *European Journal of Mineralogy*, **13**, 901-920.
- Tullis, J., Yund, R.A., 1987, Transition from cataclastic flow to dislocation creep of feldspar: mechanisms and microstructures, *Geology*, **15**, 606-609.
- Tullis, J., Yund, R.A., 1980, Hydrolytic weakening of experimentally deformed Westerly granite and Hale albite rock, *Journal of Structural Geology*, **2**, 439-451.
- Tullis, J., Yund, R.C., 1985, Dynamic recrystallization of feldspar: A mechanism for ductile shear zone formation, *Geology*, **13**, 238-241.
- Tullis, J.A., Snoke, A.W., Tood, V.R., 1982, Penrose Conference Report: significance and petrogenesis of mylonitic rocks, *Geology*, **10**, 227-230.
- Tullis, T.E., 1978, Mylonites - natural and experimental: Processes and conditions of mylonite formation as inferred from experimental deformation studies, *Geological Society of America Short Course Notes*, 7-8 March, 1978, Boston, Massachusetts.
- Tullis, T.E., 1983, Deformation of feldspars, In: Ribbe, P.H. (ed), *Feldspar Mineralogy* (Reviews in Mineralogy Volume 2), Mineralogical Society of America, p. 297-323.
- Turner, F.J., 1981, *Metamorphic Petrology*, 2nd Edition, McGraw-Hill Book Company, New York, 524p.
- Tuttle, O.F., Bowens, N.L., 1958, Origin of granite in the light of experimental studies in the system NaAlSi₃O₈-KAlSi₃O₈-SiO₂-H₂O, *Sciences de la Terre*, **3**, 299-309.
- Twidale, C.R., 1982, *Granite Landforms*, Elsevier, Amsterdam, 372p.
- Twiss, R.J., 1977, Theory and applicability of recrystallized grain size palaeopiezometer, *Pure and Applied Geophysics*, **115**, 227-244.
- Twiss, R.J., Moores, E.M., 1992, *Structural Geology*, W.H. Freeman and Company, New York, 532p.
- Urai, J.L., Schuiling, R.D., Jansen, J.B.H., 1990, Alpine deformation on Naxos (Greece), In: Knipe, R.J., Rutter, E.H. (eds), *Deformation mechanisms, Rheology and Tectonics*, Geological Society, London, Special Publications, **54**, 509-522.
- Vanderberg, L.C., Lister, G.S., 1996, Structural analysis of basement tectonites from the Aegean metamorphic core complex of Ios, Cyclades, Greece, *Journal of Structural Geology*, **18**, 1437-1454.
- Verge, N.J., 1995, Oligo-Miocene extensional exhumation of the Menderes Massif, western Anatolia, *Terra Abstracts*, **7**, 117.
- Vidal, J., Kybin, L., Debat, D., Soula, J.C., 1980, Deformation and dynamic recrystallization of K-feldspar augen in orthogneiss from Montagne Noire, Occitania, Southern France, *Lithos*, **13**, 247-255.

- Von Platen, H., 1965, Experimental anatexis and genesis of migmatites, In: Pitcher, W.S., Flinn, G.W. (eds), *Controls on Metamorphism*, Oliver and Boyd, Edinburgh, p. 203-218.
- Ward, P., 1991, On plate tectonics and the geologic evolution of southwestern North America, *Journal of Geophysical Research*, **96**, 12479-12496.
- Watts, M.J., Williams, G.D., 1979, Fault rocks as indicators of progressive shear deformation in the Guingamp region, Brittany, *Journal of Structural Geology*, **1**, 323-332.
- Wegmann, C.E., 1935, Zur Deutung der Migmatite, *Geologische Rundschau*, **26**, 305-350.
- Weinberg, R.F., Searle, M.P., 1998, The Pangong Injection Complex, Indian Karakoram: A case of pervasive granite flow through hot viscous crust, *Journal of the Geological Society, London*, **155**, 883-891.
- Westaway, R., 1994a, Present-day kinematics of the Middle East and Eastern Mediterranean, *Journal of Geophysical Research*, **99**, 12071-12090.
- Westaway, R., 1994b, Evidence for dynamic coupling of surface processes with isostatic compensation in the lower crust during active extension of western Turkey, *Journal of Geophysical Research*, **99**, 20203-20223.
- Westaway, R., 2003, Kinematics of the Middle East and Eastern Mediterranean Updated, *Turkish Journal of Earth Sciences*, **12**, 5-46.
- Westaway, R., Pringle, M., Yurmen, S., Demir, T., 2004, Pliocene and Quaternary regional uplift in western Turkey: The Gediz river terrace and staircase and the volcanism at Kula. *Tectonophysics* [in press].
- Westaway, R., Pringle, M., Yurtmen, S., Demir, T., Bridgland, D., Rowbotham, G., Maddy, D., 2003, Pliocene and Quaternary surface uplift of western Turkey revealed by long-term river terrace sequences, *Current Science*, **84**, 1090-1101.
- White, A.J.R., 1966, Genesis of migmatites from the Palmer region of south Australia, *Chemical Geology*, **1**, 165-200.
- White, J.C., White, S.H., 1983, Semi-brittle deformation within the Alpine fault zone, New Zealand, *Journal of Structural Geology*, **5**, 579-589.
- White, R.W., Powell, R., Clarke, G.L., 2003, Prograde metamorphic assemblage evolution during partial melting of metasedimentary rocks at low pressures: Migmatites from Mt Stafford, central Australia, *Journal of Petrology*, **44**, 1937-1960.
- White, S.H., 1975, Tectonic deformation and recrystallization of Oligoclase, *Contributions to Mineralogy and Petrology*, **50**, 287-304.
- White, S.H., 1977, Geological significance of recovery and recrystallization process in quartz, *Tectonophysics*, **39**, 143-170.
- White, S.H., Burrows, S.E., Carreras, J., Shaw, N.D., Humphreys, F.J., 1980, On mylonites in ductile shear zones, *Journal of Structural Geology*, **2**, 175-187.
- Whitney, D.L., Bozkurt, E., 2002, Metamorphic history of the southern Menderes Massif, western Turkey, *Geological Society of America Bulletin*, **114**, 829-838.
- Wijbrans, J.R., McDougall, I., 1986, Ar-40/Ar-39 dating of white micas from an alpine high-pressure metamorphic belt on Naxos (Greece) - the resetting of the argon isotopic system, *Contributions to Mineralogy and Petrology*, **93**, 187-194.
- Wijbrans, J.R., McDougall, I., 1988, Metamorphic evolution of the Attic Cycladic Metamorphic Belt on Naxos (Cyclades, Greece) utilizing $^{40}\text{Ar}/^{39}\text{Ar}$ age spectrum measurements, *Journal of Metamorphic Geology*, **6**, 571-594.
- Willis, B., 1934, Inselbergs, *Assoc. Amor. Geogr. Ann.*, **24**, 123-129.
- Willis, B., 1936, East African plateaus and rift valleys, In: *Studies in Comparative Seismology*, Carnegie Institute, Washington D.C. Publications, 470 p.
- Wilson, C.J.L., 1980, Shear zones in a pegmatite: a study of albite-mica-quartz deformation, *Journal of Structural Geology*, **2**, 203-209.
- Wilson, M., 1989, *Igneous Petrogenesis: A Global Tectonic Approach*, Unwin Hyman Limited, London, 446 p.

- Wilson, M., 1993, Magmatism and the geodynamics of basin formation, *Sedimentary Geology*, **86**, 5-29.
- Winchester, J.A., 1972, The petrology of Moinian calc-silicate gneisses from Fannich Forest and their significance as indicators of metamorphic grade, *Journal of Petrology*, **13**, 405-424.
- Winchester, J.A., 1974, The zonal pattern of regional metamorphism in the Scottish Caledonides, *Journal of the Geological Society, London*, **130**, 509-524.
- Winkler, H.G.F., 1974, *Petrogenesis of Metamorphic Rocks*, 2nd Edition, Springer-Verlag, New York, 320 p.
- Winkler, H.G.F., 1976, *Petrogenesis of Metamorphic Rocks*, 3rd Edition, Springer-Verlag, New York, 320 p.
- Yardley, B.W.D., 1978, Genesis of the Skagit Gneiss migmatites, Washington, and the distinction between possible mechanisms of migmatization, *Geological Society of America Bulletin*, **89**, 941-951.
- Yardley, B.W.D., 1989, *An introduction to Metamorphic Petrology*, Longman, Harlow, 248p.
- Yılmaz, Y., 1989, An approach to the origin of young volcanic rocks of western Turkey, In: Şengör, A.M.C. (ed), *Tectonic Evolution of the Tethyan Region*, Kluwer Academic Publishers, p.159-189.
- Yılmaz, Y., Genç, S.C., Gürer, Ö.F., Bozcu, M., Yılmaz, K., Karacık, Z., Altunkaynak, Ş., Elmas, A., 2000, When did the western Anatolian grabens begin to develop?. In: Bozkurt, E., Winchester, J.A., Piper, J.D.A (eds), *Tectonics and Magmatism in Turkey and the Surrounding Area*, Geological Society, London, Special Publications, **173**, 353-384.
- Yılmaz, Y., Genç, S.C., Karacık, Z., 2001, Two contrasting magmatic associations of NW Anatolia and their tectonic significance, *Journal of Geodynamics*, **31**, 243-271.
- Yılmaz, Y., Karacık, Z., 2001, Geology of the northern side of the Gulf of Edremit and its tectonic significance for the development of the Aegean grabens, *Geodinamica Acta*, **14**, 31-40.
- Ziegler, P., Cloetingh, S., 2004, Dynamic processes controlling evolution of rifted basins, *Earth Science Review*, **65**, 1-73.
- Ziegler, P.A., 1995, Cenozoic rift system of western and Central Europe: an overview, *Geologie en Mijnbouw*, **73**, 99-127.
- Zimmerman, J.L., Saupe, F., Özgen, S., Anil, M., 1989, Oligocene-Miocene K-Ar ages of the quartz-monzonite stocks from Nevruz-Çakıroba (Yenice, Çanakkale, Northwest Turkey), *Terra Abstracts*, **1**, p. 354.